

**MECH541**  
**KINEMATIC SYNTHESIS**  
**Lecture Notes**

**Jorge Angeles**

Department of Mechanical Engineering &  
Centre for Intelligent Machines  
McGill University, Montreal (Quebec), Canada

**Shaoping Bai**

Department of Mechanical Engineering  
Aalborg University  
Aalborg, Denmark

© January 2016

These lecture notes are not as yet in final form.

Please report corrections & suggestions to

Prof. J. Angeles

Department of Mechanical Engineering &

McGill Centre for Intelligent Machines

McGill University

817 Sherbrooke St. W.

Montreal, Quebec

CANADA H3A 0C3

FAX: (514) 398-7348

[angeles@cim.mcgill.ca](mailto:angeles@cim.mcgill.ca)

# Contents

<b>1</b>	<b>Introduction to Kinematic Synthesis</b>	<b>5</b>
1.1	The Role of Kinematic Synthesis in Mechanical Design . . . . .	5
1.2	Glossary . . . . .	9
1.3	Kinematic Analysis vs. Kinematic Synthesis . . . . .	12
1.3.1	A Summary of Systems of Algebraic Equations . . . . .	14
1.4	Algebraic and Computational Tools . . . . .	15
1.4.1	The Two-Dimensional Representation of the Cross Product . . . . .	15
1.4.2	Algebra of $2 \times 2$ Matrices . . . . .	17
1.4.3	Algebra of $3 \times 3$ Matrices . . . . .	18
1.4.4	Linear-Equation Solving: Determined Systems . . . . .	18
1.4.5	Linear-Equation Solving: Overdetermined Systems . . . . .	22
1.5	Nonlinear-equation Solving: the Determined Case . . . . .	32
1.5.1	The Newton-Raphson Method . . . . .	34
1.6	Overdetermined Nonlinear Systems of Equations . . . . .	35
1.6.1	The Newton-Gauss Method . . . . .	35
1.7	Software Tools . . . . .	38
1.7.1	ODA: Matlab and C code for Optimum Design . . . . .	38
1.7.2	Packages Relevant to Linkage Synthesis . . . . .	40
<b>2</b>	<b>The Qualitative Synthesis of Kinematic Chains</b>	<b>45</b>
2.1	Notation . . . . .	45
2.2	Background . . . . .	46
2.3	Kinematic Pairs . . . . .	51
2.4	Graph Representation of Kinematic Chains . . . . .	54
2.5	Groups of Displacements . . . . .	56
2.5.1	Displacement Subgroups . . . . .	60
2.6	Kinematic Bonds . . . . .	64
2.7	The Chebyshev-Grübler-Kutzbach-Hervé Formula . . . . .	66
2.7.1	Trivial Chains . . . . .	67

2.7.2	Exceptional Chains . . . . .	71
2.7.3	Paradoxical Chains . . . . .	74
2.8	Applications to Robotics . . . . .	74
2.8.1	The Synthesis of Robotic Architectures and Their Drives . . . . .	74
<b>3</b>	<b>Function Generation</b>	<b>79</b>
3.1	Introduction . . . . .	79
3.2	Input-Output Functions . . . . .	80
3.2.1	Planar Four-Bar Linkages . . . . .	80
3.2.2	The Denavit-Hartenberg Notation . . . . .	83
3.2.3	Spherical Four-Bar-Linkages . . . . .	84
3.2.4	Spatial Four-Bar-Linkages . . . . .	89
3.3	Exact Synthesis . . . . .	93
3.3.1	Planar Linkages . . . . .	93
3.3.2	Spherical Linkages . . . . .	98
3.3.3	Spatial Linkages . . . . .	100
3.4	Analysis of the Synthesized Linkage . . . . .	101
3.4.1	Planar Linkages . . . . .	101
3.4.2	Spherical Four-Bar Linkages . . . . .	112
3.4.3	Spatial Four-Bar Linkages . . . . .	114
3.5	Approximate Synthesis . . . . .	121
3.5.1	The Approximate Synthesis of Planar Four-Bar Linkages . . . . .	124
3.5.2	The Approximate Synthesis of Spherical Linkages . . . . .	126
3.5.3	The Approximate Synthesis of Spatial Linkages . . . . .	127
3.6	Linkage Performance Evaluation . . . . .	131
3.6.1	Planar Linkages: Transmission Angle and Transmission Quality . . . . .	131
3.6.2	Spherical Linkages: Transmission Angle and Transmission Quality . . . . .	136
3.6.3	Spatial Linkages: Transmission Angle and Transmission Quality . . . . .	137
3.7	Design Error vs. Structural Error . . . . .	139
3.7.1	Minimizing the Structural Error . . . . .	142
3.8	Synthesis Under Mobility Constraints . . . . .	145
3.9	Synthesis of Complex Linkages . . . . .	146
3.9.1	Synthesis of Stephenson Linkages . . . . .	146
<b>4</b>	<b>Motion Generation</b>	<b>147</b>
4.1	Introduction . . . . .	147
4.2	Planar Four-bar Linkages . . . . .	147
4.2.1	Dyad Synthesis for Three Poses . . . . .	149
4.2.2	Dyad Synthesis for Four Poses . . . . .	149
4.2.3	Dyad Synthesis for Five Poses . . . . .	152

4.2.4	Case Study: Synthesis of a Landing Gear Mechanism . . . . .	153
4.2.5	The Presence of a P Joint in Dyad Synthesis . . . . .	159
4.2.6	Approximate Synthesis . . . . .	164
4.3	Spherical Four-bar Linkages . . . . .	169
4.3.1	Dyad Synthesis for Three Attitudes . . . . .	171
4.3.2	Dyad Synthesis for Four Attitudes . . . . .	172
4.3.3	Dyad Synthesis Five Attitudes . . . . .	173
4.3.4	Spherical Dyads with a P Joint . . . . .	174
4.3.5	Approximate Dyad Synthesis . . . . .	175
4.3.6	Examples . . . . .	181
4.4	Spatial Four-bar Linkages . . . . .	187
<b>5</b>	<b>Path Generation</b>	<b>189</b>
5.1	Introduction . . . . .	189
5.2	Planar Path Generation . . . . .	190
5.3	Planar Path Generation With Prescribed Timing . . . . .	192
5.4	Coupler Curves of Planar Four-Bar Linkages . . . . .	197
5.5	The Theorem of Roberts-Chebyshev . . . . .	201
<b>A</b>	<b>A Summary of Dual Algebra</b>	<b>203</b>
A.1	Introduction . . . . .	203
A.2	Definitions . . . . .	204
A.3	Fundamentals of Rigid-Body Kinematics . . . . .	208
A.3.1	Finite Displacements . . . . .	209
A.3.2	Velocity Analysis . . . . .	217
A.3.3	The Linear Invariants of the Dual Rotation Matrix . . . . .	219
A.3.4	The Dual Euler-Rodrigues Parameters of a Rigid-Body Motion . . . . .	224
A.4	The Dual Angular Velocity . . . . .	229
A.5	Conclusions . . . . .	235
<b>Bibliography</b>		<b>237</b>
<b>Index</b>		<b>247</b>



# Chapter 1

## Introduction to Kinematic Synthesis

### 1.1 The Role of Kinematic Synthesis in Mechanical Design

When designing a *mechanical system*, whether a *structure* or a *machine*, the first step is to produce a *conceptual design* that will meet the *design specifications*. Broadly speaking, the main *function* of a structure is *to be capable of withstanding the anticipated loads without exhibiting major deformations that would hamper the integrity of the structure or the safety of its occupants*. Likewise, the main function of a machine is *to be able to perform the intended task, usually involving finite displacements of its parts, without major deformations that would hamper the integrity of the machine or the safety of its users*.

To be true, mechanical systems exhibit, more often than not, features of both structures and mechanisms. Such examples occur in transportation machinery, such as landing gears in aircraft. Figure 1.1 illustrates the structure of the deployed landing gear of the *Airbus A300-600* aircraft. In this *posture*, the landing gear works as a structure, to withstand not only the static load of the airplane on the tarmac, but also the dynamic load exerted by the unavoidable impact upon landing.

Transportation machinery is a domain in which mechanisms, especially linkages—the focus of this course—plays a major role. Shown in Fig. 1.2 is a depiction of the powertrain of a Class-C Mercedes Benz. A key subsystem of the system in question—the powertrain—is the steering linkage, whose main components are visible in the figure. Again, this mechanism plays the dual role of a structure and a machine, as its function is not only to properly orient the planes of the front wheels upon turning, but also to support the wheels and the loads transmitted by the ground onto the vehicle frame.

In the above preamble we have introduced concepts of *engineering design* as pertaining to mechanical systems at large. Of these, we have focused on structures and machines. In fact, design, together with *manufacturing*, is the *raison d'être* of engineers, all disciplines



Figure 1.1: The landing gear of an *Airbus A300-600*

known as *engineering science*, namely, mechanics, thermofluids and numerics, to name but just the major branches, playing a supporting role in the production process. For this reason it is necessary to dwell on this concept. Because of its importance, the *engineering design process* has been the subject of study over the centuries, starting with Marcus Vitruvius Pollio (ca. 75 BCE–ca. 15 CE) and his 10-volume work under the title *De Architectura* (Vitruvius, 28 B.C.E.). Modern engineering design theory owes its origins, to a great extent, to Franz Reuleaux (1829–1905), who first proposed a *grammar* to describe the kinematic chain of a machine (Moon, 2003). A modern model of the design process, due to French (1992), is depicted in Fig. 1.3. In this model, four stages are distinguished: a) analysis of the problem; b) conceptual design; c) embodiment design; and d) detailing, or detailed design.

In the first stage, analysis of the problem, the *functions* required from the object under design, in our case, a machine, are clearly defined, in general, but precise terms. At this stage, the task of the design engineer is to produce a) design requirements, in terms as general as possible, in order to avoid biasing the design team towards a specific layout of the solution, and b) *design specifications*, so as to satisfy the rather vaguely spelled-out needs of the *client*.

In the second stage, the design team produces a set of *design variants*, as rich as

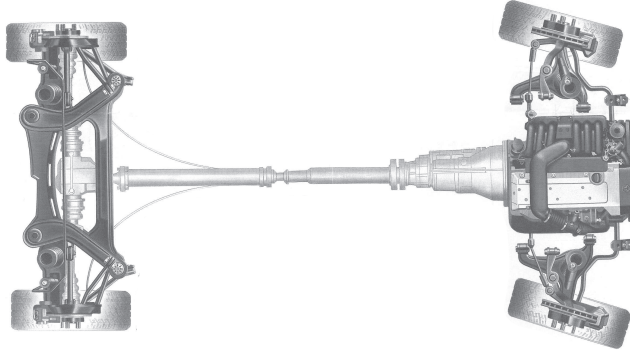


Figure 1.2: A view of the powertrain of a C-Class Mercedes Benz

possible, after several sessions, structured or unstructured, which are part of the *creative* aspect of the design process.

In the third stage, the design team focuses on a reduced set of design variants, those having the highest likelihood of succeeding in satisfying the client's demands within the resources—budget, milestones, technology—set at the disposal of the design team. In this stage, the task of the team is to produce a preliminary model of the design solution, with a clear identification of the main parameters defining a specific design variant. Further, a *parametric model* of each of the short-listed candidate variants is produced, which is then subject to optimization with the aim of finding the specific fundamental dimensions that either maximize a profit or minimize a cost of the design solution, or even do both at the same time, in a process that is known as *multiobjective optimization*. Design optimization is thus a key activity in the embodiment stage, which makes this stage *iterative*, as optimization requires several rounds of assignment of numerical values to the parameters of the mathematical model; evaluating the performance of the design solution thus resulting; improving this performance, when there is still room for improvement; and stopping when no more improvement is possible.

The final stage involves materials selection, manufacturing issues, and production-cost analysis. As a result of this stage, a set of manufacturing drawings is produced that is then sent out for prototype manufacturing, when the design job so requires, or directly to production.

*Kinematic synthesis* plays a key role in the first three stages of the foregoing design process, as pertaining to machine design. In fact, in the first stage, analysis of the problem, more than kinematic synthesis, what is required is *kinematics knowledge*, as design functions and specifications are to be understood by any engineer trained in the discipline. It is in the second and third stages where kinematic synthesis plays a fundamental role, as explained below.

As pertaining to machine design or, more specifically, to mechanism design, Hartenberg and Denavit (1964) proposed three phases of kinematic synthesis: a) *type synthesis*; b) *number synthesis*; and c) *dimensional synthesis*. Both type and number syntheses pertain

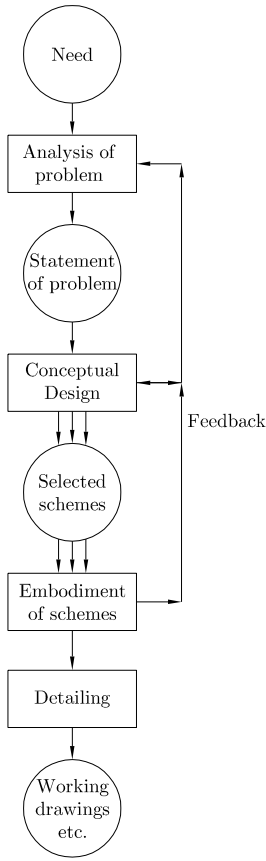


Figure 1.3: French’s model of the design process

to the *conceptual design* phase, as the former refers to choosing the type of mechanism to perform the required function, namely, a linkage, a cam-follower mechanism, a belt-pulley transmission, or a gear train, for example. Number synthesis refers to the numbers of links and joints in a linkage, along with the type of joints to be used—kinematic joints, or lower kinematic pairs, are studied in Ch. 2.

The conceptual phase of the design process is fundamental. Moreover, this phase is the one that has posed the major challenges to those attempting to automate the design process. In the realm of kinematic synthesis, we introduce a methodology, termed *qualitative synthesis*, in Ch. 2, in an attempt to provide a structure to the rather unstructured stage of conceptual mechanism design. Qualitative synthesis focuses on the synthesis of linkages.

Chapters 3–5 are devoted to what Hartenberg and Denavit call dimensional synthesis, as the main objective here is to find the dimensions defining the geometry of the various links and joints of the kinematic chain underlying the mechanism under design. In these chapters, we assume that a *preliminary layout* of the conceptual design—obtained as a result of the type and number syntheses of the kinematic chain at hand—is available, our main job being to contribute to the production of the embodiment of this design. The design embodiment is the realization of a kinematic chain as a table of what is known as

the *Denavit-Hartenberg parameters*—to be introduced in Ch. 3—that define uniquely the kinematic chain at hand.

Going back to the more general machine-design process, *dimensioning* involves two phases: functional dimensioning and mechanical dimensioning. The former is previous to the latter, and includes the determination of the *fundamental dimensions* of the machine, prior to the shaping of all its parts. It is the functional dimensioning where kinematic synthesis plays a major role. Mechanical dimensioning pertains to the dimensioning of the machine elements for stress, strength, heat capacity, and dynamic-response requirements.

Before we embark on the details of the course, a review of the glossary is in order.

## 1.2 Glossary

Some general definitions are first recalled:

- Kinematics: The branch of mechanics that studies motion, independent of its relation with forces.
- Statics: The branch of mechanics that studies the equilibrium of forces and moments acting on particles, rigid bodies, and flexible bodies.
- Kinematic constraint: The physical prevention of relative motion—rotation and translation—between two bodies in one or more directions. The term also denotes the algebraic or differential relations representing the physical constraint.
- Kinetostatics: The branch of mechanics that studies the interplay of forces and moments with motion variables under static, conservative conditions.

The concepts of *machine* and *mechanism* are frequently interchanged as if they were equivalent, but they are not. We give below some definitions from various sources, with added comments:

### Machine

- Here is an account of the definitions of machine, taken from (Dudiță et al., 1987).

Different definitions of machine have been given by scholars for more than two millennia, starting with Vitruvius in 28 BCE, namely,

- *A machine is a combination (system, assemblage) of moving material bodies* (Vitruvius, 28 B.C.E.; Hachette, 1811; Borgnis, 1818; Beck, 1859; Reuleaux, 1875; Koenigs, 1901).
- *A machine is generally composed of three parts: a motor part, a transmission part, and an execution part* (Euler, 1753; Bogolyubov, 1976).

- *A machine produces mechanical work, or performs productive operations, actions, or effects* (Vitruvius, 28 B.C.; Poncelet, 1824; Reuleaux, 1900; Koenigs, 1901; Bogolyubov, 1976).
  - *A machine transforms or transmits forces* (Vitruvius, 28 B.C.; Leupold, 1724; Euler, 1753; Bogolyubov, 1976; Reuleaux, 1900; Koenigs, 1901).
  - *A machine is characterized by deterministic motions* (Hachette, 1811; Leupold, 1724; Reuleaux, 1875; Borgnis, 1818; Reuleaux, 1900).
  - *A machine is an artifact* (Leupold, 1724).
- Some dictionary definitions:
    - *Webster's Collegiate Dictionary* (2003, on-line):
 

(archaic): a constructed thing whether material or immaterial; an assemblage of parts that transmit forces, motion, and energy one to another in a predetermined manner; an instrument (as a lever) designed to transmit or modify the application of power, force, or motion; a mechanically, electrically, or electronically operated device for performing a task (a calculating machine, a card-sorting machine.)

Comment: *comprehensive definitions when considered as a whole*
    - *The Concise Oxford Dictionary* (1995):
 

An *apparatus* for applying mechanical power, having several parts, each with a definite function

Comment: *leaves computers out*
    - *The Random House College Dictionary* (1979):
 

An *apparatus* consisting of interrelated parts with separate functions, used in the performance of some kind of work.

Comment: *ditto*
    - Le Petit Robert (Robert, 1994):
 

Any *system* in which a specific correspondence exists between an input form of energy or information and the corresponding ones at the output (loosely translated from French).

Comment: *a comprehensive definition, that includes computers*
  - *An apparatus* for transformation of power, materials, and information to substitute or simplify physical or intellectual work (Frolov, 1987).
- Comment: *a comprehensive definition, that includes computers*

- *Mechanical system* that performs a specific task, such as the forming of material, and the transference and transformation of *motion* and *force* (IFToMM PC SoT, 2003).

*Comment: leaves computers out*

## Mechanism

- A piece of machinery (Merriam Webster's Collegiate Dictionary, 2003, on-line).

*Comment: too vague*

- Definitions in (IFToMM PC SoT, 2003):

- *System* of bodies designed to convert *motions* of, and *forces* on, one or several bodies into constrained motions of, and *forces* on, other bodies.

*Comment: Could be much terser and more informative*

- *Kinematic chain* with one of its components (*link* or *joint*) connected to the *frame*.

*Comment: confuses mechanism with its kinematic chain*

- Structure, adaptation of parts of machine; system of mutually adapted parts working together (as) in machine (The Concise Oxford Dictionary, 1995).
- An assembly of moving parts performing a complete functional motion (Stein, 1979).
- A combination layout of pieces or elements, assembled with the goal of (producing) an operation as a unit (Loosely translated from (Robert, 1994)).

*Comment: In all above definitions, the concept of goal or task is present*

## Linkage

- Definitions in Merriam Webster's Collegiate Dictionary (2003, on-line):

- A system of links.

*Comment: concise and comprehensive*

- a system of links or bars which are jointed together and more or less constrained by having a link or links fixed and by means of which straight or nearly straight lines or other point paths may be traced.

*Comment: unnecessarily cumbersome and limited to path-generating linkages*

- *Kinematic chain* whose *joints* are equivalent to *lower pairs* only (IFToMM PC on SoT, 2003).

*Comment: confuses linkage with its kinematic chain*

## Rigid Body

A continuum whose points remain equidistant under any possible motion.

## Rigid-body Pose

The position of one landmark point of the body and the orientation of a coordinate frame fixed to the body with respect to a reference frame.

## Rigid-body Twist

The velocity of one landmark point of the body and the angular velocity of the body.

## Mechanical-System Posture

The set of link poses allowed by the kinematic constraints imposed by the various kinematic pairs. The concept also applies to humans and other living organisms.

## Mechanical-System Gesture

The set of link twists allowed by the kinematic constraints imposed by the kinematic pairs. The concept also applies to humans—e.g., the *surgical gesture*—and other living organisms.

## 1.3 Kinematic Analysis vs. Kinematic Synthesis

The fundamental problems in mechanism kinematics can be broadly classified into:

- (a) **Analysis:** Given a linkage, find the motion of its links, for a prescribed motion of its input joint(s).
- (b) **Synthesis:** Given a *task* to be produced by a linkage, find the linkage that *best* performs the task.

The task at hand can be one of three, in this context:

- (a) **Function generation:** the motion of the output joint(s) is prescribed as a function of the motion variable(s) of the input joint(s);
- (b) **Motion generation** (a.k.a. rigid-body guidance): the motion of the output link(s) is prescribed in terms of the motion variable(s) of the input link(s) or joint(s);
- (c) **Path generation:** the path traced by a point on a *floating link*—a link not anchored to the mechanism frame—is prescribed as a curve, possibly timed with the motion of the input joint(s).

Kinematic synthesis being a quite broad concept, it involves various aspects (Hartenberg and Denavit, 1964):

- *Type synthesis:* Given a task to be produced by a mechanism, find the type that will best perform it, e.g., a linkage, a cam mechanism, a gear train, or a combination thereof.

- *Number synthesis*: Given a task to be produced by a mechanism of a given type, find the number of links and joints that will best execute the task.
- *Dimensional synthesis*: Given a task to be produced by a mechanism, find its relevant geometric parameters.

In our case, we treat both type and number synthesis under one single umbrella, *qualitative synthesis*; for consistency, dimensional synthesis will be termed *quantitative synthesis*. There are, moreover, two types of dimensional synthesis:

1. **Exact synthesis**: Number of linkage parameters available is sufficient to produce *exactly* the prescribed motion. Problem leads to—linear or, most frequently, nonlinear—equation solving .
2. **Approximate synthesis**: Number of linkage parameters available is **not** sufficient to produce exactly the prescribed motion. Optimum dimensions are sought that *approximate* the prescribed motion with the *minimum* error. Problem leads to mathematical programming (optimization)

Furthermore, quantitative synthesis can be achieved, with a variable degree of success, via one of three types of methods:

- Graphical: Under this type, the geometric relations of the task at hand are manipulated *directly* as such. In the pre-comouter era this was done by means of drafting instruments alone. Nowadays, the drafting instruments have been replaced by CAD software. Although this tool has expanded significantly the capabilities of geometric methods, these are still limited to the *primitives* in the menu of CAD software packages.
- Algebraic: In these methods, the geometric relations in question are manipulated by algebraic means of computer-algebra software, to produce the desired linkage parameters as the solutions to the underlying *synthesis equations*. It is noteworthy that, by virtue of the Theorems of Kempe (1870) and Koenigs (1897), the geometric relations of any linkage containing any combination of five of the six lower kinematic pairs<sup>1</sup>, the screw pair excluded, lead to systems of multivariate polynomial equations. This is excellent news because most of the computer-algebra software available caters to systems of multivariate polynomial equations.
- Semigraphical: Purely algebraic methods entail some drawbacks, like *algebraic singularities*, which are conditions under which some solutions cannot be found for reasons other than kinematic. Semigraphical methods reduce the system of alge-

---

<sup>1</sup>To be introduced in Ch. 2.

braic equations to a subsystem of *bivariate equations*, i.e., equations involving only two variables. The bivariate equations defining a set of contours in the plane of those two variables, the *real* solutions to the problem at hand are found as the intersections of all those contours.

**Caveat:** Sometimes algebraic methods are billed as “analytic methods,” which is to be avoided. Reason: according to common usage—see, for example, the *The Random House College Dictionary*—“analytic” is anything “pertaining to or proceeding by analysis (opposed to synthetic)”. Careless usage of the qualifier leads to awkward phrases like “analytic synthesis.”

### 1.3.1 A Summary of Systems of Algebraic Equations

The relevance of systems of algebraic equations is to be highlighted. The synthesis of linkages, as pointed out above, *usually* leads to *algebraic* systems of equations. Non-algebraic equations are termed *transcendental*. We expand first on the former.

Systems of algebraic equations are sets of *multivariate polynomial equations*. That is, each equation, written in homogeneous form  $P_k(\mathbf{x}) = 0$ ,  $k = 1, \dots, n$ , where we have assumed that the system has as many equations as unknowns, is a linear combination of products of *integer powers* of its  $n$  unknown variables, e.g.,  $x_1^{p_1}x_2^{p_2} \cdots x_n^{p_n}$ .

The sum of the exponents of each product,  $\sum_1^n p_j$ , is known as the *degree* of the product; the highest product-degree of the system of the  $i$ th equation is termed the *degree*  $d_i$  of the same equation. Using a suitable elimination procedure, it is conceptually possible, although not really possible all the time, to reduce the system of  $n$  equations in  $n$  unknowns to one single *monovariate polynomial equation*. According to a result due to Bezout (Salmon, 1964), the degree of the resulting monovariate polynomial, the *resolvent* or *eliminant* of the algebraic system at hand, cannot be greater than the product  $P = d_1 d_2 \cdots d_n$ . The number of possible solutions, thus, can be as high as  $P$ .

While some simple kinematic synthesis problems lead to either linear or quadratic equations, some not so complicated problems can lead to polynomials of a degree of the order of 10, which in this case means that the degree of the system can be as high as  $10^n$ —the case in which all equations of the system are of the 10th degree. For example, the synthesis of a six-bar *function generator*—see Ch. 3—for eight accuracy points that approximates a parabolic function led to a resolvent polynomial of degree 64,858 (Plecnik and McCarthy, 2013). Some synthesis problems of planar four-bar linkages lead to resolvent polynomials of a degree lying in the billions! (Chen and Angeles, 2008). Because of the above reasons, we stress in this course semigraphical methods of kinematic synthesis.

One major difference between algebraic and transcendental systems of equations is recalled: an algebraic system admits a finite—predictably bounded by the system Bezout number—number of roots (solutions); systems of transcendental equations can admit

infinitely many. Examples of the latter occur in the characteristic equation of continuous bodies, e.g., a taut string with its ends fixed to an inertial frame. The roots of the characteristic equation, which involves trigonometric functions associated with a variable  $\lambda$  that has units of length-inverse, determine the infinitely many vibration modes of the string, one mode per root.

## 1.4 Algebraic and Computational Tools

In deriving the kinematic relations that lead to the various synthesis equations, we shall resort to the two-dimensional representation of the cross product. To do this, we introduce below a  $2 \times 2$  orthogonal matrix  $\mathbf{E}$  that will prove to be extremely useful. An alternative to the use of this matrix for the same purpose is the use of *complex numbers*. The problem with complex numbers is that they are quite useful to represent two-dimensional vectors, their application to three and higher dimensions being still unknown. On the contrary, the two-dimensional representation of the cross product is just a particular case of three-dimensional vector algebra.

We will also need some quick computations with  $2 \times 2$  matrices, which will be revised in this section. Methods for the numerical solution of linear systems of equations are also included.

### 1.4.1 The Two-Dimensional Representation of the Cross Product

The cross product occurs frequently in planar kinematics and statics, and hence, in planar *kinetostatics*. However, planar problems involve only two-dimensional vectors and  $2 \times 2$  matrices, while the cross product is limited to three-dimensional spaces. Here we describe how to represent in two dimensions the cross product, without resorting to three-dimensional vectors. Let:  $\mathbf{r}$  be the position vector of a point of a rigid body under planar motion;  $\boldsymbol{\omega}$  be the angular-velocity vector of the rigid body and assumed normal to the plane of motion.

Without loss of generality, assume that  $\mathbf{r}$  lies entirely in the plane of motion, which is normal to  $\boldsymbol{\omega}$ . Below we compute  $\boldsymbol{\omega} \times \mathbf{r}$  using only two-dimensional vectors.

Let  $\mathbf{E}$  be an *orthogonal matrix* that rotates vectors in the plane through an angle of  $90^\circ$  counterclockwise (ccw):

$$\mathbf{E} \equiv \begin{bmatrix} 0 & -1 \\ 1 & 0 \end{bmatrix} \quad (1.1a)$$

Note that

$$\mathbf{E}^T \mathbf{E} = \mathbf{E} \mathbf{E}^T = \mathbf{1}, \quad \mathbf{1} = \begin{bmatrix} 1 & 0 \\ 0 & 1 \end{bmatrix} \quad (1.1b)$$

with  $\mathbf{1}$  denoting the  $2 \times 2$  *identity matrix*. Also note that  $\mathbf{E}$  is *skew-symmetric*:

$$\mathbf{E} = -\mathbf{E}^T \quad \Rightarrow \quad \mathbf{E}^2 = -\mathbf{1}, \quad \mathbf{E}^{-1} = -\mathbf{E} \quad (1.1c)$$

Therefore,  $\mathbf{E}$  rotates vectors  $\mathbf{r}$  in the plane through an angle of  $90^\circ$  ccw, as depicted in Fig. 1.4, i.e.,

$$\mathbf{r} = \begin{bmatrix} x \\ y \end{bmatrix} \quad \Rightarrow \quad \mathbf{E}\mathbf{r} = \begin{bmatrix} -y \\ x \end{bmatrix} \quad (1.1d)$$

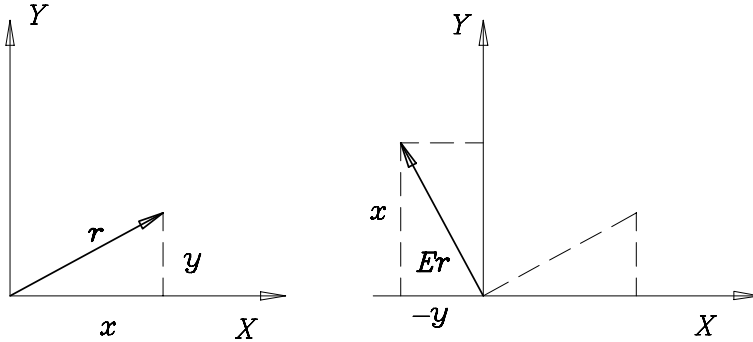


Figure 1.4: Vector  $\mathbf{r}$  and its image under  $\mathbf{E}$

Now, for the purpose at hand, we start with the usual three-dimensional vectors  $\mathbf{r}$  and  $\boldsymbol{\omega}$  and assume an *orthonormal basis* for the three-dimensional space,  $\{\mathbf{i}, \mathbf{j}, \mathbf{k}\}$ , with  $\mathbf{k}$  defined normal to the plane of motion and pointing toward the viewer. Thus,

$$\boldsymbol{\omega} = \omega \mathbf{k} = \begin{bmatrix} 0 \\ 0 \\ \omega \end{bmatrix}, \quad \mathbf{r} = \begin{bmatrix} x \\ y \\ 0 \end{bmatrix} \quad (1.2)$$

where  $\omega > 0$  if the angular velocity is ccw; if cw, then  $\omega < 0$ . Therefore,

$$\boldsymbol{\omega} \times \mathbf{r} = \det \begin{bmatrix} \mathbf{i} & \mathbf{j} & \mathbf{k} \\ 0 & 0 & \omega \\ x & y & 0 \end{bmatrix} = -\omega y \mathbf{i} + \omega x \mathbf{j}$$

Then, the two-dimensional form of the foregoing product is

$$[\boldsymbol{\omega} \times \mathbf{r}]_{2D} = \omega \begin{bmatrix} -y \\ x \end{bmatrix} \equiv \omega \mathbf{E}\mathbf{r} \quad (1.3)$$

As a second use of matrix  $\mathbf{E}$ , we derive the two-dimensional form of the cross product  $\mathbf{r} \times \mathbf{f}$  yielding the moment of force  $\mathbf{f}$  about the origin. We assume that  $\mathbf{r}$  and  $\mathbf{f}$  both lie in a plane normal to the unit vector  $\mathbf{k}$ .

First, we start with the usual three-dimensional representation of vectors  $\mathbf{r}$  and  $\mathbf{f}$ , and hence,

$$\mathbf{r} \times \mathbf{f} = \det \begin{bmatrix} \mathbf{i} & \mathbf{j} & \mathbf{k} \\ x & y & 0 \\ f_x & f_y & 0 \end{bmatrix} = (xf_y - yf_x)\mathbf{k}$$

Now, let

$$xf_y - yf_x \equiv n \quad (1.4)$$

which can be readily recognized as the dot product of the two-dimensional vectors  $\mathbf{Er}$  and  $\mathbf{f}$ , i.e.,

$$n = \mathbf{f}^T \mathbf{Er} \equiv (\mathbf{Er})^T \mathbf{f} = -\mathbf{r}^T \mathbf{Ef} \quad (1.5)$$

If  $n > 0$ , then the moment is ccw; otherwise, cw. We have thus shown that the cross product of two two-dimensional vectors reduces to a scalar, i.e.,  $n$ .

Matrix  $\mathbf{E}$  also appears in the representation of the rotation of a rigid body in planar motion through an angle  $\theta$ . This rotation is represented algebraically by means of a *proper orthogonal matrix*  $\mathbf{Q}$ . This matrix is proper orthogonal because it is orthogonal and its determinant is +1. Matrix  $\mathbf{Q}$  is given by

$$\mathbf{Q} = \begin{bmatrix} \cos \theta & -\sin \theta \\ \sin \theta & \cos \theta \end{bmatrix} \equiv (\cos \theta) \mathbf{1} + (\sin \theta) \mathbf{E} \quad (1.6)$$

Thus, if a vector  $\mathbf{r}_0$  is “fixed” to a rigid body rotating about the origin through an angle  $\theta$ , after the rotation,  $\mathbf{r}_0$  becomes  $\mathbf{r}$ , which is given by

$$\mathbf{r} = \mathbf{Q}\mathbf{r}_0 = (\cos \theta)\mathbf{r}_0 + (\sin \theta)\mathbf{Er}_0 \quad (1.7)$$

### 1.4.2 Algebra of $2 \times 2$ Matrices

A  $2 \times 2$  matrix  $\mathbf{A}$  can be partitioned either columnwise or rowwise:

$$\mathbf{A} \equiv [\mathbf{a} \ \mathbf{b}] \equiv \begin{bmatrix} \mathbf{c}^T \\ \mathbf{d}^T \end{bmatrix}$$

where  $\mathbf{a}$ ,  $\mathbf{b}$ ,  $\mathbf{c}$ , and  $\mathbf{d}$  are all two-dimensional column vectors. We have

#### Fact 1.4.1

$$\det(\mathbf{A}) = -\mathbf{a}^T \mathbf{Eb} = \mathbf{b}^T \mathbf{Ea} = -\mathbf{c}^T \mathbf{Ed} = \mathbf{d}^T \mathbf{Ec}$$

and

#### Fact 1.4.2

$$\mathbf{A}^{-1} = \frac{1}{\det(\mathbf{A})} \begin{bmatrix} \mathbf{b}^T \\ -\mathbf{a}^T \end{bmatrix} \mathbf{E} = \frac{1}{\det(\mathbf{A})} \mathbf{E} [-\mathbf{d} \ \mathbf{c}] \quad (1.8)$$

Componentwise, if  $a_{ij}$  denotes the  $i$ th entry of the  $j$ th column of  $\mathbf{A}$ ,

$$\mathbf{A}^{-1} = \frac{1}{\det(\mathbf{A})} \begin{bmatrix} a_{22} & -a_{12} \\ -a_{21} & a_{11} \end{bmatrix}$$

That is, the inverse of a  $2 \times 2$  nonsingular matrix is obtained upon:

- (a) exchanging the diagonal entries of the given matrix;
- (b) reversing the sign of its off-diagonal entries; and
- (c) dividing the matrix thus resulting by the determinant of the given matrix.

Notice that the two  $2 \times 2$  matrix factors multiplying the reciprocal of  $\det(\mathbf{A})$  in eq. (1.8) are both, in fact, nothing but  $\text{Adj}(\mathbf{A})$ , the adjoint of  $\mathbf{A}$ .

### 1.4.3 Algebra of $3 \times 3$ Matrices

A  $3 \times 3$  matrix  $\mathbf{A}$  can be partitioned columnwise into three columns, each having as entries the components of a three-dimensional vector, namely,

$$\mathbf{A} = [\mathbf{a}_1 \quad \mathbf{a}_2 \quad \mathbf{a}_3]$$

its determinant being readily computed as the *mixed* vector-scalar product of its column vectors:

$$\det(\mathbf{A}) = \mathbf{a}_1 \times \mathbf{a}_2 \cdot \mathbf{a}_3$$

The inverse of  $\mathbf{A}$  can also be readily computed symbolically if we resort to the concept of *reciprocal bases*:

$$\mathbf{A}^{-1} = \frac{1}{\Delta} \begin{bmatrix} (\mathbf{a}_2 \times \mathbf{a}_3)^T \\ (\mathbf{a}_3 \times \mathbf{a}_1)^T \\ (\mathbf{a}_1 \times \mathbf{a}_2)^T \end{bmatrix} \quad (1.9a)$$

where

$$\Delta \equiv \mathbf{a}_1 \times \mathbf{a}_2 \cdot \mathbf{a}_3 \quad (1.9b)$$

The reader can verify the validity of the foregoing formula by straightforward computation of the product  $\mathbf{A}\mathbf{A}^{-1}$  or, equivalently, of  $\mathbf{A}^{-1}\mathbf{A}$ , which should yield the  $3 \times 3$  identity matrix.

### 1.4.4 Linear-Equation Solving: Determined Systems

Consider solving for  $\mathbf{x}$  the system below:

$$\mathbf{Ax} = \mathbf{b} \quad (1.10)$$

where  $\mathbf{A}$  is a  $n \times n$  matrix of *known* coefficients;  $\mathbf{b}$  is the  $n$ -dimensional right-hand side *known* vector; and  $\mathbf{x}$  is the  $n$ -dimensional vector of *unknowns*.

**Definition:**  $\mathbf{A}$  is said to be *singular* if

$$\det(\mathbf{A}) = 0 \quad (1.11)$$

Otherwise,  $\mathbf{A}$  is *nonsingular*

**Fact 1.4.3** If  $\mathbf{A}$  is nonsingular, then eq.(1.10) has a unique solution, namely,

$$\mathbf{x} = \mathbf{A}^{-1}\mathbf{b} \quad (1.12)$$

**Caveat:** Never compute—unless instructed to do so!— $\mathbf{A}^{-1}$  explicitly. A matrix inverse is seldom needed and incurs a waste of precious CPU time! Instead, find a *good* numerical approximation to the solution, while taking into account that  $\mathbf{A}$  and  $\mathbf{b}$  are usually known only up to a certain roundoff error.

In computing the solution of system (1.10) for  $\mathbf{x}$ , we must take into account the unavoidable roundoff error of the data,  $\mathbf{A}$  and  $\mathbf{b}$ . Let:

- $\delta\mathbf{A}$  be the matrix roundoff error in  $\mathbf{A}$
- $\delta\mathbf{b}$  be the vector roundoff-error in  $\mathbf{b}$
- $\delta\mathbf{x}$  be the vector roundoff-error incurred when solving eq.(1.10) for  $\mathbf{x}$ , by virtue of  $\delta\mathbf{A}$  and  $\delta\mathbf{b}$

The *relative* roundoff errors in the data,  $\epsilon_{\mathbf{A}}$  and  $\epsilon_{\mathbf{b}}$ , and in the computed solution,  $\epsilon_{\mathbf{x}}$ , are defined as

$$\epsilon_{\mathbf{x}} \equiv \frac{\|\delta\mathbf{x}\|}{\|\mathbf{x}\|}, \quad \epsilon_{\mathbf{A}} \equiv \frac{\|\delta\mathbf{A}\|}{\|\mathbf{A}\|}, \quad \epsilon_{\mathbf{b}} \equiv \frac{\|\delta\mathbf{b}\|}{\|\mathbf{b}\|} \quad (1.13)$$

where  $\|\cdot\|$  denotes *any* vector or matrix norm<sup>2</sup>.

The relative roundoff error in the computed solution is known to be related to the relative roundoff error in the data via the relation (Golub and Van Loan, 1983)

$$\epsilon_{\mathbf{x}} \leq \kappa(\mathbf{A})(\epsilon_{\mathbf{A}} + \epsilon_{\mathbf{b}}) \quad (1.14)$$

where  $\kappa(\mathbf{A})$  is the *condition number* of matrix  $\mathbf{A}$  of eq.(1.10):

$$\kappa(\mathbf{A}) \equiv \|\mathbf{A}\| \|\mathbf{A}^{-1}\| \quad (1.15)$$

Various matrix norms are at our disposal, such as the *Euclidean norm*, a.k.a. the *2-norm*, the *Frobenius norm* and the *infinity norm*, a.k.a. the *Chebyshev norm*, denoted, respectively, by  $\|\mathbf{A}\|_2$ ,  $\|\mathbf{A}\|_F$  and  $\|\mathbf{A}\|_\infty$ . The definitions of these norms are given below:

$$\|\mathbf{A}\|_2 \equiv \max_i \{ \sqrt{\lambda_i} \}_1^n \quad (1.16a)$$

$$\|\mathbf{A}\|_F \equiv \sqrt{\text{tr}(\mathbf{A}^T \mathbf{A})} \quad (1.16b)$$

$$\|\mathbf{A}\|_\infty \equiv \max_j \{ \max_i |a_{ij}| \}_{i,j=1}^n \quad (1.16c)$$

---

<sup>2</sup>The matrix norm is a generalization of the vector norm, the latter being, in turn, a generalization of the module of complex numbers or the absolute value of real numbers.

where  $\{\lambda_i\}_1^n$  denotes the set of eigenvalues of  $\mathbf{A}\mathbf{A}^T$ , and  $\mathbf{W}$  is a *weighting* positive-definite matrix, that is defined according to the user's needs. For example, if  $\mathbf{W} = (1/n)\mathbf{1}$ , with  $\mathbf{1}$  defined as the  $n \times n$  identity matrix, then the Frobenius norm of the identity matrix is unity, regardless of the value of  $n$ , which is convenient. Not only this; with the foregoing value of  $\mathbf{W}$ ,  $\|\mathbf{A}\|_F$  is the rms value of the *singular values*<sup>3</sup> of  $\mathbf{A}$ . Moreover,  $\text{tr}(\cdot)$  denotes the *trace* of its  $n \times n$  matrix argument  $(\cdot)$ , i.e., the sum of the diagonal entries of the matrix. Also notice that the eigenvalues of  $\mathbf{A}$  can be real or complex,  $|\lambda_i|$  denoting the *module* of  $\lambda_i$ . Computing the eigenvalues of arbitrary matrices is cumbersome because of the complex nature of the eigenvalues, in general. Computing the eigenvalues of symmetric matrices, on the contrary, is much simpler, because these are known to be real. In fact, the set  $\{\lambda_i\}_1^n$  is most conveniently computed as the eigenvalues of  $\mathbf{A}\mathbf{A}^T$ , which is not only symmetric, but also positive-definite, and hence, its eigenvalues are all positive. In fact, if  $\mathbf{A}$  is singular, then  $\mathbf{A}\mathbf{A}^T$  is only positive-semidefinite, meaning that some of its eigenvalues vanish, but none is negative. We thus have

$$\lambda_i \geq 0, \quad i = 1, \dots, n \quad (1.17)$$

Whenever we have chosen one specific norm to define the condition number, we indicate the condition number as  $\kappa_2$ ,  $\kappa_F$  or  $\kappa_\infty$ . In particular,

$$\kappa_2 = \frac{\sqrt{\lambda_l}}{\sqrt{\lambda_s}} \quad (1.18)$$

where  $\lambda_l$  and  $\lambda_s$  denote the largest and the smallest eigenvalues of  $\mathbf{A}\mathbf{A}^T$ , respectively. In fact,  $\{\sqrt{\lambda_i}\}_1^n$  is known as the set of *singular values* of matrix  $\mathbf{A}$ . Moreover,

$$\kappa_F = \sqrt{\frac{1}{n} \text{tr}(\mathbf{A}\mathbf{A}^T)} \sqrt{\frac{1}{n} \text{tr}(\mathbf{A}^{-1}\mathbf{A}^{-T})} \quad (1.19)$$

where  $\mathbf{A}^{-T}$  denotes the inverse of the transpose of  $\mathbf{A}$  or, equivalently, the transpose of the inverse of the same matrix.

It is now apparent that  $\kappa$ , regardless of the matrix norm used to compute it, is bounded from below but unbounded from above:

$$1 \leq \kappa < \infty \quad (1.20)$$

**Remark 1.4.1** *The condition number of a singular matrix is infinitely large.*

**Remark 1.4.2** *If a matrix  $\mathbf{A}\mathbf{A}^T$  has all its eigenvalues identical, then  $\mathbf{A}$  is said to be isotropic. Isotropic matrices have a  $\kappa = 1$ , regardless of the matrix norm used to compute  $\kappa$ . Isotropic matrices are optimally conditioned.*

---

<sup>3</sup>The singular values of a  $m \times n$  matrix  $\mathbf{A}$ , with  $m \leq n$  are the (nonnegative) eigenvalues of the

Methods for computing a good numerical approximation to *the* solution (1.12):

- Gaussian elimination, a.k.a. LU-decomposition: Based on the observation that a *triangular system* is readily solved by either *backward* or *forward substitution*.  $\mathbf{A}$  is decomposed into a *lower-* and an *upper-triangular* factors,  $\mathbf{L}$  and  $\mathbf{U}$ , respectively.
- Iteratively: Various types of methods, by the names Gauss-Jordan, Gauss-Seidel, successive-overrelaxation (SOR), etc. Used mainly for “large” systems (hundreds or thousands of unknowns) that we will not be handling
- Symbolically: Only possible for certain classes of  $\mathbf{A}$  matrices, like tridiagonal, and for arbitrary matrices of modest size ( $n$  is below 5 or so)

We focus here on Gaussian elimination, or LU-decomposition. We start by *decomposing* the  $n \times n$  matrix  $\mathbf{A}$  in the form

$$\mathbf{A} = \mathbf{LU} \quad (1.21)$$

where  $\mathbf{L}$  and  $\mathbf{U}$  take the forms

$$\mathbf{L} = \begin{bmatrix} 1 & 0 & \cdots & 0 \\ l_{21} & 1 & \cdots & 0 \\ \vdots & \vdots & \ddots & \vdots \\ l_{n1} & l_{n2} & \cdots & 1 \end{bmatrix}, \quad \mathbf{U} = \begin{bmatrix} u_{11} & u_{12} & \cdots & u_{1n} \\ 0 & u_{22} & \cdots & u_{2n} \\ \vdots & \vdots & \ddots & \vdots \\ 0 & 0 & \cdots & u_{nn} \end{bmatrix} \quad (1.22)$$

Now eq.(1.10) is rewritten as

$$\mathbf{LUx} = \mathbf{b} \Rightarrow \begin{cases} \mathbf{Ly} = \mathbf{b} \\ \mathbf{Ux} = \mathbf{y} \end{cases} \quad (1.23)$$

and hence,  $\mathbf{x}$  is computed in two stages: First,  $\mathbf{y}$  is computed from a lower-triangular system; then,  $\mathbf{x}$  is computed from an upper-triangular system. The lower-triangular system is solved for  $\mathbf{y}$  by *forward substitution*; the upper-triangular system is solved for  $\mathbf{x}$  by *backward substitution*.

Note that

$$\det(\mathbf{A}) = \det(\mathbf{L})\det(\mathbf{U}) \quad (1.24a)$$

But, apparently,

$$\det(\mathbf{L}) = 1, \quad \det(\mathbf{U}) = \prod_1^n u_{ii} \quad (1.24b)$$

Hence,

$$\det(\mathbf{A}) = \det(\mathbf{U}) = \prod_1^n u_{ii} \quad (1.24c)$$

Therefore,  $\mathbf{A}$  is singular if any of the diagonal entries of  $\mathbf{U}$  vanishes.

product  $\mathbf{AA}^T$

## The Case of a Positive-Definite Matrix

A  $n \times n$  matrix  $\mathbf{A}$  is said to be *positive-definite* if (i) it is symmetric and (ii) all its eigenvalues are positive. Under these conditions, the quadratic form  $\mathbf{x}^T \mathbf{A} \mathbf{x} > 0$ , for any  $\mathbf{x} \in \mathbb{R}^n$ . If the same matrix verifies property (i) but verifies property (ii) in the alternative form (ii-alt) none of its eigenvalues is negative, then the matrix is said to be *positive-semidefinite* and the foregoing quadratic form becomes  $\mathbf{x}^T \mathbf{A} \mathbf{x} \geq 0$ .

If  $\mathbf{A}$  is at least *positive-definite*, then it admits the **Cholesky decomposition**:

$$\mathbf{A} = \mathbf{C}^T \mathbf{C} \quad (1.25a)$$

where  $\mathbf{C}$  is a *real, lower-triangular* matrix, namely,

$$\mathbf{C} = \begin{bmatrix} c_{11} & 0 & \cdots & 0 \\ c_{21} & c_{22} & \cdots & 0 \\ \vdots & \vdots & \ddots & \vdots \\ c_{n1} & c_{n2} & \cdots & c_{nn} \end{bmatrix} \quad (1.25b)$$

According to *Sylvester's Theorem*<sup>4</sup>,  $\mathbf{C}$  is invertible if  $\mathbf{A}$  is positive-definite; if positive-semidefinite,  $\mathbf{C}$  is singular, of the same rank as  $\mathbf{A}$ .

The solution of system (1.10) proceeds as in the general case, in two steps:

$$\mathbf{C}^T \mathbf{y} = \mathbf{b} \quad (1.26)$$

$$\mathbf{C} \mathbf{x} = \mathbf{y} \quad (1.27)$$

### 1.4.5 Linear-Equation Solving: Overdetermined Systems

We are now confronted with solving a system of linear equations formally identical to that given in eq.(1.10). The difference now is that matrix  $\mathbf{A}$  is no longer square, but rectangular, with  $n$  columns of dimension  $m$ , namely,

$$\mathbf{A} \mathbf{x} = \mathbf{b}, \quad \mathbf{A} : m \times n, \quad m > n \quad (1.28)$$

where  $\mathbf{b}$  is, obviously,  $m$ -dimensional. Now, given that we have a surplus of equations over the number of unknowns, it is not possible, in general, to find a vector  $\mathbf{x}$  that will verify all  $m$  equations, and hence, an error will be incurred, the purpose here being to find the vector  $\mathbf{x}$  that renders the error of minimum norm. That is, we cannot *actually solve* system (1.28); all we can do is find an acceptable approximation  $\mathbf{x}$  to the system. The *error vector*  $\mathbf{e}$  in this approximation is defined as

$$\mathbf{e} \equiv \mathbf{b} - \mathbf{A} \mathbf{x} \quad (1.29)$$

---

<sup>4</sup>See Theorem 1.4.3.

Again, we have various norms at our disposal that we can choose to minimize. All norms of  $\mathbf{e}$  can be expressed as

$$\|\mathbf{e}\|_p \equiv \left( \sum_1^m |e_k|^p \right)^{1/p} \quad (1.30)$$

with  $e_k$  being understood as the  $k$ th component of the  $m$ -dimensional vector  $\mathbf{e}$ . When  $p = 2$ , the foregoing norm is known as the *Euclidean norm*, which is used most frequently in mechanics. When  $p \rightarrow \infty$ , the *infinity norm*, also known as the *Chebyshev norm*, is obtained. This norm is, in fact, nothing but the largest absolute value of the components of the vector at hand; finding this norm, thus, incurs no computational cost. It turns out that upon seeking the value of  $\mathbf{x}$  that minimizes a norm of  $\mathbf{e}$ , the simplest is the Euclidean norm, for the minimization of its square leads to a linear system of equations whose solution can be obtained *directly*, as opposed to *iteratively*. Indeed, let us set up the minimization problem below:

$$z(\mathbf{x}) \equiv \frac{1}{2} \|\mathbf{e}\|_2^2 \quad \rightarrow \quad \min_{\mathbf{x}} \quad (1.31)$$

The *normality condition* of the minimization problem at hand is derived upon setting the gradient of  $z$  with respect to  $\mathbf{x}$  equal to zero, i.e.,

$$\frac{dz}{d\mathbf{x}} = \mathbf{0} \quad (1.32a)$$

which is *shorthand notation* for

$$\frac{dz}{dx_1} = 0, \quad \frac{dz}{dx_2} = 0, \quad \dots, \quad \frac{dz}{dx_n} = 0 \quad (1.32b)$$

However,  $z$  is not an explicit function of  $\mathbf{x}$ , but of  $\mathbf{e}$ , while  $\mathbf{e}$  is an explicit function of  $\mathbf{x}$ . Hence, in order to find  $dz/d\mathbf{x}$ , the “chain rule” has to be applied. As this is to be applied over vectors, an explanation is in order: first,  $d\mathbf{e}$  is derived upon a differential increment  $dx_i$  of the  $i$ th component of  $\mathbf{x}$ , for  $i = 1, 2, \dots, n$ :

$$d\mathbf{e} = \frac{d\mathbf{e}}{dx_1} dx_1 + \frac{d\mathbf{e}}{dx_2} dx_2 + \dots + \frac{d\mathbf{e}}{dx_n} dx_n$$

or, in array form,

$$d\mathbf{e} = \underbrace{\begin{bmatrix} \frac{d\mathbf{e}}{dx_1} & \frac{d\mathbf{e}}{dx_2} & \dots & \frac{d\mathbf{e}}{dx_n} \end{bmatrix}}_{\equiv \frac{d\mathbf{e}}{d\mathbf{x}}} \underbrace{\begin{bmatrix} dx_1 \\ dx_2 \\ \vdots \\ dx_n \end{bmatrix}}_{d\mathbf{x}}$$

where  $d\mathbf{e}/d\mathbf{x}$  is, apparently, a  $m \times n$  array, namely,

$$\frac{d\mathbf{e}}{d\mathbf{x}} = \begin{bmatrix} \frac{de_1}{dx_1} & \frac{de_1}{dx_2} & \dots & \frac{de_1}{dx_n} \\ \frac{de_2}{dx_1} & \frac{de_2}{dx_2} & \dots & \frac{de_2}{dx_n} \\ \vdots & \vdots & \ddots & \vdots \\ \frac{de_m}{dx_1} & \frac{de_m}{dx_2} & \dots & \frac{de_m}{dx_n} \end{bmatrix} \in \mathbb{R}^{m \times n} \quad (1.33)$$

On the other hand, upon application of the “chain rule” to  $z$  in terms of the components of  $\mathbf{e}$ ,

$$\frac{dz}{d\mathbf{x}} = \frac{de_1}{d\mathbf{x}} \frac{dz}{de_1} + \frac{de_2}{d\mathbf{x}} \frac{dz}{de_2} + \dots + \frac{de_m}{d\mathbf{x}} \frac{dz}{de_m}$$

or, in array form,

$$\frac{dz}{d\mathbf{x}} = \left[ \frac{de_1}{d\mathbf{x}} \quad \frac{de_2}{d\mathbf{x}} \quad \dots \quad \frac{de_m}{d\mathbf{x}} \right] \begin{bmatrix} \frac{dz}{de_1} \\ \frac{dz}{de_2} \\ \vdots \\ \frac{dz}{de_m} \end{bmatrix}$$

If the first factor in the foregoing product is expressed in component form, then

$$\frac{dz}{d\mathbf{x}} = \begin{bmatrix} \frac{de_1}{dx_1} & \frac{de_2}{dx_1} & \dots & \frac{de_m}{dx_1} \\ \frac{de_1}{dx_2} & \frac{de_2}{dx_2} & \dots & \frac{de_m}{dx_2} \\ \vdots & \vdots & \ddots & \vdots \\ \frac{de_1}{dx_n} & \frac{de_2}{dx_n} & \dots & \frac{de_m}{dx_n} \end{bmatrix} \begin{bmatrix} \frac{dz}{de_1} \\ \frac{dz}{de_2} \\ \vdots \\ \frac{dz}{de_m} \end{bmatrix} \quad (1.34)$$

whose first factor can be readily identified, in light of eq. (1.33), as  $(d\mathbf{e}/d\mathbf{x})^T$ , and hence,

$$\frac{dz}{d\mathbf{x}} = \left( \frac{d\mathbf{e}}{d\mathbf{x}} \right)^T \frac{dz}{d\mathbf{e}} \quad (1.35)$$

an expression that can be fairly termed the *chain rule* for vector arrays.

Now, from eq.(1.29),

$$\frac{d\mathbf{e}}{d\mathbf{x}} = -\mathbf{A} \quad (1.36)$$

Hence, the final expression for the gradient of  $z$ ,  $dz/d\mathbf{x}$ , is

$$\frac{dz}{d\mathbf{x}} = -\mathbf{A}^T \mathbf{e} \quad (1.37)$$

Therefore, the error vector of minimum Euclidean norm, or *least-square error* for brevity, represented henceforth by  $\mathbf{e}_0$ , satisfies the *normality condition*

$$\mathbf{A}^T \mathbf{e}_0 = \mathbf{0}_n \quad (1.38)$$

with  $\mathbf{0}_n$  denoting the  $n$ -dimensional zero vector. Now we have the first result:

**Theorem 1.4.1** *The least-square error  $\mathbf{e}_0$  of the overdetermined system of linear equations (1.10) lies in the null space of the transpose of the full-rank  $m \times n$  matrix  $\mathbf{A}$ , with  $m > n$ .*

In order to gain insight into the above result, let  $\{\mathbf{a}_i\}_1^n$  represent the  $n$   $m$ -dimensional columns of matrix  $\mathbf{A}$ . Hence,  $\mathbf{A}^T$  can be expressed as a column array of vectors  $\mathbf{a}_i^T$ , for  $i = 1, \dots, n$ , eq.(1.38) thus leading to

$$\mathbf{a}_i^T \mathbf{e}_0 = \mathbf{0}_n \quad (1.39)$$

Furthermore, if eq.(1.29) is substituted into eq.(1.37), and the product thus resulting is substituted, in turn, into the normality condition (1.32a), we obtain

$$\mathbf{A}^T \mathbf{A} \mathbf{x} = \mathbf{A}^T \mathbf{b} \quad (1.40)$$

which is known as the *normal equations* of the minimization problem at hand. By virtue of the assumption on the rank of  $\mathbf{A}$ , the product  $\mathbf{A}^T \mathbf{A}$  is *positive-definite* and hence, invertible. As a consequence, the value  $\mathbf{x}_0$  of  $\mathbf{x}$  that minimizes the Euclidean norm of the approximation error of the given system is

$$\mathbf{x}_0 = (\mathbf{A}^T \mathbf{A})^{-1} \mathbf{A}^T \mathbf{b} \quad (1.41)$$

the matrix coefficient of  $\mathbf{b}$  being known as a *generalized inverse* of  $\mathbf{A}$ ; we shall refer to this generalized inverse here as  $\mathbf{A}^I$ , i.e.,

$$\mathbf{A}^I \equiv (\mathbf{A}^T \mathbf{A})^{-1} \mathbf{A}^T \quad (1.42)$$

More specifically,  $\mathbf{A}^I$  is known as the *left Moore-Penrose generalized inverse* of  $\mathbf{A}$ , because, when  $\mathbf{A}$  is multiplied by  $\mathbf{A}^I$  from the left, the product becomes

$$\mathbf{A}^I \mathbf{A} = \mathbf{1}_n \quad (1.43)$$

in which  $\mathbf{1}_n$  denotes the  $n \times n$  identity matrix. The error obtained with this value is known as the *least-square error* of the approximation, i.e.,

$$\mathbf{e}_0 \equiv \mathbf{b} - \mathbf{A} \mathbf{x}_0 \quad (1.44)$$

Now we have one more result:

**Theorem 1.4.2 (Projection Theorem)** *The least-square error is orthogonal to  $\mathbf{A} \mathbf{x}_0$ , i.e.,*

$$\mathbf{e}_0^T \mathbf{A} \mathbf{x}_0 \equiv \mathbf{x}_0^T \mathbf{A}^T \mathbf{e}_0 = 0 \quad (1.45)$$

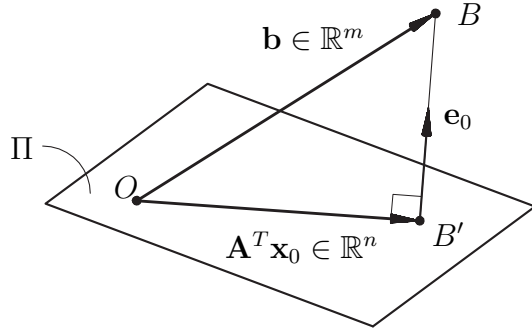


Figure 1.5: The Projection Theorem

*Proof:* Readily follows from eq.(1.38), and hence, from Theorem 1.4.1.

The Projection Theorem is illustrated in Fig. 1.5.

While the formula yielding the foregoing generalized inverse is quite simple to implement, the number of floating-point operations (flops) it takes to evaluate, along with the ever-present roundoff errors in both the data and the results, renders it not only *inefficient*, but also *unreliable*, if applied verbatim. What is at stake here is the concept of condition number, introduced in Subsection 1.4.4 for square matrices. The same concept can be applied to rectangular matrices, if the matrix inverse is replaced by its left Moore-Penrose generalized inverse. In fact, the singular values of rectangular  $\mathbf{A}$  are the non-negative square roots of the non-negative eigenvalues of the  $n \times n$  positive-semidefinite matrix  $\mathbf{A}^T \mathbf{A}$ , exactly as in the case of square matrices. If  $\mathbf{A}$  is of full rank, i.e., if its  $n$   $m$ -dimensional columns are linearly independent, then  $\mathbf{A}^T \mathbf{A}$  is positive-definite. However, note that  $\mathbf{A} \mathbf{A}^T$  is singular, regardless of whether  $\mathbf{A}$  is of full rank or not. The foregoing statement is a result of Sylvester's Theorem (Strang, 1988):

**Theorem 1.4.3 (Sylvester's Theorem)** *Let  $p \times q$   $\mathbf{A}$  and  $q \times r$   $\mathbf{B}$  be two arbitrary matrices, which are thus compatible under multiplication. Then,*

$$\text{rank}(\mathbf{AB}) \leq \min\{\text{rank}(\mathbf{A}), \text{rank}(\mathbf{B})\} \quad (1.46)$$

Therefore, if  $\mathbf{A}$  is of full rank, then  $\text{rank}(\mathbf{A}) = n$ , and hence,  $\text{rank}(\mathbf{AA}^T) = n < m$ , which means that the product  $\mathbf{AA}^T \in \mathbb{R}^{m \times m}$  is rank-deficient, i.e., singular in this case.

**Remark 1.4.3** *If the working condition number is either  $\kappa_2$  or  $\kappa_F$ , then the condition number of  $\mathbf{A}^T \mathbf{A}$  is exactly the square of the condition number of  $\mathbf{A}$ .*

As a consequence, then, even if  $\mathbf{A}$  is only slightly ill-conditioned, the product  $\mathbf{A}^T \mathbf{A}$  can be catastrophically ill-conditioned, the moral being that the normal equations (1.40) are much more sensitive to data roundoff error than the original equations (1.28). Therefore, **the normal equations should be avoided**. Below we outline two procedures to

calculate efficiently the least-square approximation of the overdetermined system (1.10) that do not resort to the normal equations, and hence, preserve the condition number of  $\mathbf{A}$  and do this with a low number of flops.

In figuring out a numerical method suitable to finding the *least-square approximation* of the overdetermined system of linear equations (1.28) it is convenient to resort to the geometric interpretation of the problem at hand: Let us assume that  $\mathbf{A}$  is of full rank, and hence, its  $n$   $m$ -dimensional columns  $\{\mathbf{a}_i\}_1^n$ , introduced in eq.(1.39), are linearly independent. However, notice that this set cannot constitute a basis of the  $m$ -dimensional space of these vectors, or of vector  $\mathbf{b}$  for that matter, because of a deficit of  $m - n$  vectors in the set. Hence, there is no guarantee that, given an arbitrary  $m$ -dimensional vector  $\mathbf{b}$ , we can find  $n$  real numbers  $\{x_k\}_1^n$  that will produce  $\mathbf{b}$  as a linear combination of the given set of vectors—the columns of  $\mathbf{A}$ . Now, let us regard  $\mathbf{b}$  as the position vector of a point  $B$  in  $m$ -dimensional space, with  $\mathbf{l}$  denoting the vector spanned by the linear combination

$$\mathbf{l} \equiv \mathbf{a}_1 x_1 + \mathbf{a}_2 x_2 + \cdots + \mathbf{a}_n x_n \quad (1.47)$$

We can also regard  $\mathbf{l}$  as the position vector of a point  $L$  in the same space, the purpose of the numerical method sought being to find the set  $\{x_i\}_1^n$  that yields a vector  $\mathbf{l}$  corresponding to a point  $L$  lying a minimum distance from  $B$ . If vector  $\mathbf{a}_i$  were represented in a basis in which only its first  $i$  components were nonzero, then  $\mathbf{A}$  would be upper-triangular, and the task at hand would be straightforward: it would be obvious then that we would be able to match the first  $n$  components of  $\mathbf{b}$  with a suitable choice of numbers  $\{x_i\}_1^n$ —these numbers could be found by backward substitution! However the last  $m - n$  components of  $\mathbf{b}$  would remain unmatched, and hence, would contain the error in the approximation.

Now, in general, the columns of  $\mathbf{A}$  most likely will be full. Nevertheless, it is always possible to find a suitable coordinate system, i.e., a suitable basis, under which the columns of  $\mathbf{A}$  will have the special structure described above.

In seeking the new coordinate system, we aim at a transformation of both all columns of  $\mathbf{A}$  and  $\mathbf{b}$  that will render  $\mathbf{A}$  in upper-triangular form, similar to the effect of the LU-decomposition applied to the solution of system (1.10). However, in seeking the suitable transformation in the case at hand, we should preserve the distances between points in  $m$ -dimensional space; else, the Euclidean norm will not be preserved and the approximation obtained will not yield the minimum distance between points  $B$  and  $L$ . A safe numerical procedure should thus preserve the Euclidean norm of the columns of  $\mathbf{A}$  and, hence, the inner product between any two columns of this matrix. Therefore, a triangularization procedure like LU-decomposition would not work, because this does not preserve inner products. Obviously, the transformations that do preserve these inner products are orthogonal, either rotations or reflections. Examples of these methods are (a) the Gram-Schmidt orthogonalization procedure and (b) *Householder reflections*, which

are outlined below<sup>5</sup>.

## The Gram-Schmidt Orthogonalization Procedure

This procedure consists in regarding the columns of  $\mathbf{A}$  as a set of  $n$   $m$ -dimensional vectors  $\{\mathbf{a}_k\}_1^n$ . From this set, a new set  $\{\mathbf{e}_k\}_1^n$  is obtained that is *orthonormal*. The first step consists in defining a *normal* vector—i.e., of *unit norm*— $\mathbf{e}_1$  as<sup>6</sup>

$$\mathbf{e}_1 = \frac{\mathbf{a}_1}{\|\mathbf{a}_1\|} \quad (1.48)$$

Further, we define  $\mathbf{e}_2$  as the *normal component* of  $\mathbf{a}_2$  onto  $\mathbf{e}_1$ , namely,

$$\mathbf{b}_2 \equiv (\mathbf{1} - \mathbf{e}_1 \mathbf{e}_1^T) \mathbf{a}_2 \quad (1.49a)$$

$$\mathbf{e}_2 \equiv \frac{\mathbf{b}_2}{\|\mathbf{b}_2\|} \quad (1.49b)$$

In the next step, we define  $\mathbf{e}_3$  as the unit vector normal to the plane defined by  $\mathbf{e}_1$  and  $\mathbf{e}_2$  and in the direction in which the inner product  $\mathbf{e}_3^T \mathbf{a}_3$  is positive, which is possible because all vectors of the set  $\{\mathbf{a}_k\}_1^m$  have been assumed to be linearly independent—remember that  $\mathbf{A}$  has been assumed to be of full rank. To this end, we subtract from  $\mathbf{a}_3$  its projection onto the plane mentioned above, i.e.,

$$\mathbf{b}_3 = (\mathbf{1} - \mathbf{e}_1 \mathbf{e}_1^T - \mathbf{e}_2 \mathbf{e}_2^T) \mathbf{a}_3 \quad (1.50a)$$

$$\mathbf{e}_3 \equiv \frac{\mathbf{b}_3}{\|\mathbf{b}_3\|} \quad (1.50b)$$

and so on, until we obtain  $\mathbf{e}_{n-1}$ , the last unit vector of the orthogonal set,  $\mathbf{e}_n$ , being obtained as

$$\mathbf{b}_n = (\mathbf{1} - \mathbf{e}_1 \mathbf{e}_1^T - \mathbf{e}_2 \mathbf{e}_2^T - \cdots - \mathbf{e}_{n-1} \mathbf{e}_{n-1}^T) \mathbf{a}_n \quad (1.51a)$$

Finally,

$$\mathbf{e}_n \equiv \frac{\mathbf{b}_n}{\|\mathbf{b}_n\|} \quad (1.51b)$$

In the next stage, we represent all vectors of the set  $\{\mathbf{a}_k\}_1^n$  in *orthogonal coordinates*, i.e., in the base  $\mathcal{O} = \{\mathbf{e}_k\}_1^n$ , which are then arranged in a  $m \times n$  array  $\mathbf{A}_o$ . By virtue of the form in which the set  $\{\mathbf{e}_k\}_1^n$  was defined, the last  $m - k$  components of vector  $\mathbf{a}_k$  vanish.

---

<sup>5</sup>These methods are implemented in Maple, a language for computer algebra, under the command `LeastSquares(A, B, ...)`.

<sup>6</sup>In the balance of this section only the Euclidian norm is used; for the sake of brevity, this norm is simply referred to as “the norm”.

We thus have, in the said orthonormal basis,

$$[\mathbf{a}_k]_{\mathcal{O}} = \begin{bmatrix} \alpha_{1k} \\ \alpha_{2k} \\ \vdots \\ \alpha_{kk} \\ 0 \\ \vdots \\ 0 \end{bmatrix}, \quad [\mathbf{b}]_{\mathcal{O}} = \begin{bmatrix} \beta_1 \\ \beta_2 \\ \vdots \\ \beta_m \end{bmatrix}$$

Therefore, eq.(1.28), when expressed in  $\mathcal{O}$ , becomes

$$\begin{bmatrix} \alpha_{11} & \alpha_{12} & \cdots & \alpha_{1n} \\ 0 & \alpha_{22} & \cdots & \alpha_{2n} \\ \vdots & \vdots & \ddots & \vdots \\ 0 & 0 & \cdots & \alpha_{nn} \\ 0 & 0 & \cdots & 0 \\ \vdots & \vdots & \ddots & \vdots \\ 0 & 0 & \cdots & 0 \end{bmatrix} \begin{bmatrix} x_1 \\ x_2 \\ \vdots \\ x_n \end{bmatrix} = \begin{bmatrix} \beta_1 \\ \beta_2 \\ \vdots \\ \beta_n \\ \beta_{n+1} \\ \vdots \\ \beta_m \end{bmatrix} \quad (1.52)$$

whence  $\mathbf{x}$  can be computed by back-substitution. It is apparent, then, that the last  $m - n$  equations of the foregoing system are incompatible: their left-hand sides are zero, while their right-hand sides are not necessarily so. What the right-hand sides of these equations represent, then, is the approximation error in orthogonal coordinates. Its Euclidean norm is, then,

$$\|\mathbf{e}_0\| \equiv \sqrt{\beta_{n+1}^2 + \dots + \beta_m^2} \quad (1.53)$$

## Householder Reflections

The familiar concept of reflection about a plane—that of a flat mirror, for example—in 3D space can be generalized to  $n$ -dimensional spaces. Indeed, a reflection onto a plane  $\Pi$  of unit normal  $\mathbf{n}$  is illustrated in Fig. 1.6. In that figure, the projection of point  $P$ , of position vector  $\mathbf{p}$ , from an origin lying in the plane—this is necessary in order for  $\Pi$  to be a *vector space*—onto  $\Pi$  is labelled  $P'$ , of position vector  $\mathbf{p}'$ . Obviously, point  $P'$  is the intersection of the normal to  $\Pi$  from  $P$  with  $\Pi$  itself. If now a third point  $P''$  is found on the extension of the normal from  $P$  lying exactly the same distance  $d$  between  $P$  and  $P'$ , then  $P''$  becomes the reflection of  $P$  with respect to  $\Pi$ .

Now it is apparent that the position vector  $\mathbf{p}''$  of  $P''$  is given by

$$\mathbf{p}'' = \mathbf{p} - 2(\mathbf{p}^T \mathbf{n})\mathbf{n} \quad (1.54)$$

or

$$\mathbf{p}'' = (\mathbf{1} - 2\mathbf{n}\mathbf{n}^T)\mathbf{p} \quad (1.55)$$

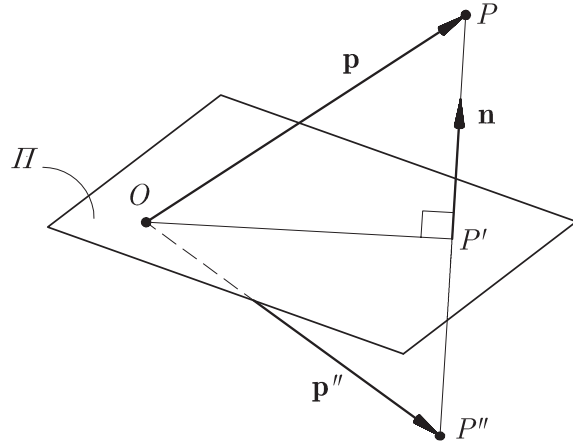


Figure 1.6: A reflection onto a plane  $\Pi$  of unit normal  $\mathbf{n}$

whence the reflection is represented algebraically by a matrix  $\mathbf{R}$  given by

$$\mathbf{R} = \mathbf{1} - 2\mathbf{n}\mathbf{n}^T \quad (1.56)$$

The extension of the 3D concept of reflection is now straightforward: vector  $\mathbf{n}$  in eq.(1.56) can be thought of as being  $n$ -dimensional.

With the above background, the second method discussed here, based on the application of a chain of  $n$  transformations  $\{\mathbf{H}_k\}_1^n$ , known as *Householder reflections*, to both sides of eq.(1.10), can now be introduced. The purpose of these reflections is, again, to obtain a representation of matrix  $\mathbf{A}$  in upper-triangular form (Golub and Van Loan, 1989). The algorithm proceeds as follows: We assume that we have applied reflections  $\mathbf{H}_1, \mathbf{H}_2, \dots, \mathbf{H}_{i-1}$ , in this order, to  $\mathbf{A}$  that have rendered it in *upper-trapezoidal form*, i.e.,

$$\mathbf{A}_{i-1} \equiv \mathbf{H}_{i-1} \dots \mathbf{H}_2 \mathbf{H}_1 \mathbf{A} \quad (1.57)$$

or

$$\mathbf{A}_{i-1} = \begin{bmatrix} a_{11}^* & a_{12}^* & \cdots & a_{1,i-1}^* & a_{1i}^* & \cdots & a_{1n}^* \\ 0 & a_{22}^* & \cdots & a_{2,i-1}^* & a_{2i}^* & \cdots & a_{2n}^* \\ 0 & 0 & \cdots & a_{3,i-1}^* & a_{3i}^* & \cdots & a_{3n}^* \\ \vdots & \vdots & \ddots & \vdots & \vdots & \ddots & \vdots \\ 0 & 0 & \cdots & a_{i-1,i-1}^* & a_{i-1,i}^* & \cdots & a_{i-1,n}^* \\ 0 & 0 & \cdots & 0 & a_{ii}^* & \cdots & a_{i,n}^* \\ \vdots & \vdots & \ddots & \vdots & \vdots & \ddots & \vdots \\ 0 & 0 & \cdots & 0 & a_{m,i}^* & \cdots & a_{mn}^* \end{bmatrix} \quad (1.58)$$

The next Householder reflection,  $\mathbf{H}_i$ , is determined so as to render the last  $m - i$  components of the  $i$ th column of  $\mathbf{H}_i \mathbf{A}_{i-1}$  equal to zero, while leaving its first  $i - 1$  columns unchanged. We do this by setting

$$\alpha_i = \text{sgn}(a_{ii}^*) \sqrt{(a_{ii}^*)^2 + (a_{i+1,i}^*)^2 + \cdots + (a_{mi}^*)^2} \quad (1.59a)$$

$$\mathbf{u}_i = [0 \ 0 \ \cdots \ 0 \ a_{ii}^* + \alpha_i \ a_{i+1,i}^* \ \cdots \ a_{mi}^*]^T \quad (1.59b)$$

$$\mathbf{H}_i = \mathbf{1} - \frac{\mathbf{u}_i \mathbf{u}_i^T}{\|\mathbf{u}_i\|^2/2} \quad (1.59c)$$

where  $\text{sgn}(x)$ , the *signum function* of  $x$ , is defined as  $+1$  if  $x > 0$ , as  $-1$  if  $x < 0$ , and is left undefined when  $x = 0$ . As the reader can readily verify,

$$\frac{1}{2}\|\mathbf{u}_i\|^2 = \alpha_i(\mathbf{u}_i)_i = \alpha_i(a_{ii}^* + \alpha_i) \equiv \gamma_i \quad (1.60)$$

and hence, the denominator appearing in the expression for  $\mathbf{H}_i$  is calculated with one single addition and a single multiplication. Notice that  $\mathbf{H}_i$  reflects vectors in  $m$ -dimensional space onto a hyperplane of unit normal  $\mathbf{u}_i/\|\mathbf{u}_i\|$ .

It is important to realize that

- (a)  $\alpha_i$  is defined with the sign of  $a_{ii}^*$  because the denominator  $\gamma_i$  appearing in eq.(1.60) is proportional to the sum of  $a_{ii}^*$  and  $\alpha_i$ , thereby guaranteeing that the absolute value of this sum will always be greater than the absolute value of each of its terms. If this provision were not made, then the resulting sum could be of a negligibly small absolute value, which would thus render  $\gamma_i$  a small positive number. Such a small number would thus introduce unnecessarily an inadmissibly large roundoff-error amplification upon dividing the product  $\mathbf{u}_i \mathbf{u}_i^T$  by  $\gamma_i$ ;
- (b) an arbitrary vector  $\mathbf{v}$  is transformed by  $\mathbf{H}_i$  with unusually few flops, namely,

$$\mathbf{H}_i \mathbf{v} = \mathbf{v} - \frac{1}{\gamma_i} (\mathbf{v}^T \mathbf{u}_i) \mathbf{u}_i$$

Upon application of the  $n$  Householder reflections thus defined, the system at hand becomes

$$\mathbf{H} \mathbf{A} \mathbf{x} = \mathbf{H} \mathbf{b} \quad (1.61)$$

with  $\mathbf{H}$  defined as

$$\mathbf{H} \equiv \mathbf{H}_n \dots \mathbf{H}_2 \mathbf{H}_1 \quad (1.62)$$

Similar to that in equation (1.52), the matrix coefficient of  $\mathbf{x}$  in eq.(1.61), i.e.,  $\mathbf{H} \mathbf{A}$ , is in upper-triangular form. That is, we have

$$\mathbf{H} \mathbf{A} = \begin{bmatrix} \mathbf{U} \\ \mathbf{O}_{m'n} \end{bmatrix}, \quad \mathbf{H} \mathbf{b} = \begin{bmatrix} \mathbf{b}_U \\ \mathbf{b}_L \end{bmatrix} \quad (1.63)$$

with  $\mathbf{U}$  a  $n \times n$  upper-triangular matrix identical to that appearing in eq.(1.22),  $\mathbf{O}_{m'n}$  denoting the  $(m - n) \times n$  zero matrix,  $m' \equiv m - n$ , and  $\mathbf{b}_U$  and  $\mathbf{b}_L$  being  $n$ - and  $m'$ -dimensional vectors. The unknown  $\mathbf{x}$  can thus be calculated from eq.(1.61) by back-substitution.

Note that the last  $m'$  components of the left-hand side of eq.(1.61) are zero, while the corresponding components of the right-hand side of the same equation are not necessarily

so. This apparent contradiction can be resolved by recalling that the overdetermined system at hand, in general, has no solution. The lower part of  $\mathbf{b}$ ,  $\mathbf{b}_L$ , is then nothing but an  $m'$ -dimensional array containing the nonzero components of the approximation error in the new coordinates. That is, the least-square error,  $\mathbf{e}_0$ , in these coordinates takes the form

$$[\mathbf{e}_0]_{\mathcal{O}} = \begin{bmatrix} \mathbf{0}_n \\ \mathbf{b}_L \end{bmatrix} \quad (1.64a)$$

where subscripted brackets are used to denote vector or matrix representation in a coordinate frame labelled with the subscript, usually in caligraphic fonts. In the above equation,  $\mathcal{O}$  stands for *orthogonal frame*, which defines the new coordinates. Hence, the above expression readily leads to the norm (any norm) of the least-square error, namely,

$$\|\mathbf{e}_0\| = \|\mathbf{b}_L\| \quad (1.64b)$$

## 1.5 Nonlinear-equation Solving: the Determined Case

**Definition 1.5.1** A system of algebraic equations containing some that are not linear is termed *nonlinear*. If the number of equations is identical to the number of unknowns, the system is *determined*.

**Example:** Find the intersection of the circle and the hyperbola depicted in Fig. 1.7.

*Solution:* The equations of the circle and the hyperbola are

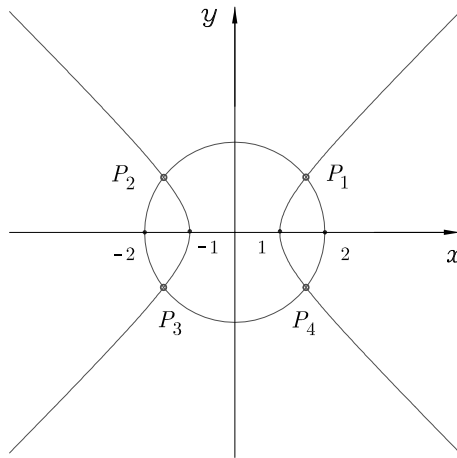


Figure 1.7: Intersection of a circle and a hyperbola

$$\begin{aligned}\phi_1(x, y) &\equiv x^2 + y^2 - 4 = 0 \\ \phi_2(x, y) &\equiv x^2 - y^2 - 1 = 0\end{aligned}$$

The solution to a nonlinear system of equations, when one exists at all, is usually *multiple*: The circle and the hyperbola of Fig. 1.7 intersect at four points  $\{P_i\}_1^4$ , of coordinates

$P_i$	$x_i$	$y_i$
1	$\sqrt{5}/2$	$\sqrt{3}/2$
2	$\sqrt{5}/2$	$-\sqrt{3}/2$
3	$-\sqrt{5}/2$	$\sqrt{3}/2$
4	$-\sqrt{5}/2$	$-\sqrt{3}/2$

Table 1.1: The four intersection points of the circle and the hyperbola of Fig. 1.7

$(x_i, y_i)$ , as displayed in Table 1.1. The problem may have **no real solution**, e.g., the circle and the hyperbola of Fig. 1.8 do not intersect. The system of equations from which the coordinates of the intersection points are to be computed is given below:

$$\begin{aligned}\phi_1(x, y) &\equiv x^2 + y^2 - 1 = 0 \\ \phi_2(x, y) &\equiv x^2 - y^2 - 16 = 0\end{aligned}$$

This system of equations admits no real solution!

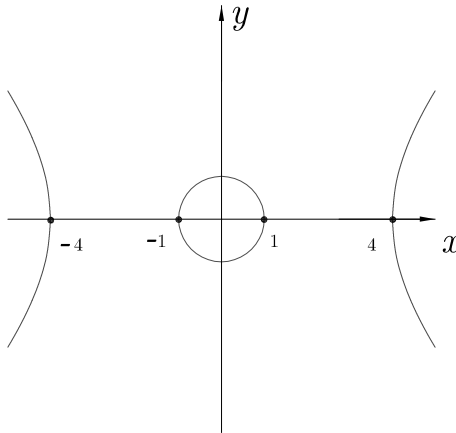


Figure 1.8: A circle and a hyperbola that do not intersect

In general, a determined nonlinear system of equations takes the form

$$\boldsymbol{\phi}(\mathbf{x}) = \mathbf{0} \quad (1.65)$$

where  $\mathbf{x}$  and  $\boldsymbol{\phi}$  are both  $n$ -dimensional vectors:

$$\mathbf{x} \equiv \begin{bmatrix} x_1 \\ x_2 \\ \vdots \\ x_n \end{bmatrix}, \quad \boldsymbol{\phi} \equiv \begin{bmatrix} \phi_1(x_1, x_2, \dots, x_n) \\ \phi_2(x_1, x_2, \dots, x_n) \\ \vdots \\ \phi_n(x_1, x_2, \dots, x_n) \end{bmatrix} \quad (1.66)$$

### 1.5.1 The Newton-Raphson Method

We outline below the method of solution of determined nonlinear systems using the Newton-Raphson method. This is an *iterative method*, whereby a sequence of approximations is obtained that, if converging, it approaches the solution in a finite number of iterations within a prescribed *tolerance*.

A value  $\mathbf{x}^0$  of  $\mathbf{x}$  is given as an *initial guess*:

$$\mathbf{x}^0 \equiv [p_1 \ p_2 \ \dots \ p_n]^T$$

and  $\boldsymbol{\phi}$  is evaluated at  $\mathbf{x}^0$ :

$$\boldsymbol{\phi}^0 \equiv \boldsymbol{\phi}(\mathbf{x}^0)$$

If the value  $\mathbf{x}^0$  was chosen arbitrarily, most likely it will not verify the given system of equations, i.e.,

$$\boldsymbol{\phi}^0 \neq \mathbf{0}$$

Next, we look for a “small” increment  $\Delta\mathbf{x}$  of  $\mathbf{x}$  (the increment is small if its norm—any norm—is small):

$$\Delta\mathbf{x} \equiv [\Delta x_1 \ \Delta x_2 \ \dots \ \Delta x_n]^T$$

Now,  $\boldsymbol{\phi}(\mathbf{x}^0 + \Delta\mathbf{x})$  is evaluated up to its linear approximation (all quadratic and higher-order terms are dropped from its series expansion):

$$\boldsymbol{\phi}(\mathbf{x}^0 + \Delta\mathbf{x}) \approx \boldsymbol{\phi}(\mathbf{x}^0) + \left. \frac{\partial \boldsymbol{\phi}}{\partial \mathbf{x}} \right|_{\mathbf{x}=\mathbf{x}^0} \Delta\mathbf{x} \quad (1.67)$$

The *Jacobian matrix* of  $\boldsymbol{\phi}$  with respect to  $\mathbf{x}$  is defined as the matrix of partial derivatives<sup>7</sup> of the components of  $\boldsymbol{\phi}$  with respect to all the components of  $\mathbf{x}$ :

$$\Phi \equiv \frac{\partial \boldsymbol{\phi}}{\partial \mathbf{x}} = \begin{bmatrix} \partial \phi_1 / \partial x_1 & \partial \phi_1 / \partial x_2 & \dots & \partial \phi_1 / \partial x_n \\ \partial \phi_2 / \partial x_1 & \partial \phi_2 / \partial x_2 & \dots & \partial \phi_2 / \partial x_n \\ \vdots & \vdots & \ddots & \vdots \\ \partial \phi_n / \partial x_1 & \partial \phi_n / \partial x_2 & \dots & \partial \phi_n / \partial x_n \end{bmatrix} \quad (1.68)$$

In the next step, we find  $\Delta\mathbf{x}$  that renders zero the linear approximation of  $\boldsymbol{\phi}(\mathbf{x}_0 + \Delta\mathbf{x})$ :

$$\boldsymbol{\phi}_0 + \Phi(\mathbf{x}^0)\Delta\mathbf{x} = \mathbf{0}$$

or

$$\Phi(\mathbf{x}^0)\Delta\mathbf{x} = -\boldsymbol{\phi}^0 \quad (1.69)$$

whence  $\Delta\mathbf{x}$  can be found using Gaussian elimination:

---

<sup>7</sup>See Subsection 1.4.5 for a derivation of the (matrix) partial derivative of a vector with respect to another vector.

$$\Delta \mathbf{x} = -\Phi_0^{-1} \phi^0, \quad \Phi_0 \equiv \Phi(\mathbf{x}^0) \quad (1.70)$$

Next,  $\mathbf{x}$  is updated:

$$\mathbf{x} \leftarrow \mathbf{x}^0 + \Delta \mathbf{x} \quad (1.71)$$

the procedure stopping when

$$\|\Delta \mathbf{x}\| \leq \epsilon_x \quad (1.72)$$

for a prescribed tolerance  $\epsilon_x$ .

### Remarks:

- Use the maximum norm to test convergence in eq.(1.72), for it costs virtually nothing;
- no guarantee that the Newton-Raphson method will converge at all;
- whether the Newton-Raphson method converges is dependent upon the initial guess,  $\mathbf{x}^0$ ;
- the boundary between regions of convergence and divergence is a *fractal* (Mandelbrot, 1983; Gleick, 1988);
- when the Newton-Raphson method converges, it does so *quadratically*: At every iteration, *two* decimal places of accuracy are gained (Dahlquist and Björck, 1974).

## 1.6 Overdetermined Nonlinear Systems of Equations

A system of nonlinear equations of the form

$$\phi(\mathbf{x}) = \mathbf{0} \quad (1.73)$$

where  $\mathbf{x}$  is a  $n$ -dimensional vector and  $\phi$  is a  $q$ -dimensional vector, is *overdetermined* if  $q > n$ . Just as in the linear case, in general, no vector  $\mathbf{x}$  can be found that verifies *all* the  $q$  scalar equations of the system. However, approximations can be found that minimize the least-square error of the approximation, as described in the balance of this Section. The method of solution adopted here is the overdetermined counterpart of the Newton-Raphson method.

### 1.6.1 The Newton-Gauss Method

**Problem:** Find an *approximate solution* to system (1.73) that verifies those equations with the *least-square error*:

$$f(\mathbf{x}) = \frac{1}{2} \phi^T \mathbf{W} \phi \rightarrow \min_{\mathbf{x}} \quad (1.74)$$

where  $\mathbf{W}$  is a  $q \times q$  positive-definite *weighting matrix*.

**Solution:** We follow a procedure similar to Newton-Raphson's, which is known as the *Newton-Gauss method*, as described below:

First, an initial guess  $\mathbf{x}^0$  of  $\mathbf{x}$  is given; then, we produce the sequence

$$\mathbf{x}^1, \mathbf{x}^2, \dots, \quad (1.75)$$

such that

$$\mathbf{x}^{k+1} = \mathbf{x}^k + \Delta\mathbf{x}^k \quad (1.76)$$

**Calculation of  $\Delta\mathbf{x}^k$ :**

- Factor  $\mathbf{W}$  into its two Cholesky factors:

$$\mathbf{W} = \mathbf{V}^T \mathbf{V} \quad (1.77)$$

which is possible because  $\mathbf{W}$  is assumed positive-definite<sup>8</sup>.

- Compute  $\Delta\mathbf{x}^k$  as the *least-square solution* of the overdetermined linear system

$$\mathbf{V}\Phi(\mathbf{x}^k)\Delta\mathbf{x}^k = -\mathbf{V}\phi(\mathbf{x}^k) \quad (1.78)$$

with  $\Phi(\mathbf{x})$  defined as the  $q \times n$  Jacobian matrix of the vector function  $\phi(\mathbf{x})$ , i.e.,

$$\Phi(\mathbf{x}) = \frac{\partial \phi(\mathbf{x})}{\partial \mathbf{x}} \quad (1.79)$$

Drop superscripts for the sake of notation-simplicity and recall eq.(1.41):

$$\Delta\mathbf{x} = -(\Phi^T \mathbf{W} \Phi)^{-1} \Phi^T \mathbf{W} \phi \quad (1.80)$$

This procedure is iterative, stopping when a *convergence criterion is met*.

## The Damping Factor

When implementing the Newton-Gauss method, the objective function  $f$  may increase upon correcting  $\mathbf{x}^k$  according to eq.(1.76), i.e.

$$f(\mathbf{x}^{k+1}) > f(\mathbf{x}^k) \quad (1.81)$$

This increase gives rise to oscillations and sometimes even leads to divergence. One way to cope with this situation is by introducing *damping*. Instead of using the whole increment  $\Delta\mathbf{x}^k$ , we use a fraction of it, i.e.

$$\mathbf{x}^{k+1} = \mathbf{x}^k + \alpha \Delta\mathbf{x}^k, \quad 0 < \alpha < 1 \quad (1.82)$$

where  $\alpha$  is known as the *damping factor*.

---

<sup>8</sup>In fact, the Cholesky decomposition is also possible for positive semi-definite matrices, as stated in

## Convergence Criterion

Calculate first  $\nabla f(\mathbf{x})$ :

$$\nabla f(\mathbf{x}) \equiv \frac{\partial f}{\partial \mathbf{x}} = \left( \frac{\partial \phi}{\partial \mathbf{x}} \right)^T \frac{\partial f}{\partial \phi} \quad (1.83)$$

$$\frac{\partial \phi}{\partial \mathbf{x}} \equiv \Phi, \quad \frac{\partial f}{\partial \phi} = \mathbf{W}\phi \quad (1.84)$$

Hence, the condition for a stationary point is

$$\Phi^T \mathbf{W}\phi = \mathbf{0} \quad (1.85)$$

which is the *normality condition* of the problem stated in eq.(1.74).

If now eq.(1.80) is recalled, it is apparent that  $\Delta\mathbf{x}$  vanishes when the normality condition (1.85) has been met.

It is thus apparent that, at a stationary point of  $f$ ,  $\phi(\mathbf{x})$  **need not vanish**, as is the case in overdetermined systems; however,  $\phi(\mathbf{x})$  **must lie in the null space of  $\Phi^T \mathbf{W}$** . Moreover, from eqs.(1.80) and (1.85) follows that, at a stationary point,  $\Delta\mathbf{x}$  vanishes. Hence, the convergence criterion is

$$\|\Delta\mathbf{x}\| < \epsilon \quad (1.86)$$

where  $\epsilon$  is a prescribed tolerance.

### Remarks:

- The normality condition (1.85) alone does not guarantee a minimum, but only a *stationary point*.
- However, as it turns out, if the procedure converges, then it does so, to a second-order approximation, to a minimum, and neither to a maximum nor a saddle point, as we prove below.

The sequence  $f(\mathbf{x}^0), f(\mathbf{x}^1), \dots, f(\mathbf{x}^k), f(\mathbf{x}^{k+1}), \dots$ , obtained from the sequence of  $\mathbf{x}$  values, evolves, to a first order, as  $\Delta f(\mathbf{x})$ , given by

$$\Delta f = \left( \frac{\partial f}{\partial \mathbf{x}} \right)^T \Delta\mathbf{x} \quad (1.87)$$

i.e.,

$$\Delta f = \phi^T \mathbf{W}\Phi \Delta\mathbf{x} \quad (1.88)$$

Upon plugging expression (1.80) of  $\Delta\mathbf{x}$  into eq. (1.88), we obtain

$$\Delta f = -\phi^T \underbrace{\mathbf{W}\Phi(\Phi^T \mathbf{W}\Phi)^{-1} \Phi^T \mathbf{W}}_{\mathbf{M}} \phi = -\phi^T \mathbf{M}\phi \quad (1.89)$$

where, apparently,  $\mathbf{M}$  is a  $q \times q$  positive-definite matrix. As a consequence,  $\boldsymbol{\phi}^T \mathbf{M} \boldsymbol{\phi}$  becomes a positive-definite quadratic expression of  $\boldsymbol{\phi}$ ; hence,  $\Delta f$  is negative definite. Thus, the second-order approximation of  $f(\mathbf{x})$  is negative-definite, and hence, the sequence of  $f$  values *decreases monotonically*. That is, in the neighbourhood of a stationary point the first-order approximation of  $\boldsymbol{\phi}(\mathbf{x})$  is good enough, and hence, if the procedure **converges**, it does so to a **minimum**.

The reader may wonder whether the Newton-Raphson method can be used to solve nonlinear least-square problems. Although the answer is *yes*, the Newton-Raphson method is not advisable in this case, as made apparent below.

Recall  $\nabla f$  from eqs.(1.74) and (1.75):

$$\begin{aligned}\nabla f(\mathbf{x}) &= \frac{\partial f}{\partial \mathbf{x}} = \underbrace{\Phi^T(\mathbf{x})}_{n \times q} \underbrace{\mathbf{W}}_{q \times q} \underbrace{\boldsymbol{\phi}(\mathbf{x})}_{q-\text{dim}} \\ \nabla f(\mathbf{x}) = \mathbf{0} &\Rightarrow \underbrace{\Phi^T(\mathbf{x}) \mathbf{W} \boldsymbol{\phi}(\mathbf{x})}_{\equiv \boldsymbol{\psi}(\mathbf{x}) \in \mathbb{R}^n} = \mathbf{0}\end{aligned}\tag{NC}$$

thereby obtaining a determined system of  $n$  equations in  $n$  unknowns. This system can be solved using Newton-Raphson method, which requires  $\nabla \boldsymbol{\psi}(\mathbf{x})$ :

$$\nabla \boldsymbol{\psi}(\mathbf{x}) = \frac{\partial \boldsymbol{\psi}}{\partial \mathbf{x}} = \frac{\partial}{\partial \mathbf{x}} \left[ \underbrace{\Phi^T(\mathbf{x})}_{(\partial \boldsymbol{\phi} / \partial \mathbf{x})^T} \mathbf{W} \boldsymbol{\phi}(\mathbf{x}) \right]$$

That is,  $\nabla \boldsymbol{\psi}(\mathbf{x})$  involves second-order derivatives of  $\boldsymbol{\phi}$  with respect to  $\mathbf{x}$ :

$$\frac{\partial \psi_i}{\partial x_j} \equiv \frac{\partial^2 \phi_i}{\partial x_j \partial x_i}, \quad i, j = 1, \dots, n$$

In summary, the Newton-Raphson method is too cumbersome and prone to ill-conditioning, for it is based on the normality conditions of the least-square problem at hand. **It is strongly recommended to avoid this method when confronted with overdetermined systems of nonlinear equations.**

## 1.7 Software Tools

### 1.7.1 ODA: Matlab and C code for Optimum Design

ODA is a C library of subroutines for optimization problems, that implements the *Orthogonal-Decomposition Algorithm* (Teng and Angeles, 2001). The source file of this package, implemented in C, consists of a number of subroutines designed and classified based on their application. At the beginning of each subroutine a detailed description of the purpose and usage of the subroutine is included. Moreover, data validation has been considered

in the software. In order to solve a problem, the user simply calls one corresponding C subroutine.

Since the solutions for linear problems are *direct*—as opposed to *iterative*—the use of ODA to solve linear problems requires only information on the problem parameters, such as matrices  $\mathbf{A}$ ,  $\mathbf{C}$ , and  $\mathbf{W}$ , as well as vectors  $\mathbf{b}$  and  $\mathbf{d}$ , as applicable. For nonlinear problems, the solution is iterative, and hence, the user is required to provide functions describing  $\phi(\mathbf{x})$ ,  $\mathbf{h}(\mathbf{x})$ ,  $\Phi(\mathbf{x})$ ,  $\mathbf{J}(\mathbf{x})$ , as needed. These functions are provided via subroutines in forms that can be called by the package. In addition to this information, the user is also required to provide an initial guess  $\mathbf{x}_0$  of  $\mathbf{x}$ , so that the iterative procedure can be started.

1. **Unconstrained linear problems:** Subroutine **MNSLS** is used to find the minimum-norm solution of an underdetermined linear system, while subroutine **LSSLS** is used to find the least-square approximation of an overdetermined linear system. **LSSLS** can also handle determined systems, i.e., systems of as many equations as unknowns.
2. **Unconstrained nonlinear problems:** Subroutine **LSSNLS** is used to solve this type of problems. Since the nonlinear functions and their associated gradient matrices are problem-dependent, the user is required to provide two subroutines that are used to evaluate the foregoing items, namely,
  - **FUNPHI:** This subroutine is used to evaluate the  $q$ -dimensional vector function  $\phi(\mathbf{x})$  in terms of the given  $n$ -dimensional vector  $\mathbf{x}$ .
  - **DPHIDX:** This subroutine is used to evaluate the  $q \times n$  gradient matrix  $\Phi$  of the vector-function  $\phi(\mathbf{x})$  with respect to  $\mathbf{x}$ , at the current value of  $\mathbf{x}$ .
 Moreover, an initial guess of  $\mathbf{x}$  is required when calling this subroutine.
3. **Constrained linear problems:** Subroutine **LSSCLS** is used to solve this type of problems.
4. **Constrained nonlinear problems:** Subroutine **LSSCNL** is used for solving this type of problems. Before calling **LSSCNL**, the user is required to provide four problem-dependent subroutines: Two of these are **FUNPHI** and **DPHIDX**, already described in item 2 above. The other two are used to evaluate the left-hand sides of the constraint equations and their gradient matrix, as listed below:
  - **FUNH:** This subroutine is used to evaluate the  $l$ -dimensional constraint function  $\mathbf{h}$  in terms of the given  $n$ -dimensional vector  $\mathbf{x}$ .
  - **DHDX:** This subroutine is used to evaluate the  $l \times n$  gradient matrix  $\mathbf{J}$  of the

---

Subsection 1.4.4, but these are not of interest in the context of the Newton-Gauss method.

vector-function  $\mathbf{h}(\mathbf{x})$  in terms of the given  $n$ -dimensional vector  $\mathbf{x}$ . Moreover, an initial guess of  $\mathbf{x}$  is required when calling LSSCNL.

5. **Constrained problems with arbitrary objective function:** Subroutine ARBITRARY is used for solving this type of problems. Before calling ARBITRARY, the user is required to provide four problem-dependent subroutines: Two of these are FUNPHI and DPHIDX, as described in item 2 above. The other two subroutines are used to evaluate the left-hand sides of the constraint equations and their gradient matrix, as listed below:

- **phi:** Subroutine used to evaluate the objective function  $\phi(\mathbf{x})$  in terms of the given  $n$ -dimensional vector  $\mathbf{x}$ .
- **h:** Subroutine used to evaluate the  $l$ -dimensional constraint function  $\mathbf{h}$  in terms of the given  $n$ -dimensional vector  $\mathbf{x}$ .
- **J:** Subroutine used to evaluate the  $l \times n$  gradient matrix  $\mathbf{J}$  of the vector-function  $\mathbf{h}(\mathbf{x})$  at the current value of  $\mathbf{x}$ .
- **gradient:** Subroutine used to evaluate the  $n$ -dimensional gradient  $\nabla f$  of the objective function  $f(\mathbf{x})$  at the current value of vector  $\mathbf{x}$ .
- **Hessian:** Subroutine used to evaluate the  $n \times n$  Hessian matrix  $\nabla \nabla f$  of the objective function  $f(\mathbf{x})$  at the current value of vector  $\mathbf{x}$ . Moreover, an initial guess of  $\mathbf{x}$  is required when calling ARBITRARY.

### 1.7.2 Packages Relevant to Linkage Synthesis

Several software packages of interest to kinematic synthesis are currently available, either commercially or semi-commercially. A list, with some features, follows:

- SAM: Package intended not only for kinematics, but also for static analysis. Runs only on Windows and is commercially available from *Artas Engineering Software*, of RJ Neuen, The Netherlands:

[www.artas.nl](http://www.artas.nl)

- PRO/ENGINEER: Comprehensive package for mechanical design and analysis at large. Its PRO/MECHANICA module provides motion analysis, simulation, and animation of fairly complex mechanisms. Runs on Windows and Unix. Vendor: *Parametric Technology, Inc.* (USA):

<http://www.ptc.com/>

- UNIGRAPHICS: High-end, comprehensive package with modules for finite-element analysis, CAD/CAM, and CAE (Computer-Aided Engineering). Vendor: *Siemens PLM Software*

<http://www.plm/automation.siemens.com>

- CATIA: The most widespread CAE package, in CAD, CAE, CAM. Manufacturer: *Dassault Systèmes*

<http://www.3ds.com/contact/>

- ADAMS, a general tool for mechanism and multibody-system analysis, produced by *MSC.ADAMS Software*. No synthesis features are supported.
- AUTOCAD: Comprehensive package for mechanical design and geometric analysis. To be used as a CAD support for linkage synthesis. No special features for linkage synthesis available. Runs mostly on Windows. Old versions run also on Unix. Vendor: *Autodesk, Inc.* with

[www.autodesk.com](http://www.autodesk.com)

- MATLAB: General-purpose numerical analysis package with excellent routines for equation-solving and optimization. To be used as a support for linkage synthesis. A few Matlab routines are specifically geared to linkage analysis. Package is produced by *The MathWorks* with

[www.mathworks.com](http://www.mathworks.com)

- MACSYMA, MAPLE, and MATHEMATICA: commercial packages for symbolic computations. MAPLE

[www.maplesoft.com](http://www.maplesoft.com)

and MATHEMATICA

[www.wolfram.com/mathematica4/isp](http://www.wolfram.com/mathematica4/isp)

provide for numerical computations

- MOBILE : Excellent object-oriented modeller and simulator of mechanical systems composed mostly of rigid bodies. No synthesis capabilities. Semicommercial. Available from the University of Duisburg-Essen. For information, contact: Martin Tändl: [m.taendl@uni-duisburg.de](mailto:m.taendl@uni-duisburg.de)

- BERTINI: Developed by Bates, Hauenstein, Sommese, and Wampler (2013), a C program for solving polynomial systems. Key features:
  - Finds isolated solutions by total degree or multihomogeneous degree homotopies.
  - Implements the latest method, called “regeneration,” which efficiently finds isolated solutions by introducing the equations one-by-one.
  - Finds positive dimensional solution sets and breaks them into irreducible components.
  - Has adaptive multiprecision arithmetic for maintaining accuracy in larger problems.
  - Endgames for fast, accurate treatment of singular roots.
  - Simple input file format.
  - Provides parameter homotopy, useful for efficiently solving multiple examples in a parameterized family of systems.
  - Allows user-defined homotopies.
  - Supports parallel computing.
  - A detailed users manual is available from SIAM Books. See Charles W. Wampler’s publications in:

<http://www3.nd.edu/~cwampl1/Software.htm>

- HOMLAB: Developed by Charles Wampler, a suite of MatLab routines for learning about polynomial continuation. Although created for use with the book by Sommese and Wampler (2005), HomLab is a general-purpose solver, fast enough for moderately-sized systems. If you are concerned about speed, numerical accuracy, and user-friendliness, try Bertini. If you want to learn the techniques of polynomial continuation from the inside, HomLab is your entry point.
- PHC: A code written in Ada, by Jan Verschelde. Key features:
  - Treatment of isolated solutions, including polyhedral homotopy (also known as the BKK approach, mixed volume, or polytope method).
  - Treatment of positive-dimensional solutions includes irreducible decomposition and diagonal homotopy.
  - The PHC pages also include a large collection of interesting examples.
- HOM4PS: Developed by T.-Y. Li, T.-L. Lee, T. Chen and N. Owenhouse, a piece of code for polyhedral homotopy (Li and Tsai, 2009). Very fast polyhedral homotopy method.

- Ch: C/C++ code for numerical computations, of special interest to solving complex kinematics problems. It handles dual numbers.



# Chapter 2

## The Qualitative Synthesis of Kinematic Chains

li·ai·son 1: a binding or thickening agent used in cooking

2 a) a close bond or connection : INTERRELATIONSHIP

b): an illicit sexual relationship : AFFAIR

*Merriam Webster's Collegiate Dictionary*, Tenth Edition (C)1997,  
1996 Zane Publishing, Inc.

*Qui pourrait ne pas frémir en songeant aux malheurs  
que peut causer une seule liaison dangereuse!*

Lettre CLXXV. Madame DE VOLANGES  
à Madame DE ROSEMONDE (de Laclos, 1782).

The fundamental concepts of motion representation and groups of displacements, as pertaining to rigid bodies, are recalled. These concepts are then applied to: a) the classification of kinematic chains according to their mobility; b) the determination of the degree of freedom of kinematic chains; and c) the qualitative synthesis of multiloop chains occurring in various types of machines, including parallel robots.

### 2.1 Notation

In following the notation introduced in Ch. 1, we will denote with lower-case boldfaces all vectors; with upper-case boldfaces all matrices. Additionally, sets will be denoted with calligraphic fonts, e.g.,  $\mathcal{A}$ ,  $\mathcal{B}$ , etc., while lower kinematic pairs (LKP), to be introduced in Section 2.3, are denoted with *sans-serif* upper cases: R, P, H, C, F, and S.

## 2.2 Background

The notion of *rigid body* is fundamental in the study of kinematic chains. A rigid body is a geometric concept that stems from the more general concept of *continuum*: *A rigid body  $\mathcal{B}$  is an unbounded continuum of points such that, under any possible transformation, two arbitrary points of  $\mathcal{B}$  remain equidistant.*

A rigid body  $\mathcal{B}$  is thus a set of points that fills continuously the three-dimensional Euclidean space  $\mathcal{E}$ . That is, between any two distinct points of  $\mathcal{B}$  we can always find an infinite, nondenumerable set of points of  $\mathcal{B}$ . A rigid body, as any set of points, is capable of undergoing transformations. In the case at hand, these transformations preserve the distance between any two points of  $\mathcal{B}$ ; as a consequence, the same transformation preserves the angle between any two lines of the body. Any such transformation is called an *isometry*—from Greek *isos* for “equal” and *metron* for “measure.” We must, however, distinguish between two kinds of isometries, as described below: Choose any four points  $O$ ,  $A$ ,  $B$ , and  $C$  of the body, not lying in a plane. If, when the last three points, as viewed from  $O$ , lie in the ccw order  $A$ ,  $B$ ,  $C$ , the trihedron defined by segments  $OA$ ,  $OB$  and  $OC$  is said to be *right-handed*; otherwise, it is *left-handed*. If a “hand” can be attributed to a set, we refer to this feature as the *chirality*—Greek: *chéir* = hand. It is apparent that under any *physically possible* motion of  $\mathcal{B}$ , a right-handed (left-handed) trihedron remains right-handed (left-handed). Isometries that do not preserve the hand of the trihedron are *reflections*, examples of which are the two shoes, or the two gloves, or the two eyes, etc., of the same individual. One is a reflection, or a mirror-image, of the other. A hand-preserving isometry of  $\mathcal{B}$  is implicit in a *displacement* of  $\mathcal{B}$  from a reference *pose*—both position and orientation—to its current pose. To simplify matters, we will denote body and pose with the same calligraphic letter, while distinguishing among various poses of the same body by subscripts, whenever needed. Thus,  $\mathcal{B}_0$  denotes a reference pose of  $\mathcal{B}$ , while its current pose can be represented by  $\mathcal{B}$ , as long as no confusion arises. Chirality-preserving isometries are involved in *rigid-body motions*.

Rigid-body pose and displacement are thus two abstract concepts. To quantify the pose we resort to *coordinate frames*. A coordinate frame is attached to a rigid body  $\mathcal{B}$ . The *orientation* of  $\mathcal{B}$  with respect to a reference frame is thus given by the orientation of the body-frame with respect to that of the reference frame. The position of  $\mathcal{B}$ , in turn, is given by that of the origin of the body-frame in the reference frame. The body-pose thus comprises both body-position and body-orientation. Body-position is thus defined by the *position vector*  $\mathbf{o}_B$  of the origin  $O_B$  of the body-frame, while body-orientation by the *rotation matrix*  $\mathbf{Q}$  carrying the reference frame into an attitude coincident with that of the body-frame.

According to Euler’s Theorem (Angeles, 2014), the displacement of a rigid body about a fixed point  $O$ , called a *pure rotation*, is fully characterized by an axis passing through

$O$  and parallel to the unit vector  $\mathbf{e}$ , and an angle  $\phi$ , as depicted in Fig. 2.1. Prior to introducing the rotation matrix, some preliminaries are invoked in the paragraphs below.

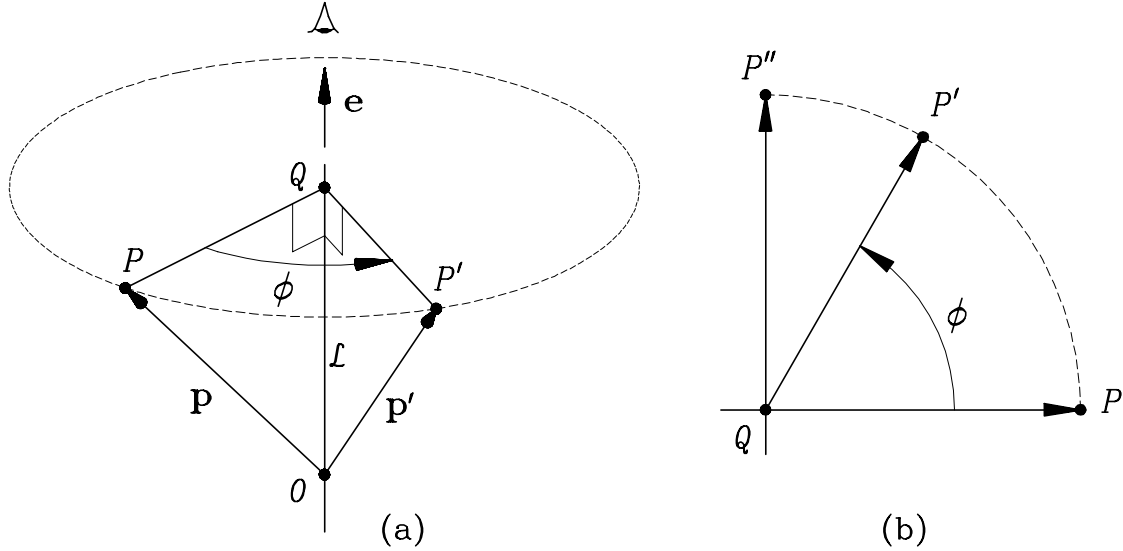


Figure 2.1: Rotation of a rigid body about a line

Given two vectors  $\mathbf{u}, \mathbf{v} \in \mathbb{R}^n$ , the product  $\mathbf{u}\mathbf{v}^T$  is termed a rank-one matrix because any  $\mathbf{w} \in \mathbb{R}^n$  normal to  $\mathbf{v}$  is mapped by  $\mathbf{u}\mathbf{v}^T$  into  $\mathbf{0}_n \in \mathbb{R}^n$ . As there are  $n - 1$  linearly independent vectors normal to  $\mathbf{v}$ , the *nullity* of  $\mathbf{u}\mathbf{v}^T$ , i.e., the dimension of its null space, is  $n - 1$ . As a consequence,  $\text{rank}(\mathbf{u}\mathbf{v}^T) = 1$ , hence the name.

The foregoing motion is represented algebraically by a rotation matrix, i.e., a  $3 \times 3$  *proper orthogonal* matrix  $\mathbf{Q}$ —a matrix is said to be proper-orthogonal if and only if its inverse equals its transpose and its determinant is  $+1$ ; if the said determinant is  $-1$ , the matrix is said to be *improper-orthogonal*—that adopts any of the equivalent forms given below:

$$\mathbf{Q} = e^{\phi\mathbf{E}} \quad (2.1a)$$

$$\mathbf{Q} = \mathbf{1} + \sin \phi \mathbf{E} + (1 - \cos \phi) \mathbf{E}^2 \quad (2.1b)$$

$$\mathbf{Q} = \mathbf{e}\mathbf{e}^T + \cos \phi (\mathbf{1} - \mathbf{e}\mathbf{e}^T) + \sin \phi \mathbf{E} \quad (2.1c)$$

In the above expressions we have resorted to the matrix exponential in the first representation of  $\mathbf{Q}$ . Moreover, we introduced matrices  $\mathbf{1}$ ,  $\mathbf{e}\mathbf{e}^T$ , and  $\mathbf{E}$ , that will be described presently. Matrix  $\mathbf{1}$  denotes the  $3 \times 3$  *identity matrix*, while  $\mathbf{e}\mathbf{e}^T$  is a *symmetric, rank-one matrix*; finally,  $\mathbf{E}$  denotes the *cross-product matrix* (CPM) of the unit vector  $\mathbf{e}$ , the CPM being defined as: Given any three-dimensional vector  $\mathbf{a}$ , the cross-product matrix  $\mathbf{A}$  of  $\mathbf{a}$  is given by

$$\mathbf{A} \equiv \frac{\partial(\mathbf{a} \times \mathbf{v})}{\partial \mathbf{v}} = \text{CPM}(\mathbf{a}) \quad (2.1d)$$

for any three-dimensional vector  $\mathbf{v}$ . More concretely, if  $\mathbf{a}$  has components  $[a_1 \ a_2 \ a_3]^T$  in a given coordinate frame, then, in the same frame,

$$\mathbf{a}\mathbf{a}^T = \begin{bmatrix} a_1^2 & a_1a_2 & a_1a_3 \\ a_1a_2 & a_2^2 & a_2a_3 \\ a_1a_3 & a_2a_3 & a_3^2 \end{bmatrix}, \quad \mathbf{A} = \begin{bmatrix} 0 & -a_3 & a_2 \\ a_3 & 0 & -a_1 \\ -a_2 & a_1 & 0 \end{bmatrix} \quad (2.2a)$$

An identity that the reader is invited to verify follows: if  $\mathbf{A} = \text{CPM}(\mathbf{a})$ , for any three-dimensional vector  $\mathbf{a}$ , then

$$\mathbf{A}^2 = -\|\mathbf{a}\|^2 \mathbf{1} + \mathbf{a}\mathbf{a}^T \quad (2.3)$$

In particular, if  $\|\mathbf{a}\| = 1$ , then  $\mathbf{A}^2 = -\mathbf{1} + \mathbf{a}\mathbf{a}^T$ . Now it should be apparent that expression (2.1c) follows from expression (2.1b) upon application of the foregoing identity.

Now, given a rigid body in two poses,  $\mathcal{B}_1$  and  $\mathcal{B}_2$ , characterized by the position vectors  $\mathbf{o}_1$  and  $\mathbf{o}_2$ , and the rotation matrices  $\mathbf{Q}_1$  and  $\mathbf{Q}_2$ , the displacement of the body from  $\mathcal{B}_1$  to  $\mathcal{B}_2$  is *represented* by a) the vector difference  $\mathbf{u} = \mathbf{o}_2 - \mathbf{o}_1$  and b) the matrix product  $\mathbf{Q} = \mathbf{Q}_2\mathbf{Q}_1$ . Special cases of displacements are the *pure rotation*, as introduced above, for which  $\mathbf{u} = \mathbf{0}$ , and the *pure translation*, for which  $\mathbf{Q} = \mathbf{1}$ .

The concept inverse to the CPM of a 3D vector is the axial vector of a  $3 \times 3$  matrix. The *Cartesian decomposition* of a  $n \times n$  matrix  $\mathbf{A}$  is

$$\mathbf{A} = \mathbf{A}_S + \mathbf{A}_{SS} \quad (2.4)$$

where  $\mathbf{A}_S$  is symmetric and  $\mathbf{A}_{SS}$  is skew-symmetric.

The reader can readily prove that

$$\mathbf{A}_S \equiv \frac{1}{2}(\mathbf{A} + \mathbf{A}^T), \quad \mathbf{A}_{SS} \equiv \frac{1}{2}(\mathbf{A} - \mathbf{A}^T) \quad (2.5)$$

**Definition 2.2.1** For  $n = 3$ , let  $\mathbf{v}$  be any 3D vector. Then there exists a vector  $\mathbf{a}$  such that

$$\mathbf{A}_{SS}\mathbf{v} \equiv \mathbf{a} \times \mathbf{v} \quad (2.6)$$

Vector  $\mathbf{a}$  is called the *axial vector* of  $\mathbf{A}_{SS}$ :

$$\mathbf{a} = \text{vect}(\mathbf{A}_{SS}) = \text{vect}(\mathbf{A}) \quad (2.7)$$

### Theorem 2.2.1

$$\mathbf{A}_{SS} = \text{CPM}(\mathbf{a}) \quad (2.8)$$

*Proof:* trivial. DIY.

**Theorem 2.2.2** Operations  $\text{CPM}(\cdot)$  and  $\text{vect}(\cdot)$  are linear, i.e., if  $\mathbf{A}$  and  $\mathbf{B}$  are  $3 \times 3$  matrices and  $\mathbf{a}$  and  $\mathbf{b}$  are 3D vectors, while  $\alpha$  and  $\beta$  are real numbers, then

$$\text{CPM}(\alpha\mathbf{a} + \beta\mathbf{b}) = \alpha\text{CPM}(\mathbf{a}) + \beta\text{CPM}(\mathbf{b}) \quad (2.9a)$$

while

$$\text{vect}(\alpha\mathbf{A} + \beta\mathbf{B}) = \alpha\text{vect}(\mathbf{A}) + \beta\text{vect}(\mathbf{B}) \quad (2.9b)$$

*Proof:* follows directly from the definitions of  $\text{CPM}(\cdot)$  and  $\text{vect}(\cdot)$  plus that of the cross product.

If  $a_{ij}$  is the  $(i, j)$  entry of  $\mathbf{A}$ , below we find the entries of  $\mathbf{a}$ :

$$\mathbf{A}_S = \begin{bmatrix} a_{11} & (a_{12} + a_{21})/2 & (a_{13} + a_{31})/2 \\ & a_{22} & (a_{23} + a_{32})/2 \\ \text{sym} & & a_{33} \end{bmatrix} \quad (2.10a)$$

$$\mathbf{A}_{SS} = \begin{bmatrix} 0 & (a_{12} - a_{21})/2 & (a_{13} - a_{31})/2 \\ & 0 & (a_{23} - a_{32})/2 \\ \text{skew-sym} & & 0 \end{bmatrix} \quad (2.10b)$$

Further, if  $a_i$  denotes the  $i^{th}$  component of  $\mathbf{a}$  with a similar definition for  $v_i$ ,

$$\mathbf{a} \times \mathbf{v} = \det \left( \begin{bmatrix} \mathbf{i} & \mathbf{j} & \mathbf{k} \\ a_1 & a_2 & a_3 \\ v_1 & v_2 & v_3 \end{bmatrix} \right) = \begin{bmatrix} a_2 v_3 - a_3 v_2 \\ a_3 v_1 - a_1 v_3 \\ a_1 v_2 - a_2 v_1 \end{bmatrix} \quad (2.11)$$

As well,

$$\mathbf{A}_{SS}\mathbf{v} = \frac{1}{2} \begin{bmatrix} (a_{12} - a_{21})v_2 + (a_{13} - a_{31})v_3 \\ -(a_{12} - a_{21})v_1 + (a_{23} - a_{32})v_3 \\ -(a_{13} - a_{31})v_1 - (a_{23} - a_{32})v_2 \end{bmatrix} \quad (2.12)$$

As per eq. (2.6), equate eqs. (2.11) and (2.12):

$$a_2 = \frac{1}{2}(a_{13} - a_{31}), \quad a_3 = -\frac{1}{2}(a_{12} - a_{21}), \quad a_1 = -\frac{1}{2}(a_{23} - a_{32}) \quad (2.13)$$

or

$$\mathbf{a} = \frac{1}{2} \begin{bmatrix} a_{32} - a_{23} \\ a_{13} - a_{31} \\ a_{21} - a_{12} \end{bmatrix} \quad (2.14)$$

**Facts:** for any  $n \times n$  matrix  $\mathbf{M}$  and any  $n$ -dimensional vectors  $\mathbf{a}$  and  $\mathbf{b}$ ,

**Fact 2.2.1**

$$\text{tr}(\mathbf{M}) = m_{11} + m_{22} + \dots + m_{nn}$$

**Fact 2.2.2**

$$\text{tr}(\mathbf{ab}^T) = a_1b_1 + a_2b_2 + \cdots + a_nb_n = \mathbf{a}^T\mathbf{b}$$

**Fact 2.2.3** If  $\mathbf{M} = -\mathbf{M}^T$ , then all its diagonal entries vanish, and hence,  $\text{tr}(\mathbf{M}) = 0$

**Theorem 2.2.3** If  $\mathbf{A} = \mathbf{A}^T$ , then  $\text{vect}(\mathbf{A}) = \mathbf{0}$

*Proof:* follows from eq. (2.14).

**Theorem 2.2.4** the trace( $\cdot$ ) operation is linear, i.e.,

$$\text{tr}(\alpha\mathbf{A} + \beta\mathbf{B}) = \alpha\text{tr}(\mathbf{A}) + \beta\text{tr}(\mathbf{B})$$

*Proof:* follows from its definition.

The foregoing concepts are now applied to find the *natural invariants* of  $\mathbf{Q}$ , i.e., the unit vector  $\mathbf{e}$ , its cross-product matrix  $\mathbf{E}$ , and angle  $\phi$ , as per eqs. (2.1a–2.1c).

$$\begin{aligned} \text{tr}(\mathbf{Q}) &= \underbrace{\text{tr}(\mathbf{ee}^T)}_{\text{Theorem 2.2.4}} + \underbrace{\text{tr}[\cos \phi(\mathbf{1} - \mathbf{ee}^T)]}_{\text{Fact 2.2.2}} + \underbrace{\text{tr}(\sin \phi \mathbf{E})}_{\text{Theorem 2.2.4}} \\ &= \underbrace{\mathbf{e}^T\mathbf{e}}_{\text{Fact 2.2.2}} + \cos \phi \underbrace{[\text{tr}(\mathbf{1}) - \mathbf{e}^T\mathbf{e}]}_{\text{Theorem 2.2.4}} + \sin \phi \underbrace{\text{tr}(\mathbf{E})}_{\text{Fact 2.2.3}} \\ &= 1 + 2 \cos \phi \end{aligned} \tag{2.15}$$

$$\begin{aligned} \text{vect}(\mathbf{Q}) &= \underbrace{\text{vect}(\mathbf{ee}^T)}_{\text{Theorem 2.2.2}} + \underbrace{\text{vect}[\cos \phi(\mathbf{1} - \mathbf{ee}^T)]}_{\text{Fact 2.2.3}} + \underbrace{\text{vect}(\sin \phi \mathbf{E})}_{\text{Theorem 2.2.2}} \\ &= \underbrace{\mathbf{0}}_{\text{Theorem 2.2.3}} + \underbrace{\mathbf{0}}_{\text{Theorem 2.2.3}} + \underbrace{\sin \phi \text{vect}(\mathbf{E})}_{\text{Theorem 2.2.2}} \\ &= \underbrace{\sin \phi \mathbf{e}}_{\text{eq. (2.7)}} \end{aligned} \tag{2.16}$$

which leads to an uncertainty, as  $\phi$  can be associated to one of two possible quadrants. Moreover, a reversal in the sign of  $\phi$ , which does not change the direction of the axis of rotation, can be compensated with a reversal of the sign of the components of  $\mathbf{e}$ , to leave  $\mathbf{Q}$  immutable. For concreteness, and without loss of generality, we shall assume

henceforth that  $\sin \phi \geq 0$ , and hence, that  $\phi$  lies either in the first or the second quadrant. The quadrant ambiguity is resolved by the sign of  $\cos \phi$ :

$$\begin{aligned} & \text{if } \cos \phi = \frac{\text{tr}(\mathbf{Q}) - 1}{2} > 0, \text{ then } \phi \text{ in 1st quadrant} \\ & \text{if } \cos \phi = \frac{\text{tr}(\mathbf{Q}) - 1}{2} < 0, \text{ then } \phi \text{ in 2nd quadrant} \end{aligned}$$

**Example 2.2.1** For  $\mathbf{Q}_1$  of eq. (2.21a), find  $\mathbf{e}$  and  $\phi$ .

$$\begin{aligned} \text{vect}(\mathbf{Q}_1) &= \frac{1}{2} \begin{bmatrix} 3/2 \\ \sqrt{3}/2 \\ \sqrt{3}/2 \end{bmatrix} = \frac{1}{4} \begin{bmatrix} 3 \\ \sqrt{3} \\ \sqrt{3} \end{bmatrix} \Rightarrow \sin \phi = \|\text{vect}(\mathbf{Q}_1)\| = \sqrt{15}/4 \\ \Rightarrow \phi &= 75.52^\circ \text{ or } 104.48^\circ \\ \mathbf{e} &= \text{vect}(\mathbf{Q}_1)/\|\text{vect}(\mathbf{Q}_1)\| = \frac{\sqrt{15}}{15} \begin{bmatrix} 3 \\ \sqrt{3} \\ \sqrt{3} \end{bmatrix} \\ \text{tr}(\mathbf{Q}_1) &= \frac{1}{2} \Rightarrow \cos \phi = -\frac{1}{4} \Rightarrow \phi = 104.48^\circ \end{aligned}$$

## 2.3 Kinematic Pairs

The concepts, and to a great extent the notation and nomenclature that follow, are taken from (Hervé, 1978; 1999).

The kinematics of machines is studied via their underlying *kinematic chains*. A kinematic chain is the result of the coupling of rigid bodies, called *links*. Upon coupling *two* links, a kinematic pair is obtained. When the coupling takes place in such a way that the two links share a common surface, a *lower kinematic pair* results; when the coupling takes place along a common line or a common point of the two links, a *higher kinematic pair* is obtained.

If every link of a chain is coupled to at most two other links, then the chain is said to be *simple*. If all the links of a simple kinematic chain are coupled to two other links, then a *closed kinematic chain* is obtained. Moreover, this chain constitutes a *single loop*. If a simple chain has a link coupled to only one other link, then it has necessarily a second link coupled to only one other link, an *open chain* thus resulting. A multiloop chain can have open *subchains*. Single-loop kinematic chains are present in single-degree-of-freedom mechanisms, but a single-loop chain may have a degree of freedom (dof) greater than or less than unity. Simple kinematic chains of the open type are present in robotic manipulators of the *serial* type. Multiloop kinematic chains occur in both single-degree-of-freedom machines, e.g., in automobile suspensions, and in multi-dof robotic manipulators of the *parallel type*, paradigms of which are flight simulators. We shall elaborate on these concepts in this course.

Lower kinematic pairs deserve special attention for various reasons: One is that they model fairly well the mechanical couplings in a variety of machines; one more is that they are known to occur in exactly six types, to be described presently. Higher kinematic pairs occur in cam-follower mechanisms and in gears, in which contact occurs along common lines or common points of the coupled bodies.

The six lower kinematic pairs, displayed in Fig. 2.2, are listed below:

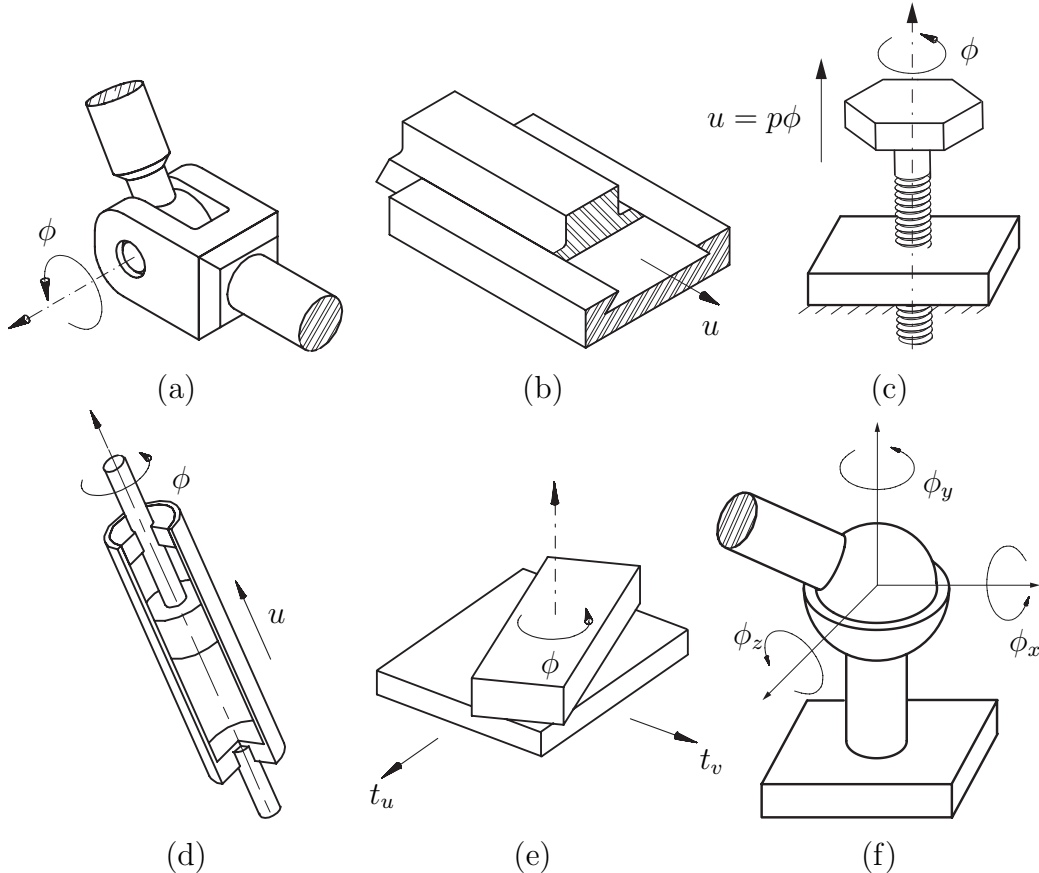


Figure 2.2: The six lower kinematic pairs: (a) revolute (**R**); (b) prismatic (**P**); (c) screw (**H**); (d) cylindrical (**C**); (e) planar (**F**); and (f) spherical (**S**)

- (i) The *revolute pair* **R** allows a relative rotation through an angle  $\phi$  about one axis  $\mathcal{A}$  passing through a point  $A$  of position vector  $\mathbf{a}$  and parallel to the unit vector  $\mathbf{e}$ ;
- (ii) The *prismatic pair* **P** allows a relative translation  $u$  in the direction of a unit vector  $\mathbf{e}$ ;
- (iii) The *screw pair* **H** allows both a relative rotation through an angle  $\phi$  about an axis  $\mathcal{A}$  passing through a point  $A$  of position vector  $\mathbf{a}$  and parallel to the unit vector  $\mathbf{e}$ , and a relative translation  $u$  in the direction of  $\mathbf{e}$ . However, the rotation and

the translation are not independent, for they are related by the *pitch*  $p$  of the pair:  
 $u = p\phi$ ;

- (iv) The *cylindrical pair*  $C$  allows both a relative rotation through an angle  $\phi$  about an axis  $A$  passing through a point  $A$  of position vector  $\mathbf{a}$  and parallel to the unit vector  $\mathbf{e}$ , and a relative translation  $u$  in the direction of  $\mathbf{e}$ , rotation and translation being independent;
- (v) The *planar pair*  $F$  allows two independent translations  $t_u$  and  $t_v$  in the directions of the *distinct* unit vectors  $\mathbf{u}$  and  $\mathbf{v}$ , respectively, and a rotation  $\phi$  about an axis normal to the plane of these two vectors; and
- (vi) The *spherical pair*  $S$ , allowing one independent rotation about each of three non-coplanar axes concurrent at a point  $O$ . The relative motion allowed by  $S$  is thus characterized by point  $O$ , and is associated with an axis parallel to the unit vector  $\mathbf{e}$  and with the angle of rotation  $\phi$  about this axis, as per Euler's Theorem.

**Remark 2.3.1** While the  $R$ ,  $H$ , and  $C$  pairs are characterized by an axis, the  $P$  pair is characterized by a direction alone; not by an axis!

## The $\Pi$ Kinematic Pair

Besides the six LKPs, the  $\Pi$  pair will be introduced in this chapter. This joint is a *parallelogram four-bar linkage*, as depicted in Fig. 2.3, which couples two links, 1, that is considered *fixed*, and 3. The latter moves under *pure translation*, all its points describing circles of variable location and radius identical to the common length of links 2 and 4.

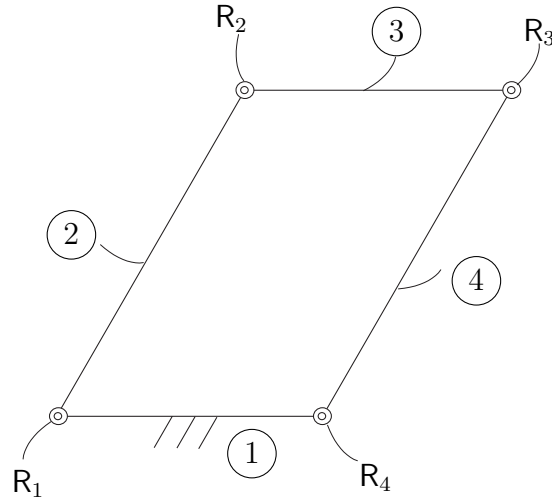


Figure 2.3: The  $\Pi$  joint, a four-bar parallelogram coupling links 1 and 3

In the standard terminology, link 3 is termed the *coupler*. The linkage thus provides a kinematic pair of the coupler link with respect to the fixed link. Hervé and Sparacino

(1992) termed this coupling a  $\Pi$  kinematic pair, a.k.a. a  $\Pi$ -joint. At about the same time, Wohlhart (1991, 1992) and Dietmaier (1992) reported work on the use of the same type of joints in mechanisms.

Note that the  $\Pi$  joint does not belong to the class of lower kinematic pairs. The  $\Pi$  pair can be shown to be equivalent to a  $P$  pair of continuously variable direction. Indeed, the instant centre (Uicker, Jr. et al., 2011) of the coupler link 3 with respect to link 1 of the parallelogram linkage lies at infinity, in the direction of the axes of the parallel links 2 and 4 of Fig. 2.3<sup>1</sup>. This point thus changes continuously its location, depending on the angle of inclination of the axes of links 2 and 3 with respect to line  $\overline{R_1 R_4}$ . The same point is thus common to both links 1 and 3, but it is the only common point. If the linkage is regarded as a three-dimensional object, then the instant centre is, in fact, a line, the instant screw axis—see Theorem A.3.5—and hence, contact between the two coupled links takes place not along a surface, but along a line, which disqualifies the  $\Pi$  pair from being a LKP. The interest of this pair lies in its ability to generate pure translations when combined with other  $\Pi$ -joints or with lower kinematic pairs, as discussed below.

## 2.4 Graph Representation of Kinematic Chains

Figure 2.3 depicts a planar four-bar linkage in the most common way: its  $R$  joints are represented as small circles—with smaller circles inside that most often are replaced by dots or even left empty—their centre denoting the projection of the  $R$  axis onto the plane of the figure. The joints are coupled by means of straight lines representing the mechanism links. These lines convey geometric information, as their lengths are the distances between neighbouring-joint axes. An alternative representation of linkages, particularly useful in the preliminary stages of mechanism design, in which dimensions are yet to be found, is in terms of *graphs*. A graph is a two-dimensional sketch that is composed of nodes and edges (Harary, 1972). The nodes are objects—e.g., pieces of land in the famous Königsberg/Kaliningrad—related by the edges—e.g., the seven Königsberg/Kaliningrad bridges that so much attracted Leonhard Euler’s attention. In kinematic synthesis, the objects are the mechanism links, the edges the joints that couple them. The graph representation of the four-bar linkage of Fig. 2.3, or of any four-bar linkage for that matter, as dimensions become immaterial in a graph, is depicted in Fig. 2.4

Apparently, a mechanism graph encapsulates non-dimensional, *relational information* on the *architecture* of a linkage. This information includes connectivity—which link is coupled to which—and layout—whether the chain is closed, as in the above case, or open, as in the case of an industrial robot of the serial type, e.g., the one shown in Fig. 2.5. In the graph representation, link 1 is the base, link 7 the end-effector.

The architecture of some machines is more complex in that it contains several loops.

---

<sup>1</sup>Remember the Aronhold-Kennedy Theorem of elementary mechanisms courses!

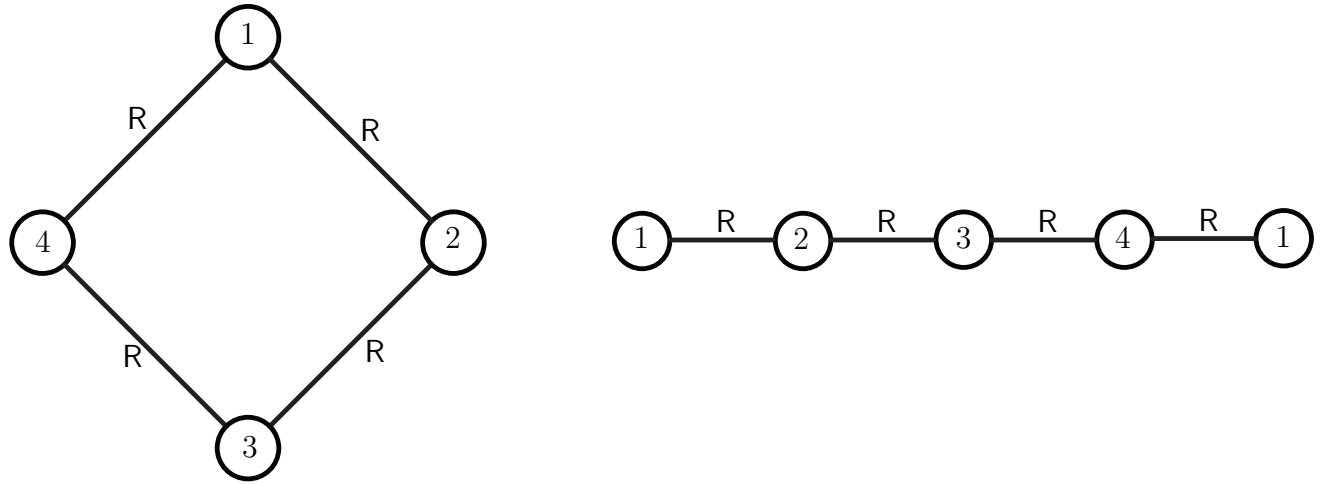


Figure 2.4: Two alternative graphs of a four-bar linkage

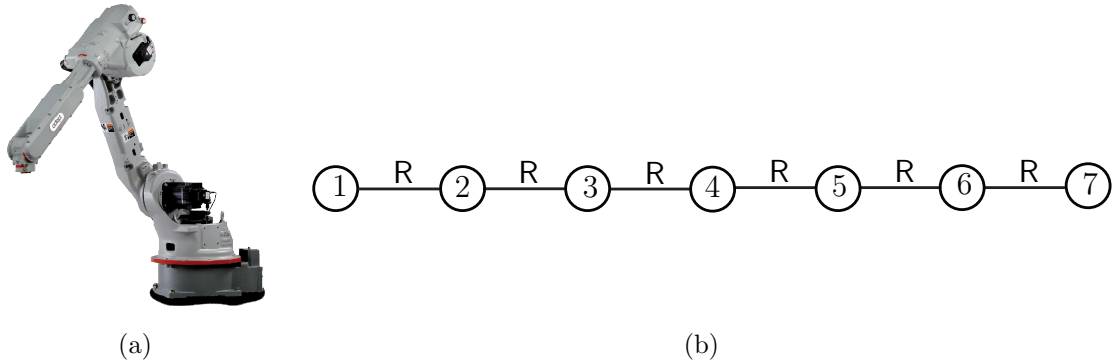
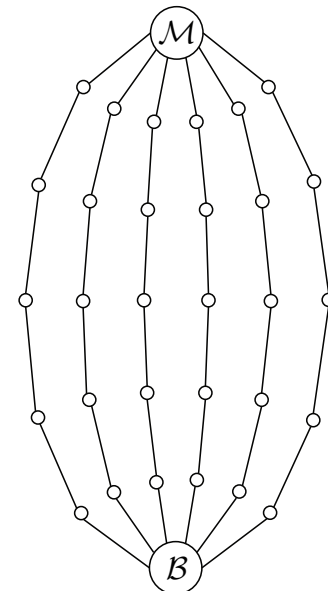


Figure 2.5: A six-axis industrial robot of the serial type: (a) its photograph and (b) its graph (Permission to reproduce from Adept Technology, Inc. is pending)

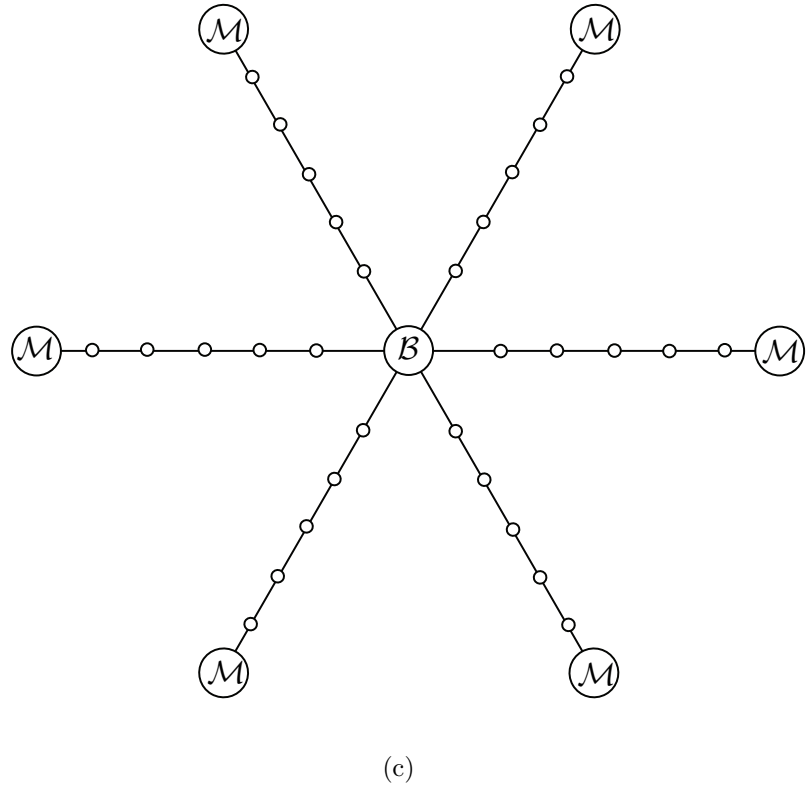
For example, the flight simulator of Fig. 2.6(a) comprises one base platform ( $\mathcal{B}$ ), the ground, one moving platform ( $\mathcal{M}$ ), the one carrying the aircraft cockpit, both coupled by means of six extensible limbs. Its graph, in two versions, being shown in Figs. 2.6(b) and (c). As a matter of fact, each limb is itself a serial kinematic chain of the serial type, its architecture being depicted in Fig. 2.7, which is, again, a six-joint open chain, similar to the one of Fig. 2.5(a), with one difference: its third joint from the base (1) is of the P type, instead of the R type of Fig. 2.5(b). One more difference, not affecting its topology but worth pointing out, is that, of all six joints of the chain shown in Fig. 2.7, only the P joint is actuated, all R joints being *passive*.



(a)



(b)



(c)

Figure 2.6: A flight simulator: (a) its photograph; and (b) & (c) two alternatives of its graph representation (Permission to reproduce from CAE Electronics Ltd. is pending)

## 2.5 Groups of Displacements

In the sequel, we shall resort to the algebraic concept of *group*. A group is a set  $\mathcal{G}$  of elements related by a *binary operation*  $\star$  with four properties:

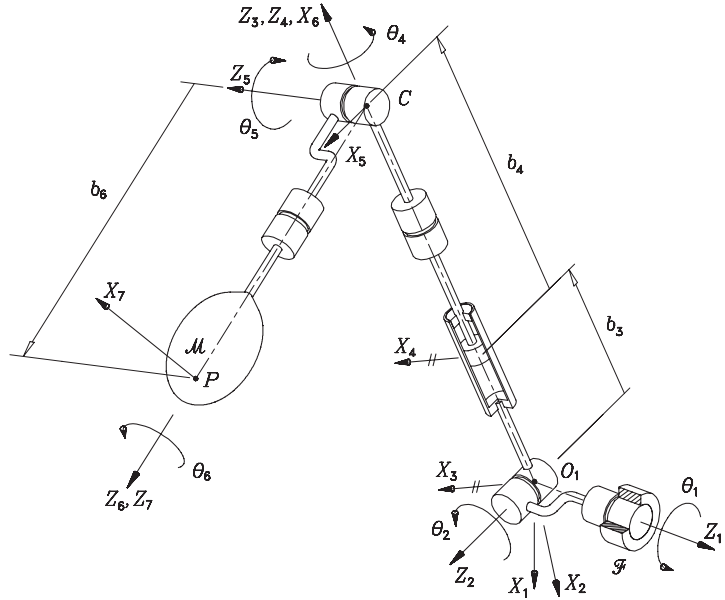


Figure 2.7: The kinematic chain of a flight-simulator limb

- P1 if  $a$  and  $b \in \mathcal{G}$ , then  $a * b \in \mathcal{G}$ ;
- P2 if  $a$ ,  $b$ , and  $c \in \mathcal{G}$ , then  $a * (b * c) = (a * b) * c$ ;
- P3  $\mathcal{G}$  contains an element  $\iota^2$  called the *identity* of  $\mathcal{G}$  under  $*$ , such that  $a * \iota = \iota * a = a$ ; and
- P4 for every  $a \in \mathcal{G}$ , there exists an element  $a^{-1}$ , called the *inverse of  $a$  under  $*$*  such that  $a * a^{-1} = a^{-1} * a = \iota$ .

Two types of groups are found, discrete and continuous. The former have a discrete set of elements, the later a continuum. An example of a discrete group is the *symmetry group* of a regular polygon, defined as the set of rotations about the centre of the polygon that leaves the figure unchanged. Continuous groups, or Lie groups, named after the Norwegian mathematician Sophus Lie (1842–1899), are of interest to this chapter.

If the elements of a set  $\mathcal{D}$  are the displacements undergone by a rigid body, then we can define a binary operation  $\odot$ —read “o-dot”—of displacements as the *composition* of displacements: As the body undergoes first a displacement  $d_a$  and then a displacement  $d_b$ , taking the body, successively, from pose  $\mathcal{B}_0$  to pose  $\mathcal{B}_a$ , and then to pose  $\mathcal{B}_b$ , it is intuitively apparent that the composition of the two displacements,  $d_a \odot d_b$ , is in turn a rigid-body displacement.

More concretely, a rigid-body displacement, illustrated in Fig. 2.8, is defined by a translation  $\mathbf{b}$  of a landmark point, say  $O$  in the figure, and a rotation  $\mathbf{Q}$  about the same

---

<sup>2</sup> $\iota$  is the Greek letter *iota*.

point. Point  $P$  in the displaced posture is assumed to be the displaced counterpart of a point  $P_0$ —not shown in the figure—of position vector  $\boldsymbol{\pi}_0$  in the reference posture. Under these conditions, the position vector  $\mathbf{p}$  of  $P$  in the reference frame  $\mathcal{A}$  can be expressed as

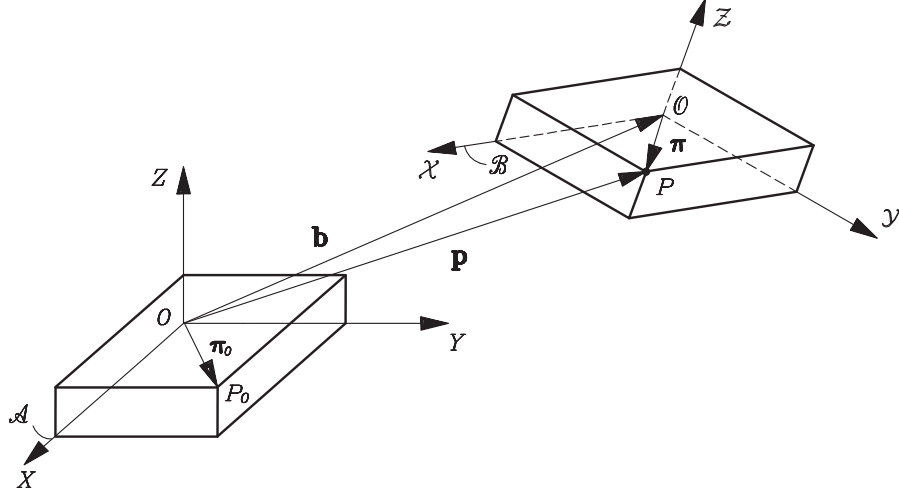


Figure 2.8: Coordinate frames with different origins

$$\mathbf{p} = \mathbf{b} + \underbrace{\mathbf{Q}\boldsymbol{\pi}_0}_{\mathbf{Q}\boldsymbol{\pi}} = \mathbf{b} + \mathbf{Q}\boldsymbol{\pi}_0 \quad (2.17)$$

which gives the displaced position of  $P$  as a sum of vectors, the second being, in turn, the product of a matrix by a vector. A terser representation can be obtained, involving only a product of a matrix by a vector, if *homogeneous coordinates* are introduced. The homogeneous coordinates of a *finite point*, i.e., a point whose Cartesian coordinates are finite real numbers, are grouped in a four-dimensional array  $\{\mathbf{p}\}$ , whose first three components are the Cartesian coordinates of  $P$ , the fourth being the real unity, i.e.,

$$\{\mathbf{p}\} \equiv \begin{bmatrix} \mathbf{p} \\ 1 \end{bmatrix}, \quad \{\mathbf{p}_0\} \equiv \begin{bmatrix} \boldsymbol{\pi}_0 \\ 1 \end{bmatrix} \quad (2.18)$$

where  $\{\mathbf{p}_0\}$  are the homogeneous coordinates of  $P_0$ . Now, with the aid of the above definitions and relation (2.17), the same relation can be expressed as a product of a matrix by a vector array in the form

$$\{\mathbf{p}\} = \{\mathbf{T}\}\{\mathbf{p}_0\}, \quad \{\mathbf{T}\} \equiv \begin{bmatrix} \mathbf{Q} & \mathbf{b} \\ \mathbf{0}^T & 1 \end{bmatrix} \quad (2.19)$$

where  $\{\mathbf{T}\}$  is termed a *homogeneous-transformation matrix*. Notice that homogeneous transformations, as defined above, are represented by  $4 \times 4$  matrices that involve four blocks: the upper left block is a proper orthogonal matrix, accounting for the rigid-body rotation; the upper-right three-dimensional vector block  $\mathbf{b}$ , accounting for the translation

of the landmark point  $O$ , the designated origin of frame  $\mathcal{A}$ ; the lower-left three-dimensional row block  $\mathbf{0}^T$ ; and the lower-right  $1 \times 1$  “block” that is the real unity.

It is left as an exercise to the reader to prove that homogeneous transformations form a continuous group under the operation of matrix multiplication.

Hence, with the notation introduced above, for the rigid-body displacements  $d_a$  and  $d_b$ :

- (a)  $d_a \odot d_b \in \mathcal{D}$ ;
- (b) a third displacement  $d_c$  is introduced, carrying  $\mathcal{B}$  from pose  $\mathcal{B}_b$  to pose  $\mathcal{B}_c$ . Then,  

$$d_a \odot (d_b \odot d_c) = (d_a \odot d_b) \odot d_c;$$
- (c) under no motion, any pose  $\mathcal{B}$  of a rigid body is preserved, the motion undergone by the body then being represented by a displacement  $\iota$ —read “iota”—that can be defined as the *identity element* of  $\mathcal{D}$ , such that, for any displacement  $d$ ,  $d \odot \iota = \iota \odot d = d$ ; and
- (d) for any displacement  $d$  carrying the body from pose  $\mathcal{B}_0$  to pose  $\mathcal{B}$ , the *inverse displacement*  $d^{-1}$  is defined as that bringing back the body from  $\mathcal{B}$  to  $\mathcal{B}_0$ , and hence,  

$$d \odot d^{-1} = d^{-1} \odot d = \iota.$$

From the foregoing discussion it is apparent that the set of rigid-body displacements  $\mathcal{D}$  has the algebraic structure of a group. Henceforth, we refer to the set of displacements of a rigid body as *group*  $\mathcal{D}$ . The interest in studying rigid-body displacements as algebraic groups lies in that, on the one hand,  $\mathcal{D}$  includes interesting and practical subgroups that find relevant applications in the design of production-automation and prosthetic devices. On the other hand, the same subgroups can be *combined* to produce novel mechanical layouts that would be insurmountably difficult to produce by sheer intuition. The combination of subgroups, in general, can take place via the standard set operations of *union* and *intersection*. As we shall see, however, the set defined as that comprising the elements of two displacement subgroups is not necessarily a subgroup, and hence, one cannot speak of the union of displacement subgroups. On the contrary, the intersection of two displacement subgroups is always a subgroup itself, and hence, the *intersection of displacement subgroups* is a valid group operation.

Rather than the union of groups, what we have is the *product* of groups. Let  $\mathcal{G}_1$  and  $\mathcal{G}_2$  be two groups defined over the same binary operation  $\star$ ; if  $g_1 \in \mathcal{G}_1$  and  $g_2 \in \mathcal{G}_2$ , then the product of these two groups, represented by  $\mathcal{G}_1 \bullet \mathcal{G}_2$ , is the *set* of elements of the form  $g_1 \star g_2$ , where the order is important, for commutativity is not to be taken for granted in group theory.

The intersection of the two foregoing groups, represented by the usual set-theoretic symbol  $\cap$ , i.e.,  $\mathcal{G}_1 \cap \mathcal{G}_2$ , is the group of elements  $g$  belonging to both  $\mathcal{G}_1$  and  $\mathcal{G}_2$ , and hence, the order is not important.

### 2.5.1 Displacement Subgroups

A *subgroup*  $\mathcal{G}_s$  of a given group  $\mathcal{G}$  is a set of objects such that: (a) they all belong to  $\mathcal{G}$ , although some objects, or elements, of  $\mathcal{G}$  may not belong to  $\mathcal{G}_s$ , and (b)  $\mathcal{G}_s$  has the algebraic structure of a group. Therefore, a subgroup  $\mathcal{D}_s$  of the group of rigid-body displacements  $\mathcal{D}$  is itself a group of displacements, but may lack some rigid-body displacements. If  $\mathcal{D}$  includes elements not included in  $\mathcal{D}_s$ , then the latter is said to be a *proper subset* of the former.

The six lower kinematic pairs can be regarded as *generators* of displacement subgroups. We thus have:

- (i) The revolute pair  $R$  of axis  $\mathcal{A}$  generates the subgroup  $\mathcal{R}(\mathcal{A})$  of rotations about  $\mathcal{A}$ . Each element of this subgroup is characterized by the angle  $\phi$  of the corresponding rotation;
- (ii) the prismatic pair in the direction  $\mathbf{e}$  generates the subgroup  $\mathcal{P}(\mathbf{e})$  of translations along  $\mathbf{e}$ . Each element of  $\mathcal{P}(\mathbf{e})$  is characterized by the translation  $u$  along  $\mathbf{e}$ ;
- (iii) the screw pair of axis  $\mathcal{A}$  and pitch  $p$  generates the subgroup  $\mathcal{H}(\mathcal{A}, p)$  of rotations  $\phi$  about  $\mathcal{A}$  and translations  $u$  along the direction of the same axis, translations and rotations being related by the pitch  $p$  in the form  $u = p\phi$ , as described when the screw pair was introduced. Each element of  $\mathcal{H}(\mathcal{A}, p)$  can thus be characterized either by  $u$  or by  $\phi$ ;
- (iv) the cylindrical pair of axis  $\mathcal{A}$  generates the subgroup  $\mathcal{C}(\mathcal{A})$  of independent rotations about and translations along  $\mathcal{A}$ . Each element of  $\mathcal{C}(\mathcal{A})$  is thus characterized by both the displacement  $u$  and the rotation  $\phi$ ;
- (v) the planar pair generates the subgroup  $\mathcal{F}(\mathbf{u}, \mathbf{v})$  of two independent translations in the directions of the *distinct* unit vectors  $\mathbf{u}$  and  $\mathbf{v}$ , and one rotation about an axis normal to both  $\mathbf{u}$  and  $\mathbf{v}$ . Each element of  $\mathcal{F}(\mathbf{u}, \mathbf{v})$  is thus characterized by the two translations  $t_u$ ,  $t_v$  and the rotation  $\phi$ ;
- (vi) the spherical pair generates the subgroup  $\mathcal{S}(O)$  of rotations about point  $O$ . Each element of  $\mathcal{S}(O)$ , a rotation about  $O$ , is characterized by the axis of rotation passing through  $O$  in the direction of a unit vector  $\mathbf{e}$  and through an angle  $\phi$ . Alternatively, each rotation about  $O$  can be characterized by the independent rotations about three designated axes, e.g., the well-known Euler angles.

Besides the six foregoing subgroups, we can define six more, namely,

- (vii) The *identity subgroup*  $\mathcal{I}$ , whose single element is the identity displacement  $\iota$  introduced above;

- (viii) the *planar-translation subgroup*  $\mathcal{T}_2(\mathbf{u}, \mathbf{v})$  of translations in the directions of the two distinct unit vectors  $\mathbf{u}$  and  $\mathbf{v}$ . Each element of this group is thus characterized by two translations,  $t_u$  and  $t_v$ ;
- (ix) the *translation subgroup*  $\mathcal{T}_3$  of translations in  $\mathcal{E}$ , each element of which is characterized by three independent translations  $t_u$ ,  $t_v$ , and  $t_w$ ;
- (x) the subgroup  $\mathcal{Y}(\mathbf{e}, p) = \mathcal{T}_2(\mathbf{u}, \mathbf{v}) \bullet \mathcal{H}(\mathcal{A}, p)$ , with  $\mathbf{u} \times \mathbf{v} = \mathbf{e} \parallel \mathcal{A}$  of motions allowed by a screw of pitch  $p$  and axis parallel to  $\mathbf{e}$  undergoing arbitrary translations in a direction normal to  $\mathbf{e}$ . Each element of this subgroup is thus characterized by the two independent translations  $t_u$ ,  $t_v$  of the axis, and either the rotation  $\phi$  about this axis or the translation  $t_w$  along the axis. Faute-de-mieux, we shall call this subgroup the *translating-screw group*;
- (xi) the subgroup  $\mathcal{X}(\mathbf{e}) = \mathcal{F}(\mathbf{e}) \bullet \mathcal{P}(\mathbf{e})$ , resulting of the product of the planar subgroup of plane normal to  $\mathbf{e}$  and the prismatic subgroup of direction  $\mathbf{e}$ . Each element of this subgroup is thus characterized by the two translations  $t_u$ ,  $t_v$  and the angle  $\phi$  of the planar subgroup plus the translation  $t_w$  in the direction of  $\mathbf{e}$ . Moreover, note that  $\mathcal{F}(\mathbf{e}) \bullet \mathcal{P}(\mathbf{e}) = \mathcal{P}(\mathbf{e}) \bullet \mathcal{F}(\mathbf{e})$ . This subgroup, named after the German mathematician and mineralogist Arthur Moritz Schönflies (1853–1928), is known as the *Schönflies subgroup*, and is generated most commonly by what is known as SCARA systems, for *Selective-Compliance Assembly Robot Arm*;
- (xii) the group  $\mathcal{D}$  itself. Each element of this subgroup is characterized by three independent translations and three independent rotations.

It is thus apparent that each subgroup includes a set of displacements with a specific *degree of freedom*. We shall need below an extension of the concept of dof, for which reason we term the dof of each subgroup its *dimension*, and denote the dimension of any subgroup  $\mathcal{G}_s$  by  $\dim[\mathcal{G}_s]$ . Thus,

$$\dim[\mathcal{I}] = 0 \tag{2.20a}$$

$$\dim[\mathcal{R}(\mathcal{A})] = \dim[\mathcal{P}(\mathbf{e})] = \dim[\mathcal{H}(\mathcal{A}, p)] = 1 \tag{2.20b}$$

$$\dim[\mathcal{T}_2(\mathbf{u}, \mathbf{v})] = \dim[\mathcal{C}(\mathcal{A})] = 2 \tag{2.20c}$$

$$\dim[\mathcal{T}_3] = \dim[\mathcal{F}(\mathbf{e})] = \dim[\mathcal{S}(O)] = \dim[\mathcal{Y}(\mathbf{e}, p)] = 3 \tag{2.20d}$$

$$\dim[\mathcal{X}(\mathbf{e})] = 4 \tag{2.20e}$$

$$\dim[\mathcal{D}] = 6 \tag{2.20f}$$

The foregoing list of *twelve* displacement subgroups is *exhaustive*, none of which is of dimension five. The reader may wonder whether displacement products are missing from the list that might be subgroups. However, any displacement product not appearing in

the above list *is not a subgroup*. As a matter of fact, any set of displacements including rotations about *two axes*, and no more than two, fails to have a group structure. Consider, for example, the set of rotations  $\mathcal{W}$  produced by a (two-dof) *pitch-roll wrist* (PRW), as depicted in Fig. 2.9. With reference to this figure, frame  $\mathcal{F}_0$ , serving as the *reference*

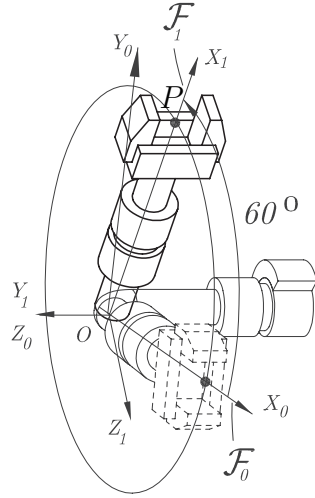


Figure 2.9: A pitch-roll wrist producing a first rotation

*frame*, is defined with  $X_0$  along the roll axis, passing through the *operation point*  $P$ , while  $Z_0$  is defined along the pitch axis.

Now we introduce a first rotation  $\mathbf{Q}_1$  (not a coordinate transformation!): Define  $\mathcal{F}_1$  with  $X_1$  along the displaced roll axis, passing through  $P$  in the displaced pose of the end-effector (EE), and making an angle of  $60^\circ$  with  $X_0$ ,  $Z_1$  lying in the  $X_0$ - $Y_0$  plane, and making an angle of  $-30^\circ$  with  $X_0$ , when measured in the direction of  $Z_0$ . Matrix  $\mathbf{Q}_1$ , rotating  $\mathcal{F}_0$  into  $\mathcal{F}_1$  as illustrated in Fig. 2.9, is obtained, in  $\mathcal{F}_0$ -coordinates, upon assigning to its first column the  $\mathcal{F}_0$ -components of the unit vector  $\mathbf{i}_1$ , parallel to  $X_1$ , its second column being given by the  $\mathcal{F}_0$ -components of the unit vector  $\mathbf{j}_1$ , parallel to  $Y_1$ ; its third column follows the same pattern<sup>3</sup>. The rotation  $\mathbf{Q}_1$  carrying  $\mathcal{F}_0$  into  $\mathcal{F}_1$  as depicted in Fig. 2.9 is, hence,

$$\mathbf{Q}_1 = \begin{bmatrix} 1/2 & 0 & \sqrt{3}/2 \\ \sqrt{3}/2 & 0 & -1/2 \\ 0 & 1 & 0 \end{bmatrix} \quad (2.21a)$$

Next, we introduce a second rotation  $\mathbf{Q}_2$ : Define a new frame  $\mathcal{F}_2$  with  $X_2$  along the displaced roll axis, passing through  $P$  in the displaced pose of the EE, and making an angle of  $30^\circ$  with  $X_0$ , when measured in the direction of  $Z_0$ ,  $Z_2$  coinciding with  $Z_0$ . Hence, in  $\mathcal{F}_0$ -coordinates as well,

---

<sup>3</sup>The matrix transforming  $\mathcal{F}_0$ -coordinates into  $\mathcal{F}_1$ -coordinates is  $\mathbf{Q}_1^T$ .

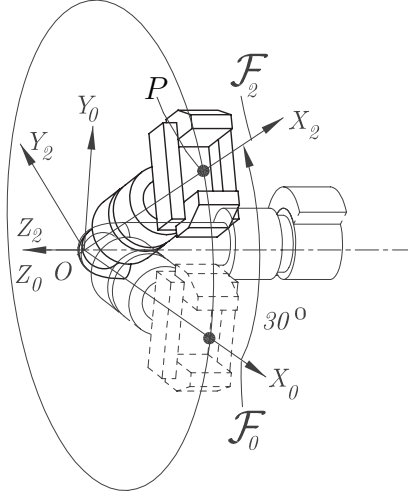


Figure 2.10: A pitch-roll wrist producing a second rotation

$$\mathbf{Q}_2 = \begin{bmatrix} \sqrt{3}/2 & -1/2 & 0 \\ 1/2 & \sqrt{3}/2 & 0 \\ 0 & 0 & 1 \end{bmatrix} \quad (2.21b)$$

Moreover, let  $\mathbf{Q}_3 = \mathbf{Q}_1\mathbf{Q}_2$ , a third rotation obtained as the product of the first two, namely,

$$\mathbf{Q}_3 = \begin{bmatrix} \sqrt{3}/4 & -1/4 & \sqrt{3}/2 \\ 3/4 & -\sqrt{3}/4 & -1/2 \\ 1/2 & \sqrt{3}/2 & 0 \end{bmatrix} \quad (2.21c)$$

which yields a third attitude of the EE, as depicted in Fig. 2.11.

We note that, in an arbitrary configuration, the roll axis remains normal to  $Z_0$ . Hence, any rotation produced by the PRW takes the EE to a pose in which the roll axis is normal to  $Z_0$ , i.e., the set of possible displaced configurations of the roll axis is a pencil of lines passing through the origin and normal to  $Z_0$ . The roll axis in the displaced pose of the EE thus lies in the  $X_0$ - $Y_0$  plane. Any EE pose whereby the roll axis lies outside of the  $X_0$ - $Y_0$  plane is attained by a rotation *outside* of  $\mathcal{W}$ .

As it turns out, the roll axis is carried by  $\mathbf{Q}_3$  into a configuration parallel to  $\mathbf{i}_3$ , the image of  $\mathbf{i}_0$  under  $\mathbf{Q}_3$ , as depicted in Fig. 2.11, i.e.,

$$\mathbf{i}_3 = \mathbf{Q}_3\mathbf{i}_0 = [\sqrt{3}/4 \quad 3/4 \quad 1/2]^T \quad (2.22)$$

which, apparently, is not normal to  $Z_0$ —its  $Z_0$ -component is  $1/2 \neq 0$ —and, hence,  $\mathbf{Q}_3$  lies outside of the set  $\mathcal{W}$  of feasible rotations produced by the PRW. Therefore, the set of rotations produced by a PRW does not have the algebraic structure of a group.

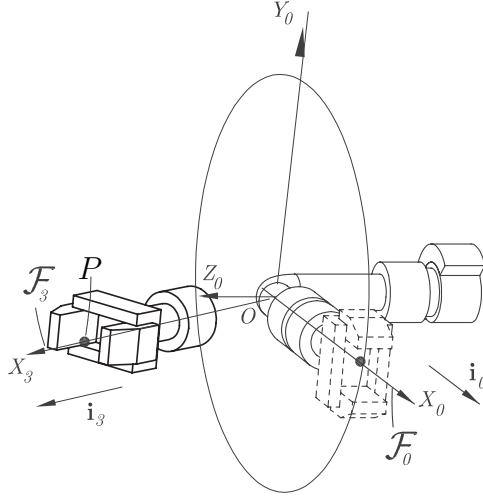


Figure 2.11: The EE of a pitch-roll wrist undergoing a third, unfeasible, rotation

## 2.6 Kinematic Bonds

Displacement subgroups can be combined to produce new sets of displacements that may or may not be displacement subgroups themselves. To combine subgroups, we resort to the group operations of product ( $\bullet$ ) and intersection ( $\cap$ ).

Now we introduce the concept of *kinematic bond*, which is a generalization of kinematic pair, as first proposed by Hervé (1978), who called this concept *liaison cinématique* in French. This concept has been termed *kinematic liaison* (Angeles, 1982) or *mechanical connection* (Hervé, 1999) in English. Since “liaison” in English is usually applied to human relations, the term “bond” seems more appropriate, and is thus adopted here.

We illustrate the concept with an example: Let us assume three links, numbered from 1 to 3, and coupled by two kinematic pairs generating the two subgroups  $\mathcal{G}_1$  and  $\mathcal{G}_2$ , where these two subgroups are instanced by specific displacement subgroups below. We then have

$$\mathcal{G}_1 \bullet \mathcal{G}_2 = \mathcal{R}(\mathcal{A}) \bullet \mathcal{P}(\mathbf{e}) = \mathcal{C}(\mathcal{A}), \quad \text{for } \mathbf{e} \parallel \mathcal{A} \quad (2.23a)$$

$$\mathcal{G}_1 \bullet \mathcal{G}_2 = \mathcal{R}(\mathcal{A}) \bullet \mathcal{T}_2(\mathbf{u}, \mathbf{v}) = \mathcal{F}(\mathbf{e}), \quad \text{for } \mathbf{e}, \mathcal{A} \perp \mathbf{u}, \mathbf{v} \quad (2.23b)$$

$$\mathcal{G}_1 \bullet \mathcal{G}_2 = \mathcal{R}(\mathcal{A}) \bullet \mathcal{R}(\mathcal{B}) = \mathcal{L}(1, 3) \quad (2.23c)$$

$$\mathcal{G}_1 \cap \mathcal{G}_2 = \mathcal{R}(\mathcal{A}) \cap \mathcal{C}(\mathcal{A}) = \mathcal{R}(\mathcal{A}) \quad (2.23d)$$

$$\mathcal{G}_1 \cap \mathcal{G}_2 = \mathcal{R}(\mathcal{A}) \cap \mathcal{S}(O) = \mathcal{R}(\mathcal{A}), \quad \text{for } O \in \mathcal{A} \quad (2.23e)$$

$$\mathcal{G}_1 \cap \mathcal{G}_2 = \mathcal{R}(\mathcal{A}) \cap \mathcal{P}(\mathbf{e}) = \mathcal{I}, \quad \text{for any } \mathcal{A}, \mathbf{e} \quad (2.23f)$$

All of the above examples, except for the third one, amount to a displacement subgroup. This is why no subgroup symbol is attached to that set. Instead, we have used the symbol  $\mathcal{L}(1, 3)$  to denote the kinematic bond between the first and third links of the

chain. In general, a kinematic bond between links  $i$  and  $n$  of a kinematic chain, when no ambiguity is possible, is denoted by  $\mathcal{L}(i, n)$ . When the chain connecting these two links is not unique, such as in a closed chain, where these two links can be regarded as connected by two possible *paths*, a subscript will be used, e.g.,  $\mathcal{L}_I(i, j)$ ,  $\mathcal{L}_{II}(i, j)$ , etc. A kinematic bond is, thus, a set of displacements, as stemming from a binary operation of displacement subgroups, although the bond itself need not be a subgroup. Obviously, the 12 subgroups described above are themselves special cases of kinematic bonds.

The kinematic bond between links  $i$  and  $n$  can be conceptualized as the product of the various subgroups associated with the kinematic pairs between the  $i$ th and the  $n$ th links. To keep the discussion general enough, we shall denote the subgroup associated with the kinematic pair coupling links  $i$  and  $i + 1$  as  $\mathcal{L}(i, i + 1)$ , with a similar notation for all other kinematic-pair subgroups. Thus,

$$\mathcal{L}(i, n) = \mathcal{L}(i, i + 1) \bullet \mathcal{L}(i + 1, i + 2) \bullet \cdots \bullet \mathcal{L}(n - 1, n) \quad (2.24)$$

For example, in a six-axis serial manipulator, like the one shown in Fig. 2.5, we can set  $i = 1$ ,  $n = 7$ , all six kinematic pairs in-between being revolutes of independent axes  $\mathcal{R}(\mathcal{A}_1), \mathcal{R}(\mathcal{A}_2), \dots, \mathcal{R}(\mathcal{A}_6)$ . Then,

$$\mathcal{L}(1, 7) = \mathcal{D}$$

That is, the manipulator is a generator of the general six-dimensional group of rigid-body displacements  $\mathcal{D}$ .

As an example of group-intersection, let us consider the *Sarrus mechanism*, depicted in Fig. 2.12.

A less common realization of the Sarrus mechanism is depicted in Fig. 2.13. This is a  $\Pi\Pi\Pi\Pi$  closed kinematic chain, modelled as a *compliant mechanism*, which bears a *monolithic* structure, made of a polymer. The R joints of the mechanism are realized by removing material at the joint locations, so as to render these areas much more compliant than the other areas. The mechanism is designed so as to serve as a uniaxial accelerometer.

In the Sarrus mechanism of Fig. 2.12, we have six links, coupled by six revolute pairs. Moreover, the revolute pairs occur in two triplets, each on one leg of the mechanism. The axes of the three revolute pairs of each leg are parallel to each other. The bond  $\mathcal{L}(1, 4)$ , apparently, is not unique, for it can be defined by traversing any of the two legs. Let the leg of links 1, 2, 3 and 4, coupled by revolutes of axes parallel to the unit vector  $\mathbf{u}$ , be labelled  $I$ ; the other leg, of links 4, 5, 6 and 1, coupled by revolutes of axes parallel to the unit vector  $\mathbf{v}$ , is labelled  $II$ . It is apparent that, upon traversing leg  $I$ , we obtain

$$\mathcal{L}_I(1, 4) = \mathcal{F}(\mathbf{u})$$

Moreover, upon traversing leg  $II$ ,

$$\mathcal{L}_{II}(1, 4) = \mathcal{F}(\mathbf{v})$$

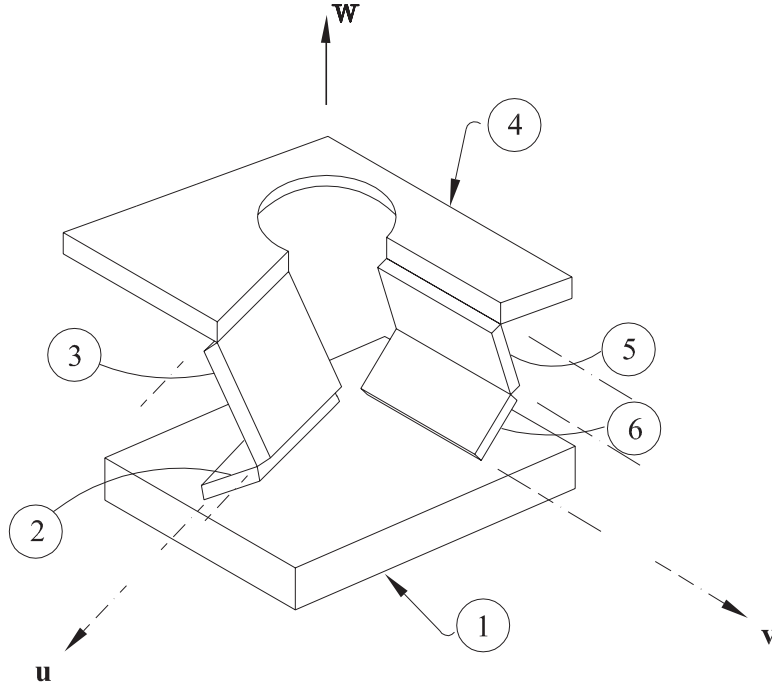


Figure 2.12: The Sarrus mechanism

That is, leg  $I$  is a generator of the planar subgroup  $\mathcal{F}$  of plane normal to vector  $\mathbf{u}$ , while leg  $II$  is that of the subgroup  $\mathcal{F}$  of plane normal to vector  $\mathbf{v}$ . Therefore, the intersection  $\mathcal{L}_I(1, 4) \cap \mathcal{L}_{II}(1, 4)$  is the set of displacements common to the two  $\mathcal{F}$ -subgroups, namely, the prismatic subgroup of translations in the direction  $\mathbf{w} = \mathbf{v} \times \mathbf{u}$ , i.e.,

$$\mathcal{L}_I(1, 4) \cap \mathcal{L}_{II}(1, 4) = \mathcal{P}(\mathbf{w})$$

The Sarrus mechanism is thus a revolute realization of the prismatic joint.

## 2.7 The Chebyshev-Grübler-Kutzbach-Hervé Formula

Finding the degree of freedom (dof)  $f$  of a given kinematic chain has been an elusive task for over a century. Here we adopt the methodology proposed by Hervé (1978), based on the concept of *groups of displacements*.

Essentially, Hervé considers whether the *topology* of a kinematic chain suffices to predict its dof or not. The topology of a kinematic chain pertains to the numbers of links and joints as well as their layouts, regardless of the values of the geometric parameters of the chain, such as distances and angles between pair axes and the like. According to Hervé (1978), kinematic chains can be classified in three categories, based on their mobility:

- (a) *Trivial*, when all the possible kinematic bonds between any pair of links is a subset

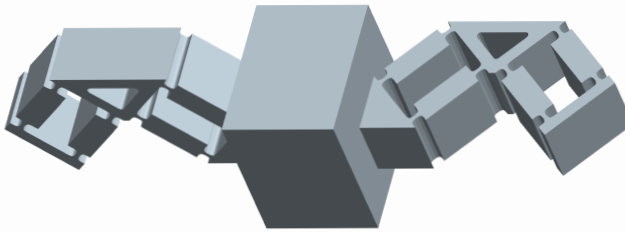


Figure 2.13: An alternative realization of the Sarrus mechanism

of one particular subgroup of  $\mathcal{D}$ , including  $\mathcal{D}$  itself, but excluding  $\mathcal{I}$ . When the common subgroup of interest is  $\mathcal{D}$  itself, the chain is trivial if the product of the subgroups of all the foregoing kinematic pairs yields  $\mathcal{D}$ . The dof of a trivial kinematic chain can be determined with the aid of the formula derived below, which takes into account only the topology of the chain. **Caveat: An algorithm to decide, with knowledge only of the topology of a linkage, whether the linkage is trivial, is still to be devised.**

- (b) If the chain (i) is not trivial; (ii) all its possible kinematic bonds between any pair of its links form a subset  $\mathcal{D}_s$  of  $\mathcal{D}$  that does not bear the group property; and (iii) the bond between two of its links can be expressed as the *intersection*  $\mathcal{D}_g$  of a number of kinematic bonds that is a subgroup of  $\mathcal{D}$ , then the chain is said to be *exceptional*. In this case, the dof of the chain is the dimension of  $\mathcal{D}_g$ .
- (c) *paradoxical*, when the topology of the kinematic chain alone does not suffice to determine the chain dof. In this case, special relations among the various geometric parameters of the chain yield a mobility that would be absent under general values of those parameters, for the same topology.

### 2.7.1 Trivial Chains

Regarding trivial chains, let  $\mathcal{G}_m$  be the subgroup of the *least dimension*  $d_m$ , containing all possible bonds between any pair of links of the chain.  $\mathcal{G}_m$  can thus be thought of as a kind of *least common multiple* of all possible bonds of the chain. Moreover, let  $d_i$  be the

dimension of the subgroup associated with the  $i$ th kinematic pair, and  $r_i \equiv d_m - d_i$  be its degree of constraint, termed its *restriction* for brevity. In determining the dof of a chain, we are interested in the *relative* motion capability of the chain, and hence, we consider arbitrarily one link *fixed*. It is immaterial which specific link is the designated fixed one. If the chain is composed of  $l$  links and  $p$  kinematic pairs, then its dof  $f$  is given by the difference between its total dof before coupling and the sum of its restrictions, i.e.,

$$f = d_m(l - 1) - \sum_{i=1}^p r_i \quad (2.25)$$

The above relation can be termed a *generalized Chebyshev-Grübler-Kutzbach* (CGK) formula in that it generalizes the concept involved in parameter  $d_m$  above. Conventional CGK formulas usually consider that  $d_m$  can attain one of two possible values, 3 for planar and spherical chains and 6 for spatial chains. In the generalized formula,  $d_m$  can attain any of the values 2, 3, 4, or 6. Moreover, rather than considering only three subgroups of displacements, we consider all 12 described above, none of which is of dimension five.

As an example of the application of the above formula, we consider the *vise mechanism*, displayed in Fig. 2.14. In that figure, we distinguish three links and three LKPs. The links are the frame 1, the crank 2 and the slider 3, which define three bonds, namely,

$$\mathcal{L}(1, 2) = \mathcal{R}(\mathcal{A}), \quad \mathcal{L}(2, 3) = \mathcal{H}(\mathcal{A}), \quad \mathcal{L}(3, 1) = \mathcal{P}(\mathbf{a})$$

in which  $\mathcal{A}$  is the common axis of the R and the H pairs, while  $\mathbf{a}$  is the unit vector parallel to  $\mathcal{A}$ . In this case, it is apparent that all three bonds lie in the  $\mathcal{C}(\mathcal{A})$  subgroup, and hence,  $d_m = 2$ . Moreover, if we number the three joints in the order R, H, P, and notice that the dimension  $d_i$  associated with each of the three joints is unity, then  $r_i = 1$ , for  $i = 1, 2, 3$ . Application of the generalized CGK formula (2.25) yields

$$f = 2(3 - 1) - 3 \times 1 = 4 - 3 = 1$$

which is indeed the correct value of the vise dof.

While the generalized CGK formula is more broadly applicable and less error-prone than its conventional counterpart, it is not error-free. Indeed, let us consider the HHHRRH closed chain of Fig. 2.15, first proposed by Hervé (1978). The four H pairs of this figure have distinct pitches.

It is apparent that all links move in parallel planes, and that these planes also translate along their common normal direction. The displacement subgroup containing all possible kinematic bonds of the mechanism under study, of minimum dimension, is thus the Schönflies subgroup  $\mathcal{X}(\mathbf{u})$ , and hence,  $d_m = 4$ . Since we have six links and six joints, each of restriction  $r_i = d_m - f_i$ , for  $f_i = 1$  and  $i = 1, \dots, 6$ , the dof of the mechanism is obtained from the CGK formula as

$$f = 4(6 - 1) - 6 \times 3 = 2$$

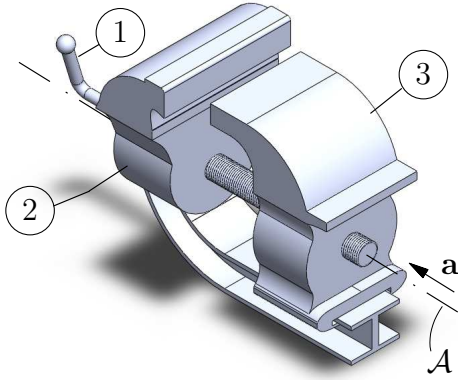


Figure 2.14: The well-known vise mechanism

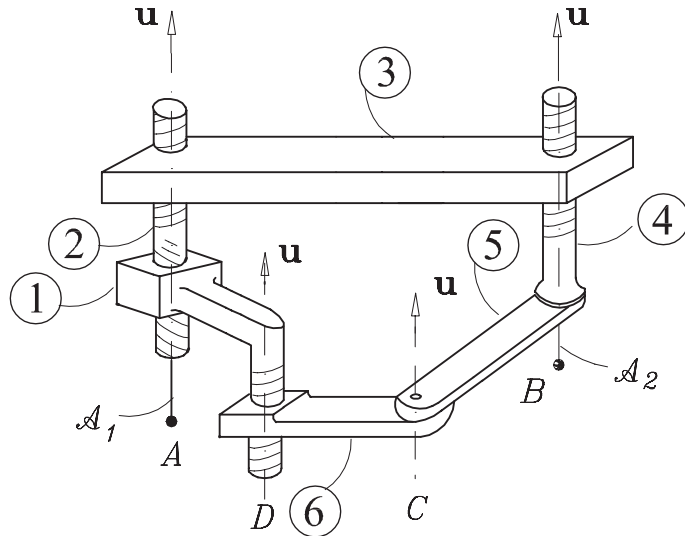


Figure 2.15: The HHHRRH mechanism

However, the above result is wrong, for it predicts a too large dof. Indeed, the mechanism has one idle dof, as can be readily shown by means of a bond analysis: Let us compute  $\dim[\mathcal{L}(1, 5)]$ :

$$\mathcal{L}(1, 5) = \underbrace{\mathcal{L}(1, 2) \bullet \mathcal{L}(2, 3)}_{\mathcal{C}(\mathcal{A}_1)} \bullet \underbrace{\mathcal{L}(3, 4) \bullet \mathcal{L}(4, 5)}_{\mathcal{C}(\mathcal{A}_2)}$$

where  $\mathcal{A}_1$  and  $\mathcal{A}_2$  are axes parallel to vector  $\mathbf{u}$  and pass through points  $A$  and  $B$ , respectively, of Fig. 2.15. Now we find the above-mentioned idle dof. To this end, we compute  $\dim[\mathcal{L}(1, 5)]$ , which may appear to be the sum of the dimensions of the two subgroups,  $\mathcal{C}(\mathcal{A}_1)$  and  $\mathcal{C}(\mathcal{A}_2)$ . However, notice that these two subgroups include one common translation along  $\mathbf{u}$ , and hence, in computing the said dimension, care should be taken in not counting this translation twice. What this means is that the dimension of the intersection



Figure 2.16: A five-point automotive suspension

of the above two factors must be subtracted from the sum of their dimensions, i.e.,

$$\dim[\mathcal{L}(1, 5)] = \dim[\mathcal{C}(\mathcal{A}_1)] + \dim[\mathcal{C}(\mathcal{A}_2)] - \dim[\mathcal{C}(\mathcal{A}_1) \cap \dim[\mathcal{C}(\mathcal{A}_2)] = 2 + 2 - 1 = 3$$

We have thus shown that the chain entails one idle dof. In order to obtain the correct dof of the chain from the generalized CGK formula, then, the total number  $m$  of idle dof must be subtracted from the dof predicted by that formula, i.e.,

$$f = d_m(n - 1) - \sum_{i=1}^p r_i - m \quad (2.26)$$

which can be fairly called the *Chebyshev-Grübler-Kutzbach-Hervé* formula. In the case at hand,  $m = 1$ , and hence, the dof of the chain of Fig. 2.15 is unity.

**Exercise 2.7.1** *A model of an automotive five-point suspension is included in Fig. 2.16<sup>4</sup>. This system is used to support and guide the front wheels upon turning and allowing for relative motion of each wheel with respect to the vehicle chassis. By moving a front wheel on a suspension of this kind while the vehicle is lifted from ground, it is possible to realize that the suspension has one single degree of freedom. Moreover, the mechanical system in question includes one fixed base, the chassis, one mobile platform, the metal frame on which the wheel is mounted, chassis and frame coupled by five links by means of S joints.*

- (i) Produce a graph representation of the suspension linkage;
- (ii) Determine the degree of freedom of the linkage.

---

<sup>4</sup>Taken from (Plecnik and McCarthy, 2013)

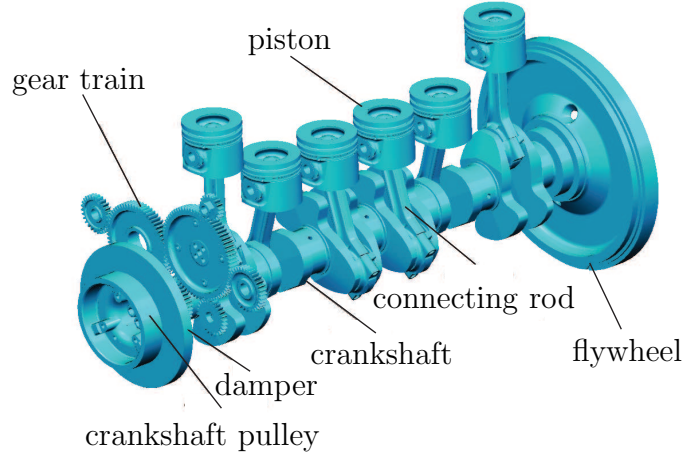


Figure 2.17: The slider-crank mechanism as a key component of an internal combustion engine: a power-generation system with six cylinders in line (courtesy of MMM International Motores, Campinas, Brazil)

### 2.7.2 Exceptional Chains

The Sarrus mechanism of Figs. 2.12 and 2.13 is an example of an exceptional chain. Indeed, all its links undergo motions of either one of two planar subgroups,  $\mathcal{F}(\mathbf{u})$  and  $\mathcal{F}(\mathbf{v})$ . Moreover, the product of these two subgroups does not yield the group  $\mathcal{D}$ —notice that the linkage has two sets of R pairs, each parallel to a distinct unit vector,  $\mathbf{u}$  or  $\mathbf{v}$ . The dof of this mechanism can still be found, but not with the aid of the CGK formula of eq.(2.25), for all its kinematic bonds do not belong to the same subgroup of  $\mathcal{D}$ . This dof is found, rather, as the dimension of the intersection of the two foregoing subgroups, i.e.,

$$f = \dim[\mathcal{F}(\mathbf{u}) \cap \mathcal{F}(\mathbf{v})] = \dim[\mathcal{P}(\mathbf{u} \times \mathbf{v})] = 1$$

Another example of exceptional chain is the familiar slider-crank mechanism of internal combustion engines and compressors, as shown in Fig. 2.17. It is customary to represent this mechanism as a planar RRRP mechanism. However, a close look at the coupling of the piston with its chamber reveals that this coupling is not via a prismatic, but rather via a cylindrical pair. It is thus apparent that the displacements of all the links lie not in one single subgroup of  $\mathcal{D}$ , but rather in a subset that can be decomposed into two kinematic bonds, which happen to be subgroups of  $\mathcal{D}$ , the  $\mathcal{F}(\mathbf{e})$  subgroup of motions generated by the RRR subchain and the  $\mathcal{C}(\mathcal{A})$  subgroup of the piston-chamber coupling  $\mathbf{C}$ . Here,  $\mathcal{A}$  is the axis of the cylindrical chamber and  $\mathbf{e}$  is the unit vector parallel to the axes of the three R pairs. Apparently, the product of these two subgroups does not generate all of  $\mathcal{D}$ , for it is short of rotations about an axis normal to both  $\mathbf{e}$  and  $\mathcal{A}$ . Nevertheless, the dof of this chain can be determined as the dimension of the intersection of the two subgroups,

i.e.,

$$f = \dim[\mathcal{F}(\mathbf{e}) \cap \mathcal{C}(\mathcal{A})] = \dim[\mathcal{P}(\mathbf{u})] = 1, \quad \mathbf{u} \parallel \mathcal{A}$$

Now, why would such a simple planar mechanism—the slider-crank—as portrayed in elementary books on mechanisms, be built with a spatial structure? The answer to this question lies in the *assemblability* of the mechanism: a planar RRRP mechanism requires a highly accurate machining of the crankshaft, connecting rod, piston and chamber, in order to guarantee that the axes of the three R pairs are indeed parallel and that the axis of the cylindrical chamber is normal to the three R axes, which is by no means a simple task!

One more example of exceptional chain is the parallel robot of Fig. 2.18, consisting of four identical limbs that join a base  $A_I A_{II} A_{III} A_{IV}$  with a moving plate  $D_I D_{II} D_{III} D_{IV}$ . Each limb, moreover, is a PRIIRR chain (Altuzarra et al., 2009).

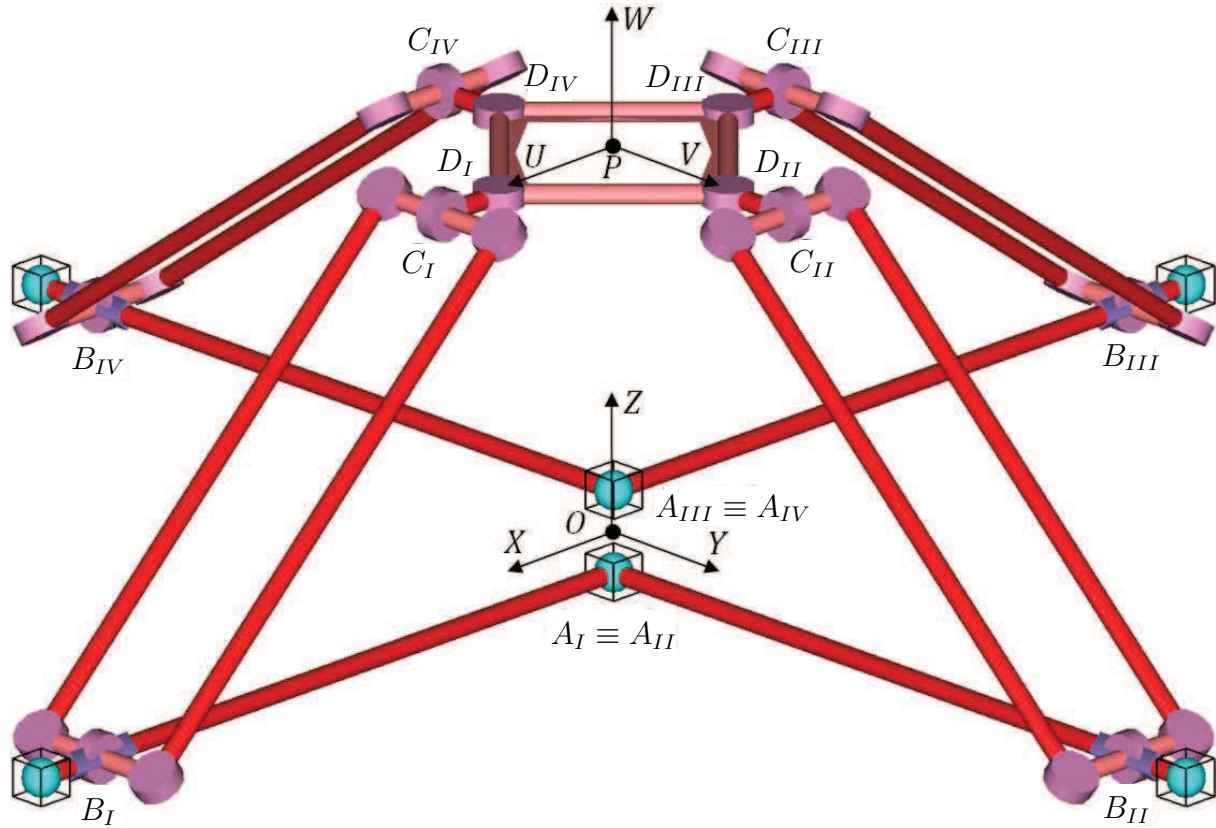


Figure 2.18: The Schönflies-motion generator developed at the University of the Basque Country, in Bilbao, Spain

The kinematic chain thus contains five joints per limb and 18 links: the base plate, the mobile plate and four intermediate links per limb. If the CGK formula is applied for the general kinematic chain, with  $d_m = 6$ ,  $l = 18$ ,  $r_i = 5$ , for  $i = 1, \dots, 18$ , the dof  $f$  thus resulting turns out to be

$$f = 6(18 - 1) - 20 \times 5 = 102 - 100 = 2$$

which is not what the authors claim, namely, four. In order to elucidate the apparent contradiction, we conduct below a group-theoretic analysis of the chain mobility: first, let  $\mathcal{R}(P, \mathbf{e})$  denote the subgroup generated by a R joint of axis passing through point  $P$  and parallel to the unit vector  $\mathbf{e}$ ; then, let  $\mathcal{L}_J$  denote the kinematic bond of the  $J$ th limb, which is the product of five simple bonds, each with a dimension equal to one, namely,

1. Either the prismatic subgroup  $\mathcal{P}(\mathbf{i})$  of displacements parallel to  $\mathbf{i}$ , for  $J = I, III$ , or its counterpart  $\mathcal{P}(\mathbf{j})$  of displacements parallel to  $\mathbf{j}$ , for  $J = II, IV$ ;
2. the rotation subgroup  $\mathcal{R}(B_J, \mathbf{j})$ , of axis of rotation passing through point  $B_J$  and parallel either to  $\mathbf{j}$ , for  $J = I, III$ , or its counterpart  $\mathcal{R}(B_J, \mathbf{i})$ , for  $J = II, IV$ ;
3. the subset of displacements  $\mathcal{D}_{\Pi}(\mathbf{n}_J)$  associated with the  $\Pi$ -joint, characterized by translations along circles of radius  $\overline{B_J C_J}$  lying in the plane of the  $J$ th parallelogram, of normal  $\mathbf{n}_J$ ;
4. the rotation subgroup  $\mathcal{R}(C_J, \mathbf{j})$ , of axis of rotation passing through point  $C_J$  and parallel either to  $\mathbf{j}$ , for  $J = I, III$  or to  $\mathbf{i}$  for  $J = II, IV$ ;
5. the rotation subgroup  $\mathcal{R}(D_J, \mathbf{k})$  of axis of rotation passing through  $D_J$  and parallel to  $\mathbf{k}$ .

Therefore,

$$\mathcal{L}_J = \underbrace{\mathcal{P}(\mathbf{i}) \bullet \mathcal{R}(B_J, \mathbf{j}) \bullet \mathcal{D}_{\Pi}(\mathbf{n}_J) \bullet \mathcal{R}(C_J, \mathbf{j})}_{\mathcal{X}(\mathbf{j})} \bullet \mathcal{R}(D_J, \mathbf{k}) = \mathcal{X}(\mathbf{j}) \bullet \mathcal{R}(D_J, \mathbf{k}), \quad J = I, III$$

Likewise,

$$\mathcal{L}_J = \mathcal{X}(\mathbf{i}) \bullet \mathcal{R}(D_J, \mathbf{k}), \quad J = II, IV$$

Notice that none of the four bonds derived above is a subgroup of  $\mathcal{D}$ , which disqualifies the multiloop kinematic chain from being trivial. However, notice also that

$$\mathcal{X}(\mathbf{j}) \bullet \mathcal{R}(D_J, \mathbf{k}) = \mathcal{X}(\mathbf{k}) \bullet \mathcal{R}(C_J, \mathbf{j}), \quad J = I, III$$

and

$$\mathcal{X}(\mathbf{i}) \bullet \mathcal{R}(D_J, \mathbf{k}) = \mathcal{X}(\mathbf{k}) \bullet \mathcal{R}(C_J, \mathbf{i}), \quad J = II, IV$$

Therefore,

$$\mathcal{L}_J \cap \mathcal{L}_K = \mathcal{X}(\mathbf{k}), \quad J, K = I, \dots, IV, \quad J \neq K$$

thereby proving that, indeed, the intersection of all limb bonds is a subgroup of  $\mathcal{D}$ , namely, the Schönflies subgroup  $\mathcal{X}(\mathbf{k})$ . The dof  $f$  of the robot at hand is, thus,

$$f = \dim[\mathcal{X}(\mathbf{k})] = 4$$

and, according to Hervé's classification, the multiloop chain can be considered exceptional.

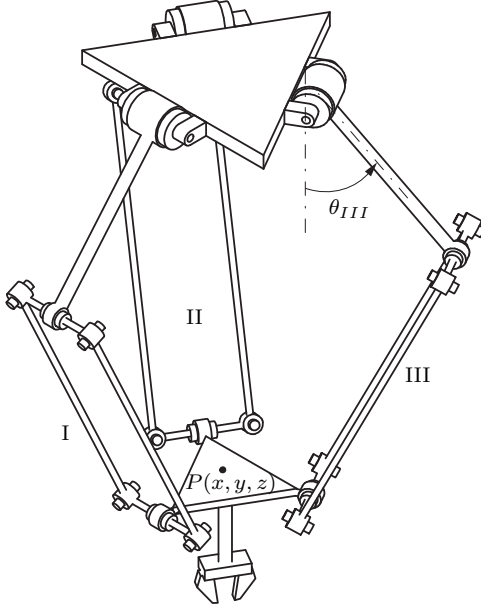


Figure 2.19: Kinematic chain of the Clavel Delta robot

### 2.7.3 Paradoxical Chains

Examples of paradoxical chains are well documented in the literature (Bricard, 1927; Angeles, 1982). These include the *Bennett mechanism* and the *Bricard mechanism*, among others.

## 2.8 Applications to Robotics

The foregoing concepts are now applied to the *qualitative* synthesis of parallel robotic architectures. By qualitative we mean here the determination of the topology of the kinematic chain, not including the corresponding dimensions. These dimensions are found at a later stage, by means of methods of *quantitative synthesis*, which Hartenberg and Denavit (1964) term dimensional synthesis, the subject of Chs. 3–5. The full determination of the kinematic chain, including dimensions, yields what is known as the *architecture* of the robotic system at hand.

### 2.8.1 The Synthesis of Robotic Architectures and Their Drives

The first robotic architecture with  $\Pi$ -joints was proposed by Clavel in what he called the *Delta Robot* (Clavel, 1988). The kinematic chain of this robot is displayed in Fig. 2.19. Delta is a generator of the  $T_3$  displacement subgroup; it is thus capable of three-dof translations.

The kinematic chain of the Delta robot is composed of two triangular plates, the top ( $\mathcal{A}$ ) and the bottom ( $\mathcal{B}$ ) plates. The top plate supports the three (direct-drive) motors,

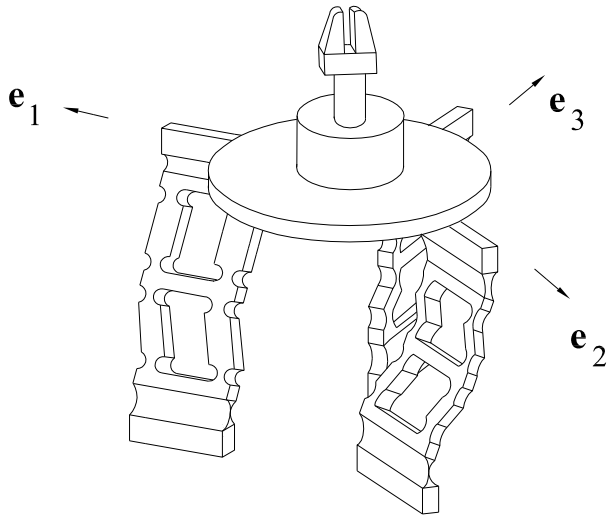


Figure 2.20: The MEL microfinger

the bottom plate the gripper, and hence, constitutes the moving-platform (MP) of the robot. The MP is capable of translating in 3D space with respect to the upper plate, which is considered fixed. The two plates are coupled by means of three legs, each with a RRIIR chain.

To be true, the  $\Pi$ -joints of the actual Delta are not composed of R joints, but rather of *orientable pin joints*, equivalent to S joints. The reason is that providing parallelism between any pair of R axes is physically impossible. To allow for *assemblability*, then, a margin of manoeuvre must be provided.

While Clavel did not cite any group-theoretical reasoning behind his ingenious design, an analysis in this framework will readily explain the principle of operation of the robot. This analysis is conducted on the ideal kinematic chain displayed in Fig. 2.19.

The  $i$ th leg is a generator of the Schönflies  $\mathcal{X}(\mathbf{e}_i)$  subgroup, with  $\mathbf{e}_i$  denoting the unit vector parallel to the axis of the  $i$ th motor. That is, the  $i$ th leg generates a Schönflies subgroup of displacements comprising translations in 3D space and one rotation about an axis parallel to  $\mathbf{e}_i$ . The subset of EE displacements is thus the intersection of the three subgroups  $\mathcal{X}(\mathbf{e}_i)$ , for  $i = 1, 2, 3$ , i.e., the subgroup  $\mathcal{T}_3$ . Therefore, the EE is capable of pure translations in 3D space. This kinematic chain is, thus, of the exceptional type.

One second applications example is the microfinger of Japan's Mechanical Engineering Laboratory (MEL) at Tsukuba (Arai et al., 1996), as displayed in Fig. 2.20. In the MEL

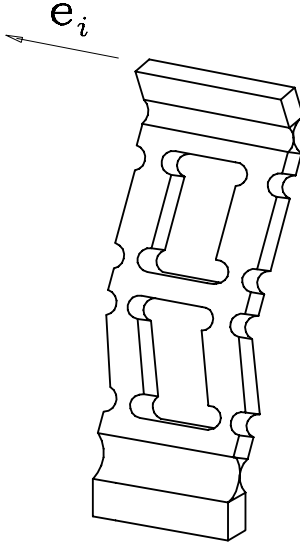


Figure 2.21: The  $i$ th leg of the MEL microfinger

design, the authors use a structure consisting of two plates that translate with respect to each other by means of three legs coupling the plates. The  $i$ th leg entails a RIIIIR chain, shown in Fig. 2.21, that generates the Schönflies subgroup in the direction of a unit vector  $\mathbf{e}_i$ , for  $i = 1, 2, 3$ . The three unit vectors, moreover, are coplanar and make angles of  $120^\circ$  pairwise. The motion of the moving plate is thus the result of the intersection of these three subgroups, which is, in turn, the  $\mathcal{T}_3$  subgroup. Moreover, the kinematic chain of each leg is made of an elastic material in one single piece, in order to allow for micrometric displacements.

Another example is the Y-Tristar robot, developed at Ecole Centrale de Paris by Hervé and Sparacino (1992). One more application of the same concepts is the four-dof SCARA-motion generator proposed by Angeles et al. (2000), and displayed in Fig. 2.22. This robot entails a kinematic chain of the RIIIRII type with two vertical revolutes and two  $\Pi$ -pairs lying in distinct, vertical planes. The Schönflies subgroup generated by this device is of vertical axis. While Delta and Y-Tristar are made up of Schönflies motion generators, the intersection of all these is the translation subgroup  $\mathcal{T}_3$ . A Schönflies motion generator with parallel architecture is possible, as shown in Fig. 2.23. This architecture is the result of coupling two identical Schönflies motion generators of the type displayed in Fig. 2.22, each generating the same Schönflies subgroup. As a result, the two-legged parallel robot generates the intersection of two identical subgroups, which is the same subgroup. Yet another application of the  $\Pi$  pair is found in the four-degree-of-freedom parallel robot patented by Company et al. (2001), and now marketed by Adept Technology, Inc. under the trade mark Quattro s650. A photograph of this robot is displayed in Fig. 2.24.

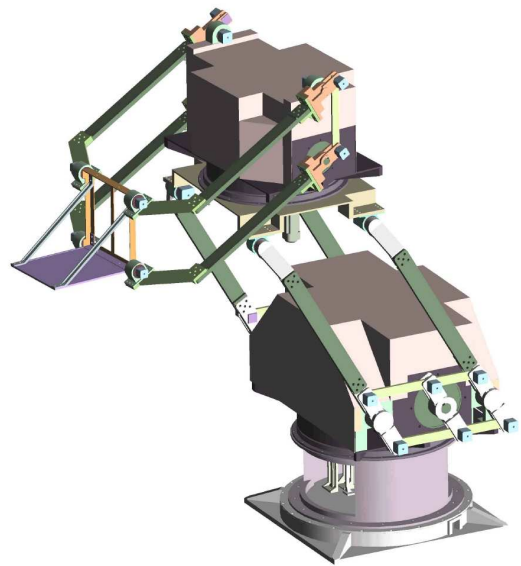


Figure 2.22: A serial Schönflies-motion generator with a RΠRΠ architecture

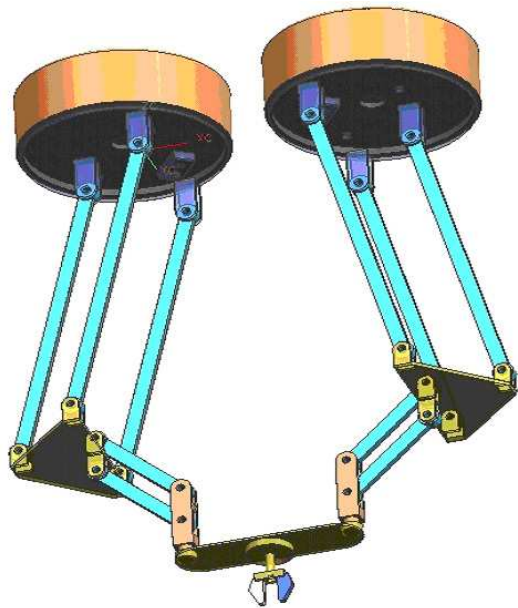


Figure 2.23: A parallel Schönflies–motion generator composed of two RΠRΠ legs



Figure 2.24: Adept Technology's Quattro robot, a parallel Schonflies-motion generator

# Chapter 3

## Function Generation

### 3.1 Introduction

Linkages are the most common means of producing a large variety of motions of a rigid body, termed the *output link*, about an axis fixed to the machine frame. In the best known applications, motion is produced by a motor, usually running at a constant rpm, and coupled by means of a speed reducer—gear train, harmonic drive, or similar—to the *input link*. Under these conditions, the input link moves at a constant speed as well. Other applications of linkages involve alternative forms of actuation, such as motors under computer control, whose motion is all but uniform, and dictated by unpredictable changes in the environment. In these cases, changes are detected by means of sensors sending their input signals to the computer generating the output signals, that are fed into the motor. Such applications fall in the realm of *mechatronic systems*.

In one more class of applications, the linkage is driven by a human actuator. Examples of this class are numerous, and sometimes taken for granted, e.g., when cutting a paper sheet with scissors, when pedalling a bicycle, etc. In the case of scissors, the two blades of this tool form a two-link open chain coupled by a R pair. When held by a user, this chain is coupled to a second, similar chain formed by the proximal phalanx of the thumb and the intermediate phalanx of the index finger, thereby forming a four-bar linkage. Likewise, in the case of a bicycle, the frame and one of the two pedals form an open chain, which couples with a second, similar chain, formed by the calf and the thigh of a human user, coupled by the R pair of the knee, thereby forming, again, a four-bar linkage.

One more application of the concepts studied in this chapter involves *parameter identification*, whereby a linkage exists but is not accessible for measurements, and we want to know its dimensions. Take the case of the subtalar and ankle-joint complex, which is known to entail a closed kinematic chain, i.e., a linkage, but its joints are not readily accessible for measurement. We can cite here a case in which a series of experiments was conducted, measuring input and output angles, from which linkage dimensions were

estimated by fitting the measurements to a linkage kinematic model (Wright et al, 1964).

## 3.2 Input-Output Functions

### 3.2.1 Planar Four-Bar Linkages

The classical problem of function generation was first formulated algebraically by Freudenstein in a seminal paper that has been recognized as the origin of modern kinematics (Freudenstein, 1955). In that paper, Freudenstein set to finding the link lengths  $\{a_i\}_1^4$  of the planar four-bar linkage displayed in Fig. 3.1 so as to obtain a prescribed relation between the angles  $\psi$  and  $\phi$ .

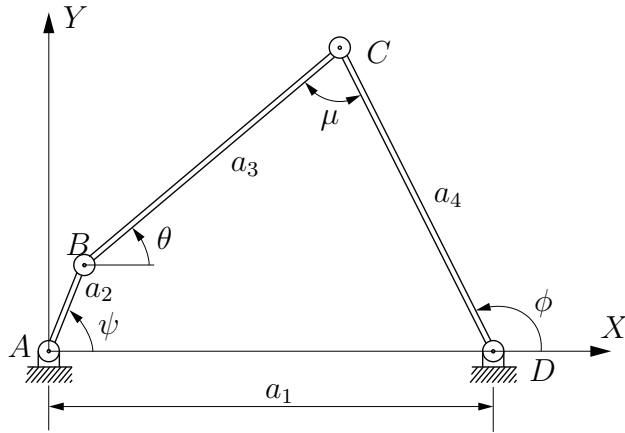


Figure 3.1: A four-bar linkage for function generation

In Fig. 3.1,  $\psi$  denotes the *input angle* of the linkage,  $\phi$  the *output angle*,  $\theta$  the *coupler angle*, and  $\mu$  the *transmission angle*, which will be studied in Section 3.6. We state below the *function-generation problem* associated with the linkage of Fig. 3.1:

*Find  $\{a_k\}_1^4$  that will allow the linkage to produce the set of  $m$  input-output pairs  $\{\psi_k, \phi_k\}_1^m$ .*

In the foregoing statement an algebraic relation between the two angles,  $\psi$  and  $\phi$ , known as the *input-output (IO) equation*, is assumed to be available in the form of an *implicit function*, namely,

$$F(\psi, \phi) = 0 \quad (3.1)$$

In formulating the input-output equation, we introduce four two-dimensional vectors, all represented in the coordinate frame of Fig. 3.1:

$$\mathbf{r}_1 \equiv \overrightarrow{AB} = a_2 \begin{bmatrix} \cos \psi \\ \sin \psi \end{bmatrix}, \quad \mathbf{r}_2 \equiv \overrightarrow{BC} = a_3 \begin{bmatrix} \cos \theta \\ \sin \theta \end{bmatrix}, \quad (3.2a)$$

$$\mathbf{r}_3 \equiv \overrightarrow{AD} = a_1 \begin{bmatrix} 1 \\ 0 \end{bmatrix}, \quad \mathbf{r}_4 \equiv \overrightarrow{DC} = a_4 \begin{bmatrix} \cos \phi \\ \sin \phi \end{bmatrix} \quad (3.2b)$$

From Fig. 3.1 follows that

$$\mathbf{r}_1 + \mathbf{r}_2 = \mathbf{r}_3 + \mathbf{r}_4 \quad (3.3)$$

Obviously, we need a *scalar* relation between the input and output angles, but we have derived above a vector equation. Note, however, that the angles of interest appear in  $\mathbf{r}_1$  and  $\mathbf{r}_4$ ;  $\mathbf{r}_3$  remains constant throughout the linkage motion; and  $\mathbf{r}_2$  contains an *unwanted unknown*,  $\theta$ . This is eliminated below: From eq.(3.3),

$$\mathbf{r}_2 = \mathbf{r}_3 + \mathbf{r}_4 - \mathbf{r}_1 \quad (3.4)$$

Now, the right-hand side of the above equation is independent of this angle. If we take the *Euclidean norm*, a.k.a. the *magnitude*, of both sides of eq.(3.4), then angle  $\theta$  is eliminated, for the magnitude of  $\mathbf{r}_2$  is independent of this angle; in fact, this magnitude is nothing but the link length  $a_3$ . We thus have

$$\|\mathbf{r}_2\|^2 = \|\mathbf{r}_3 + \mathbf{r}_4 - \mathbf{r}_1\|^2 \quad (3.5)$$

Upon expansion,

$$\|\mathbf{r}_2\|^2 = \|\mathbf{r}_3\|^2 + \|\mathbf{r}_4\|^2 + \|\mathbf{r}_1\|^2 + 2\mathbf{r}_3^T \mathbf{r}_4 - 2\mathbf{r}_3^T \mathbf{r}_1 - 2\mathbf{r}_4^T \mathbf{r}_1 \quad (3.6)$$

where

$$\begin{aligned} \|\mathbf{r}_1\|^2 &= a_2^2, & \|\mathbf{r}_2\|^2 &= a_3^2, & \|\mathbf{r}_3\|^2 &= a_1^2, & \|\mathbf{r}_4\|^2 &= a_4^2 \\ \mathbf{r}_3^T \mathbf{r}_4 &= a_1 a_4 \cos \phi, & \mathbf{r}_3^T \mathbf{r}_1 &= a_1 a_2 \cos \psi, & \mathbf{r}_4^T \mathbf{r}_1 &= a_2 a_4 \cos(\phi - \psi) \end{aligned}$$

Plugging the foregoing expressions into eq.(3.6) yields a form of the input-output (IO) equation:

$$a_3^2 = a_1^2 + a_4^2 + a_2^2 + 2a_1 a_4 \cos \phi - 2a_1 a_2 \cos \psi - 2a_2 a_4 \cos(\phi - \psi) \quad (3.7)$$

which is already a scalar relation between the input and the output angles, with the link lengths as parameters, free of any other linkage variable, like  $\theta$  and  $\mu$ . However, this relation is not yet in the most suitable form for our purposes. Indeed, it is apparent that a scaling of the link lengths by the same factor does not change the input-output relation, and hence, the above equation cannot yield all four link lengths. This means that we can only obtain the relative values of the link lengths for a set of prescribed input-output angles. One more remark is in order: the link lengths appear as unknowns when a pair of input-output angles is given; moreover, these unknowns appear quadratically in that equation. Thus, simply dividing the two sides of the equation by any link length will still yield a quadratic equation in the link-length ratios. What Freudenstein (1955) cleverly realized was that by means of a suitable *nonlinear mapping* from link lengths into nondimensional parameters, a linear equation in these parameters can be produced. To

this end, both sides of eq.(3.7) are divided by  $2a_2a_4$ . Once this is done, the definitions below are introduced:

$$k_1 \equiv \frac{a_1^2 + a_2^2 - a_3^2 + a_4^2}{2a_2a_4}, \quad k_2 \equiv \frac{a_1}{a_2}, \quad k_3 \equiv \frac{a_1}{a_4} \quad (3.8)$$

which are the *Freudenstein parameters* of the linkage at hand. The inverse relations are readily derived, if in terms of one of the link lengths, say  $a_1$ :

$$a_2 = \frac{1}{k_2}a_1, \quad a_4 = \frac{1}{k_3}a_1, \quad a_3 = \sqrt{a_1^2 + a_2^2 + a_4^2 - 2k_1a_2a_4} \quad (3.9)$$

The IO equation (3.7) then becomes

$$k_1 + k_2 \cos \phi - k_3 \cos \psi = \cos(\phi - \psi) \quad (3.10)$$

thereby obtaining the *Freudenstein equation*. Notice that, upon writing this equation in homogeneous form, we obtain  $F(\psi, \phi)$  of eq.(3.1), namely,

$$F(\psi, \phi) \equiv k_1 + k_2 \cos \phi - k_3 \cos \psi - \cos(\phi - \psi) = 0 \quad (3.11)$$

If we now write eq.(3.10) for  $\{\psi_k, \phi_k\}_1^m$ , we obtain  $m$  linear equations in the three Freudenstein parameters, arrayed in vector  $\mathbf{k}$ , namely,

$$\mathbf{S}\mathbf{k} = \mathbf{b} \quad (3.12)$$

where  $\mathbf{S}$  is the  $m \times 3$  *synthesis matrix*;  $\mathbf{k}$  is the 3-dimensional vector of unknown Freudenstein parameters; and  $\mathbf{b}$  is an  $m$ -dimensional vector of known components, i.e.,

$$\mathbf{S} \equiv \begin{bmatrix} 1 & \cos \phi_1 & -\cos \psi_1 \\ 1 & \cos \phi_2 & -\cos \psi_2 \\ \vdots & \vdots & \vdots \\ 1 & \cos \phi_m & -\cos \psi_m \end{bmatrix}, \quad \mathbf{k} \equiv \begin{bmatrix} k_1 \\ k_2 \\ k_3 \end{bmatrix}, \quad \mathbf{b} \equiv \begin{bmatrix} \cos(\phi_1 - \psi_1) \\ \cos(\phi_2 - \psi_2) \\ \vdots \\ \cos(\phi_m - \psi_m) \end{bmatrix} \quad (3.13)$$

Three cases arise:

$m < 3$ : Case  $m = 1$  reduces to the synthesis of a quadrilateron with two given angles, which admits infinitely many solutions. Case  $m = 2$  seldom occurs in practice without additional conditions, that render the problem more complex, e.g., in the synthesis of quick-return mechanisms;

$m = 3$ : The number of equations coincides with the number of unknowns, and hence, the problem admits one *unique* solution—unless the synthesis matrix is **singular**. We are in the case of *exact synthesis*;

$m > 3$ : The number of equations exceeds the number of unknowns, which leads to an over-determined system of equations. Hence, no solution is possible, in general, but an optimum solution can be found that best approximates the synthesis equations in the least-square sense. Problem falls in the category of *approximate synthesis*.

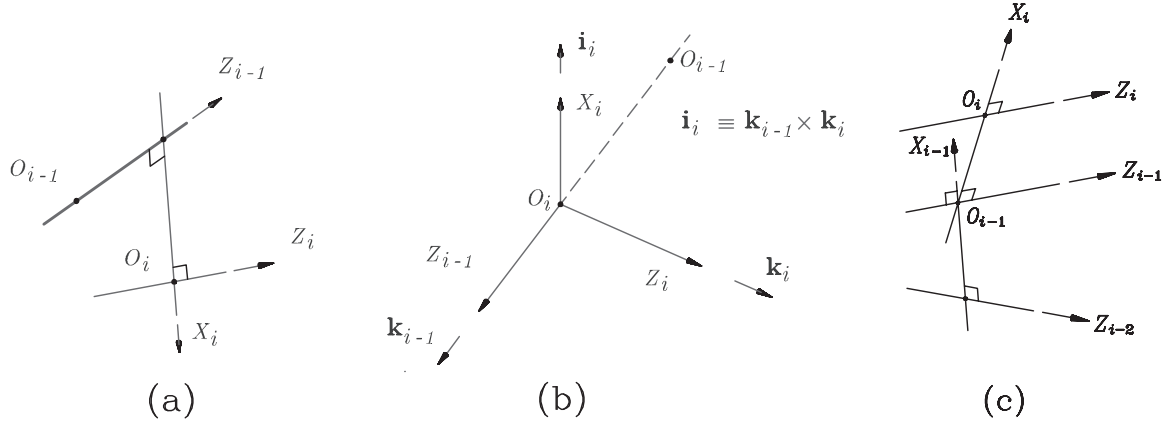


Figure 3.2: Definition of  $X_i$  when  $Z_{i-1}$  and  $Z_i$ : (a) are skew; (b) intersect; and (c) are parallel.

### 3.2.2 The Denavit-Hartenberg Notation

Prior to deriving the IO equations of spherical and spatial linkages, we introduce the *Denavit-Hartenberg (DH) notation*, which is extremely useful in the analysis of kinematic chains in three dimensions.

In order to uniquely describe the *architecture* of a kinematic chain, i.e., the relative location and orientation of its neighbouring-pair axes, the Denavit-Hartenberg notation (Hartenberg and Denavit, 1964) is introduced. To this end, we assume a *simple kinematic chain*, open or closed, with links numbered  $1, \dots, n$ , the  $i$ th pair being defined as that coupling the  $(i-1)$ st link with the  $i$ th link. Next, a coordinate frame  $\mathcal{F}_i$  is defined with origin  $O_i$  and axes  $X_i, Y_i, Z_i$ . This frame is attached to the  $(i-1)$ st link—not to the  $i$ th link!—for  $i = 1, \dots, n$ . This is done by following the rules given below:

1.  $Z_i$  is the axis of the  $i$ th pair. Notice that there are two possibilities of defining the positive direction of this axis, since each pair axis is only a line, not a directed segment. Moreover, the  $Z_i$  axis of a prismatic pair can be located arbitrarily, since only its direction is defined by the axis of this pair.
2.  $X_i$  is defined as the common perpendicular to  $Z_{i-1}$  and  $Z_i$ , directed from the former to the latter, as shown in Fig. 3.2a. Notice that if these two axes intersect, the positive direction of  $X_i$  is undefined and hence, can be freely assigned. Henceforth, we will follow the *right-hand rule* in this case. This means that if unit vectors  $\mathbf{i}_i, \mathbf{k}_{i-1}$ , and  $\mathbf{k}_i$  are attached to axes  $X_i, Z_{i-1}$ , and  $Z_i$ , respectively, as indicated in Fig. 3.2b, then  $\mathbf{i}_i$  is defined as  $\mathbf{k}_{i-1} \times \mathbf{k}_i$ . Moreover, if  $Z_{i-1}$  and  $Z_i$  are parallel, the location of  $X_i$  is undefined. In order to define it uniquely, we will specify  $X_i$  as passing through the origin of the  $(i-1)$ st frame, as shown in Fig. 3.2c.
3. The *distance* between  $Z_i$  and  $Z_{i+1}$  is defined as  $a_i$ , which is thus *nonnegative*.

4. The  $Z_i$ -coordinate of the intersection  $O'_i$  of  $Z_i$  with  $X_{i+1}$  is denoted by  $d_i$ . Since this quantity is a coordinate, it can be either positive or negative. Its absolute value is the distance between  $X_i$  and  $X_{i+1}$ , also called the *offset* between successive common perpendiculars.
5. The angle between  $Z_i$  and  $Z_{i+1}$  is defined as  $\alpha_i$  and is measured about the positive direction of  $X_{i+1}$ . This item is known as the *twist angle* between successive pair axes.
6. The angle between  $X_i$  and  $X_{i+1}$  is defined as  $\theta_i$  and is measured about the positive direction of  $Z_i$ .

### 3.2.3 Spherical Four-Bar-Linkages

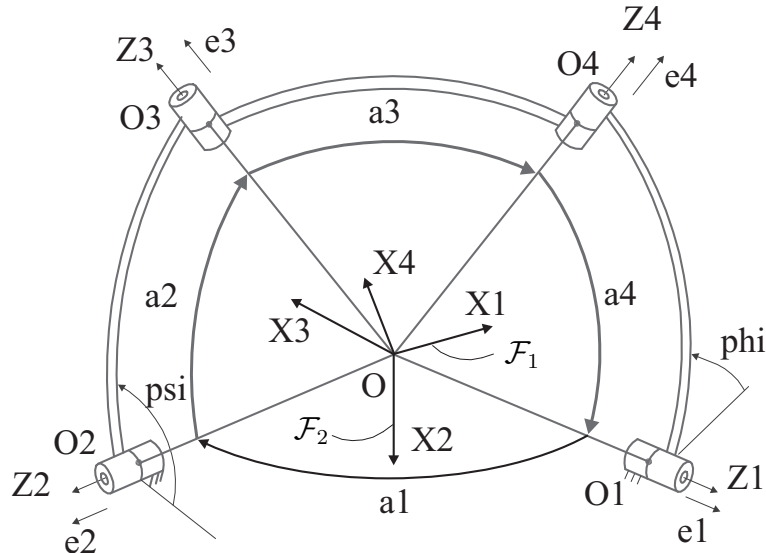


Figure 3.3: A spherical four-bar linkage for function generation

A spherical four-bar linkage for function generation is depicted in Fig. 3.3. In this case we are interested, as in the planar case, in deriving a relation between the input angle  $\psi$  and the output angle  $\phi$ , that should include the *linkage dimensions*  $\{\alpha_i\}_1^4$  as parameters. To this end, we introduce the unit vectors  $\{e_i\}_1^4$ , directed along the concurrent axes of the four revolutes, as depicted in Fig. 3.3. Notice that, in order to bring the notation adopted for planar four-bar linkages, as proposed by Freudenstein and displayed in Fig. 3.1, in line with the Denavit-Hartenberg notation, we have placed  $Z_1$  along the axis of the output joint and  $Z_2$  along that of the input joint.

Deriving the desired relation is now a simple matter, for we have one geometric relation at our disposal, namely,

$$e_3 \cdot e_4 = \cos \alpha_3 \quad (3.14)$$

Now, in order to compute the foregoing dot product, we need its two factors (*i*) *in the same coordinate frame*, and (*ii*) in terms of the input and output angles. Apparently, if we choose  $\mathcal{F}_2$ , the coordinate frame fixed to the mechanism frame, to represent the two unit vectors in question, we will have the desired expressions.

Under the Denavit-Hartenberg notation, the  $Z_i$ -axis is defined as the axis of the  $i$ th revolute, while  $X_i$  is defined as the common perpendicular to  $Z_{i-1}$  and  $Z_i$ , directed from the former to the latter, according to the *right-hand rule*. These axes are illustrated in Fig. 3.3.

Now, the matrix rotating  $\mathcal{F}_i$  into  $\mathcal{F}_{i+1}$  is denoted  $\mathbf{Q}_i$ . This matrix is given as (Hartenberg and Denavit, 1964; Angeles, 2014):

$$\mathbf{Q}_i \equiv [\mathbf{Q}_i]_i \equiv \begin{bmatrix} \cos \theta_i & -\lambda_i \sin \theta_i & \mu_i \sin \theta_i \\ \sin \theta_i & \lambda_i \cos \theta_i & -\mu_i \cos \theta_i \\ 0 & \mu_i & \lambda_i \end{bmatrix} \quad (3.15)$$

where  $\lambda_i \equiv \cos \alpha_i$  and  $\mu_i \equiv \sin \alpha_i$ , while  $\theta_i$  was already defined in Subsection 3.2.2. Apparently, vector  $\mathbf{e}_i$  in  $\mathcal{F}_i$ , denoted  $[\mathbf{e}_i]_i$ , is given by

$$[\mathbf{e}_i]_i = \begin{bmatrix} 0 \\ 0 \\ 1 \end{bmatrix} \quad (3.16)$$

Moreover,  $\mathbf{Q}_i$  can be regarded as the matrix transforming  $\mathcal{F}_{i+1}$ -coordinates into  $\mathcal{F}_i$ -coordinates, i.e., for *any* three-dimensional vector  $\mathbf{v}$ ,

$$[\mathbf{v}]_i = \mathbf{Q}_i [\mathbf{v}]_{i+1} \quad (3.17)$$

Likewise,

$$[\mathbf{v}]_{i+1} = [\mathbf{Q}_i^T]_i [\mathbf{v}]_i \quad (3.18)$$

More specifically, we represent the foregoing transformations in the abbreviated form:

$$\mathbf{Q}_1: \mathcal{F}_1 \rightarrow \mathcal{F}_2, \quad \mathbf{Q}_2: \mathcal{F}_2 \rightarrow \mathcal{F}_3, \quad \mathbf{Q}_3: \mathcal{F}_3 \rightarrow \mathcal{F}_4, \quad \mathbf{Q}_4: \mathcal{F}_4 \rightarrow \mathcal{F}_1 \quad (3.19a)$$

$$\mathbf{Q}_1: [\cdot]_2 \rightarrow [\cdot]_1, \quad \mathbf{Q}_2: [\cdot]_3 \rightarrow [\cdot]_2, \quad \mathbf{Q}_3: [\cdot]_4 \rightarrow [\cdot]_3, \quad \mathbf{Q}_4: [\cdot]_1 \rightarrow [\cdot]_4 \quad (3.19b)$$

$$\mathbf{Q}_1^T: \mathcal{F}_2 \rightarrow \mathcal{F}_1, \quad \mathbf{Q}_2^T: \mathcal{F}_3 \rightarrow \mathcal{F}_2, \quad \mathbf{Q}_3^T: \mathcal{F}_4 \rightarrow \mathcal{F}_3, \quad \mathbf{Q}_4^T: \mathcal{F}_1 \rightarrow \mathcal{F}_4 \quad (3.19c)$$

$$\mathbf{Q}_1^T: [\cdot]_1 \rightarrow [\cdot]_2, \quad \mathbf{Q}_2^T: [\cdot]_2 \rightarrow [\cdot]_3, \quad \mathbf{Q}_3^T: [\cdot]_3 \rightarrow [\cdot]_4, \quad \mathbf{Q}_4^T: [\cdot]_4 \rightarrow [\cdot]_1 \quad (3.19d)$$

In particular, given expression (3.16) for  $[\mathbf{e}_i]_i$ , it is apparent that the third column of  $\mathbf{Q}_i^T$  or, equivalently, the third row of  $\mathbf{Q}_i$ , is  $[\mathbf{e}_i]_{i+1}$ . By the same token, the third column of  $\mathbf{Q}_i$  is  $[\mathbf{e}_{i+1}]_i$ , i.e.,

$$[\mathbf{e}_i]_{i+1} = \begin{bmatrix} 0 \\ \mu_i \\ \lambda_i \end{bmatrix}, \quad [\mathbf{e}_{i+1}]_i = \begin{bmatrix} \mu_i \sin \theta_i \\ -\mu_i \cos \theta_i \\ \lambda_i \end{bmatrix} \quad (3.20)$$

The vector representations required are derived below. We do this by recalling that  $[\mathbf{e}_3]_2$  is the third column of  $\mathbf{Q}_2$ , while  $[\mathbf{e}_4]_1$  is the third row of  $\mathbf{Q}_4$ .

$$[\mathbf{e}_3]_2 = \begin{bmatrix} \mu_2 \sin \theta_2 \\ -\mu_2 \cos \theta_2 \\ \lambda_2 \end{bmatrix} \quad (3.21)$$

$$[\mathbf{e}_4]_2 = \mathbf{Q}_1^T [\mathbf{e}_4]_1 \equiv \begin{bmatrix} \cos \theta_1 & \sin \theta_1 & 0 \\ -\lambda_1 \sin \theta_1 & \lambda_1 \cos \theta_1 & \mu_1 \\ \mu_1 \sin \theta_1 & -\mu_1 \cos \theta_1 & \lambda_1 \end{bmatrix} \begin{bmatrix} 0 \\ \mu_4 \\ \lambda_4 \end{bmatrix} \quad (3.22)$$

$$= \begin{bmatrix} \mu_4 \sin \theta_1 \\ \mu_4 \lambda_1 \cos \theta_1 + \lambda_4 \mu_1 \\ -\mu_4 \mu_1 \cos \theta_1 + \lambda_4 \lambda_1 \end{bmatrix} \quad (3.23)$$

which are the expressions sought. Hence,

$$[\mathbf{e}_3^T]_2 [\mathbf{e}_4]_2 = \mu_2 \mu_4 \sin \theta_1 \sin \theta_2 - \mu_2 \cos \theta_2 (\mu_4 \lambda_1 \cos \theta_1 + \lambda_4 \mu_1) + \lambda_2 (-\mu_4 \mu_1 \cos \theta_1 + \lambda_4 \lambda_1) \quad (3.24)$$

Upon substituting the above expression into eq.(3.14), we obtain

$$\lambda_1 \lambda_2 \lambda_4 - \lambda_3 - \lambda_4 \mu_1 \mu_2 \cos \theta_2 - \lambda_1 \mu_2 \mu_4 \cos \theta_1 \cos \theta_2 - \lambda_2 \mu_1 \mu_4 \cos \theta_1 + \mu_2 \mu_4 \sin \theta_1 \sin \theta_2 = 0 \quad (3.25)$$

which is a form of the input-output equation sought. This equation can be simplified upon realizing that the last coefficient of its left-hand side cannot vanish, least one of the input and output links, or even both, shrinks to one point on the sphere—a consequence of at least one of  $\alpha_2$  and  $\alpha_4$  vanishing or equating  $\pi$ . In this light, we can safely divide both sides of the above equation by  $\mu_2 \mu_4$ . Moreover, in order to render the same equation terser, we introduce the *Freudenstein parameters for the spherical linkage* below:

$$k_1 \equiv \frac{\lambda_1 \lambda_2 \lambda_4 - \lambda_3}{\mu_2 \mu_4}, \quad k_2 = \frac{\lambda_4 \mu_1}{\mu_4}, \quad k_3 = \lambda_1, \quad k_4 = \frac{\lambda_2 \mu_1}{\mu_2} \quad (3.26)$$

Now the two sides of eq.(3.25) are divided by  $\mu_2 \mu_4$ , and definitions (3.26) are introduced in the equation thus resulting, which leads to

$$k_1 - k_2 \cos \theta_2 - k_3 \cos \theta_1 \cos \theta_2 - k_4 \cos \theta_1 + \sin \theta_1 \sin \theta_2 = 0 \quad (3.27)$$

This equation, however, involves a relation between angles  $\theta_1$  and  $\theta_2$  of the DH notation, which are different from, although related to, the input and the output angles  $\psi$  and  $\phi$ . To better understand the relation between the two pairs of angles, we sketch these in Fig. 3.4. From this figure, it is apparent that

$$\theta_2 = \psi + \pi, \quad \theta_1 = 2\pi - \phi \quad \text{or} \quad \theta_1 = -\phi \quad (3.28)$$

Hence,

$$\cos \theta_2 = -\cos \psi, \quad \sin \theta_2 = -\sin \psi, \quad \cos \theta_1 = \cos \phi, \quad \sin \theta_1 = -\sin \phi \quad (3.29)$$

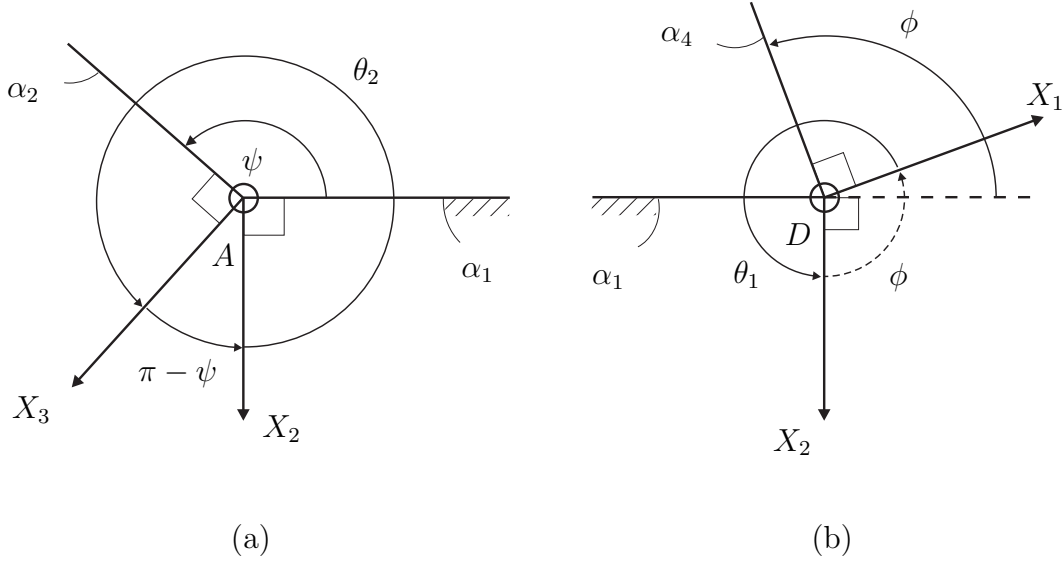


Figure 3.4: Relation between input and output angles with their counterparts in the DH notation: (a)  $\psi$  and  $\theta_2$ ; and (b)  $\phi$  and  $\theta_1$

Substitution of relations (3.29) into eq.(3.27) leads to

$$F(\psi, \phi) \equiv k_1 + k_2 \cos \psi + k_3 \cos \psi \cos \phi - k_4 \cos \phi + \sin \psi \sin \phi = 0 \quad (3.30)$$

which is the *input-output equation for spherical linkages*, written in terms of the input and output angles  $\psi$  and  $\phi$ , respectively. Either eq.(3.27) or eq.(3.30) can be used to find the output angle  $\phi$  for a given linkage and a given value of the input angle  $\psi$ , which constitutes the *analysis problem*. The same equation is to be used for synthesis, as described below.

In a synthesis problem, we aim to calculate the set of unknown linkage angles  $\{\alpha_i\}_1^4$ , for a *given* set of pairs  $\{(\psi_i, \phi_i)\}_1^m$  of IO angle values that the linkage is to meet. In order to obtain the synthesis equations allowing us to compute the set of Freudenstein parameters leading to the desired linkage, we proceed as in the planar case and write eq.(3.30) for the given set of pairs of angle values, thus obtaining the *synthesis equations* in the form of eq.(3.12), as derived for planar four-bar linkages. Obviously, the synthesis matrix  $\mathbf{S}$  and vectors  $\mathbf{b}$  and  $\mathbf{k}$  now change to

$$\mathbf{S} \equiv \begin{bmatrix} 1 & \cos \psi_1 & \cos \psi_1 \cos \phi_1 & -\cos \phi_1 \\ 1 & \cos \psi_2 & \cos \psi_2 \cos \phi_2 & -\cos \phi_2 \\ \vdots & \vdots & \vdots & \vdots \\ 1 & \cos \psi_m & \cos \psi_m \cos \phi_m & -\cos \phi_m \end{bmatrix}, \quad \mathbf{k} \equiv \begin{bmatrix} k_1 \\ k_2 \\ k_3 \\ k_4 \end{bmatrix}, \quad \mathbf{b} \equiv \begin{bmatrix} -\sin \psi_1 \sin \phi_1 \\ -\sin \psi_2 \sin \phi_2 \\ \vdots \\ -\sin \psi_m \sin \phi_m \end{bmatrix} \quad (3.31)$$

Similar to the planar case, we have exact synthesis when the number  $m$  of given pairs of input-output angular values equals the number of Freudenstein parameters at hand, which in this case happens when  $m = 4$ . When  $m > 4$ , then we have a problem of approximate synthesis.

However, eq.(3.30) only provides values for the linkage parameters  $\{k_i\}_1^4$ . Hence, we need a means to convert the latter into the former.

Notice that the relations between the two sets,  $\{\alpha_i\}_1^4$  and  $\{k_i\}_1^4$ , are nonlinear, and hence, solving eqs.(3.26) for the former needs careful planning. For starters, the foregoing equations are rewritten explicitly in terms of the linkage dimensions  $\{\alpha_i\}_1^4$ , and reordered conveniently:

$$c\alpha_1 - k_3 = 0 \quad (3.32a)$$

$$c\alpha_4 s\alpha_1 - k_2 s\alpha_4 = 0 \quad (3.32b)$$

$$c\alpha_2 s\alpha_1 - k_4 s\alpha_2 = 0 \quad (3.32c)$$

$$c\alpha_1 c\alpha_2 c\alpha_4 - c\alpha_3 - k_1 s\alpha_2 s\alpha_4 = 0 \quad (3.32d)$$

In many instances,  $\alpha_1$  is given—not up to the designer to find it!—and hence, the problem of finding the remaining DH parameters simplifies tremendously. This can be done sequentially, from eqs. (3.32b) to (3.32d), in this order.

In a semigraphical method, based on *contour-intersection* and favored in this course, all but two of the unknowns are first eliminated from the set of nonlinear equations, thereby ending up with a reduced number of equations in the two remaining unknowns. Each of these equations is then plotted in the plane of the two unknowns, which yields one contour per bivariate equation, in that plane. All real solutions are then found by *inspection*, at the intersections of all the contours. Notice that, if the reduced system comprises more than two bivariate equations, then the system entails algebraic redundancy, which is convenient, as this adds *robustness* to the system.

In the particular case at hand, the transformation sought can be most readily found by noticing the structure of eqs.(3.32a–d): The first equation involves one single unknown,  $\alpha_1$ ; the second only *one new* unknown,  $\alpha_4$ ; the third only *one new* unknown,  $\alpha_2$ ; and the fourth only one new unknown as well,  $\alpha_3$ . Hence, we devise the *algorithm* below:

- i) From eq.(3.32a), compute  $\alpha_1 = \cos^{-1}(k_3) \Rightarrow$  two possible values of  $\alpha_1$ ;
- ii) From eq.(3.32b), compute  $\alpha_4 = \tan^{-1}(\sin \alpha_1 / k_2) \Rightarrow$  two possible values of  $\alpha_4$  for each value of  $\alpha_1$ ;
- iii) From eq.(3.32c), compute  $\alpha_2 = \tan^{-1}(\sin \alpha_1 / k_4) \Rightarrow$  two possible values of  $\alpha_2$  for each value of  $\alpha_1$  *and its corresponding* value of  $\alpha_4$ , thereby leading to four possible values of  $\alpha_2$ ;
- iv) From eq.(3.32d), compute  $\alpha_3 = \cos^{-1}(\cos \alpha_1 \cos \alpha_2 \cos \alpha_4 - k_1 \sin \alpha_2 \sin \alpha_4) \Rightarrow$  two possible values for  $\alpha_3$  for each pair of values of  $\alpha_1$ ,  $\alpha_2$  and  $\alpha_4$ .

In summary, then, we have: two possible values of  $\alpha_1$ ; four possible values of  $\alpha_4$ ; four possible values of  $\alpha_2$ , which can be combined in  $2 \times 4 \times 4 = 32$  forms. Hence, we

end up with up to  $2 \times 32 = 64$  values of  $\alpha_3$ . Therefore, we can expect up to 64 sets of  $\{\alpha_i\}_1^4$  values for one single set  $\{k_i\}_1^4$ . However, some of the 64 sets of linkage dimensions found above may be complex, and hence, uninteresting. The problem may also not admit any single real solution, for example, if  $|k_3| > 1$ . As well,  $\alpha_3$  becomes complex when  $|\cos \alpha_1 \cos \alpha_2 \cos \alpha_4 - k_1 \sin \alpha_2 \sin \alpha_4| > 1$ . That is, for a feasible linkage, two conditions must be imposed on the Freudenstein parameters  $\{k_i\}_1^4$ :

$$|k_3| \leq 1, \quad |\cos \alpha_1 \cos \alpha_2 \cos \alpha_4 - k_1 \sin \alpha_2 \sin \alpha_4| \leq 1 \quad (3.33)$$

Note that the semigraphical method *filters* all complex solutions and is guaranteed to yield all real solutions if the two contours in question are plotted inside a square of side  $\pi$  centred at the origin of the  $\alpha_2$ - $\alpha_3$  plane. In order to implement the semigraphical method, first four pairs of values  $(\alpha_1, \alpha_4)$  are computed from eqs.(3.32a & b). Each of these pairs is then substituted into eqs.(3.32c & d), thereby obtaining four pairs of contours in the  $\alpha_2$ - $\alpha_3$  plane. The intersections of each pair of contours, which can be estimated by inspection, yield one subset of real solutions. Each of these estimates of  $\alpha_3$  and  $\alpha_4$  values can then be used as an *initial guess* for a Newton-Raphson solution of the two equations. Due to the proximity of each estimate from the pair of real roots, the Newton-Raphson method should converge in a pair of iterations for a reasonable tolerance. Once all four pairs of contours have been exhausted, *all real roots* of the problem have been computed.

Finally, notice that any *spherical triangle* and, in fact, any *spherical polygon* defined on the surface of the unit sphere has an *antipodal* counterpart. In this light, then, even if we end up with a full set of feasible linkage dimensions, only 32 four-bar linkages defined by this set are distinct.

### 3.2.4 Spatial Four-Bar-Linkages

The analysis of spatial four-bar linkages relies heavily on the algebra of *dual numbers*, which is extensively discussed in Appendix A. What we should recall now is (a) the usual representation of dual quantities, by means of a “hat” ( $\hat{\cdot}$ ) on top of the variable in question and (b) the definition of the *dual unit*,  $\epsilon$ , via its two properties

$$\epsilon \neq 0, \quad \epsilon^2 = 0 \quad (3.34)$$

A general layout of a spatial four-bar linkage is included in Fig. 3.5, in which we use the Denavit-Hartenberg notation, introduced in Subsection 3.2.2. Similar to that subsection, we have laid the ouput axis along  $Z_1$ , in order to comply both with the DH notation and with the notation adopted in Figs. 3.1 and 3.3. In this case,  $\psi$  and  $\phi$  denote the input and the output angles, as in Subsection 3.2.3, their relations with angles  $\theta_1$  and  $\theta_2$  of the DH notation being exactly as in the spherical case, namely,

$$\psi = \theta_2 - \pi, \quad \phi = 2\pi - \theta_1 \quad (3.35)$$

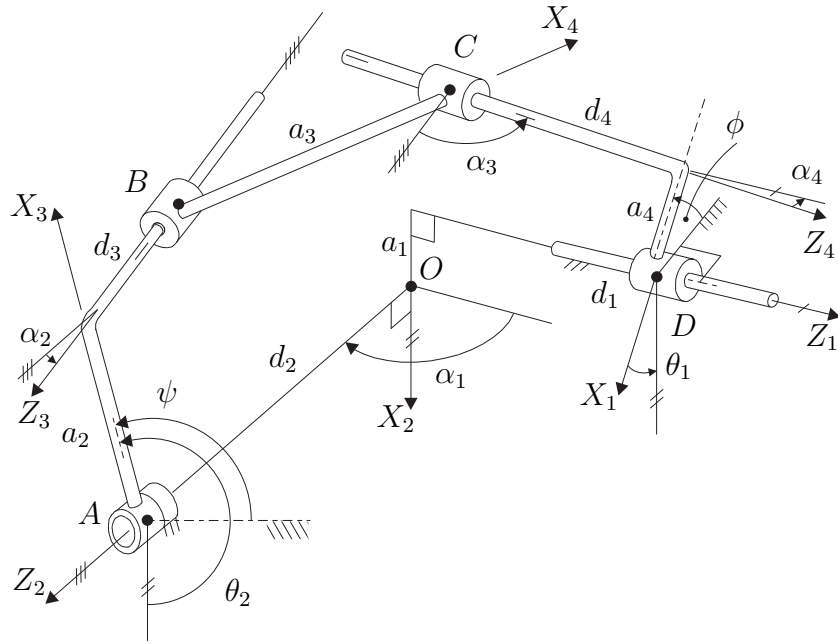


Figure 3.5: A RCCC linkage for function generation

The IO equation of the RCCC linkage is most readily derived by resorting to the *Principle of Transference* (Dimentberg, 1965; Rico Martínez and Duffy, 1995), which is cited below:

*The kinematics and statics relations of spatial linkages and cam mechanisms can be derived upon replacing the real variables occurring in the corresponding relations for spherical linkages by dual numbers.*

Put quite simply, the IO equation of the RCCC linkage can be derived from that of the spherical RRRR linkage upon “putting hats” on the variables and the (Freudenstein) parameters occurring in eq.(3.30), thereby obtaining

$$\hat{F}(\hat{\psi}, \hat{\phi}) \equiv \hat{k}_1 + \hat{k}_2 \cos \hat{\psi} + \hat{k}_3 \cos \hat{\psi} \cos \hat{\phi} - \hat{k}_4 \cos \hat{\phi} + \sin \hat{\psi} \sin \hat{\phi} = 0 \quad (3.36)$$

Furthermore, *dualization* of an angular displacement  $\theta$  about an axis  $\mathcal{A}$  is an operation by which a sliding  $d_o$  is introduced in a direction parallel to the same axis, the dual angle  $\hat{\theta}$  then being represented as

$$\hat{\theta} = \theta + \epsilon d_o \quad (3.37)$$

The variable  $\theta$  is referred to as the *primal part* of  $\hat{\theta}$ ,  $d_o$  as the *dual part*. Notice that the latter being a sliding, its units are those of length; the dual unit  $\epsilon$  can then be thought of as “having units of length-inverse.” The *dualization operation* can thus be kinematically interpreted as the replacement of a R joint of axis  $\mathcal{A}$  by a C joint of the same axis. Hence, the RCCC linkage of Fig. 3.5 is obtained by replacing all R joints of the spherical linkage of Fig. 3.3, but that associated with the input angle  $\psi$ , with a C joint. In this light, then,

the dual quantities appearing in eq.(3.36) are to be interpreted as

$$\hat{F}(\hat{\psi}, \hat{\phi}) = F(\hat{\psi}, \hat{\phi}) + \epsilon F_o(\hat{\psi}, \hat{\phi}) \quad (3.38a)$$

with

$$\hat{\psi} = \psi + \epsilon d_2, \quad \hat{\phi} = \phi + \epsilon d_1, \quad \hat{k}_i \equiv k_i + \epsilon k_{oi}, \quad i = 1, \dots, 4 \quad (3.38b)$$

Consistently, then, the  $k_i$  parameters are dimensionless, while their dual counterparts  $k_{oi}$ , for  $i = 1, \dots, 4$ , have all units of length. The former are displayed in eq.(3.26) for the spherical four-bar linkage; they are the same for its spatial counterpart. The latter are obtained below upon extracting them from the dual version of the expressions displayed in the above equation. The computations are lengthy and time-consuming, for which reason the dual expressions were obtained using computer algebra<sup>1</sup>. In deriving the desired expressions, the relation that gives the dual version  $\hat{f}(\hat{x})$  of a real function  $f(x)$  of a real variable  $x$ , whereby the dual argument is defined as  $\hat{x} \equiv x + \epsilon x_o$ , is given in eq.(A.3), and reproduced below for quick reference.

$$\hat{f}(\hat{x}) = \hat{f}(x + \epsilon x_o) \equiv f(x) + \epsilon x_o \frac{df(x)}{dx}$$

Hence,

$$\cos \hat{\psi} \equiv \cos \psi - \epsilon d_2 \sin \psi, \quad \sin \hat{\psi} \equiv \sin \psi + \epsilon d_2 \cos \psi \quad (3.39a)$$

$$\cos \hat{\phi} \equiv \cos \phi - \epsilon d_1 \sin \phi, \quad \sin \hat{\phi} \equiv \sin \phi + \epsilon d_1 \cos \phi \quad (3.39b)$$

in which  $d_2$  is constant, while  $d_1$  is variable, as per Fig. 3.5.

Likewise, for the dual angles  $\hat{\alpha}_i \equiv \alpha_i + \epsilon a_i$ ,

$$\cos \hat{\alpha}_i \equiv \cos \alpha_i - \epsilon a_i \sin \alpha_i, \quad \sin \hat{\alpha}_i \equiv \sin \alpha_i + \epsilon a_i \cos \alpha_i \quad (3.40)$$

Further, the primal parts  $\{k_i\}_1^4$  of the dual Freudenstein parameters  $\{\hat{k}_i\}_1^4$  are identical to those of the spherical linkage, displayed in eq.(3.26). For quick reference, the same parameters are reproduced below:

$$k_1 \equiv \frac{\lambda_4 \lambda_1 \lambda_2 - \lambda_3}{\mu_2 \mu_4}, \quad k_2 = \frac{\lambda_4 \mu_1}{\mu_4}, \quad k_3 = \lambda_1, \quad k_4 = \frac{\mu_1 \lambda_2}{\mu_2} \quad (3.41)$$

their dual counterparts being

$$\begin{aligned} k_{o1} &= -\frac{a_1 \lambda_2 \lambda_4 \mu_1 \mu_2 \mu_4 + a_2 (\lambda_1 \lambda_4 - \lambda_2 \lambda_3) \mu_4 - a_3 \mu_2 \mu_3 \mu_4 + a_4 (\lambda_1 \lambda_2 - \lambda_3 \lambda_4) \mu_2}{\mu_2^2 \mu_4^2} \\ k_{o2} &= \frac{a_1 \lambda_1 \lambda_4 \mu_4 - a_4 \mu_1}{\mu_4^2}, \quad k_{o3} = -a_1 \mu_1, \quad k_{o4} = \frac{a_1 \lambda_1 \lambda_2 \mu_2 - a_2 \mu_1}{\mu_2^2} \end{aligned} \quad (3.42)$$

Moreover, if the angle of rotation  $\theta_i$ , associated with the  $i$ th R joint of Fig. 3.3 under

---

<sup>1</sup>See the Maple 15 worksheet DualRCCC-I0131224.mw.

the DH notation, for  $i = 1, 3, 4$ , is dualized, the *dual angles* thus resulting become, in the notation of Fig. 3.5,

$$\hat{\theta}_1 = \theta_1 + \epsilon d_1 = -\phi + \epsilon d_1, \quad \hat{\theta}_2 = \theta_2 = \psi + \pi, \quad \hat{\theta}_3 = \theta_3 + \epsilon d_3, \quad \hat{\theta}_4 = \theta_4 + \epsilon d_4 \quad (3.43)$$

where

$$-\infty < d_i < \infty, \quad i = 1, 3, 4$$

which is an unbounded real number, with units of length. Notice that  $d_i$  is not a “length,” properly speaking, because a length is positive, while  $d_i$  can be negative, exactly the same as a joint angle. Moreover,  $F_o(\psi, \phi, d_1)$  is given below:

$$\begin{aligned} F_o(\psi, \phi, d_1) = & k_{o1} - k_2 d_2 \sin(\psi) + k_{o2} \cos(\psi) - k_3 d_1 \cos(\psi) \sin(\phi) \\ & - k_3 d_2 \sin(\psi) \cos(\phi) + k_{o3} \cos(\psi) \cos(\phi) + k_4 d_1 \sin(\phi) \\ & - k_{o4} \cos(\phi) + d_1 \sin(\psi) \cos(\phi) + d_2 \cos(\psi) \sin(\phi) = 0 \end{aligned} \quad (3.44)$$

Further, the synthesis equations for the spatial four-bar linkage can be readily set up by dualizing those derived for the spherical case, with the synthesis matrix  $\mathbf{S}$  and the right-hand side  $\mathbf{b}$  of eq.(3.31) substituted by their “hatted” counterparts, namely,

$$\hat{\mathbf{S}}\hat{\mathbf{k}} = \hat{\mathbf{b}} \quad (3.45)$$

where, as usual,

$$\hat{\mathbf{S}} = \mathbf{S} + \epsilon \mathbf{S}_o, \quad \hat{\mathbf{k}} = \mathbf{k} + \epsilon \mathbf{k}_o, \quad \hat{\mathbf{b}} = \mathbf{b} + \epsilon \mathbf{b}_o \quad (3.46)$$

the primal part  $\mathbf{k}$  of vector  $\hat{\mathbf{k}}$ , it is recalled, being the same as that of the spherical linkage, and displayed componentwise in eq.(3.26). The dual part is displayed likewise in eqs.(3.42). The primal and dual parts of  $\mathbf{S}$  and  $\mathbf{b}$  are derived below: Upon dualizing  $\mathbf{S}$  of eq.(3.31) componentwise, the relation below is obtained:

$$\hat{\mathbf{S}} = \begin{bmatrix} 1 & c\psi_1 - \epsilon d_2 s\psi_1 & c\psi_1(c\phi_1 - \epsilon u_1 s\phi_1) & -c\phi_1 + \epsilon u_1 s\phi_1 \\ 1 & c\psi_2 - \epsilon d_2 s\psi_2 & c\psi_2(c\phi_2 - \epsilon u_2 s\phi_2) & -c\phi_2 + \epsilon u_2 s\phi_2 \\ \vdots & \vdots & \vdots & \vdots \\ 1 & c\psi_m - \epsilon d_2 s\psi_m & c\psi_m(c\phi_m - \epsilon u_m s\phi_m) & -c\phi_m + \epsilon u_m s\phi_m \end{bmatrix} \quad (3.47)$$

or

$$\hat{\mathbf{S}} = \underbrace{\begin{bmatrix} 1 & c\psi_1 & c\psi_1 c\phi_1 & -c\phi_1 \\ 1 & c\psi_2 & c\psi_2 c\phi_2 & -c\phi_2 \\ \vdots & \vdots & \vdots & \vdots \\ 1 & c\psi_m & c\psi_m c\phi_m & -c\phi_m \end{bmatrix}}_{\mathbf{S}} + \epsilon \underbrace{\begin{bmatrix} 0 & -d_2 s\psi_1 & -u_1 c\psi_1 s\phi_1 & u_1 s\phi_1 \\ 0 & -d_2 s\psi_2 & -u_2 c\psi_2 s\phi_2 & u_2 s\phi_2 \\ \vdots & \vdots & \vdots & \vdots \\ 0 & -d_2 s\psi_m & -u_m c\psi_m s\phi_m & u_m s\phi_m \end{bmatrix}}_{\mathbf{S}_o} \quad (3.48)$$

where the definition  $u_i \equiv (d_1)_i$  has been introduced, to avoid a double subscript. Likewise,

$$\hat{\mathbf{k}} = \underbrace{\begin{bmatrix} k_1 \\ k_2 \\ k_3 \\ k_4 \end{bmatrix}}_{\mathbf{k}} + \epsilon \underbrace{\begin{bmatrix} k_{o1} \\ k_{o2} \\ k_{o3} \\ k_{o4} \end{bmatrix}}_{\mathbf{k}_o}, \quad \hat{\mathbf{b}} = \underbrace{\begin{bmatrix} -s\psi_1 s\phi_1 \\ -s\psi_2 s\phi_2 \\ \vdots \\ -s\psi_m s\phi_m \end{bmatrix}}_{\mathbf{b}} + \epsilon \underbrace{\begin{bmatrix} -u_1 s\psi_1 c\phi_1 - d_2 c\psi_1 s\phi_1 \\ -u_2 s\psi_2 c\phi_2 - d_2 c\psi_2 s\phi_2 \\ \vdots \\ -u_m s\psi_m c\phi_m - d_2 c\psi_m s\phi_m \end{bmatrix}}_{\mathbf{b}_o} \quad (3.49)$$

Now, upon equating the primal and the dual parts of eq.(3.45), two real vector equations are obtained, namely,

$$\mathbf{Sk} = \mathbf{b}, \quad \mathbf{Sk}_o + \mathbf{S}_o \mathbf{k} = \mathbf{b}_o \quad (3.50)$$

As the reader can readily verify, the first of the two foregoing equations is identical to that derived for spherical linkages in eq.(3.31). That is, the problem of synthesis of a spatial function generator has been *decoupled* into two, the synthesis procedure then being straightforward:

1. Synthesize first a spherical linkage for the angular input-output data given at the outset;
2. Substitute vector  $\mathbf{k}$ , as obtained from step 1, along with the additional data  $\{(d_1)_i\}_1^m$ , with  $u_i \leftarrow (d_1)_i$ , for  $i = 1, \dots, m$ , and solve the second vector equation of (3.50) for  $\mathbf{k}_o$ , thereby completing the synthesis problem.

**Remark 3.2.1** Given that the output involves a sliding variable  $d_1$ , besides the angle  $\phi$ , two sets of data-points must be prescribed:  $\{\psi_i, \phi_i\}_1^m$  and  $\{\psi_i, (d_1)_i\}_1^m$ .

### 3.3 Exact Synthesis

#### 3.3.1 Planar Linkages

We have  $m = 3$  in this case, and hence, the synthesis equations look like

$$\begin{bmatrix} 1 & c\phi_1 & -c\psi_1 \\ 1 & c\phi_2 & -c\psi_2 \\ 1 & c\phi_3 & -c\psi_3 \end{bmatrix} \begin{bmatrix} k_1 \\ k_2 \\ k_3 \end{bmatrix} = \begin{bmatrix} c(\phi_1 - \psi_1) \\ c(\phi_2 - \psi_2) \\ c(\phi_3 - \psi_3) \end{bmatrix} \quad (3.51a)$$

where

$$c(\cdot) \equiv \cos(\cdot) \quad \text{and} \quad s(\cdot) \equiv \sin(\cdot) \quad (3.51b)$$

Solving *numerically* for  $\{k_i\}_1^3$  is straightforward, if Gaussian elimination, or LU-decomposition, is applied—as, implemented, e.g., in Matlab. Given the simple structure of the system at hand, however, a solution in *closed form* is also possible: To this end, subtract the first

equation from the second and third equations:

$$\begin{bmatrix} 1 & c\phi_1 & -c\psi_1 \\ 0 & c\phi_2 - c\phi_1 & -c\psi_2 + c\psi_1 \\ 0 & c\phi_3 - c\phi_1 & -c\psi_3 + c\psi_1 \end{bmatrix} \begin{bmatrix} k_1 \\ k_2 \\ k_3 \end{bmatrix} = \begin{bmatrix} c(\phi_1 - \psi_1) \\ c(\phi_2 - \psi_2) - c(\phi_1 - \psi_1) \\ c(\phi_3 - \psi_3) - c(\phi_1 - \psi_1) \end{bmatrix} \quad (3.52)$$

Note that the second and third equations are free of  $k_1$ , and hence, one can solve them first for  $k_2$  and  $k_3$ :

$$\begin{bmatrix} c\phi_2 - c\phi_1 & -c\psi_2 + c\psi_1 \\ c\phi_3 - c\phi_1 & -c\psi_3 + c\psi_1 \end{bmatrix} \begin{bmatrix} k_2 \\ k_3 \end{bmatrix} = \begin{bmatrix} c(\phi_2 - \psi_2) - c(\phi_1 - \psi_1) \\ c(\phi_3 - \psi_3) - c(\phi_1 - \psi_1) \end{bmatrix} \quad (3.53)$$

The above  $2 \times 2$  system can be solved for  $k_2$  and  $k_3$  if we recall Fact 1.4.2:

$$\begin{bmatrix} k_2 \\ k_3 \end{bmatrix} = \frac{1}{\Delta} \begin{bmatrix} -c\psi_3 + c\psi_1 & c\psi_2 - c\psi_1 \\ -c\phi_3 + c\phi_1 & c\phi_2 - c\phi_1 \end{bmatrix} \begin{bmatrix} c(\phi_2 - \psi_2) - c(\phi_1 - \psi_1) \\ c(\phi_3 - \psi_3) - c(\phi_1 - \psi_1) \end{bmatrix} \quad (3.54a)$$

where

$$\begin{aligned} \Delta &\equiv \det \begin{bmatrix} c\phi_2 - c\phi_1 & -c\psi_2 + c\psi_1 \\ c\phi_3 - c\phi_1 & -c\psi_3 + c\psi_1 \end{bmatrix} \\ &= (c\phi_2 - c\phi_1)(-c\psi_3 + c\psi_1) + (c\psi_2 - c\psi_1)(c\phi_3 - c\phi_1) \end{aligned} \quad (3.54b)$$

With  $k_2$  and  $k_3$  obtained from eqs.(3.54a & b),  $k_1$  is derived from the first of eqs.(3.52). The final result is

$$k_i = \frac{N_i}{\Delta}, \quad i = 1, 2, 3 \quad (3.55)$$

with numerators  $N_i$  calculated sequentially:

$$\begin{aligned} N_2 &= (-c\psi_3 + c\psi_1)[c(\phi_2 - \psi_2) - c(\phi_1 - \psi_1)] \\ &\quad + (c\psi_2 - c\psi_1)[c(\phi_3 - \psi_3) - c(\phi_1 - \psi_1)] \end{aligned} \quad (3.56a)$$

$$\begin{aligned} N_3 &= (-c\phi_3 + c\phi_1)[c(\phi_2 - \psi_2) - c(\phi_1 - \psi_1)] \\ &\quad + (c\phi_2 - c\phi_1)[c(\phi_3 - \psi_3) - c(\phi_1 - \psi_1)] \end{aligned} \quad (3.56b)$$

$$N_1 = c(\phi_1 - \psi_1)\Delta - c\phi_2 N_2 + c\psi_1 N_3 \quad (3.56c)$$

The foregoing problem is therefore quite simple to solve. We just showed how to solve it in closed form. However, the solution obtained must be correctly interpreted. Indeed, upon looking at definitions (3.8), it is apparent that, all link lengths being positive,  $k_2$  and  $k_3$  should be positive as well, while  $k_1$  is capable of taking any finite positive or negative real values. However, nothing in the above formulation prevents  $k_2$  and  $k_3$  from turning out to be negative or zero. Negative values of these parameters are not to be discarded, for they have a geometric interpretation: Notice that, in eq.(3.10), if  $\phi$  is changed to  $\phi + \pi$ , then the sign of the second term of the left-hand side of that equation is reversed. Ditto the third term if  $\psi$  is changed to  $\psi + \pi$ . The conclusion then follows:

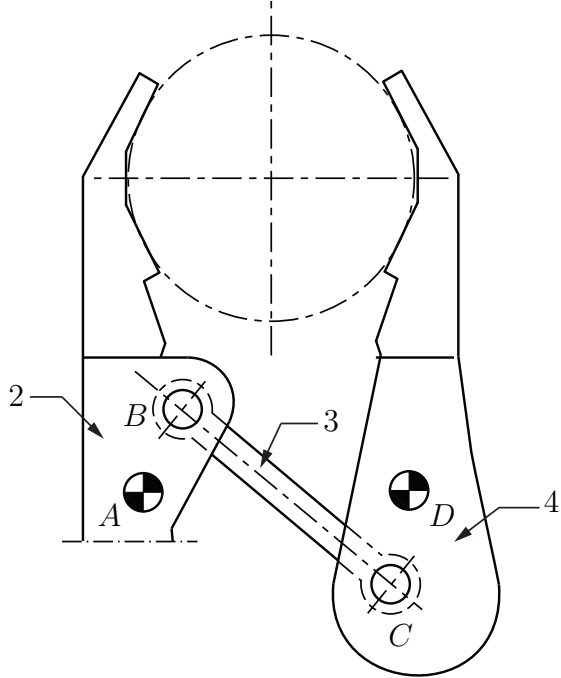


Figure 3.6: The conceptual design of the actuation mechanism for a robotic gripper

*A negative  $k_2$  ( $k_3$ ) indicates that the input (output) angle  $\psi$  ( $\phi$ ) should not be measured as indicated in Fig. 3.1, but all the way down to the extension of link  $O_1O_2$  ( $O_4O_3$ ).*

If the solution to the synthesis problem leads to  $k_2 = 0$ , then  $a_2 \rightarrow \infty$ , which means that the input link is of infinite length. The interpretation now is that the first joint of the linkage is of the P type, i.e., we end up with a PRRR linkage. Likewise, if  $k_3 = 0$ , then  $a_4 \rightarrow \infty$ , and we end up with a RRRP linkage.

Finally, even in the presence of nonzero values of the Freudenstein parameters, nothing guarantees that the link lengths derived from them will yield a feasible linkage. Indeed, for a linkage to be possible, the link lengths must satisfy the *feasibility condition* :

*Any link length must be smaller than the sum of the three other link lengths.*

**Example 3.3.1 (Synthesis of a Robotic Gripper)** *Shown in Fig. 3.6 is a concept proposed by Dudić et al. (1989) to serve as the actuation mechanism of a robotic gripper. This is a four-bar linkage with a symmetric architecture,  $a_2 = a_4$ , as the two fingers of the gripper are intended to open and close with symmetric motions—form follows function!. Determine the link lengths that will produce the pairs of input-output values given in Table 3.1.*

*Solution:* The  $3 \times 3$  synthesis matrix  $\mathbf{S}$  and the 3-dimensional vector  $\mathbf{b}$  of the synthesis equation are first determined with the data of Table 3.1:

Table 3.1: Input-output values for exact function generation with three data points

$j$	$\psi [^\circ]$	$\phi [^\circ]$
1	30.0	240.0
2	45.0	225.0
3	60.0	210.0

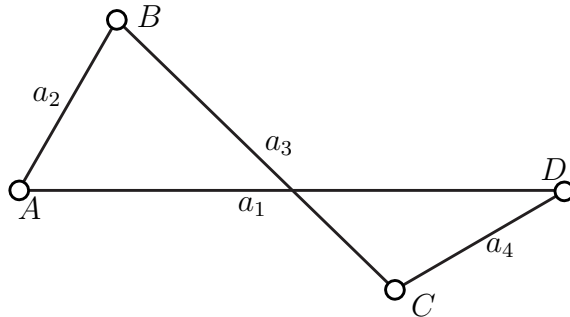


Figure 3.7: The synthesized four-bar linkage for a robotic gripper

$$\mathbf{S} = \begin{bmatrix} 1 & -0.5000 & -.8660 \\ 1 & -.7071 & -.7071 \\ 1 & -.8660 & -.5000 \end{bmatrix}, \quad \mathbf{b} = \begin{bmatrix} -.8660 \\ -1.000 \\ -.8660 \end{bmatrix}$$

The synthesis equation was solved using the LU-decomposition, as implemented by computer-algebra software<sup>2</sup>, which yielded, with four digits,

$$\mathbf{k} = [2.9319 \quad 2.7802 \quad 2.7802]^T$$

thereby obtaining the link lengths:

$$a_1 = 1.0, \quad a_2 = 0.3597, \quad a_3 = 0.7072, \quad a_4 = 0.3597$$

which indeed produce a symmetric linkage, as  $a_2 = a_4$ . The linkage thus synthesized is displayed in Fig. 3.7.

### Bloch Synthesis

A special kind of linkage synthesis occurs when input-output relations are not specified at three distinct values of the input and output angles, but rather at one single value of these angles, to which *velocity and acceleration conditions* are adjoined. The problem thus arising is known as *Bloch synthesis*. Besides its special nature, this problem becomes relevant because of its revelation:

---

<sup>2</sup>See `DuditaXactSynth.mw`

*The simultaneous vanishing of velocity and acceleration of the output link, i.e., second-order rest of the output link, cannot be obtained with a planar four-bar linkage whose input link turns at a constant angular velocity.*

The foregoing claim will be made clear in the sequel. As a matter of fact, second-order rest cannot be obtained with any linkage, but good approximations can be obtained with six-bar linkages producing short-duration dwell.

The problem at hand then can be stated as: *Synthesize a four-bar linkage that meets conditions on position, velocity and acceleration at a given position of the input link.*

In order to formulate this problem, we differentiate both sides of the Freudenstein equation, eq.(3.10), with respect to time. After rearrangement of terms and a reversal of signs, this gives

$$\dot{\phi}s\phi k_2 - \dot{\psi}s\psi k_3 = (\dot{\phi} - \dot{\psi})s(\phi - \psi) \quad (3.57a)$$

$$\begin{aligned} (\ddot{\phi}s\phi + \dot{\phi}^2c\phi)k_2 - (\ddot{\psi}s\psi + \dot{\psi}^2c\psi)k_3 &= (\ddot{\phi} - \ddot{\psi})s(\phi - \psi) \\ &\quad + (\dot{\phi} - \dot{\psi})^2c(\phi - \psi) \end{aligned} \quad (3.57b)$$

Next, we write eqs.(3.10) and (3.57a & b) at  $\psi = \psi_1$ , and cast them in vector form:

$$\mathbf{Ak} = \mathbf{b} \quad (3.58a)$$

where  $\mathbf{A}$  and  $\mathbf{b}$  are given below:

$$\mathbf{A} \equiv \begin{bmatrix} 1 & c\phi_1 & -c\psi_1 \\ 0 & \dot{\phi}_1 s\phi_1 & -\dot{\psi}_1 s\psi_1 \\ 0 & \ddot{\phi}_1 s\phi_1 + \dot{\phi}_1^2 c\phi_1 & -\ddot{\psi}_1 s\psi_1 - \dot{\psi}_1^2 c\psi_1 \end{bmatrix} \quad (3.58b)$$

$$\mathbf{b} \equiv \begin{bmatrix} c(\phi_1 - \psi_1) \\ (\dot{\phi}_1 - \dot{\psi}_1)s(\phi_1 - \psi_1) \\ (\ddot{\phi}_1 - \ddot{\psi}_1)s(\phi_1 - \psi_1) + (\dot{\phi}_1 - \dot{\psi}_1)^2 c(\phi_1 - \psi_1) \end{bmatrix} \quad (3.58c)$$

Notice, from eq.(3.58b), that, if both  $\dot{\phi}_1$  and  $\ddot{\phi}_1$  vanish, then the first and the second columns of  $\mathbf{A}$  become linearly dependent,  $\mathbf{A}$  thus becoming singular.

If  $\mathbf{A}$  is non-singular, the second and third of equations (3.58a) are free of  $k_1$ , and hence, can be decoupled from the first equation to solve for  $k_2$  and  $k_3$ , namely,

$$\begin{bmatrix} \dot{\phi}_1 s\phi_1 & -\dot{\psi}_1 s\psi_1 \\ \ddot{\phi}_1 s\phi_1 + \dot{\phi}_1^2 c\phi_1 & -(\ddot{\psi}_1 s\psi_1 + \dot{\psi}_1^2 c\psi_1) \end{bmatrix} \begin{bmatrix} k_2 \\ k_3 \end{bmatrix} = \begin{bmatrix} (\dot{\phi}_1 - \dot{\psi}_1)s(\phi_1 - \psi_1) \\ (\ddot{\phi}_1 - \ddot{\psi}_1)s(\phi_1 - \psi_1) \\ + (\dot{\phi}_1 - \dot{\psi}_1)^2 c(\phi_1 - \psi_1) \end{bmatrix} \quad (3.59)$$

In solving the above system, we shall need the determinant  $\Delta$  of the above  $2 \times 2$  matrix, which is computed below:

$$\Delta \equiv \det \begin{bmatrix} \dot{\phi}_1 s\phi_1 & -\dot{\psi}_1 s\psi_1 \\ \ddot{\phi}_1 s\phi_1 + \dot{\phi}_1^2 c\phi_1 & -\ddot{\psi}_1 s\psi_1 - \dot{\psi}_1^2 c\psi_1 \end{bmatrix} \quad (3.60)$$

which, upon expansion, yields

$$\Delta = -\dot{\phi}_1 s \phi_1 (\ddot{\psi}_1 s \psi_1 + \dot{\psi}_1^2 c \psi_1) + \dot{\psi}_1 s \psi_1 (\ddot{\phi}_1 s \phi_1 + \dot{\phi}_1^2 c \phi_1) \quad (3.61)$$

thereby making it apparent that, indeed, if  $\dot{\phi}_1 = 0$  and  $\ddot{\phi}_1 = 0$ , then  $\Delta = 0$ , and the above  $2 \times 2$  matrix is singular, and hence,  $\mathbf{A}$  itself is singular as well, thereby proving that a four-bar linkage cannot produce zero velocity and zero acceleration concurrently at the output link when its input link turns at a constant rpm.

Now we recall expression (1.4.2) to invert the  $2 \times 2$  matrix coefficient of vector  $[k_2, k_3]^T$ , thus obtaining

$$\begin{bmatrix} k_2 \\ k_3 \end{bmatrix} = \frac{1}{\Delta} \begin{bmatrix} -(\ddot{\psi}_1 s \psi_1 + \dot{\psi}_1^2 c \psi_1) & \dot{\psi}_1 s \psi_1 \\ -(\ddot{\phi}_1 s \phi_1 + \dot{\phi}_1^2 c \phi_1) & \dot{\phi}_1 s \phi_1 \end{bmatrix} \begin{bmatrix} (\dot{\phi}_1 - \dot{\psi}_1) s (\phi_1 - \psi_1) \\ (\ddot{\phi}_1 - \ddot{\psi}_1) s (\phi_1 - \psi_1) \\ + (\dot{\phi}_1 - \dot{\psi}_1)^2 c (\phi_1 - \psi_1) \end{bmatrix} \quad (3.62)$$

Hence,

$$k_2 = \frac{N_2}{\Delta}, \quad k_3 = \frac{N_3}{\Delta} \quad (3.63a)$$

with

$$\begin{aligned} N_2 \equiv & -(\ddot{\psi}_1 s \psi_1 + \dot{\psi}_1^2 c \psi_1)(\dot{\phi}_1 - \dot{\psi}_1) s (\phi_1 - \psi_1) + \dot{\psi}_1 s \psi_1 [(\ddot{\phi}_1 - \ddot{\psi}_1) s (\phi_1 - \psi_1) \\ & + (\dot{\phi}_1 - \dot{\psi}_1)^2 c (\phi_1 - \psi_1)] \end{aligned} \quad (3.63b)$$

$$\begin{aligned} N_3 \equiv & -(\ddot{\phi}_1 s \phi_1 + \dot{\phi}_1^2 c \phi_1)(\dot{\phi}_1 - \dot{\psi}_1) s (\phi_1 - \psi_1) + \dot{\phi}_1 s \phi_1 [(\ddot{\phi}_1 - \ddot{\psi}_1) s (\phi_1 - \psi_1) \\ & + (\dot{\phi}_1 - \dot{\psi}_1)^2 c (\phi_1 - \psi_1)] \end{aligned} \quad (3.63c)$$

Once  $k_2$  and  $k_3$  are known, we can calculate  $k_1$  from the first of eqs.(3.58a). After simplifications,

$$k_1 = \frac{c(\phi_1 - \psi_1)\Delta - N_2 c \phi_1 + N_3 c \psi_1}{\Delta} \quad (3.63d)$$

thereby completing the solution of the problem at hand.

### 3.3.2 Spherical Linkages

In this case, the synthesis matrix of eq.(3.31) becomes of  $4 \times 4$ , while vector  $\mathbf{b}$  of the same equation becomes four-dimensional, the synthesis equations thus taking the form

$$\begin{bmatrix} 1 & \cos \psi_1 & \cos \psi_1 \cos \phi_1 & -\cos \phi_1 \\ 1 & \cos \psi_2 & \cos \psi_2 \cos \phi_2 & -\cos \phi_2 \\ 1 & \cos \psi_3 & \cos \psi_3 \cos \phi_3 & -\cos \phi_3 \\ 1 & \cos \psi_4 & \cos \psi_4 \cos \phi_4 & -\cos \phi_4 \end{bmatrix} \begin{bmatrix} k_1 \\ k_2 \\ k_3 \\ k_4 \end{bmatrix} = \begin{bmatrix} -\sin \psi_1 \sin \phi_1 \\ -\sin \psi_2 \sin \phi_2 \\ -\sin \psi_3 \sin \phi_3 \\ -\sin \psi_4 \sin \phi_4 \end{bmatrix} \quad (3.64)$$

The structure of the synthesis matrix is strikingly similar to that of the planar case, with the entries of its first column being all unity. Hence, similar to the planar case of Subsection 3.3.1, the equations can be reduced by *elementary operations on the synthesis*

*matrix* to a subsystem of three equations in three unknowns. This is readily done upon subtracting the first equation from the remaining three, which is equivalent to subtracting the first row of the synthesis matrix from its remaining three rows, and subtracting the first component of vector  $\mathbf{b}$  from its remaining three components, namely,

$$\begin{bmatrix} 1 & c\psi_1 & c\psi_1 c\phi_1 & -c\phi_1 \\ 0 & c\psi_2 - c\psi_1 & c\psi_2 c\phi_2 - c\psi_1 c\phi_1 & -c\phi_2 + c\phi_1 \\ 0 & c\psi_3 - c\psi_1 & c\psi_3 c\phi_3 - c\psi_1 c\phi_1 & -c\phi_3 + c\phi_1 \\ 0 & c\psi_4 - c\psi_1 & c\psi_4 c\phi_4 - c\psi_1 c\phi_1 & -c\phi_4 + c\phi_1 \end{bmatrix} \begin{bmatrix} k_1 \\ k_2 \\ k_3 \\ k_4 \end{bmatrix} = \begin{bmatrix} -s\psi_1 s\phi_1 \\ -s\psi_2 s\phi_2 + s\psi_1 s\phi_1 \\ -s\psi_3 s\phi_3 + s\psi_1 s\phi_1 \\ -s\psi_4 s\phi_4 + s\psi_1 s\phi_1 \end{bmatrix} \quad (3.65)$$

The foregoing system can be now cast in a more suitable block-form:

$$\begin{bmatrix} 1 & \mathbf{a}^T \\ \mathbf{0}_3 & \mathbf{A}_3 \end{bmatrix} \mathbf{k} = \begin{bmatrix} b_1 \\ \mathbf{b}_3 \end{bmatrix} \quad (3.66a)$$

with blocks defined as

$$\mathbf{a} \equiv \begin{bmatrix} c\psi_1 \\ c\psi_1 c\phi_1 \\ -c\phi_1 \end{bmatrix}, \quad \mathbf{A}_3 \equiv \begin{bmatrix} c\psi_2 - c\psi_1 & c\psi_2 c\phi_2 - c\psi_1 c\phi_1 & -c\phi_2 + c\phi_1 \\ c\psi_3 - c\psi_1 & c\psi_3 c\phi_3 - c\psi_1 c\phi_1 & -c\phi_3 + c\phi_1 \\ c\psi_4 - c\psi_1 & c\psi_4 c\phi_4 - c\psi_1 c\phi_1 & -c\phi_4 + c\phi_1 \end{bmatrix}, \quad (3.66b)$$

$$b_1 \equiv -s\psi_1 s\phi_1, \quad \mathbf{b}_3 \equiv \begin{bmatrix} -s\psi_2 s\phi_2 + s\psi_1 s\phi_1 \\ -s\psi_3 s\phi_3 + s\psi_1 s\phi_1 \\ -s\psi_4 s\phi_4 + s\psi_1 s\phi_1 \end{bmatrix} \quad (3.66c)$$

and  $\mathbf{0}_3$  is the three-dimensional zero vector. We can thus identify in the above system a reduced system of three equations in three unknowns that has been decoupled from the original system of four equations, namely,

$$\mathbf{A}_3 \mathbf{k}_3 = \mathbf{b}_3, \quad \mathbf{k}_3 \equiv \begin{bmatrix} k_2 \\ k_3 \\ k_4 \end{bmatrix} \quad (3.67)$$

Further,  $\mathbf{A}_3$  is partitioned columnwise as done in Subsection 1.4.3:

$$\mathbf{A}_3 = [\mathbf{c}_1 \quad \mathbf{c}_2 \quad \mathbf{c}_3] \quad (3.68)$$

Therefore, the inverse of  $\mathbf{A}_3$  can be computed in this case symbolically, by means of *reciprocal bases*, as per eq.(1.9a):

$$\mathbf{A}_3^{-1} = \frac{1}{\Delta} \begin{bmatrix} (\mathbf{c}_2 \times \mathbf{c}_3)^T \\ (\mathbf{c}_3 \times \mathbf{c}_1)^T \\ (\mathbf{c}_1 \times \mathbf{c}_2)^T \end{bmatrix} \quad (3.69a)$$

where

$$\Delta \equiv \mathbf{c}_1 \times \mathbf{c}_2 \cdot \mathbf{c}_3 \quad (3.69b)$$

and hence,

$$\mathbf{k}_3 = \frac{1}{\Delta} \begin{bmatrix} (\mathbf{c}_2 \times \mathbf{c}_3)^T \mathbf{b}_3 \\ (\mathbf{c}_3 \times \mathbf{c}_1)^T \mathbf{b}_3 \\ (\mathbf{c}_1 \times \mathbf{c}_2)^T \mathbf{b}_3 \end{bmatrix} \quad (3.69c)$$

thereby computing  $k_2$ ,  $k_3$  and  $k_4$ . The remaining unknown,  $k_1$ , is computed from the first equation of the array (3.65):

$$k_1 + k_2 c\psi_1 + k_3 c\psi_1 c\phi_1 - k_4 c\phi_1 = -s\psi_1 s\phi_1$$

Therefore,

$$k_1 = -s\psi_1 s\phi_1 - k_2 c\psi_1 - k_3 c\psi_1 c\phi_1 + k_4 c\phi_1 \quad (3.69d)$$

all unknowns having thus been found.

**Remark 3.3.1** *The foregoing closed-form solution of the exact synthesis problem at hand is apparently elegant and gives some insight into the relations among the variables involved, e.g., the problem has no solution when the three columns of  $\mathbf{A}_3$ , or its three rows for that matter, are coplanar. Moreover, the numerical evaluation of the Freudenstein parameters is exactly that obtained with Cramer's rule, which is notorious for being inefficient and prone to roundoff-error amplification. In our case, all four components of  $\mathbf{k}$  have been obtained symbolically, and hence, can be safely evaluated using computer algebra.*

**Remark 3.3.2** *Given that  $k_3 = \lambda_1 = \cos \alpha_1$ , the computed  $k_3$  must be smaller than unity in absolute value, and hence, any solution with  $|k_3| > 1$  must be rejected. By the same token,  $c\alpha_3 = c\alpha_1 c\alpha_2 c\alpha_4 - k_1 s\alpha_2 s\alpha_4$ , and hence, the absolute value of the foregoing difference must be smaller than unity.*

### 3.3.3 Spatial Linkages

The two synthesis matrices,  $\mathbf{S}$  and  $\mathbf{S}_o$ , of eq.(3.48) become now of  $4 \times 4$ , while vectors  $\mathbf{b}$  and  $\mathbf{b}_o$  of eq.(3.49) become four-dimensional. As a matter of fact,  $\mathbf{S}$ ,  $\mathbf{k}$  and  $\mathbf{b}$  are exactly the same as their counterparts in the spherical case, the first synthesis equation of eq.(3.50) thus being identical to eq.(3.64).

The second synthesis equation of the same eq.(3.50) is rewritten below in the standard form in which the left-hand side includes only the terms in the unknowns, namely,

$$\mathbf{S}\mathbf{k}_o = \mathbf{b}_o - \mathbf{S}_o\mathbf{k} \quad (3.70)$$

where, now,  $\mathbf{S}$  and  $\mathbf{S}_o$  are  $4 \times 4$  instances of the more general matrices of eq.(3.48), while  $\mathbf{b}$  and  $\mathbf{b}_o$  are 4-dimensional instances of their counterparts in eq.(3.49).

In the spherical case, the system (3.64) was solved in closed form upon reducing it to a system of three equations in three unknowns, which was done by subtracting the

first equation from the other three, thereby ending up with a new, reduced system of three equations in three unknowns, namely, eq.(3.67). The reader is invited to obtain the reduced equations that would allow for a closed-form solution of both the primal Freudenstein-parameter vector  $\mathbf{k}$  and its dual counterpart  $\mathbf{k}_o$ .

It is noteworthy that the foregoing computations lead to the solution of a system of three equations in three unknowns, which can be solved symbolically by means of reciprocal bases. Remarks 3.3.1 and 3.3.2 apply in this case as well.

## 3.4 Analysis of the Synthesized Linkage

After a linkage is synthesized, its performance should be evaluated, which is done by means of analysis. The first step in analyzing a linkage synthesized for function generation is to produce its *Denavit-Hartenberg parameters*, for all we have is its *Freudenstein parameters*. Below we derive analysis algorithms for planar, spherical and spatial four-bar linkages.

### 3.4.1 Planar Linkages

We start by recalling the inverse relations of eqs.(3.11), which we reproduce below for quick reference:

$$a_2 = \frac{1}{k_2}a_1, \quad a_4 = \frac{1}{k_3}a_1, \quad a_3 = \sqrt{a_1^2 + a_2^2 + a_4^2 - 2k_1a_2a_4} \quad (3.71)$$

Two remarks are in order:

- (i) The link lengths are given in terms of  $a_1$ , which is thus the link length that determines the scale of the linkage, but any other length can be used for the same purpose; and
- (ii) all lengths are positive. However, negative signs for  $k_2$  and  $k_3$  can occur, that hence lead to negative values of  $a_2$  or, correspondingly,  $a_4$ . As we saw in Subsection 3.3.1, negative values of any of these variables, or of both for that matter, bear a straightforward interpretation.

We now proceed to derive an algorithm for the fast and reliable computation of the output values of  $\phi$  corresponding to a) a given linkage of feasible link lengths  $\{a_i\}_1^4$  and b) a given input value  $\psi$ . We can do this in several ways. We start by recalling the IO equation of the planar four-bar linkage in homogeneous form, eq.(3.11):

$$k_1 + k_2 \cos \phi - k_3 \cos \psi - \cos(\phi - \psi) = 0$$

Upon expansion of the fourth term in the left-hand side, the foregoing equation can be rewritten as

$$A(\psi) \cos \phi + B(\psi) \sin \phi + C(\psi) = 0 \quad (3.72a)$$

with coefficients defined as

$$A(\psi) = k_2 - \cos \psi, \quad B(\psi) = -\sin \psi, \quad C(\psi) = k_1 - k_3 \cos \psi \quad (3.72b)$$

One approach to solving this equation for  $\phi$  consists in transforming it into an algebraic equation<sup>3</sup>. This is done by means of the tan-half identities, which are recalled below, as applied to angle  $\phi$ :

$$\cos \phi \equiv \frac{1 - T^2}{1 + T^2}, \quad \sin \phi \equiv \frac{2T}{1 + T^2}, \quad T \equiv \tan\left(\frac{\phi}{2}\right) \quad (3.73)$$

Upon substitution of the foregoing identities into eq.(3.72a), a quadratic equation in  $T$  is obtained:

$$D(\psi)T^2 + 2E(\psi)T + F(\psi) = 0 \quad (3.74a)$$

whose coefficients are given below:

$$D(\psi) \equiv k_1 - k_2 + (1 - k_3) \cos \psi \quad (3.74b)$$

$$E(\psi) \equiv -\sin \psi \quad (3.74c)$$

$$F(\psi) \equiv k_1 + k_2 - (1 + k_3) \cos \psi \quad (3.74d)$$

Now  $\phi$  can be readily computed once the two roots of eq.(3.74a) are available. Here, a caveat is in order: during the linkage motion, the three coefficients  $D(\psi)$ ,  $E(\psi)$  and  $F(\psi)$  vary as  $\psi$  does. Now, given that the above-mentioned roots are computed *automatically* using scientific code, the algorithm implementing the computations must account for *pitfalls* brought about by special numerical conditions. Thus, rather than naively using *verbatim* the formula for the roots of the quadratic equation, we follow here a *robust* approach, as suggested by Forsythe (1970): in order to avoid *catastrophic cancelations* when  $E^2 \gg DF$ , that would lead to an erroneous zero root, we first compute the root with the *larger* absolute value, namely,

$$T_1 = \frac{-E - \text{sgn}(E)\sqrt{E^2 - DF}}{D}, \quad \phi_1 = 2 \tan^{-1}(T_1) \quad (3.75)$$

where  $\text{sgn}(\cdot)$  is the *signum function* introduced in Section 1.4 when we studied Householder reflections.

Now we distinguish two cases:

1. Assume  $B(\psi) \equiv E(\psi) = -\sin \psi \neq 0$ . In this case,  $T_1$  is calculated as in eq.(3.75), while  $T_2$  is calculated upon recalling that the independent term is proportional to the product  $T_1 T_2$ , and hence,

$$T_2 = \frac{F}{DT_1}, \quad \phi_2 = 2 \tan^{-1}(T_2) \quad (3.76a)$$

---

<sup>3</sup>That is, a *polynomial equation*.

2. Now assume  $B(\psi) \equiv E(\psi) = -\sin \psi = 0$ . Under this condition, the term linear in  $T$  in eq.(3.74a) vanishes, the two roots being symmetric, namely,

$$T_{1,2} = \pm \sqrt{-\frac{F(\psi)}{D(\psi)}} \quad (3.76b)$$

Thus, cancellations are avoided upon *first* computing  $T_1$ ; then,  $T_2$  is computed safely because the denominator appearing in eq.(3.76a) has the largest possible absolute value. However, notice that the quadratic equation can degenerate into a linear equation under two cases: (a)  $F(\psi) = 0$  or (b)  $D(\psi) = 0$ . The first case simply means that one root,  $T_1$ , is zero,  $T_2$  being computed from the linear equation derived upon dividing the two sides of that quadratic by  $T$ . The second case is a bit more elusive, but it can be handled as the limiting case  $D(\psi) \rightarrow 0$ . To this end, let us divide both sides of eq.(3.74a) by  $T^2$ :

$$D(\psi) + \frac{2E(\psi)}{T} + \frac{F(\psi)}{T^2} = 0$$

Now, upon taking the limit of both sides of the above equation when  $D(\psi) \rightarrow 0$ , we obtain

$$\lim_{D(\psi) \rightarrow 0} T \rightarrow \infty$$

and hence,

$$\lim_{D(\psi) \rightarrow 0} \phi = \pi \quad (3.77)$$

In any event, the two possible solutions of the quadratic equation obtained above lead to one of three possible cases:

1. The two roots  $\{T_i\}_1^2$  are real and distinct: the corresponding angles  $\{\phi_i\}_1^2$  provide the two *conjugate* postures of the linkage. As the linkage moves, the two conjugate postures generate, correspondingly, two *conjugate branches* of the linkage motion, as shown in Fig. 3.8(a);
2. The two roots  $\{T_i\}_1^2$  are real and identical: the corresponding single value of  $\phi_1 = \phi_2$  indicates the merging of the two branches. This indicates in turn that the output link reached one extreme position, which is known as a *deadpoint*, as illustrated in Fig. 3.8(b);
3. The two roots are complex conjugate: this indicates two possibilities:
  - (a) The link lengths are unfeasible: they do not define a quadrilateron; or
  - (b) The linkage is feasible, but its input link does not move through a full turn, i.e., it is a *rocker*, the given value of  $\psi$  lying outside of its range of motion.

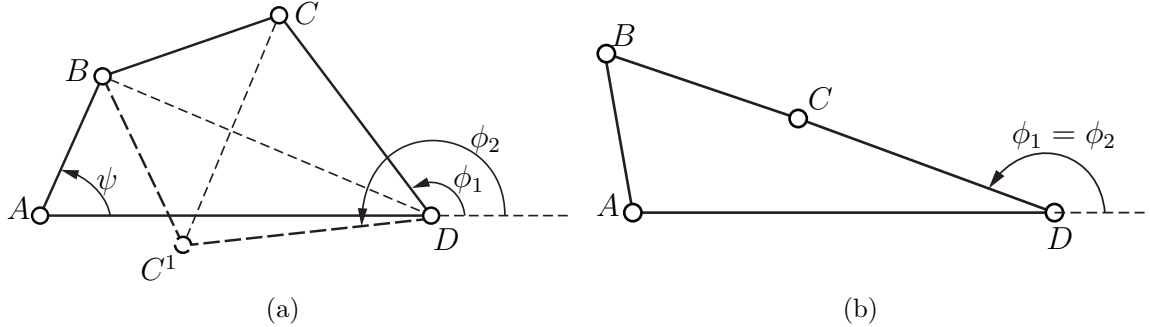


Figure 3.8: Postures of a four-bar linkage: (a) two distinct, conjugate postures; (b) deadpoint, where the two conjugate postures merge

Because of the *two conjugate branches* of the planar four-bar linkage, the linkage is said to be *bimodal*.

It is apparent that the quadratic-equation approach to the input-output analysis of the four-bar linkage must be handled with care, especially when writing code to implement it. As an alternative, we can pursue a more geometric, straightforward approach, free of the *singularity*  $T \rightarrow \infty$  of the transformation (3.73), as described below: We go back to eq.(3.72a), and rewrite it in a slightly different form

$$\mathcal{L} : \quad A(\psi)u + B(\psi)v + C(\psi) = 0 \quad (3.78a)$$

where

$$u \equiv \cos \phi, \quad v \equiv \sin \phi \quad (3.78b)$$

and hence,  $u$  and  $v$  are subject to the constraint

$$\mathcal{C} : \quad u^2 + v^2 = 1 \quad (3.78c)$$

The input-output equation thus defines a line  $\mathcal{L}$  in the  $u$ - $v$  plane, while the constraint (3.78c) defines a unit circle  $\mathcal{C}$  centred at the origin of the same plane. The circle is fixed, but the location of the line in the  $u$ - $v$  plane depends on both the linkage parameters  $k_1, k_2, k_3$  and the input angle  $\psi$ . Therefore, depending upon the linkage at hand and the position of its input link, the line may intersect the circle or not. If it does, then, additionally, the line either intersects the circle at two distinct points or, as a special case, at one single point, in which case the line is tangent to the circle, the two intersection points thus merging into a single one. In the absence of intersections, either the linkage is unfeasible or its input link is a rocker, the given input angle lying outside of its mobility range. In the case of two distinct intersections, these determine the two conjugate postures of the linkage. In the case of tangency, the linkage is at a deadpoint. Figure 3.9 depicts the case of two distinct intersection points.

Let the distance of the line to the origin be denoted by  $d$ . Apparently, we have the three cases below:

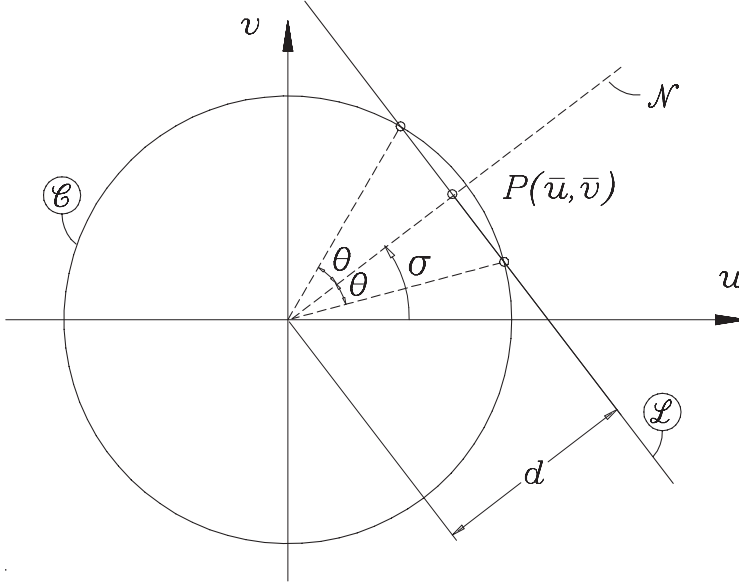


Figure 3.9: Line and circle in the **u-v** plane

$d < 1$ :  $\mathcal{L}$  intersects  $\mathcal{C}$  at two distinct points;

$d = 1$ :  $\mathcal{L}$  is tangent to  $\mathcal{C}$ ;

$d > 1$ :  $\mathcal{L}$  does not intersect  $\mathcal{C}$ .

The distance  $d$  can be readily found to be

$$d = \frac{|C(\psi)|}{S(\psi)} \quad (3.79a)$$

where  $C(\psi)$  was defined in eq.(3.72b) and

$$S(\psi) \equiv \sqrt{A(\psi)^2 + B(\psi)^2} = \sqrt{(k_2 - \cos \psi)^2 + \sin^2 \psi} \quad (3.79b)$$

An interesting *singularity* occurs whereby the foregoing calculations break down: If coefficients  $A(\psi)$ ,  $B(\psi)$ , and  $C(\psi)$  in eq.(3.78a) all vanish, then the line  $\mathcal{L}$  disappears and *any* value of  $\phi$  satisfies the input-output equation for the given value of  $\psi$ . The vanishing of these three coefficients is written below:

$$k_2 - \cos \psi = 0 \quad (3.80a)$$

$$\sin \psi = 0 \quad (3.80b)$$

$$k_1 - k_3 \cos \psi = 0 \quad (3.80c)$$

The second equation leads to  $\psi = 0$  or  $\pi$ . For  $\psi = 0$ , the first equation yields  $k_2 = 1$  and the third equation  $k_1 = k_3$ . Now,  $k_2 = 1$  means  $a_2 = a_1$ , which, together with  $k_1 = k_3$ , means  $a_4 = a_3$ , the result being a set of linkage postures whereby joint centres  $B$  and  $D$

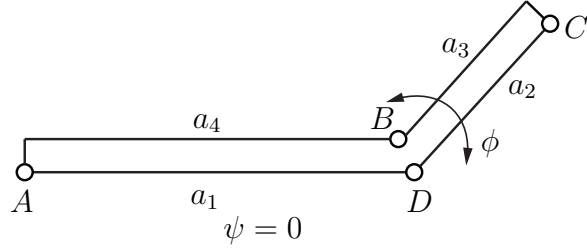


Figure 3.10: Pathological case of a four-bar linkage with special link lengths

coincide, the coupler and the output links thus being free to turn about joint centre  $D$  as one single rigid-body.

For  $\psi = \pi$ , the first equation yields  $k_2 = -1$ , which leads to  $a_2 = -a_1$ , i.e., a “negative” link length. As we saw in Subsection 3.3.1, a negative  $a_2$  means that the input angle should be measured “all the way down to the extension of the input link,” and we fall into the case  $\psi = 0$ .

Notice that this pathological case, or singularity, is not apparent from the quadratic equation. It is illustrated in Fig. 3.10.

Furthermore, in order to compute the two conjugate values  $\phi_1$  and  $\phi_2$ , we calculate first the intersection of  $\mathcal{L}$  with its normal  $\mathcal{N}$  from the origin. The intersection point  $P$  has coordinates  $(\bar{u}, \bar{v})$ , given below:

$$\bar{u} = \frac{C(\psi)(k_2 - \cos \psi)}{S(\psi)^2}, \quad \bar{v} = \frac{-C(\psi) \sin \psi}{S(\psi)^2} \quad (3.81a)$$

Now, the angle  $\sigma$  that  $\mathcal{N}$  makes with the  $u$  axis, when  $d > 0$ , and angle  $\theta$ , half the angle subtended by the chord defined by the intersections of  $\mathcal{L}$  with  $\mathcal{C}$ , are given by

$$\sigma = \arctan\left(\frac{\bar{v}}{\bar{u}}\right) \quad (3.81b)$$

$$\theta = \arccos(d) \quad (3.81c)$$

When  $d = 0$ ,  $\sigma$  cannot be calculated from the above expression, but rather as  $\arctan(-1/m)$ , where  $m$  is the slope of  $\mathcal{L}$ . Nevertheless, in this case  $\sigma$  is not needed, for the two conjugate values of the output angle can be calculated directly. Thus,

$$\phi_1 = \sigma + \theta, \quad \phi_2 = \sigma - \theta, \quad \text{for } d > 0 \quad (3.81d)$$

$$\phi_2 = \arctan\left(\frac{k_2 - \cos \psi}{\sin \psi}\right), \quad \phi_1 = \phi_2 + \pi, \quad \text{for } d = 0 \quad (3.81e)$$

We thus have devised the algorithm below for computing the two conjugate values of the output angle, in Maple code:

**Algorithm pl4bar-io(k, input)**

This algorithm computes the intersection of one line  $L$  and the unit circle

centred at the origin of the  $\cos(\phi)$ - $\sin(\phi)$  plane. The intersection points, when they exist, are returned in array `out`, with `out[1]` and `out[2]` denoting the two conjugate values of the output angle  $\phi$

```

read k[1], k[2], k[3], input;
> pl4bar-io:=proc(k,input) #Use this
> procedure only if are sure that your linkage is feasible
> local dpoint,feasible,pathos,D_d,N_d,d,u,v,sigma,theta; global
> out;
> dpoint:=false; #we assume that we are not in the presence of a
> deadpoint
> feasible:=true; #we assume that current psi-value is feasible
> pathos:=false; #we assume that we are not in the presence of
> pathological case whereby linkage becomes a one-dof open chain if
> k[2]=1 and psi=0 then pathos:=true; print(patholo=pathos); return;
> fi;
> #if k[2]=1, then a[1]=a[2]
> D_d:=k[2]*(k[2]-2*cos(input))+1: N_d:=-k[1]+k[3]*cos(input):
> d:=abs(N_d)/sqrt(D_d): #print(dd=d); #distance of line L to origin
> if d>1.0 then feasible:=false; print(feas=feasible); return; fi;
> if d=1.0 then dpoint:=true; print(dead=dpoint); theta=0; fi;
> u:=(N_d/D_d^2)*(k[2]-cos(input)): v:=-(N_d/D_d^2)*sin(input):
> #coordinates of intersection of line L and its normal N
> passing through the origin sigma:=arctan(v,u): #print(sig=sigma);
> #angle that normal makes with u-axis if dpoint=false then
> theta:=arccos(d); fi; #print(th=theta); #(1/2)angle subtended by
> secant to circle out[1]:=sigma-theta: out[2]:=sigma+theta: if v<0
> and u>0 then out[1]:=sigma+theta: out[2]:=sigma-theta: fi: #Note:
> this line does not appear in the Lecture Notes, but it is needed
> #print(out1=out[1]); print(out2=out[2]);
> end proc;
```

Various issues stem from the foregoing discussion, namely,

- (a) Linkage feasibility: For the four link lengths to yield a *feasible linkage*, they must define a quadrilateron. The condition on four given side lengths to close a quadrilateron, as given in Subsection 3.3.1, is that every length be smaller than the sum of the remaining three. When four link lengths are given as candidates to define a planar four-bar linkage, these lengths must first and foremost be capable of defining a quadrilateron. If they do, the lengths are said to be *feasible*; otherwise, they are *unfeasible*.
- (b) Link mobility: A link may or may not be capable of a full turn; if capable, it is called a *crank*; otherwise, it is called a *rocker*. This gives rise to various types of linkages, depending on the type of its input and output links, namely, *double crank*, *crank-rocker*, *rocker-crank*, or *double rocker*. Double-crank linkages are known as

*drag-link* mechanisms. This variety of linkage type leads, in turn, to what is known as *Grashof mechanisms*.

A major fundamental result in linkage theory is the *Grashof classification* of planar four-bar linkages. This classification looks at the mobility of three links with respect to the remaining one. Obviously, which of the four links is considered the “remaining one” is immaterial. According to Grashof’s classification, a linkage is termed *Grashof* if *at least one* of its links is capable of a full turn with respect to any other link. Otherwise, the linkage is termed *non-Grashof*. Now we have the main result—for a proof, see, e.g., (Waldron and Kinzel, 1999)—below:

*A planar four-bar linkage is Grashof if and only if the sum of the lengths of its shortest and longest links is smaller than or equal to the sum of the two other link lengths.*

In linkage synthesis, we are interested in meeting mobility conditions either on the input or on the output links, or even on both. We derive below these conditions in terms of the Freudenstein parameters.

### Mobility of the Input and Output Links

The condition under which the input link is a crank is quite useful because four-bar linkages are frequently driven at a constant angular velocity, and hence, the input link would better be capable of a full turn. To find this condition, we recall eq.(3.74a), whose discriminant is a function not only of constants  $k_1$ ,  $k_2$  and  $k_3$ , but also of  $\psi$  and, hence, it is not only linkage- but also posture-dependent. In the discussion below, we assume that the linkage parameters are fixed, and hence, the *linkage discriminant*  $\Delta(\psi)$ , stemming from eq.(3.74a), will be regarded as a function of  $\psi$  only. This is given by

$$\Delta(\psi) \equiv E^2(\psi) - D(\psi)F(\psi) \quad (3.82a)$$

Upon expansion, the above discriminant becomes

$$\Delta(\psi) \equiv -k_3^2 \cos^2 \psi + 2(k_1 k_3 - k_2) \cos \psi + (1 - k_1^2 + k_2^2) \quad (3.82b)$$

which is, clearly, a parabola in  $\cos \psi$  with concavity downward—its second derivative w.r.t.  $\cos \psi$  is  $-2k_3^2$ . Moreover, since  $\Delta(\psi)$  is a function only of  $\cos \psi$ , which is an *even function* of  $\psi$ ,  $\Delta(\psi)$  is also an even function of  $\psi$ , i.e.,

$$\Delta(\psi) = \Delta(-\psi)$$

For the input link to be a crank, then, the discriminant  $\Delta(\psi)$  should attain nonnegative values in the range  $-1 \leq \cos \psi \leq +1$ . Moreover, by virtue of the parabolic shape of the

$\Delta(\cos \psi)$  vs.  $\cos \psi$  plot,  $\Delta$  is nonnegative for *any* value of  $\psi$  if and only if  $\Delta(\cos \psi) \geq 0$  when  $\cos \psi = \pm 1$ . It is noteworthy that, even though  $\Delta(\psi)$  is an even function,  $\Delta(\cos \psi)$  is not; in general, then,  $\Delta(\cos \psi)$  attains distinct values at  $\cos \psi = -1$  and at  $\cos \psi = +1$ . Let  $\Delta_1$  and  $\Delta_2$  denote the values that  $\Delta$  attains when  $\cos \psi$  equals  $+1$  and  $-1$ , respectively, which are given below:

$$\Delta_1 = -k_3^2 + 2(k_1 k_3 - k_2) + 1 - k_1^2 + k_2^2, \quad \Delta_2 = -k_3^2 - 2(k_1 k_3 - k_2) + 1 - k_1^2 + k_2^2$$

The necessary and sufficient conditions for a nonnegative linkage discriminant, for any value of  $\psi$ , are now derived. Note first that  $\Delta_1$  and  $\Delta_2$  can be expressed as differences of squares, namely,

$$\Delta_1 = (1 - k_2)^2 - (k_1 - k_3)^2, \quad \Delta_2 = (1 + k_2)^2 - (k_1 + k_3)^2$$

Apparently,  $\Delta_1$  and  $\Delta_2$  are nonnegative if and only if the relations below hold:

$$(k_1 - k_3)^2 - (1 - k_2)^2 \leq 0 \quad \text{and} \quad (k_1 + k_3)^2 - (1 + k_2)^2 \leq 0 \quad (3.83)$$

Upon expressing left-hand sides of the foregoing inequalities as the products of conjugate binomials, the inequalities become

$$(k_1 - k_3 - 1 + k_2)(k_1 - k_3 + 1 - k_2) \leq 0 \quad (3.84a)$$

$$(k_1 + k_3 - 1 - k_2)(k_1 + k_3 + 1 + k_2) \leq 0 \quad (3.84b)$$

Each of the above inequalities holds if its two left-hand side factors have opposite signs, the first inequality thus leading to

$$k_1 - k_3 - 1 + k_2 \geq 0 \quad \& \quad k_1 - k_3 + 1 - k_2 \leq 0 \quad (3.84c)$$

or

$$k_1 - k_3 - 1 + k_2 \leq 0 \quad \& \quad k_1 - k_3 + 1 - k_2 \geq 0 \quad (3.84d)$$

The second inequality, likewise, leads to

$$k_1 + k_3 - 1 - k_2 \geq 0 \quad \& \quad k_1 + k_3 + 1 + k_2 \leq 0 \quad (3.84e)$$

or

$$k_1 + k_3 - 1 - k_2 \leq 0 \quad \& \quad k_1 + k_3 + 1 + k_2 \geq 0 \quad (3.84f)$$

Thus, the region of the  $\mathbf{k}$ -space  $\mathcal{K}$  containing input cranks is the *intersection* of two subregions, that defined by the four inequalities (3.84c & d) and that defined by their counterparts (3.84e & f). Moreover, the subregion represented by each quadruplet is the *union* of the intersections of the regions defined by each pair of linear inequalities. Let  $\mathcal{C}_1$  and  $\mathcal{C}_2$  be the subregions defined by the first and the second inequalities (3.84c), with similar definitions for subregions  $\mathcal{D}_1$ ,  $\mathcal{D}_2$ ,  $\mathcal{E}_1$ ,  $\mathcal{E}_2$ ,  $\mathcal{F}_1$  and  $\mathcal{F}_2$ . Let, further,  $\mathcal{R}_1$  denote the subregion defined by the four inequalities (3.84c) & (3.84d), and hence,

$$\mathcal{R}_1 = (\mathcal{C}_1 \cap \mathcal{C}_2) \cup (\mathcal{D}_1 \cap \mathcal{D}_2) \quad (3.85a)$$

with a similar definition for the subregion  $\mathcal{R}_2$ , stemming from the four inequalities (3.84e) & (3.84f):

$$\mathcal{R}_2 = (\mathcal{E}_1 \cap \mathcal{E}_2) \cup (\mathcal{F}_1 \cap \mathcal{F}_2) \quad (3.85b)$$

Therefore, the region  $\mathcal{R}_I$  containing input cranks is

$$\mathcal{R}_I = (\mathcal{R}_1 \cap \mathcal{R}_2) \quad (3.86)$$

Each inequality, furthermore, divides  $\mathcal{K}$  into two halves, one on each side of the plane obtained when turning the inequality sign of each relation into an equality sign. As the reader can readily notice, inequalities (3.84c & d) lead to the same pair of planes; likewise inequalities (3.84e & f) lead to a second pair of planes, namely,

$$\begin{aligned} k_1 + k_2 - k_3 - 1 &= 0, & k_1 - k_2 - k_3 + 1 &= 0 \\ k_1 - k_2 + k_3 - 1 &= 0, & k_1 + k_2 + k_3 + 1 &= 0 \end{aligned}$$

In summary, then, the two original quadratic inequalities of eq.(3.83) represent a region of  $\mathcal{K}$  bounded by four planes, as displayed in Fig. 3.11. Hence, the region containing input cranks comprises a regular tetrahedron with its centroid located at the origin of the above space, and two open convexes. Thus, all points within that region represent linkages whose input link is a crank.

It is noteworthy that the  $k_1$ -axis represents linkages for which  $a_2, a_4 \rightarrow \infty$ , i.e., the  $k_1$ -axis represents, actually, all PRRP linkages. However, as the reader is invited to verify, the origin does not represent a feasible linkage.

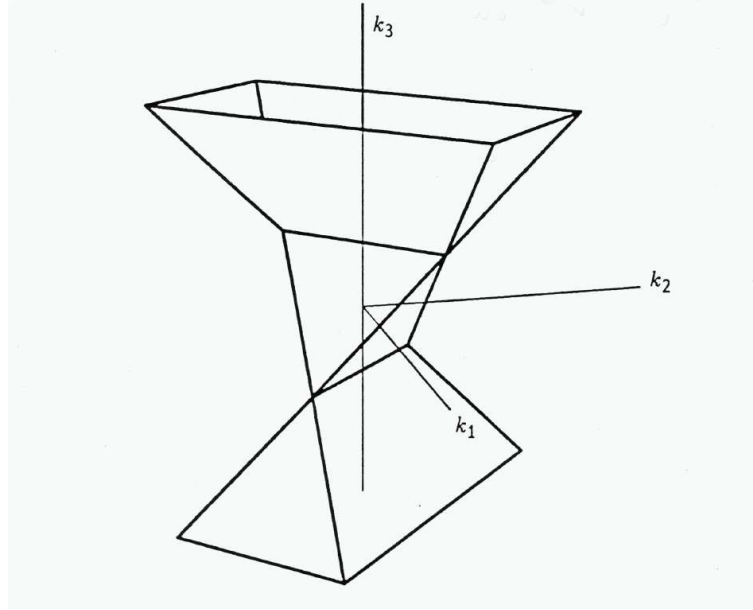


Figure 3.11: Region comprising planar four-bar linkages with an input crank

Now, in order to analyze the mobility of the output link, we simply exchange the roles of  $k_2$  and  $k_3$  in the foregoing results, which is apparent from the definitions of the linkage

parameters  $\{k_i\}_1^3$ , as given in eqs.(3.71) and the Freudenstein equation (3.10). Actually, then, the region containing output cranks can be obtained by mapping that containing input cranks by means of a linear transformation:

$$k_1 = k_1, \quad k_2 = -k_3, \quad k_3 = -k_2$$

The above transformation can be represented in matrix form as a *reflection*  $\mathbf{R}$  about a plane of unit normal  $[0, \sqrt{2}/2, \sqrt{2}/2]^T$ , given by (Angeles, 2014)

$$\mathbf{R} = \begin{bmatrix} 1 & 0 & 0 \\ 0 & 0 & -1 \\ 0 & -1 & 0 \end{bmatrix}$$

As the reader can readily verify,  $\mathbf{R}\mathbf{R}^T = \mathbf{1}$ , with  $\mathbf{1}$  denoting the  $3 \times 3$  identity matrix and  $\det(\mathbf{R}) = -1$ , which shows that  $\mathbf{R}$  is a reflection.

By means of the foregoing exchange in eqs.(3.84a & b), the inequalities leading to an output crank are obtained as

$$(k_1 - k_2)^2 < (1 - k_3)^2 \quad (3.87a)$$

$$(k_1 + k_2)^2 < (1 + k_3)^2 \quad (3.87b)$$

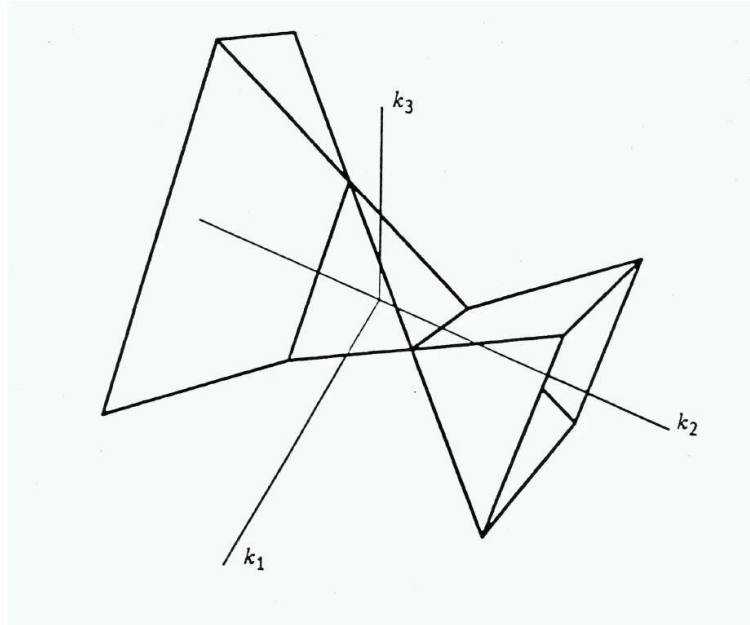


Figure 3.12: Region comprising four-bar linkages with an output crank

The mobility region  $\mathcal{R}_O$  represented by the two foregoing inequalities comprises all four-bar linkages with an *output crank*. This region is, then, the mirror image of that of Fig. 3.11 when reflected about a plane  $\Pi$  passing through the  $k_1$ -axis and intersecting the  $k_2$ - $k_3$  plane along a line passing through the origin and contained in the third and fourth quadrants of this plane. The foregoing region is represented in Fig. 3.12. Note that this region comprises a tetrahedron identical to that of Fig. 3.11 and, hence, the tetrahedron

is common to both mobility regions. Thus, any point within this tetrahedron represents a double-crank four-bar linkage, except for the origin, of course.

Furthermore, the central tetrahedron of Figs. 3.11 and 3.12 can be shown to have axes of length  $2\sqrt{2}$ .

All linkages outside of the two foregoing regions are either of the rocker-rocker type or unfeasible.

### 3.4.2 Spherical Four-Bar Linkages

The analysis of the spherical four-bar linkage parallels that of its planar counterpart. Indeed, upon introduction of the tan-half identities of eq.(3.73) into the IO equation of the spherical linkage, eq.(3.27), we obtain, again, a quadratic equation in  $T$  of the form of eq.(3.74a), namely,

$$D(\psi)T^2 + 2E(\psi)T + F(\psi) = 0 \quad (3.88a)$$

but now with coefficients that are given below:

$$D(\psi) \equiv k_1 + (k_2 - k_3) \cos \psi + k_4 \quad (3.88b)$$

$$E(\psi) \equiv \sin \psi \quad (3.88c)$$

$$F(\psi) \equiv k_1 + (k_2 + k_3) \cos \psi - k_4 \quad (3.88d)$$

Similar to the planar case, rather than attempting a solution of the quadratic equation as such, we cast the input-output equation (3.27) in the same form as we did for the planar case:

$$\mathcal{L}: \quad A(\psi)u + B(\psi)v + C(\psi) = 0 \quad (3.89a)$$

with coefficients given below:

$$A(\psi) = k_3 \cos \psi - k_4, \quad B(\psi) = \sin \psi, \quad C(\psi) = k_1 + k_2 \cos \psi \quad (3.89b)$$

which is, again, the equation of a line  $\mathcal{L}$  in the  $u$ - $v$  plane, with  $u$  and  $v$  defined, again, as

$$u \equiv \cos \phi, \quad v \equiv \sin \phi \quad (3.89c)$$

and hence, these variables are subject to the constraint

$$\mathcal{C}: \quad u^2 + v^2 = 1 \quad (3.89d)$$

The two conjugate values of  $\phi$  for a given value of  $\psi$  can thus be computed as the intersection of the line  $\mathcal{L}$  with the circle  $\mathcal{C}$ , in exactly the same way as in the planar case. As in the planar case, an interesting singularity occurs when coefficients  $A(\psi)$ ,  $B(\psi)$ , and  $C(\psi)$  of the line equation (3.89a) all vanish. In this case, we have the conditions

$$k_3 \cos \psi - k_4 = 0, \quad \sin \psi = 0, \quad k_1 + k_2 \cos \psi = 0 \quad (3.90)$$

The second of the foregoing equations leads to  $\psi = 0$  or  $\pi$ . If  $\psi = 0$ , then the first equation implies  $k_3 = k_4$ , and hence,

$$\cos \alpha_1 \sin \alpha_2 - \sin \alpha_1 \cos \alpha_2 = 0$$

i.e.,

$$\alpha_2 = \alpha_1 \quad \text{or} \quad \alpha_2 = \alpha_1 + \pi$$

If  $\alpha_2 = \alpha_1$ , then the third equation leads to  $\cos \alpha_4 = \cos \alpha_3$ , and hence,  $\alpha_4 = \pm \alpha_3$ . If  $\psi = \pi$ , a similar reasoning to that introduced for the planar case leads exactly to the same result as for  $\psi = 0$ .

As a consequence, then, the singularity under study leads to a set of postures of the spherical linkage under which the joint axes  $OA$  and  $OD$  coincide, the coupler and the output links then being free to move as a single rigid body.

A procedure written on Maple to produce the input-output analysis of spherical four-bar linkages is included below.

### Input-Output Analysis of Spherical Four-Bar Linkages

The procedure below is based on the *graphical* solution of the input-output equation for spherical mechanisms: the intersection of a line  $\mathcal{L}$ , describing the underlying linear relation between the cosine and the sine of the output angle, and the unit circle  $\mathcal{C}$  centred at the origin of the  $\cos(\text{output})$ - $\sin(\text{output})$  plane, is determined. Line  $\mathcal{L}$  depends on the linkage parameters,  $k[1], k[2], k[3]$  and  $k[4]$ , which are entered into the procedure as array  $k$ , as well as on the input-angle value, which is entered as variable "input." If  $\mathcal{L}$  does not intersect  $\mathcal{C}$ , then either the linkage is unfeasible in that its link lengths do not form a quadrilateron, or the input link is a rocker and the prescribed value of the input angle lies outside its range of motion. If  $\mathcal{L}$  intersects  $\mathcal{C}$ , then it does normally so at two points, the procedure returning the two conjugate values of the output angle as  $\text{out}[1]$  and  $\text{out}[2]$ . In case  $\mathcal{L}$  is tangent to  $\mathcal{C}$ , the procedure detects a deadpoint, and returns  $\text{out}[2] = \text{out}[1]$ .

```

> restart:
> with(plots): with(plottools):
> sph4barIO:= proc( k, input )#Computes the intersection of one line L
> and the unit circle centred at the origin of the
> cos(output)-sin(output) plane. The intersection points, when they
> exist, are returned in array out, with out[1] and out[2] denoting
> the two conjugate values of the output angle
> local dpoint, feasible, pathos, D_d, N_d, d, q, u, v, sigma, theta;
> global out;
> dpoint:=false;#we assume that we are not in the presence of a
> deadpoint
> feasible:=true;#we assume that current psi-value is feasible

```

```

> pathos:=false;#we assume that we are not in the presence of
> pathological case whereby linkage becomes a one-dof open chain
> if k[3]=k[4] and input=0 then pathos:=true; print(patholo=pathos);
> return; fi; #Note that, if k[3] = k[4], then alpha[1]= alpha[2]
> D_d:=(k[3]*cos(input)-k[4])^2 + (sin(input))^2: #Maple reserves D
> for differential operator!
> N_d:=-k[1] - k[2]*cos(input): q:= N_d/D_d: print(Num, Den = N_d,
> D_d);
> d:=abs(N_d)/sqrt(D_d): print(distance = d);#distance of line L to
> origin
> if d > 1.0 then feasible:=false; print(feas=feasible); return; fi;
> if d = 1.0 then dpoint:=true; print(dead=dpoint); fi;
> u:=q*(k[3]*cos(input)-k[4]): v:=q*sin(input): print(inters = u,
> v);#coordinates of intersection of line L and its normal N passing
> through the origin
> if d = 0 then sigma:=arctan(-sin(input), k[3]*cos(input)-k[4]) else
> sigma:=arctan(v,u); fi: print(sig=sigma);#angle that normal makes
> with u-axis
> theta:=arccos(d); print(th=theta); #(1/2) angle subtended by secant
> to circle
> if d=0 then out[2]:=sigma; out[1]:=evalf(out[2]+Pi) else
> out[1]:=sigma-theta; out[2]:=sigma+theta end if; print(out1=out[1]);
> print(out2=out[2]);
> end;

```

### Mobility of the Input and Output Links

This analysis is conducted in the space of the four Freudenstein parameters  $\{k_i\}_1^4$ , with results similar to the planar case. Obviously, in this case the visualization is more challenging.

#### 3.4.3 Spatial Four-Bar Linkages

The analysis of the spatial four-bar linkage parallels that of its planar and spherical counterparts. There are, however, a few remarkable differences, as described below.

For starters, we cast the input-output equation (3.36) in the form

$$\hat{A}\hat{u} + \hat{B}\hat{v} + \hat{C} = 0 \quad (3.91a)$$

where

$$\hat{u} = u - \epsilon d_1 v, \quad \hat{v} = v + \epsilon d_1 u, \quad u \equiv \cos \phi, \quad v \equiv \sin \phi \quad (3.91b)$$

with  $d_1$  denoting the translation of the output cylindrical pair, while  $\epsilon$  is the dual unit, which has the properties  $\epsilon \neq 0$  and  $\epsilon^2 = 0$ . Moreover,

$$\hat{A} = A(\psi) + \epsilon A_o(\psi), \quad \hat{B} = B(\psi) + \epsilon B_o(\psi), \quad \hat{C} = C(\psi) + \epsilon C_o(\psi) \quad (3.91c)$$

whose primal parts  $A(\psi)$ ,  $B(\psi)$  and  $C(\psi)$  are identical to those of the spherical linkage, as displayed in eqs.(3.89b), their dual parts  $A_o(\psi)$ ,  $B_o(\psi)$  and  $C_o(\psi)$  being obtained with the aid of computer algebra and the rules of operations with dual numbers, namely,

$$A_o = k_{3o}c\psi - k_3d_2s\psi - k_{4o} \quad (3.92a)$$

$$B_o = s\psi + d_2c\psi \quad (3.92b)$$

$$C_o = k_{1o} + k_{2o}c\psi - k_2d_2s\psi \quad (3.92c)$$

in which the Freudenstein parameters are now dual numbers:  $\hat{k}_i = k_i + \epsilon k_{io}$ , for  $i = 1, \dots, 4$ . Moreover, their primal part is identical to that of the spherical four-bar linkages, their dual parts being displayed in eqs.(3.42) and reproduced below for quick reference.

$$\begin{aligned} k_{o1} &= -\frac{a_1\lambda_2\lambda_4\mu_1\mu_2\mu_4 + a_2(\lambda_1\lambda_4 - \lambda_2\lambda_3)\mu_4 - a_3\mu_2\mu_3\mu_4 + a_4(\lambda_1\lambda_2 - \lambda_3\lambda_4)\mu_2}{\mu_2^2\mu_4^2} \\ k_{o2} &= \frac{a_1\lambda_1\lambda_4\mu_4 - a_4\mu_1}{\mu_4^2}, \quad k_{o3} = -a_1\mu_1, \quad k_{o4} = \frac{a_1\lambda_1\lambda_2\mu_2 - a_2\mu_1}{\mu_2^2} \end{aligned}$$

Once we have obtained the input-output equation in terms of dual angles, it is possible to analyze the RCCC linkage, which allows us, in turn, to compute all the joint rotations and translations. The input-output equation above can be generally written as

$$\hat{\mathcal{L}} : \quad \hat{A}\hat{u} + \hat{B}\hat{v} + \hat{C} = 0 \quad (3.93a)$$

and

$$\hat{\mathcal{C}} : \quad \hat{u}^2 + \hat{v}^2 = 1 \quad (3.93b)$$

where

$$\hat{u} = \cos \hat{\phi}, \quad \hat{v} = \sin \hat{\phi} \quad (3.93c)$$

Equations (3.93a–c) represent a *dual line*  $\hat{\mathcal{L}}$  and a *dual unit circle*  $\hat{\mathcal{C}}$  in the dual  $\hat{u}$ - $\hat{v}$  plane, respectively. Now, it is possible to decompose the equation of the “line”  $\hat{\mathcal{L}}$  into two real equations, one for its primal, and one for its dual part, namely,

$$\mathcal{P} : \quad Au + Bv + C = 0 \quad (3.94a)$$

$$\mathcal{H} : \quad (A_o + Bd_1)u - Ad_1v + C_o = 0 \quad (3.94b)$$

For the circle  $\hat{\mathcal{C}}$ , the dual part vanishes identically, the primal part leading to a *real circle*, namely,

$$\mathcal{C} : \quad u^2 + v^2 = 1 \quad (3.94c)$$

Equation (3.94a) represents a plane  $\mathcal{P}$  parallel to the  $d_1$ -axis in the  $(u, v, d_1)$ -space, while eq.(3.94b) represents a hyperbolic paraboloid  $\mathcal{H}$  in the same space. Moreover, eq.(3.94c) represents a cylinder  $\mathcal{C}$  of unit radius and axis parallel to the  $d_1$ -axis, all foregoing items being shown in Figs. 3.13a & b.

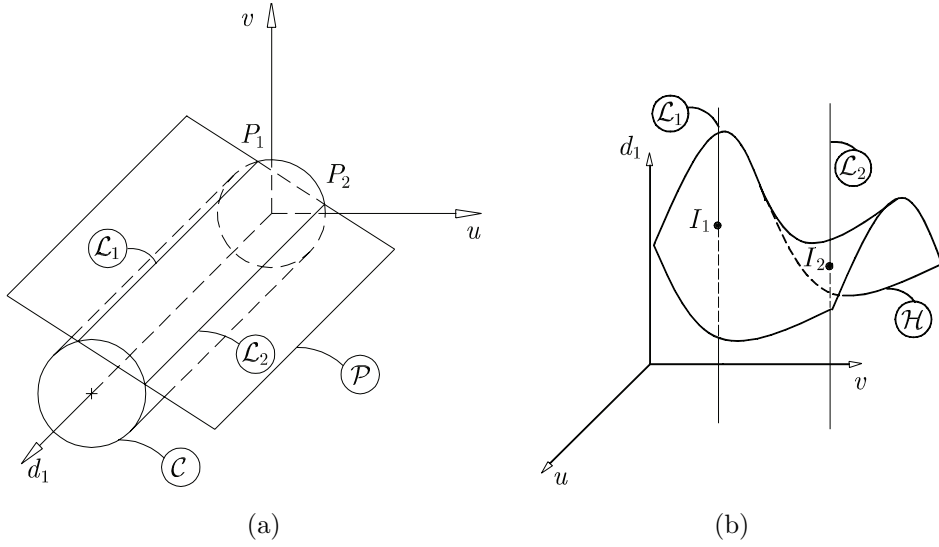


Figure 3.13: Intersections of (a)  $\mathcal{P}$  and  $\mathcal{C}$ ; and (b)  $\mathcal{L}_i$  and  $\mathcal{H}$ , for  $i = 1, 2$

The three-dimensional interpretation of eqs.(3.94a–c) is illustrated in Figs. 3.13(a) and (b), whereby line  $\mathcal{L}_i$ , for  $i = 1, 2$ , is defined by the intersection of the plane of eq.(3.94a) with the cylinder (3.94c). Moreover, each line  $\mathcal{L}_i$  intersects the paraboloid (3.94b) at one single point, as illustrated in Fig. 3.13b, and as made apparent below.

The system of equations (3.94a–c) should be solved for  $u, v$  and  $d_1$  in order to calculate the two conjugate output angles and their corresponding output translations. The intersections  $\mathcal{L}_1$  and  $\mathcal{L}_2$  of the plane  $\mathcal{P}$  and the cylinder intersect the  $u$ - $v$  plane at points  $P_1$  and  $P_2$ , as shown in Fig. 3.13a, while  $\mathcal{L}_1$  and  $\mathcal{L}_2$  intersect the hyperbolic paraboloid  $\mathcal{H}$  at points  $I_1$  and  $I_2$ , as depicted in Fig. 3.13b. The intersection points  $P_1$  and  $P_2$  thus yield the two conjugate output angles  $\phi_1$  and  $\phi_2$ . Once the two conjugate solutions  $u$  and  $v$  are known, via the coordinates of  $P_1$  and  $P_2$ , the unique value of  $d_1$  corresponding to each solution, and defining the intersection points  $I_1$  and  $I_2$ , is determined from eq.(3.94b), namely,

$$d_1(\psi) = \frac{A_o u + C_o}{Av - Bu}, \quad Av \neq Bu \quad (3.95)$$

where we have dispensed with the argument  $\psi$  in coefficients  $A$ ,  $A_o$ ,  $B$  and  $C_o$  for simplicity.

Note that the denominator of eq.(3.95) vanishes if  $Av = Bu$ ; then, as can be readily verified, the numerator of  $d_1$  in the above expression vanishes as well, and  $d_1$  is indeterminate. In this case, the surface  $\mathcal{H}$  disappears for all values of the output translations  $d_1$  and we are left with the plane  $\mathcal{P}$  and the cylinder  $\mathcal{C}$ , which means that  $d_1$  is free to take any value. That is, the motion of this linkage in the plane normal to its joint axes is independent of the translations along these axes. We are here in the presence of a parametric singularity producing a degeneracy of the linkage, similar to those described for the planar and spherical linkages in Subsections 3.4.1 and 3.4.2. Under this singularity,

all joint axes are parallel ( $\alpha_i = 0, i = 1, \dots, 4$ ) and, hence, the coupler and the output links can freely slide along their cylindrical-joint axes.

### Canonical Equation of the Hyperbolic Paraboloid $\mathcal{H}$

In order to gain insight into the problem geometry, we derive below the canonical equation of  $\mathcal{H}$ . To this end, we let

$$\mathbf{x} \equiv [u \ v \ d_1]^T, \quad Q(\mathbf{x}) \equiv A_o u + B d_1 u - A d_1 v + C_o = 0$$

where  $Q(\mathbf{x})$  is taken from eq.(3.94b), its Hessian matrix  $\mathbf{H}$  then being

$$\mathbf{H} \equiv \frac{\partial^2 Q}{\partial \mathbf{x}^2} = \begin{bmatrix} 0 & 0 & B \\ 0 & 0 & -A \\ B & -A & 0 \end{bmatrix} \quad (3.96)$$

whose eigenvalues are readily computed as

$$\lambda_1 = -\sqrt{A^2 + B^2}, \quad \lambda_2 = 0, \quad \lambda_3 = \sqrt{A^2 + B^2}$$

The corresponding non-normalized eigenvectors  $\mathbf{e}_i$ , for  $i = 1, 2, 3$ , are

$$\mathbf{e}_1 = \begin{bmatrix} B \\ -A \\ \sqrt{A^2 + B^2} \end{bmatrix}, \quad \mathbf{e}_2 = \begin{bmatrix} A \\ B \\ 0 \end{bmatrix}, \quad \mathbf{e}_3 = \begin{bmatrix} -B \\ A \\ \sqrt{A^2 + B^2} \end{bmatrix}$$

and hence, the canonical equation of the surface  $\mathcal{H}$  is of the form:

$$\zeta = \frac{\xi^2}{K} - \frac{\eta^2}{K}, \quad K = \frac{2A_o A}{A^2 + B^2}$$

where

$$\begin{aligned} \xi &= \frac{-\sqrt{2}}{2\sqrt{A^2 + B^2}} \left[ Bu + Av + d_1 + \frac{A_o B}{4A_o A} \right] \\ \eta &= \frac{\sqrt{2}}{4\sqrt{A^2 + B^2}} \left( Bu - Av + d_1 + \frac{A_o B}{A_o A} \right) \\ \zeta &= \frac{1}{\sqrt{A^2 + B^2}} \left[ Au + Bv + \frac{(A^2 + B^2)C_o A}{A_o A} \right] \end{aligned}$$

which proves that  $\mathcal{H}$  is indeed a hyperbolic paraboloid.

### The Case of $d_1$ Acting as Input

We include here a case that has been overlooked in the literature. In this case we regard the translational displacement of the output C joint of a RCCC linkage as input, the two outputs being angles  $\psi$  and  $\phi$ . This problem can occur when designing an analogue

temperature sensor in which temperature is measured via the expansion of a rod whose axis is offset with respect to the axis of a dial, the two axes lying at an arbitrary angle.

The problem no longer leads to a quadratic equation, but rather to a system of one quartic and one quadratic equation in two variables, as described presently.

Equations (3.94a & b) are both linear in  $u$  and  $v$ , which allows us to solve for these variables in terms of  $d_1$ , namely,

$$u = u(p, q) = \frac{-BC_o - CAD_1}{BA_o + B^2d_1 + A^2d_1} \quad (3.97a)$$

$$v = v(p, q) = \frac{-CA_o - AC_o + CBD_1}{BA_o + B^2d_1 + A^2d_1} \quad (3.97b)$$

where, in light of eqs.(3.92a), with  $p = \cos \psi$  and  $q = \sin \psi$ ,  $u$  and  $v$  become functions of  $p$  and  $q$ . The latter, moreover, are subject to

$$p^2 + q^2 = 1 \quad (3.98)$$

Substituting the values of  $u$  and  $v$  given above into eq.(3.94c) produces an equation free of  $u$  and  $v$  or, correspondingly, free of  $\phi$ , namely,

$$f(p, q) = 0 \quad (3.99)$$

From eq.(3.72b) and eqs.(3.92a–c), both  $u$  and  $v$ , as given by eqs.(3.97a & b), are rational functions in these variables, with both numerator and denominator quadratic in  $p$  and  $q$ . Hence,  $u^2$  and  $v^2$  are rational functions with both numerator and denominator quartic in  $p$  and  $q$ . Therefore,  $f(p, q) = 0$  leads, after clearing denominators, to a quartic equation in  $p$  and  $q$ .

The system of polynomial equations (3.98) and (3.99) apparently has a Bezout number, introduced in Section 1.3, of  $4 \times 2 = 8$ .

## Numerical Examples

The foregoing algorithm is validated with two numerical examples. All numerical and symbolic calculations were completed with the aid of computer algebra.

### Example 1: The Yang and Freudenstein Linkage

The first example is taken from (Yang and Freudenstein, 1964), with data as listed in Table 3.2. The output displacements, which vary with the input angle, are recorded in Table 3.3. For conciseness, we list only the results for  $0 \leq \psi \leq \pi$ . Our results match those reported by Yang and Freudenstein, considering the difference of input and output angles in both works, as explained in Subsections 3.2.4. It is noteworthy that only two displacement equations need be solved in our method, as compared with the system of six equations in six unknowns formulated by Yang and Freudenstein, within a purely numerical approach.

Table 3.2: D-H parameters of a RCCC mechanism

Link	1	2	3	4
$a_i$ [in]	5	2	4	3
$\alpha_i$ [deg]	60	30	55	45
$d_i$ [in]	0	variable	variable	variable

Table 3.3: RCCC displacements

$\psi$ [deg]	Branch 1		Branch 2	
	$\phi$ [deg]	$d_1$ [in]	$\phi$ [deg]	$d_1$ [in]
0	83.70015289	-0.1731633183	-83.70015289	0.1731633183
20	68.59658457	0.01107737578	-105.3298310	0.8429100445
40	64.21379652	-0.5291731100	235.9479009	1.085719194
60	67.55907283	-1.262205018	223.0109192	0.9378806915
80	75.72376603	-1.888758476	214.5328380	0.6631677103
100	87.21970033	-2.259417488	209.1315343	0.3676536240
120	101.1949772	-2.248309766	206.1460158	0.08437533590
140	116.6745934	-1.770565950	205.6297490	-0.1502382358
160	131.8997404	-0.9205435228	208.4003706	-0.2203697101
180	144.2093802	-0.1150813726	215.7906198	0.1150813650

Table 3.4: Possible values of  $\psi$  and  $\phi$ 

	$[p, q]$	$\psi$ [deg]	$\phi$ [deg]
1	[0.6047587377, -0.7964087325]	-52.78	[-65.68, -227.07]
2	[-0.9289796338, -0.3701308418]	-158.27	[-130.66, -207.99]
3	[0.5819053587, 0.8132565115]	54.41	[66.04, 226.10]
4	[0.8869350365, 0.4618941881]	27.50	[65.79, -113.02]

### Example 2: Prescribing $d_1$ as Input

In the second example, we try to find the rotations,  $\psi$  and  $\phi$ , for a given  $d_1$ , and given dimensions of a RCCC linkage. The dimensions are the same as those in Example 1, with  $d_1 = 1.0$ . In this example, eq.(3.99) takes the form:

$$A_0 p^4 + A_1(q)p^3 + A_2(q)p^2 + A_3(q)p + A_4(q) = 0 \quad (3.100)$$

where coefficients  $A_i(q)$ , for  $i = 0, \dots, 4$ , are given below:

$$\begin{aligned} A_0 &= 0.09209746694 \\ A_1(q) &= -0.06765823468q - 0.0073324502 \\ A_2(q) &= -0.1754806581q^2 + 0.01487658368q - 0.1902460942 \\ A_3(q) &= 0.1353164694q^3 + 0.1202907568q^2 + 0.2424947249q + 0.04203177757 \\ A_4(q) &= -0.015625q^4 - 0.0811898817q^3 - 0.020697377q^2 - 0.1362382267q \\ &\quad + 0.0484753242 \end{aligned}$$

Equation (3.100) represents a curve in the  $p-q$  plane, whose intersections with the circle of eq.(3.98) yield all real roots of the system at hand. Note, moreover, that all such roots are bound to lie on the above circle. The four real solutions of the foregoing system are given by the four intersections depicted in Fig. 3.14. The solutions are listed in Table 3.4, including the corresponding angles of rotation<sup>4</sup>.

### Mobility of the Input and Output Links

In this case, the mobility analysis applies *only to the input  $\psi$  and the output  $\phi$* , as this analysis decides whether a joint is fully rotatable—can sweep an angle of  $2\pi$ —or not. This analysis thus reduces to that of the spherical mechanism whose IO equation is the primal part of the dual equation of this linkage.

---

<sup>4</sup>In this table only  $p$  and  $q$  are given with 10 digits; all other values are given with only four, for the sake of economy of space.

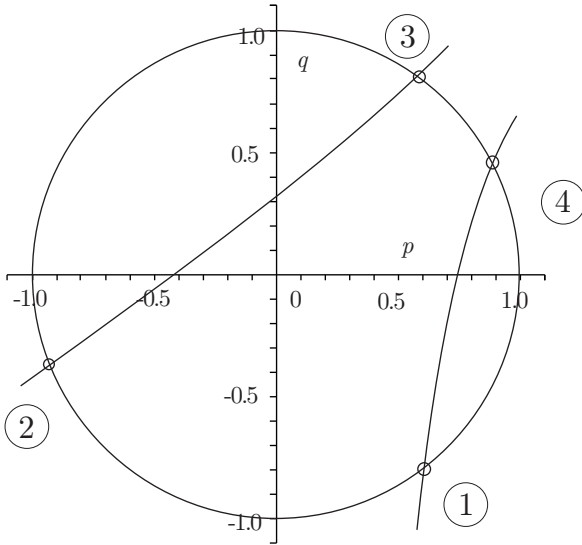


Figure 3.14: The case of an input translation

### 3.5 Approximate Synthesis

Regardless of the type of four-bar linkage,  $\mathbf{k}$  ( $\hat{\mathbf{k}}$ ) is a  $n$ -dimensional real (dual) vector; for planar linkages,  $n = 3$ , for spherical,  $n = 4$ . For spatial linkages,  $n$  is still four, but now, the parameters being dual, the total number of real parameters is eight. In general, for  $m$  input-output pairs—in the spatial case, the output is dual!—to meet with  $m > 3$  in the planar case, and  $m > 4$  in the spherical and spatial cases, no set of Freudenstein parameters can verify all synthesis equations, thereby ending up with an error vector  $\mathbf{e}$ :

$$\mathbf{e} \equiv \mathbf{b} - \mathbf{Sk} \quad (3.101a)$$

which, in the case of RCCC linkages, becomes dual, i.e.,

$$\hat{\mathbf{e}} \equiv \hat{\mathbf{b}} - \hat{\mathbf{S}}\hat{\mathbf{k}} \quad (3.101b)$$

The foregoing error vector, in its two versions, primal and dual, is termed the *design-error vector*. A positive scalar derived from this vector will be termed a *design error*.

The *design error*  $e_d$  adopted here is the rms value of the components of vector  $\mathbf{e}$ , i.e.,

$$e_d \equiv \sqrt{\frac{1}{m} \sum_1^m e_i^2} \quad (3.102a)$$

where  $e_i$  is the  $i$ th component of vector  $\mathbf{e}$ , i.e., the *residual* of the  $i$ th synthesis equation. Hence, the design error is proportional to the Euclidean norm of the design-error vector:

$$e_d \equiv \sqrt{\frac{1}{m} \|\mathbf{e}\|} \quad (3.102b)$$

It is apparent that, for fixed  $m$ , if we minimize  $\|\mathbf{e}\|$ , we minimize  $e_d$ . In the case of the spatial four-bar linkage, of course,  $e_d$  is defined as

$$\hat{e}_d = \sqrt{\frac{1}{m} \|\hat{\mathbf{e}}\|^2} \quad (3.102c)$$

where, from eq.(A.9e),

$$\|\hat{\mathbf{e}}\| = \sqrt{\hat{\mathbf{e}}^T \hat{\mathbf{e}}}, \quad \hat{\mathbf{e}}^T \hat{\mathbf{e}} = \|\mathbf{e}\|^2 + \epsilon 2\mathbf{e}^T \mathbf{e}_o \quad (3.102d)$$

The value  $\mathbf{k}_0$  of  $\mathbf{k}$  that minimizes  $\|\mathbf{e}\|$ , as derived in Subsection 1.4, is applicable to the planar and spherical cases; it is given in eq.(1.41)<sup>5</sup>—The value  $\hat{\mathbf{k}}_0$  that minimizes  $\hat{e}_d$  is discussed in Subsection 3.5.3. In the planar and spherical cases, this equation leads to

$$\mathbf{k}_0 = \mathbf{S}^I \mathbf{b} \quad (3.103a)$$

which is the *least-square approximation* of the given overdetermined system of linear equations,  $\mathbf{S}^I$  being the left Moore-Penrose generalized inverse of  $\mathbf{S}$ , as introduced in eq.(1.42), and is given by

$$\mathbf{S}^I = (\mathbf{S} \mathbf{S}^T)^{-1} \mathbf{S}^T \quad (3.103b)$$

Hence,

$$\mathbf{e}_0 \equiv \mathbf{b} - \mathbf{S} \mathbf{k}_0 \quad (3.104)$$

is the *least-square error vector*, and

$$e_{d0} \equiv \sqrt{\frac{1}{m} \|\mathbf{e}_0\|^2} \quad (3.105)$$

is the *least-square design error* of the approximation to the overdetermined system of synthesis equations.

**Remark 3.5.1** Expression (3.103a) for  $\mathbf{k}_0$  can be derived upon multiplying both sides of eq.(3.12) by  $\mathbf{S}^T$ :

$$(\mathbf{S}^T \mathbf{S}) \mathbf{k} = \mathbf{S}^T \mathbf{b} \quad (3.106)$$

where  $\mathbf{S}^T \mathbf{S}$  is a  $n \times n$  matrix. If this matrix is nonsingular, then

$$\mathbf{k} \equiv \mathbf{k}_0 = (\mathbf{S}^T \mathbf{S})^{-1} \mathbf{S}^T \mathbf{b}$$

**Remark 3.5.2** The least-square approximation  $\mathbf{k}_0$  can be thought of as being derived upon “inverting” the rectangular  $\mathbf{S}$  matrix in the original overdetermined system, eq.(3.12), with the “inverse” of  $\mathbf{S}$  understood in the generalized sense.

**Remark 3.5.3**  $\mathbf{k}_0$  minimizes the Euclidean norm of  $\mathbf{e}$ , which is proportional to the design error.

---

<sup>5</sup> $\mathbf{k}_0$  shouldn't be mistaken by  $\mathbf{k}_o$ , the dual part of  $\hat{\mathbf{k}}$ .

**Remark 3.5.4** The least-square error of the approximation of the overdetermined system of synthesis equations does not measure the positioning error, a.k.a. the structural error, but rather the design error  $\mathbf{e}$  defined above. The structural error produced by the synthesized linkage must be measured with respect to the task, not with respect to the synthesis equations. That is, if we let  $\bar{\phi}_i$  denote the prescribed value of the output angle, corresponding to the  $\psi_i$  value, with  $\phi_i$  denoting the generated value of the output angle, then the structural error is the vector  $\mathbf{s}$  given by

$$\mathbf{s} \equiv [\phi_1 - \bar{\phi}_1 \quad \phi_2 - \bar{\phi}_2 \quad \cdots \quad \phi_m - \bar{\phi}_m]^T \quad (3.107)$$

Computing the least-square approximation  $\mathbf{k}_0$  *verbatim* as appearing in eq.(3.103a) is not advisable because of Remark 1.4.3 and the discussion in the paragraph below this remark. This is, if  $\kappa(\mathbf{S})$  is moderately large, say, of the order of 1000,  $\kappa(\mathbf{S}^T \mathbf{S})$  is inadmissibly large, of the order of  $10^6$ .

Numerical methods for the solution of eq.(3.12) in the presence of a rectangular  $\mathbf{S}$  are available in the literature (Golub and Van Loan, 1983), as outlined in Subsection 1.4.5 and implemented in scientific software. The two methods outlined in Subsection 1.4.5 fall into what is called the *QR decomposition*:  $\mathbf{S}$  is factored into an orthogonal matrix  $\mathbf{Q}$  and an upper-triangular matrix  $\mathbf{R}$ .

Maple uses Householder reflections to find numerically the least-square approximation of an overdetermined system of linear equations; it uses Gram-Schmidt orthogonalization to do the same if data are given *symbolically*.

In any event, the original system (3.12) is transformed into the form

$$\mathbf{T}\mathbf{k} = \mathbf{c} \quad (3.108)$$

where  $\mathbf{T}$  and  $\mathbf{c}$  are the transforms of  $\mathbf{S}$  and  $\mathbf{b}$  of eq.(3.101a), respectively, with  $\mathbf{T}$  of the form

$$\mathbf{T} = \begin{bmatrix} \mathbf{U} \\ \mathbf{O} \end{bmatrix} \quad (3.109)$$

while  $\mathbf{U}$  and  $\mathbf{O}$  are

$$\mathbf{U} = \begin{bmatrix} u_{11} & u_{12} & \cdots & u_{1n} \\ 0 & u_{22} & \cdots & u_{2n} \\ \vdots & \vdots & \ddots & \vdots \\ 0 & 0 & \cdots & u_{nn} \end{bmatrix}, \quad \mathbf{O} : (m-n) \times n \text{ zero matrix} \quad (3.110)$$

In order to solve eq.(3.108) for  $\mathbf{k}$ , we partition vector  $\mathbf{c}$  into a  $n$ -dimensional upper part  $\mathbf{c}_U$  and a  $(m-n)$ -dimensional lower part  $\mathbf{c}_L$ :

$$\mathbf{c} = \begin{bmatrix} \mathbf{c}_U \\ \mathbf{c}_L \end{bmatrix} \quad (3.111)$$

where, in general,  $\mathbf{c}_L \neq \mathbf{0}$ .

System (3.108) thus takes the form

$$\begin{bmatrix} \mathbf{U} \\ \mathbf{O} \end{bmatrix} \mathbf{k} = \begin{bmatrix} \mathbf{c}_U \\ \mathbf{c}_L \end{bmatrix} \Rightarrow \begin{cases} \mathbf{Uk} = \mathbf{c}_U \\ \mathbf{Ok} = \mathbf{c}_L \neq \mathbf{0} \end{cases} \quad (3.112)$$

**Remark 3.5.5** If  $\mathbf{S}$  is of full rank, then so is  $\mathbf{T}$  and hence,  $\mathbf{U}$  is nonsingular.

**Remark 3.5.6** If  $\mathbf{U}$  is nonsingular, then none of its diagonal entries vanishes, for  $\det(\mathbf{U}) = u_{11}u_{22} \cdots u_{nn}$ .

**Remark 3.5.7** If  $\mathbf{U}$  is nonsingular, then  $k_1, k_2, \dots, k_n$  can be computed from the first of eqs.(3.112) by backward substitution.

**Remark 3.5.8** The second of eqs.(3.112) is a contradiction: its RHS is zero, but its LHS is not! Hence,  $\mathbf{c}_L$  is the error vector—although not in the original vector basis, but in a new, orthonormal basis—and thus, the error in the approximation of the synthesis equations is

$$e_{d0} = \sqrt{\frac{1}{m}} \|\mathbf{c}_L\| \quad (3.113)$$

### 3.5.1 The Approximate Synthesis of Planar Four-Bar Linkages

For planar linkages the procedure is straightforward, as illustrated with the example below.

**Example 3.5.1 (Approximate synthesis of the gripper mechanism)** The mechanism of Fig. 3.6 is to be synthesized, but now with a large number of input-output (IO) values. For comparison purposes, the data points used by Dudită et al. (1989) are used here, which are prescribed by equally spacing 61 IO values between  $\psi_1 = 30^\circ$ ,  $\phi = 240^\circ$  and  $\psi_{61} = 60^\circ$ ,  $\phi_{61} = 210^\circ$ , as depicted in Fig. 3.15.

Solution: The  $61 \times 3$  synthesis matrix  $\mathbf{S}$  and the 61-dimensional vector  $\mathbf{b}$  are not displayed for the sake of economy of space. Details of the solution are available in the code written for the purpose at hand<sup>6</sup>. The least-square approximation was computed using Householder reflections, which yielded, using 16 digits for comparison purposes with the results reported by Dudită et al. (1989):

$$\mathbf{k}_0 = [2.9417068638 \quad 2.7871366821 \quad 2.7869959265]^T$$

with corresponding link parameters

$$a_1 = 1.0, \quad a_2 = 0.3587911588, \quad a_3 = 0.7071482506, \quad a_4 = 0.3588092794$$

---

<sup>6</sup>See `Dudita2.mw`

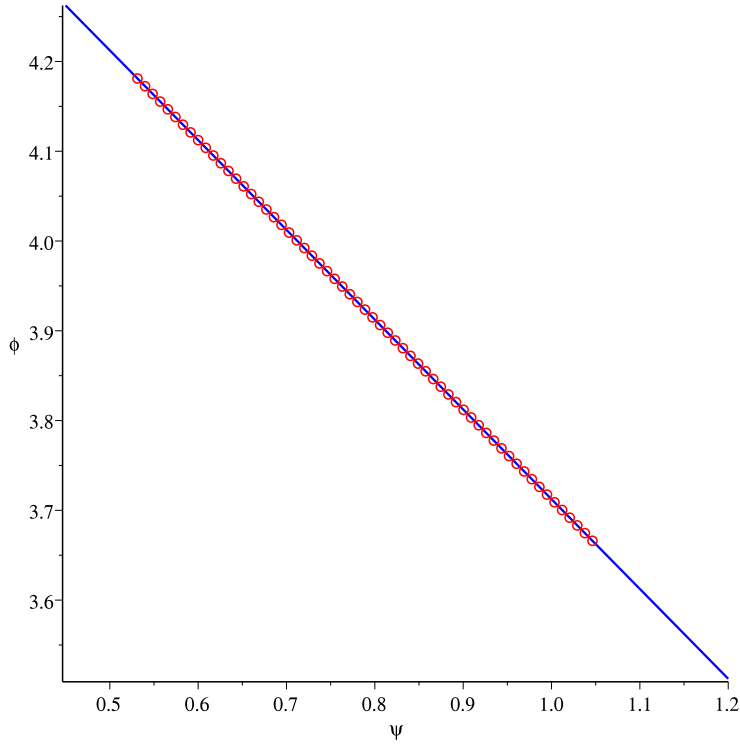


Figure 3.15: The 61 points prescribed in the  $\phi$ -vs.- $\psi$  plane

*in units of length. In the foregoing reference, the authors computed the least-square approximation using the normal equations, which produced*

$$\mathbf{k}_D = [2.9398767070 \quad 2.7857633820 \quad 2.7857633820]^T$$

*thereby obtaining the link lengths<sup>7</sup> below:*

$$a_1 = 1.0, \quad a_2 = 0.3589680324, \quad a_3 = 0.7071510069, \quad a_4 = a_2$$

*in units of length. The values of both  $\mathbf{k}$  and  $\mathbf{k}_D$  coincide up to the first two digits, those of the link lengths up to the first three digits, which is a fair matching, a consequence of the moderate condition number of the synthesis matrix, namely  $\kappa = 195$ , as computed in `Dudita2.mw`. However, the normality conditions were met, with the values provided in the foregoing reference, with an error of  $O(-4)$ ; the same conditions were met with an error of  $O(-14)$  in the code given above, which uses HHR.*

*To the naked eye, the synthesized linkage doesn't appear different from that in Fig. 3.7.*

---

<sup>7</sup>Dudiță et al. adjusted the values of the second and the third components of the  $\mathbf{k}_D$  array to be identical.

### 3.5.2 The Approximate Synthesis of Spherical Linkages

This case parallels that of planar linkages, with the provision that, as in the case of exact synthesis of spherical linkages, nothing guarantees that the computed least-square approximation complies with the two conditions (3.33). The first of these,  $|k_3| \leq 1$ , can be enforced in the least-square solution by adding one more equation,  $k_3 = 0$ , to the synthesis equations. Compliance with this condition, however, will invariably lead to a larger value of  $e_{d0}$ . Enforcing the second condition of eq.(3.33) is less straightforward, as it requires techniques for solving problems of *constrained least squares* with nonlinear equality constraints, which fall outside of the scope of this course, and will not be further discussed. The reader is referred to the literature on engineering optimization whenever confronted with this problem.

Adjoining the above equation,  $k_3 = 0$ , to the synthesis equation, then, leads to the *augmented synthesis equations*

$$\mathbf{S}_a \mathbf{k} = \mathbf{b}_a \quad (3.114a)$$

where

$$\mathbf{S}_a = \begin{bmatrix} \mathbf{S} \\ \mathbf{u}^T \end{bmatrix}, \quad \mathbf{b}_a = \begin{bmatrix} \mathbf{b} \\ 0 \end{bmatrix} \quad (3.114b)$$

with  $\mathbf{u} = [0, 0, 1, 0]^T$ , and hence,  $\mathbf{S}_a$  now becomes of  $(m + 1) \times 4$ , while  $\mathbf{b}_a$  is now  $(m + 1)$ -dimensional.

But least-square approximations allow for more flexibility, if we introduce *weights* in eq.(3.114a), by means of a  $(m + 1) \times (m + 1)$  constant matrix  $\mathbf{V}_a$ :

$$\mathbf{V}_a \mathbf{S}_a \mathbf{k} = \mathbf{V}_a \mathbf{b}_a \quad (3.115a)$$

with

$$\mathbf{V}_a = \begin{bmatrix} \mathbf{V} & \mathbf{0}_m \\ \mathbf{0}_m^T & v \end{bmatrix} \quad (3.115b)$$

in which  $\mathbf{V}$  is a  $m \times m$  block,  $\mathbf{0}_m$  is the  $m$ -dimensional zero matrix, and  $v$  is a scalar. Both  $\mathbf{V}$  and  $v$  are assigned by the user under the only constraint of avoiding the introduction of large roundoff-error amplification. We will describe presently how to prescribe  $\mathbf{V}$  and  $v$ .

Notice that the least-square approximation  $\mathbf{k}_0$  of eq.(3.115a) now becomes, symbolically,

$$\begin{aligned} \mathbf{k}_0 &= [(\mathbf{V}_a \mathbf{S}_a)^T (\mathbf{V}_a \mathbf{S}_a)]^{-1} (\mathbf{V}_a \mathbf{S}_a^T) \mathbf{V}_a \mathbf{b}_a \\ &= (\mathbf{S}_a^T \mathbf{W}_a \mathbf{S}_a)^{-1} \mathbf{S}_a^T \mathbf{W}_a \mathbf{b}_a, \quad \mathbf{W}_a \equiv \mathbf{V}_a^T \mathbf{V}_a \end{aligned} \quad (3.116)$$

in which the symmetric and positive-definite  $\mathbf{W}_a$  is termed a *weighting matrix*.

Also notice that

$$\mathbf{W}_a = \begin{bmatrix} \mathbf{V}^T & \mathbf{0}_m \\ \mathbf{0}_m^T & v_{m+1} \end{bmatrix} \begin{bmatrix} \mathbf{V} & \mathbf{0}_m \\ \mathbf{0}_m^T & v_{m+1} \end{bmatrix} = \begin{bmatrix} \mathbf{W} & \mathbf{0}_m \\ \mathbf{0}_m^T & w_{m+1} \end{bmatrix} \quad (3.117a)$$

with

$$\mathbf{W} = \mathbf{V}^T \mathbf{V}, \quad w_{m+1} \equiv v_{m+1}^2 \quad (3.117b)$$

Since no constraint is imposed on  $\mathbf{V}$ , besides robustness to round-off error amplification,  $\mathbf{V}$  can be freely chosen as *symmetric and positive-definite*, and hence, nonsingular, i.e.,

$$\mathbf{V}^2 = \mathbf{W} \Rightarrow \mathbf{V} = \sqrt{\mathbf{W}} \quad (3.118a)$$

where  $\sqrt{\mathbf{W}}$  denotes the *the positive-definite square root of  $\mathbf{W}$* . Now, the simplest matrices to square-root are diagonal matrices,  $\mathbf{W}$  then being chosen as

$$\mathbf{W} = \text{diag}(w_1, w_2, \dots, w_m) \quad (3.118b)$$

Now, the error vector in the approximation of eqs.(3.115a) is

$$\mathbf{e}_a = \mathbf{V}_a(\mathbf{b}_a - \mathbf{S}_a \mathbf{k}) = \begin{bmatrix} \mathbf{V} & \mathbf{0}_m \\ \mathbf{0}_m^T & v_{m+1} \end{bmatrix} \begin{bmatrix} \mathbf{b} - \mathbf{Sk} \\ k_3 \end{bmatrix} \quad (3.119a)$$

whose Euclidean norm is

$$\begin{aligned} \|\mathbf{e}_a\|^2 &= [\mathbf{b}^T - \mathbf{k}^T \mathbf{S}^T \quad k_3] \begin{bmatrix} \mathbf{V}^2 & \mathbf{0}_m \\ \mathbf{0}_m^T & v_{m+1}^2 \end{bmatrix} \begin{bmatrix} \mathbf{b} - \mathbf{Sk} \\ k_3 \end{bmatrix} \\ &= (\mathbf{b}^T - \mathbf{k}^T \mathbf{S}^T) \mathbf{W} (\mathbf{b} - \mathbf{Sk}) + w_{m+1} k_3^2 \\ &= \sum_{i=1}^m w_i e_i^2 + w_{m+1} k_3^2 \end{aligned} \quad (3.119b)$$

which thus yields a *weighted error-norm*. In order to avoid large roundoff-error amplification, we choose the weighting factors  $\{w_i\}_1^{m+1}$  as

$$\sum_{i=1}^{m+1} w_i = 1, \quad 0 \leq w_i \leq 1, \quad i = 1, \dots, m \quad (3.120)$$

so that  $\|\mathbf{e}_a\|^2$  becomes a *convex combination* of all  $m+1$  errors. If no preference is given to the set  $\{e_i\}_1^m$ , then the first  $m$  weights can be chosen all equal, while  $w_{m+1}$  is to be chosen so as to enforce  $|k_3|$  to be smaller than unity but, if  $w_{m+1}$  is chosen unnecessarily large, then  $|k_3|$  will be “too small” at the expense of a “large” design error. The best compromise is to be chosen by trial and error.

An application of the approximate synthesis of spherical four-bar linkages to the replacement of a bevel-gear transmission with input and output axes at right angles was reported by Alizadeh et al. (2013).

### 3.5.3 The Approximate Synthesis of Spatial Linkages

This subsubsection is largely based on (Angeles, 2012). The synthesis equations (3.50) for the spatial four-bar linkage are reproduced below for quick reference:

$$\mathbf{Sk} = \mathbf{b} \quad (3.121a)$$

$$\mathbf{Sk}_o = \mathbf{b}_o - \mathbf{S}_o \mathbf{k} \quad (3.121b)$$

which can be cast in the standard form (1.28) of an overdetermined system of linear equations, in this case of  $2m$  equations in  $2 \times 4 = 8$  unknowns, the four components of  $\mathbf{k}$  and  $\mathbf{k}_o$ . Indeed, assembling the above equations into one single system yields

$$\underbrace{\begin{bmatrix} \mathbf{S} & \mathbf{O} \\ \mathbf{S}_o & \mathbf{S} \end{bmatrix}}_{\mathbf{A}} \underbrace{\begin{bmatrix} \mathbf{k} \\ \mathbf{k}_o \end{bmatrix}}_{\mathbf{x}} = \underbrace{\begin{bmatrix} \mathbf{b} \\ \mathbf{b}_o \end{bmatrix}}_{\mathbf{r}} \quad (3.122)$$

whose matrix  $\mathbf{A}$  has four  $m \times 4$  blocks, while  $\mathbf{x}$  is an eight-dimensional vector. One could think of submitting eq.(3.122) to a linear least-square solver and, sure enough, obtain a least-square solution  $\mathbf{x}_0$  à la eq.(1.41). Problem is, this solution would be *meaningless* because the error  $\mathbf{e} \equiv \mathbf{r} - \mathbf{Ax}$  does not admit a norm. The reason is that the first  $m$  components of  $\mathbf{e}$  are dimensionless, as they refer to the spherical linkage associated with the spatial linkage at hand, while the last  $m$  bear units of length, as they refer to sliding errors. This approach is thus ruled out. Instead, the synthesis equations in dual form, eq.(3.45), with the definitions appearing in eq.(3.46), are recalled, as reproduced below for quick reference:

$$\hat{\mathbf{S}}\hat{\mathbf{k}} = \hat{\mathbf{b}} \quad (3.123)$$

which, for  $m > 4$ , cannot be satisfied exactly; the *dual error* incurred is

$$\hat{\mathbf{e}} = \hat{\mathbf{b}} - \hat{\mathbf{S}}\hat{\mathbf{k}} \quad (3.124)$$

Equation (3.123) can be shown to admit the least-square solution

$$\hat{\mathbf{k}}_0 = \hat{\mathbf{S}}^I \hat{\mathbf{b}}, \quad \hat{\mathbf{S}}^I = (\hat{\mathbf{S}}^T \hat{\mathbf{S}})^{-1} \hat{\mathbf{S}}^T \quad (3.125)$$

where

$$\hat{\mathbf{S}}^T \hat{\mathbf{S}} = \mathbf{S}^T \mathbf{S} + \epsilon (\mathbf{S}^T \mathbf{S}_o + \mathbf{S}_o^T \mathbf{S}) \quad (3.126)$$

whose inverse is readily computed using eq. (A.13) of the Appendix:

$$(\hat{\mathbf{S}}^T \hat{\mathbf{S}})^{-1} = (\mathbf{S}^T \mathbf{S})^{-1} - \epsilon (\mathbf{S}^T \mathbf{S})^{-1} (\mathbf{S}^T \mathbf{S}_o + \mathbf{S}_o^T \mathbf{S}) (\mathbf{S}^T \mathbf{S})^{-1} \quad (3.127)$$

and hence,

$$\hat{\mathbf{S}}^I = \mathbf{S}^I + \epsilon [-\mathbf{S}^I \mathbf{S}_o \mathbf{S}^I + \underbrace{(\mathbf{S}^T \mathbf{S})^{-1} \mathbf{S}_o^T}_{\Delta} - (\mathbf{S}^T \mathbf{S})^{-1} \mathbf{S}_o^T \mathbf{S} \mathbf{S}^I] \quad (3.128)$$

Were it not for the  $\Delta$  term in the above expression, it would mimic faithfully the expression for the dual inverse appearing in eq. (A.13). It will become apparent that this term can be dropped from the above expression, thereby a) simplifying the expression of interest and b) leading to a *minimum-size linkage*.

Upon substitution of expression (3.128) into eq.(3.125), and expansion of the expression thus resulting, the least-square solution  $\hat{\mathbf{k}}_0$  is obtained as

$$\hat{\mathbf{k}}_0 = \underbrace{(\mathbf{S}^T \mathbf{S})^{-1} \mathbf{S}^T \mathbf{b}}_{\mathbf{k}_0} + \epsilon \underbrace{[(\mathbf{S}^T \mathbf{S})^{-1} (\mathbf{S}_o^T \mathbf{b} + \mathbf{S}^T \mathbf{b}_o - (\mathbf{S}^T \mathbf{S}_o + \mathbf{S}_o^T \mathbf{S}) (\mathbf{S}^T \mathbf{S})^{-1} \mathbf{S}^T \mathbf{b})]}_{\mathbf{k}_{o0}} \quad (3.129)$$

While the above expressions for the least-square solution of both the primal part of  $\hat{\mathbf{k}}$ ,  $\mathbf{k}_0$ , and its dual counterpart  $\mathbf{k}_{o0}$  are theoretically sound, they are not appropriate for computations verbatim, given the large amount of floating-point operations involved, and their need of the inverse of  $\mathbf{S}^T \mathbf{S}$ . As pointed out in Remark 1.4.3, it is not advisable to compute verbatim that inverse because of the likely amplification of the condition number of the matrix product. It will be made apparent in the sequel that a terser solution  $\mathbf{k}_{o0}$  can be obtained.

Indeed, if first the least-square solution  $\mathbf{k}_0$  for the primal part of  $\hat{\mathbf{k}}$  is computed from eq.(3.121a), using the left Moore-Penrose generalized inverse  $\mathbf{S}^I$ , and then this expression is substituted into eq.(3.121b), the least-square solution  $\mathbf{k}_{o0}$  is derived as

$$\mathbf{k}_{o0} = \mathbf{S}^I(\mathbf{b}_o - \mathbf{S}_o \mathbf{S}^I \mathbf{b}) \quad (3.130)$$

which is much terser than its counterpart expression in eq.(3.129). The difference between the two expressions can be explained based on the observation that the dual generalized inverse  $\hat{\mathbf{S}}^I$  is not unique, contrary to its real counterpart. This fact is made apparent below.

Paraphrasing the derivation of the expression (A.13) for the dual inverse, let  $\hat{\mathbf{B}} = \mathbf{B} + \epsilon \mathbf{B}_o$  be the generalized inverse of a  $m \times n$  dual matrix  $\hat{\mathbf{A}} = \mathbf{A} + \epsilon \mathbf{A}_o$ , with  $m > n$ . As  $\hat{\mathbf{A}}$  has been assumed of  $m \times n$ ,  $\hat{\mathbf{B}}$  is bound to be of  $n \times m$ .

Then,

$$\hat{\mathbf{B}} \hat{\mathbf{A}} = \mathbf{1}_n \quad (3.131)$$

with  $\mathbf{1}_n$  denoting the  $n \times n$  identity matrix. Upon expansion of the left-hand side of the above equation, two real equations are obtained, one for the primal, one for the dual part:

$$\mathbf{B}\mathbf{A} = \mathbf{1}_n, \quad \mathbf{B}_o\mathbf{A} + \mathbf{B}\mathbf{A}_o = \mathbf{O}_n \quad (3.132)$$

the first equation leading to the not so unexpected result  $\mathbf{B} = \mathbf{A}^I$ , which, when substituted into the second equation, yields a matrix equation for  $\mathbf{B}_o$ :

$$\mathbf{B}_o\mathbf{A} = -\mathbf{A}^I\mathbf{A}_o$$

A more suitable form of the above equation is obtained, with the unknown  $\mathbf{B}_o$  as the right-hand factor of the left-hand side upon transposing the two sides of the equation, namely,

$$\mathbf{A}^T \mathbf{B}_o^T = -\mathbf{A}_o^T (\mathbf{A}^I)^T \equiv -\mathbf{A}_o^T \mathbf{A} (\mathbf{A}^T \mathbf{A})^{-1}$$

which is a system of  $n^2$  equations in  $m \times n > n^2$  unknowns. The system is, thus, underdetermined, thereby admitting infinitely many solutions. The conclusion is, then, that the dual left generalized inverse is not unique. Among all that many solutions, one of minimum *Frobenius* norm can be obtained if one resorts to the *right Moore-Penrose generalized inverse* of  $\mathbf{A}^T$ , denoted  $(\mathbf{A}^T)^\dagger$  (Nash and Sofer, 1996):

$$(\mathbf{A}^T)^\dagger = \mathbf{A} (\mathbf{A} \mathbf{A}^T)^{-1} \quad (3.133)$$

After some obvious manipulations,

$$\mathbf{B}_o = -\mathbf{A}^I \mathbf{A}_o \mathbf{A}^I \quad (3.134)$$

Therefore, the minimum-Frobenius-norm  $\hat{\mathbf{A}}^I$  is

$$\hat{\mathbf{A}}^I = \mathbf{A}^I - \epsilon \mathbf{A}^I \mathbf{A}_o \mathbf{A}^I \quad (3.135)$$

The reader is invited to show that, if the foregoing formula is applied to compute the least-square solution  $\hat{\mathbf{k}}_0$ , the expression below is obtained:

$$\hat{\mathbf{k}}_0 = \mathbf{S}^I \mathbf{b} + \epsilon \mathbf{S}^I (\mathbf{b}_o - \mathbf{S}_o \mathbf{S}^I \mathbf{b}) \quad (3.136)$$

whose dual part is exactly the one obtained in eq.(3.130). By the same token, the reader is invited to prove that  $\Delta^T$ , with  $\Delta$  as appearing in eq.(3.128), is *an orthogonal complement* (OC) of  $\mathbf{S}^T$ , which is the reason why this term was filtered out in eq.(3.130). Below we expand on the OC concept.

Given a  $m \times n$  matrix  $\mathbf{M}$ , with  $m < n$ , i.e., with more columns than rows—for simplicity, its  $m$  rows will be assumed linearly independent—its  $i$ th row can be regarded as a vector  $\mathbf{m}_i \in \mathbb{R}^n$ . Since  $\mathbf{M}$  has  $m$  such vectors, it is possible to find  $n - m$  linearly independent vectors  $\{\mathbf{p}_k\}_{1}^{n-m}$  orthogonal to the  $m$  rows—picture this with  $m = 2$  and  $n = 3$ . If the vectors of this set are arrayed as the columns of a  $n \times (n - m)$  matrix  $\mathbf{P}$ , then

$$\mathbf{M}\mathbf{P} = \mathbf{O}_{mn'} \quad (3.137)$$

where  $\mathbf{O}_{mn'}$  denotes the  $m \times (n - m)$  zero matrix. Every matrix  $\mathbf{P}$  that verifies eq.(3.137) is termed an orthogonal complement of  $\mathbf{M}$ . It follows that *the OC is not unique*. Indeed, a rearrangement of the columns of  $\mathbf{P}$  yields another OC of  $\mathbf{M}$ . Likewise, any multiple of a given  $\mathbf{P}$  is also an OC of  $\mathbf{M}$ .

In summary, then, the approximate synthesis of a RCCC linkage proceeds sequentially:

1. Decouple the synthesis problem into two subproblems: one leading to the optimum Freudenstein parameters of the spherical linkage associated with the spatial linkage of interest, eq.(3.121a), the other with the optimum dual counterparts of the foregoing parameters, eq.(3.121b).
2. Apply Householder reflections to the primal part  $\mathbf{S}$  of the dual synthesis matrix, thereby obtaining a  $m \times m$  orthogonal matrix  $\mathbf{H}$  and a  $m \times 4$  matrix  $\mathbf{E}$ , with an upper-triangular  $4 \times 4$  block occupying its first four rows and a  $(m - 4) \times 4$  block of zeros. Apply the same reflections to  $\mathbf{b}$  of the right-hand side of eq.(3.121a) and obtain  $\mathbf{k}_0$  by forward substitution on the first four equations.
3. Substitute  $\mathbf{k}$  into eq.(3.121b) with  $\mathbf{k}_0$  and then apply the same Householder reflections to the right-hand side of the same equations.

4. Compute  $\mathbf{k}_{o0}$  from the transformed eqs.(3.121b) by backward substitution over the same  $4 \times 4$  block.
5. Compute the skew angles  $\{\alpha_i\}_1^4$  from eqs.(3.32a)–(3.32d) by nonlinear-equation solving.
6. Compute the distances  $\{a_i\}_1^4$  from eqs.(3.42) by linear-equation solving.
7. Done!

## 3.6 Linkage Performance Evaluation

### 3.6.1 Planar Linkages: Transmission Angle and Transmission Quality

A variable of merit that is used to assess the linkage performance is the *transmission angle*  $\mu$ , illustrated in Fig. 3.1. The transmission angle is thus defined as *the angle between the axes of the output and the coupler links*.

The relevance of this angle is apparent from a kinetostatic analysis<sup>8</sup>: in Fig. 3.16, the *internal forces of constraint* are indicated as  $F_{ij}$ , to denote the force exerted by the  $i$ th link on the  $j$ th link, using a standard terminology. Therefore, the force transmitted by the output link to the frame has a magnitude  $|F_{41}|$  given by

$$|F_{41}| = |F_{14}| = |F_{34}| \quad (3.138)$$

where, from the static equilibrium of the coupler and the input links,

$$|F_{34}| = |F_{32}| = \left| \frac{\tau_\psi}{a_2 \sin(\psi - \theta)} \right| \quad (3.139)$$

and  $\tau_\psi$  is the *applied torque* that *balances statically* the *load torque*  $\tau_\phi$ .

The magnitude of the radial component of  $F_{14}$ , denoted  $|F_{14}|_r$ , is derived upon substitution of eq.(3.139) into eq.(3.138), thus obtaining

$$|F_{14}|_r \equiv |F_{14} \cos \mu| = \left| \frac{\tau_\psi}{a_2 \sin(\psi - \theta)} \cos \mu \right| \quad (3.140)$$

from which it is apparent that  $|F_{14}|_r$  is proportional to the magnitude of the applied moment and to the cosine of the transmission angle. Since this is a nonworking force, one is interested in keeping it as low as possible. However, it cannot be made zero by simply making zero the applied torque because, then, no useful force would be transmitted! Thus,

---

<sup>8</sup>This is an analysis of forces and moments of a *mechanical system in motion under static, conservative conditions*.

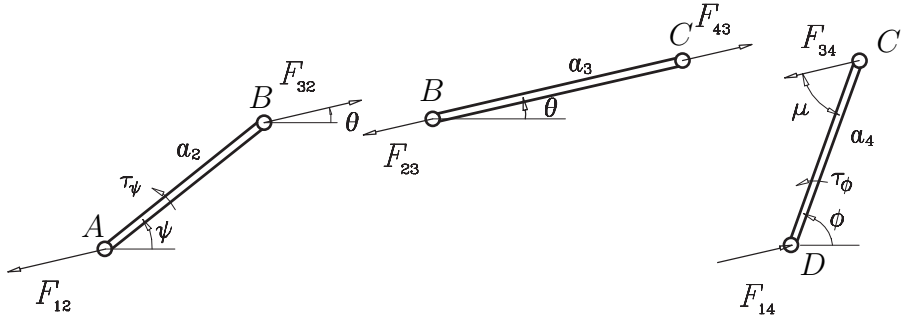


Figure 3.16: A static analysis of the four-bar linkage

the only possible way of keeping that force as small as possible is by keeping  $\cos \mu$  as small as possible, i.e., by keeping  $\mu$  as close as possible to  $\pm 90^\circ$ .

The transmission angle is posture-dependent, of course; hence, it cannot be maintained at a fixed value for all the linkage postures. In practice, a minimum allowable value on the transmission angle or, rather, on its absolute value, is prescribed. This is commonly accepted as  $45^\circ$ , i.e., a specification when designing four-bar linkages is

$$|\mu| \geq 45^\circ \quad (3.141)$$

If one is interested in a global evaluation of the performance of a four-bar linkage throughout its full range of motion, namely,  $\psi_1 \leq \psi \leq \psi_2$ , then a merit function of the linkage that takes into account *all possible postures* is needed. This quantity can be fairly termed the *transmission quality* of the linkage, which is defined as the *root-mean-square* (rms) value of  $\sin \mu$ :

$$Q \equiv \sqrt{\frac{1}{\Delta\psi} \int_{\psi_1}^{\psi_2} \sin^2 \mu d\psi}, \quad \Delta\psi \equiv \psi_2 - \psi_1 \quad (3.142)$$

From the foregoing definition, note that

$$0 < Q < 1 \quad (3.143)$$

Evaluating  $Q$  as given above is rather difficult because an expression for  $\sin \mu$  is not readily derivable. However, an expression for  $\cos \mu$  can be readily derived. Indeed, from Fig. 3.1 and the “cosine law”, two expressions for  $\overline{BD}^2$  can be derived:

$$\overline{BD}^2 = a_3^2 + a_4^2 - 2a_3a_4 \cos \mu \quad (3.144a)$$

$$\overline{BD}^2 = a_1^2 + a_2^2 - 2a_1a_2 \cos \psi \quad (3.144b)$$

Upon equating the two right-hand sides of the foregoing equations, an expression for  $\cos \mu$  is derived in terms of the input angle, namely

$$\cos \mu = \frac{a_3^2 + a_4^2 - a_1^2 - a_2^2 + 2a_1a_2 \cos \psi}{2a_3a_4} \quad (3.145)$$

If now relations (3.71) are recalled, an expression for  $\cos \mu$  in terms of the linkage parameters  $\{k_i\}_1^3$  is obtained:

$$\cos \mu = \operatorname{sgn}(k_2 k_3)(c_1 + c_2 \cos \psi) \quad (3.146a)$$

where coefficients  $c_1$  and  $c_2$  are defined as

$$c_1 \equiv \frac{k_2 - k_1 k_3}{\sqrt{D}}, \quad c_2 = \frac{k_3^2}{\sqrt{D}}, \quad D \equiv k_2^2 + k_3^2 + k_2^2 k_3^2 - 2k_1 k_2 k_3 \quad (3.146b)$$

Now the transmission quality  $Q$  can be written as  $Q = \sqrt{1 - \delta^2}$  where  $\delta$  is the integral of  $\cos^2 \mu$  over the full mobility interval of the input link, i.e.,

$$\delta \equiv \sqrt{\frac{1}{\Delta\psi} \int_{\psi_1}^{\psi_2} \cos^2 \mu d\psi}, \quad \Delta\psi \equiv \psi_2 - \psi_1 \quad (3.147)$$

and, by virtue of the relation between the transmission quality  $Q$  and  $\delta$ , namely,

$$Q^2 + \delta^2 = 1 \quad (3.148)$$

It is reasonable to call  $\delta$  the *transmission defect* of the linkage. Hence, maximizing  $Q$  is equivalent to minimizing  $\delta$ . Note that  $\delta^2$  can be written as

$$\delta^2 \equiv \frac{1}{\Delta\psi} \left[ c_1^2 \Delta\psi + 2c_1 c_2 (\sin \psi_2 - \sin \psi_1) + \frac{1}{2} c_2^2 \Delta\psi + \frac{c_2^2}{4} (\sin 2\psi_2 - \sin 2\psi_1) \right] \quad (3.149)$$

If, in particular, the input link is a crank, then,

$$\delta^2 = c_1^2 + \frac{1}{2} c_2^2 \quad (3.150)$$

In synthesizing a four-bar linkage for function generation, the location of the zeros of the dials of the  $\psi$  and  $\phi$  values is normally immaterial. What matters is the *incremental values* of these angles from those zeros. We can thus introduce parameters  $\alpha$  and  $\beta$  denoting the location of the zeros on the  $\psi$  and the  $\phi$  dials, respectively, so that now

$$\psi_i = \alpha + \Delta\psi_i, \quad \phi_i = \beta + \Delta\phi_i, \quad \text{for } i = 1, 2, \dots, m \quad (3.151)$$

We can thus regard the least-square approximation  $\mathbf{k}_0$  as a function of  $\alpha$  and  $\beta$ , i.e.,

$$\mathbf{k}_0 = \mathbf{k}_0(\alpha, \beta) \quad (3.152)$$

It is apparent, then, that the two new parameters can be used to optimize the linkage performance, e.g., by minimizing its defect  $\delta$ .

As it turns out, the transmission angle plays an important role not only in the force-transmission characteristics of the linkage, but also in the *sensitivity* of its positioning accuracy to changes in the nondimensional parameters  $\mathbf{k}$ . Indeed, if we make abstraction of the parameters  $\alpha$  and  $\beta$ , for simplicity, we can calculate the sensitivity of the synthesized

angle  $\phi_i$  to changes in  $\mathbf{k}$  from the input-output equation (3.11) written for the  $m$  prescribed input-output pairs. We display below the  $i$ th component of this vector equation:

$$F_i(\psi_i, \phi_i, \mathbf{k}) = k_1 + k_2 \cos \phi_i - k_3 \cos \psi_i - \cos(\psi_i - \phi_i) = 0, \quad i = 1, 2, \dots, m \quad (3.153)$$

where  $\phi_i$  is one of the two values of  $\phi$  that verify the above equation for  $\psi = \psi_i$ , namely, the one lying closest to  $\bar{\phi}_i$ , as introduced in eq.(3.107). The sensitivity of interest is, apparently,  $\partial \phi_i / \partial \mathbf{k}$ , which is computed below: this partial derivative is computed upon differentiation of all sides of eq.(3.153) w.r.t.  $\mathbf{k}$ , namely,

$$\frac{dF_i}{d\mathbf{k}} = \frac{\partial F_i}{\partial \phi_i} \frac{\partial \phi_i}{\partial \mathbf{k}} + \frac{\partial F_i}{\partial \mathbf{k}} = \mathbf{0}$$

Hence,

$$\frac{\partial \phi_i}{\partial \mathbf{k}} = -\frac{\partial F_i / \partial \mathbf{k}}{\partial F_i / \partial \phi_i} \quad (3.154)$$

Now, we calculate  $\partial F_i / \partial \phi_i$  from eq.(3.153):

$$\frac{\partial F_i}{\partial \phi_i} = -k_2 \sin \phi_i - \sin(\psi_i - \phi_i) = -\frac{a_1 \sin \phi_i - a_2 \sin(\phi_i - \psi_i)}{a_2} \quad (3.155)$$

A pertinent relation among the variables and parameters involved in eq.(3.155) is displayed in Fig. 3.17. From this figure,

$$a_1 \sin \phi_i - a_2 \sin(\phi_i - \psi_i) = a_3 \sin \mu_i \quad (3.156)$$

Upon substitution of eq.(3.156) into eq.(3.155), we obtain

$$\frac{\partial F_i}{\partial \phi_i} = -\frac{a_3}{a_2} \sin \mu_i \quad (3.157a)$$

which, when substituted into eq.(3.154), yields

$$\frac{\partial \phi_i}{\partial \mathbf{k}} = \frac{a_2}{a_3 \sin \mu_i} \frac{\partial F_i}{\partial \mathbf{k}} \quad (3.157b)$$

Furthermore,

$$\frac{\partial F_i}{\partial \mathbf{k}} = \begin{bmatrix} 1 \\ \cos \phi_i \\ -\cos \psi_i \end{bmatrix} \quad (3.157c)$$

and hence,

$$\frac{\partial \phi_i}{\partial \mathbf{k}} = \frac{a_2}{a_3 \sin \mu_i} \begin{bmatrix} 1 \\ \cos \phi_i \\ -\cos \psi_i \end{bmatrix} \quad (3.157d)$$

It is now apparent that the larger  $|\sin \mu_i|$ , the less sensitive the positioning accuracy of the linkage is to changes in the linkage dimensions.

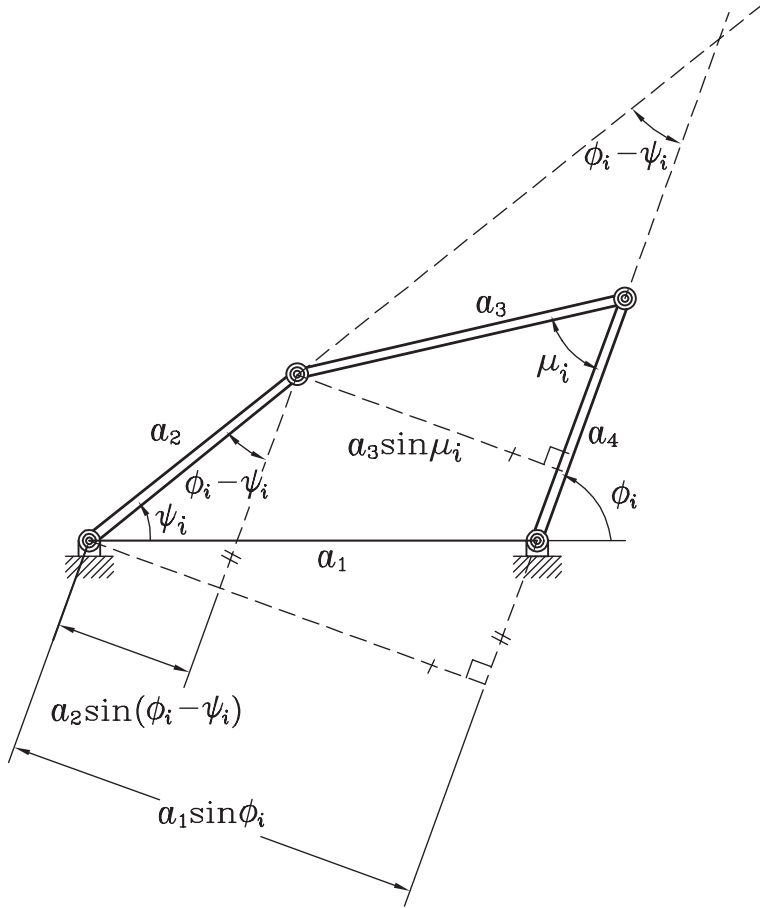


Figure 3.17: Relation between the transmission angle and the parameters and variables of a four-bar linkage

An interesting relation between the linkage discriminant defined in eq.(3.82a) and the transmission angle is now derived. From the expression for  $\cos \mu$  obtained in eqs.(3.146a), an expression for  $\sin^2 \mu$  is readily obtained, in terms of the Freudenstein parameters, as

$$\sin^2 \mu = \frac{k_3^2}{k_2^2 + k_3^2 + k_2^2 k_3^2 - 2k_1 k_2 k_3} \Delta(\psi) \quad (3.158a)$$

where  $\Delta(\psi)$  is the linkage discriminant of eq.(3.82a), reproduced below for quick reference:

$$\Delta(\psi) \equiv -k_3^2 \cos^2 \psi + 2(k_1 k_3 - k_2) \cos \psi + (1 - k_1^2 + k_2^2) \geq 0 \quad (3.158b)$$

which is nonnegative at feasible postures.

Apparently, then, for a given linkage, the square of the sine of the transmission angle is proportional to the discriminant. Hence, both vanish at dead points of the input link, which occur when this is a rocker.

### 3.6.2 Spherical Linkages: Transmission Angle and Transmission Quality

Spherical linkages are elusive to a kinetostatic analysis because they are *hyperstatic*, in that the number of static equations available under the condition that all their axes intersect at one common point is smaller than the number of reaction forces and moments to be found. Rather than deriving the transmission angle for this kind of linkages by means of a kinetostatic analysis, as in the case of planar linkages, we derive it by establishing a correspondence between its geometry and that of the planar linkage. This is done by defining coordinate frames for the planar four-bar linkage in accordance with the Denavit-Hartenberg notation introduced in Subsection 3.2.2, with axes  $X_i$ , for  $i = 1, \dots, 4$  as illustrated in Fig. 3.18. Notice that axis  $Z_1$  is defined in the foregoing figure as that of the output joint, passing through  $D$ ,  $Z_2$  as that of the input joint, passing through  $A$ , with similar definitions for axes  $Z_3$  and  $Z_4$ , all these axes pointing outside of the plane of the figure, towards the reader.

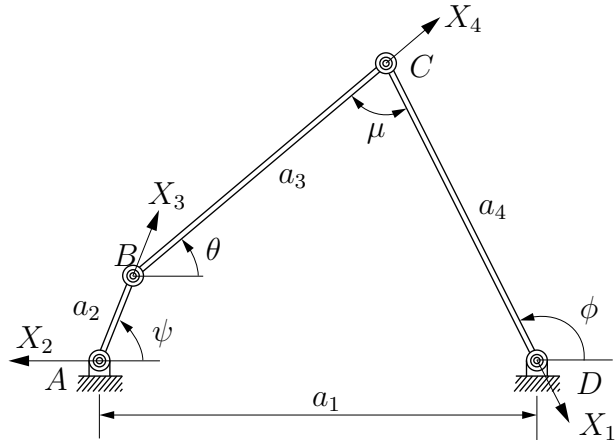


Figure 3.18: A four-bar linkage for function generation

It is now apparent that we can follow the Denavit-Hartenberg notation to define the transmission angle in this case as *the supplement* of that made by  $X_4$  and  $X_1$ , positive in the direction of  $Z_4$ , which is  $\theta_4$  by definition. Indeed, as the reader can readily verify, based on the DH notation,  $\theta_4 + \mu = \pi$  in the planar case. The same holds in the spherical case, and hence,

$$\cos \mu = -\cos \theta_4 \quad (3.159a)$$

An expression for  $\cos \mu$  in terms of the input angle  $\psi$  can be found, as in the planar case, using trigonometry. Obviously, in the case at hand, spherical trigonometry is the tool to use, which then yields (McCarthy and Soh, 2011):

$$\cos \mu = \frac{c\alpha_3 c\alpha_4 - c\alpha_1 c\alpha_2 - s\alpha_1 s\alpha_2 \cos \psi}{s\alpha_3 s\alpha_4} \quad (3.159b)$$

The mechanical significance of the transmission angle is the same as in the planar case: the closer  $\mu$  is to  $\pm 90^\circ$ , the smaller the radial component of the force transmitted by the output link to the frame, and hence, the higher the quality of the force-transmission from the input to the output links. That is, for an acceptable performance, the dihedral angle between the planes of the circular arcs of the coupler and the output links should be such that the two planes are as far from each other as possible, which happens when the angle is  $\pm 90^\circ$ , i.e., when  $\cos \mu = 0$ .

The transmission quality is defined exactly as in the planar case.

### 3.6.3 Spatial Linkages: Transmission Angle and Transmission Quality

This subsection is still under construction.

For quick reference, the spatial four-bar linkage of Fig. 3.5 is reproduced here as Fig. 3.19.

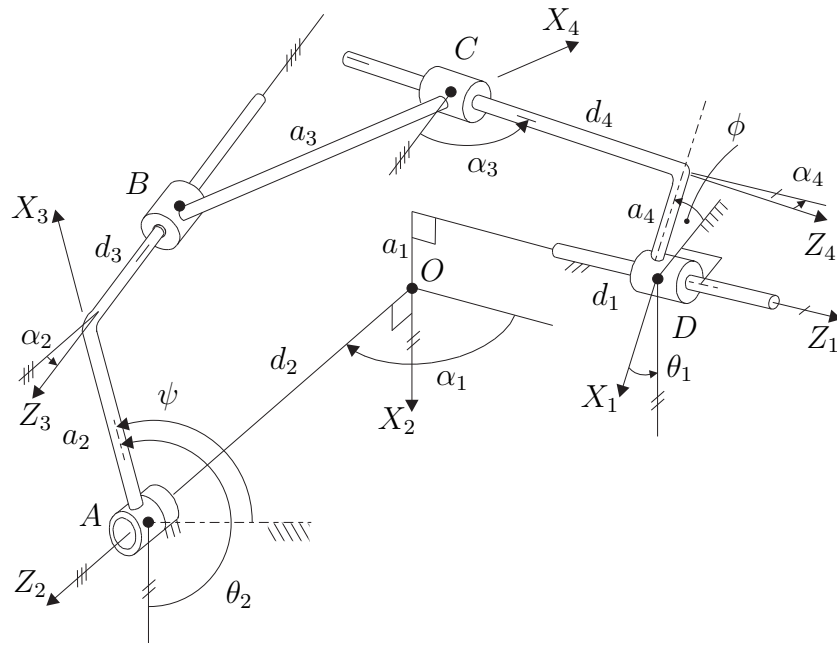


Figure 3.19: A RCCC linkage for function generation (Fig. 3.5 repeated)

Now, the simplest way of determining the transmission angle is by *dualization* of the expression in eq.(3.159a), namely, by putting hats on both  $\mu$  and  $\theta_4$ , which yields

$$\cos \hat{\mu} = -\cos \hat{\theta}_4 \quad (3.160a)$$

Similarly, an expression for  $\cos \hat{\mu}$  in terms of the input angle  $\psi$  can be found upon *dualizing* both sides of eq.(3.159b), namely,

$$\cos \hat{\mu} = \frac{c\hat{\alpha}_3 c\hat{\alpha}_4 - c\hat{\alpha}_1 c\hat{\alpha}_2 - s\hat{\alpha}_1 s\hat{\alpha}_2 \cos \hat{\psi}}{s\hat{\alpha}_3 s\hat{\alpha}_4} \quad (3.160b)$$

In the foregoing equation, according with the definition of dual angle given in eq.(A.5),

$$\hat{\mu} = \theta_4 + \epsilon d_4 \quad (3.161a)$$

where both are defined positive about and along the positive direction of  $Z_4$ . The geometric interpretation of the above expression is straightforward: while  $\theta_4$  is the angle between  $X_4$  and  $X_1$ ,  $d_4$  is the signed distance between  $X_4$  and  $X_1$ , the sign being determined by rule 5 of the DH notation. By the same token,

$$\hat{\alpha}_i = \alpha_i + \epsilon a_i \quad (3.161b)$$

which carries two constant quantities, while

$$\hat{\psi} = \psi + \epsilon d_1 \quad (3.161c)$$

carries two variable quantities, the input angle  $\psi$ , and the sliding  $d_i$ , with units of length. Moreover, the transmission quality is now a dual quantity, namely,

$$\hat{Q} \equiv \sqrt{\frac{1}{\Delta\psi} \int_{\psi_1}^{\psi_2} \sin^2 \theta_4 d\psi} + \epsilon 2 \sqrt{\frac{1}{\Delta\psi} \int_{\psi_1}^{\psi_2} d_4 \cos \theta_4 \sin \theta_4 d\psi}, \quad \Delta\psi \equiv \psi_2 - \psi_1 \quad (3.162)$$

Furthermore,  $\theta_4$  is the real angle between axes  $X_4$  and  $X_1$  in the spherical case, in which the two axes are concurrent. In the spatial case,  $\hat{\theta}_4$  is the *dual angle* between two skew lines, axes  $X_4$  and  $X_1$ . This angle, as discussed in Appendix A, comprises a primal part and a dual part, the former being the real angle between the two lines, as described above. The dual part is the signed distance between  $X_4$  and  $X_1$ , which is positive when  $Z_4$  points in the direction from  $X_4$  to  $X_1$ . Thus, in the same way that the dot product of two unit vectors provides the cosine of the angle between the two vectors, the dot product of two *dual unit vectors*—a dual vector is “of unit magnitude” when its primal part is a real unit vector—provides the cosine of the (dual) angle between two lines. The dual angle in question involves both the angle between the two lines and their signed distance.

In the planar case,  $\cos \mu$  determines “how far” the axis of the coupler link is from that of the output link, while keeping one common point,  $C$ , at any linkage posture: the larger  $|\cos \mu|$ , the “closer” the axes. In the spherical case,  $\cos \mu$  determines “how far” the plane of the circular arc of the coupler link is from its counterpart of the output link, while maintaining one common line,  $Z_4$ , at any given linkage posture: again, the larger  $|\cos \mu|$ , the “closer” the planes. In order to provide a larger *lever arm* to the transmitted force, the foregoing “distances” should be kept as large as possible, aiming at values of  $|\cos \mu|$  closer to zero than to unity.

The generalization to the spatial case then follows:  $\cos \hat{\mu}$  determines “how far”  $X_4$ , while intersecting  $Z_4$ , is from  $X_1$  at any given *linkage posture*. When the two axes coincide, the worst-case scenario, the full *wrench*—force and moment—transmitted by the coupler

link to the output link goes into the linkage support, and no part of it is used to counter the load applied on the output link. The effect of the transmitted force on the output link, under these conditions, is the same as that of a force applied to a door along a line of action that passes through the hinge axis and a moment vector lying in a plane normal to this axis. Force and moment, in this case, are incapable of turning the door.

In summary, then, maximizing the dual transmission quality of the spatial four-bar linkage is equivalent to keeping the axis of the coupler link as “far away” as possible from axis  $X_1$  of the DH notation, to increase the dual lever arm of the wrench—combination of force and moment—driving the output link directly, as transmitted by the coupler link.

**Exercise 3.6.1** Under static, conservative conditions, show that the line of action of the force transmitted by the coupler link to the output link is  $X_4$ .

**Exercise 3.6.2** Derive the expression for the dual transmission quality given in eq.(3.162), then specialize it for the case of an input crank.

## 3.7 Design Error vs. Structural Error

In this section we establish the relation between the design error and the structural error. In doing this, we build upon the analysis proposed by Tinubu and Gupta (1984).

The structural error was introduced in eq.(3.107). If now  $\phi$  and  $\bar{\phi}$  denote the  $m$ -dimensional vectors of *generated and prescribed output values*, then the structural-error vector  $\mathbf{s}$  can be expressed as

$$\mathbf{s} \equiv \phi - \bar{\phi} \quad (3.163)$$

where, it is recalled,  $\phi_i$  denotes the *generated* value,  $\bar{\phi}_i$  the *prescribed* value of the output angle for a given value  $\psi_i$  of the input angle. In the ensuing discussion we assume that the synthesis equations are cast in the general form

$$\mathbf{Sk} = \mathbf{b} \quad (3.164)$$

regardless of the type of linkage, planar, spherical or spatial. However, one should keep in mind that, in the spatial case,  $\mathbf{S}$ ,  $\mathbf{b}$  and  $\mathbf{k}$  become all dual quantities:  $\hat{\mathbf{S}}$ ,  $\hat{\mathbf{b}}$  and  $\hat{\mathbf{k}}$ . In this context,  $\mathbf{S}$  is a  $m \times n$  matrix, while  $\mathbf{k}$  and  $\mathbf{b}$ , or their dual counterparts, as the case may be, are  $n$ - and  $m$ -dimensional vectors, respectively. Again,  $n = 3$  in the planar case, 4 in the spherical and spatial cases<sup>9</sup>. In the case of spatial linkages, a second equation of the same gestalt as that of eq.(3.164), involving a second vector of Freudenstein parameters—the dual part of the dual vector  $\hat{\mathbf{k}}$ —occurs, as per eqs.(3.121a & b). The difference  $\mathbf{e} \equiv \mathbf{b} - \mathbf{Sk}$ —or its dual counterpart for that matter—is to be highlighted: minimizing a norm of  $\mathbf{e}$  is not equivalent to minimizing the same norm of  $\mathbf{s}$ . Indeed, while  $\mathbf{e}$  denotes the error in

---

<sup>9</sup>Read the opening paragraph of Section 3.5.

meeting the synthesis equations, whose components involve trigonometric functions of the input and output angles at the  $m$  prescribed pairs,  $\mathbf{s}$  denotes the error in meeting the prescribed positions, which is what really matters. Unfortunately, however, a relation of the form  $\mathbf{g} \equiv \mathbf{g}(\mathbf{e}, \mathbf{s}) = \mathbf{0}$  between the two errors is elusive. Nevertheless, a *differential* relation between the two errors can be readily obtained, as done below, and that suffices.

In minimizing the structural error, we aim at a minimum of the rms value of the components of vector  $\mathbf{s}$  by properly choosing  $\mathbf{k}$ :

$$z(\mathbf{k}) \equiv \frac{1}{2m} \|\mathbf{s}\|^2 \rightarrow \min_{\mathbf{k}} \quad (3.165)$$

where  $\|\mathbf{s}\|$  is the Euclidean norm of the structural error  $\mathbf{s}$ .

Function  $z(\mathbf{k})$  attains a *stationary* value with respect to  $\mathbf{k}$  when its *gradient* vanishes, i.e.,

$$\nabla z \equiv \frac{\partial z}{\partial \mathbf{k}} = \left( \frac{\partial \mathbf{s}}{\partial \mathbf{k}} \right)^T \frac{\partial z}{\partial \mathbf{s}} = \mathbf{0}_n \quad (3.166)$$

with  $\mathbf{0}_n$  denoting the  $n$ -dimensional zero vector. The above equation is the *normality condition* of the minimization problem at hand. Apparently,

$$\frac{\partial z}{\partial \mathbf{s}} = \frac{1}{m} \mathbf{s} \quad (3.167)$$

Now, in order to compute  $\partial \mathbf{s} / \partial \mathbf{k}$ , we recall the definition of  $\mathbf{s}$ , eq.(3.163), which leads to

$$\frac{\partial \mathbf{s}}{\partial \mathbf{k}} = \frac{\partial \boldsymbol{\phi}}{\partial \mathbf{k}} \quad (3.168)$$

as  $\bar{\boldsymbol{\phi}}$  is a constant vector of prescribed output values. Moreover, the  $i$ th row of matrix  $\partial \boldsymbol{\phi} / \partial \mathbf{k}$ , for the *planar case*, is displayed in eq.(3.157d) as a column array.

Now, in order to compute  $\partial \boldsymbol{\phi} / \partial \mathbf{k}$ , we need an equation relating the array  $\boldsymbol{\phi}$  of *generated values* of the output angle with vector  $\mathbf{k}$ . One candidate would be the  $m$  synthesis equations (3.164), which define the *design error*  $\mathbf{e}$ :

$$\mathbf{e} \equiv \mathbf{e}(\boldsymbol{\phi}, \mathbf{k}) = \mathbf{b} - \mathbf{Sk} \quad (3.169)$$

The above expression is, in general, different from zero, when evaluated at the *prescribed* values  $\bar{\phi}_i$  of the output angle, for  $i = 1, \dots, m$ , and hence, does not define an implicit equation in  $\boldsymbol{\phi}$  and  $\mathbf{k}$ . As a matter of fact, the problem of approximate synthesis consists in minimizing the Euclidean norm of the nonzero vector  $\mathbf{e}$ .

However, when the above vector is evaluated at the *generated* values  $\phi_i$  of the output angle, for  $i = 1, \dots, m$ , then it does vanish. Indeed, the  $i$ th component of  $\mathbf{e}$  as defined in eq.(3.169) is nothing but the input-output function  $F(\psi, \phi) = 0$  evaluated at  $\psi_i$  for a given linkage defined by  $\mathbf{k}$ . In our case,  $\mathbf{k}$  is the *current value*, within an iterative process, to be formulated in Subsection 3.7.1, of the unknown vector of linkage parameters, i.e., the Freudenstein parameters. Upon solving the input-output equation for  $\phi$ , two values

of  $\phi_i$  are obtained, as found in Section 3.4, and hence, the function does vanish at these two values. We will assume that, of these two values,  $\phi_i$  is chosen as the one closer to  $\bar{\phi}_i$ . We thus have

$$F(\psi_i, \phi_i) \equiv b_i - \mathbf{s}_i^T \mathbf{k} = 0 \quad (3.170)$$

in which  $\mathbf{s}_i^T$  denotes the  $i$ th row of  $\mathbf{S}$  and  $b_i$  the  $i$ th component of  $\mathbf{b}$ .

To avoid confusion, let us distinguish between the design error  $\mathbf{e}$  when evaluated at  $\phi$  and when evaluated at  $\bar{\phi}$ , by denoting the latter by  $\bar{\mathbf{e}}$ , i.e.,

$$\bar{\mathbf{e}} \equiv \mathbf{e}(\bar{\phi}, \mathbf{k}) = \bar{\mathbf{b}} - \bar{\mathbf{S}}\mathbf{k} \neq \mathbf{0} \quad (3.171)$$

where  $\bar{\mathbf{S}}$  and  $\bar{\mathbf{b}}$  denote  $\mathbf{S}$  and  $\mathbf{b}$ , respectively, when evaluated at the prescribed values of the input angle  $\{\psi_i\}_1^m$  and at the generated  $\bar{\phi}$ .

Moreover, when we evaluate  $\mathbf{e}$  at the *generated* value  $\phi$ , we obtain

$$\mathbf{e} \equiv \mathbf{e}(\phi, \mathbf{k}) = \mathbf{b} - \mathbf{S}\mathbf{k} = \mathbf{0}_m \quad (3.172)$$

which is an *implicit* vector function of  $\phi$  and  $\mathbf{k}$ , and hence, allows for the evaluation of  $\partial\phi/\partial\mathbf{k}$ . Upon differentiation of eq.(3.172) with respect to  $\mathbf{k}$ , we obtain

$$\frac{d\mathbf{e}}{d\mathbf{k}} = \frac{\partial\mathbf{e}}{\partial\mathbf{k}} + \frac{\partial\mathbf{e}}{\partial\phi} \frac{\partial\phi}{\partial\mathbf{k}} = \mathbf{O}_{mn} \quad (3.173)$$

where  $\mathbf{O}_{mn}$  is the  $m \times n$  zero matrix. Moreover, the  $m \times m$  matrix  $\partial\mathbf{e}/\partial\phi$  is computed from the input-output equation (3.170), or its dual counterpart, as the case may be. Since  $e_k$  is influenced only by  $\phi_k$ , and not by  $\phi_j$ , for  $j \neq k$ ,  $\partial\mathbf{e}/\partial\phi$  is diagonal, i.e.,

$$\frac{\partial\mathbf{e}}{\partial\phi} = \text{diag} [\partial e_1/\partial\phi_1 \quad \partial e_2/\partial\phi_2 \quad \cdots \quad \partial e_m/\partial\phi_m] \equiv \mathbf{D} \quad (3.174a)$$

Under the assumption that none of the diagonal elements of  $\mathbf{D}$  vanishes, this matrix is nonsingular, and hence, the matrix  $\partial\phi/\partial\mathbf{k}$  sought can be solved for from eq.(3.173). Furthermore, it is apparent from eq.(3.172) that  $\partial\mathbf{e}/\partial\mathbf{k}$  is nothing but the negative of the synthesis matrix  $\mathbf{S}$ , evaluated at the generated values of the output angle, i.e.,

$$\frac{\partial\mathbf{e}}{\partial\mathbf{k}} = -\mathbf{S} \quad (3.174b)$$

Hence,  $\partial\phi/\partial\mathbf{k}$ , as computed from eq.(3.173), is

$$\frac{\partial\phi}{\partial\mathbf{k}} \equiv \frac{\partial\mathbf{s}}{\partial\mathbf{k}} = \mathbf{D}^{-1}\mathbf{S} \quad (3.175)$$

Therefore, the *normality condition* (3.166) leads to

$$\mathbf{S}^T \mathbf{D}^{-1} \mathbf{s} = \mathbf{0}_n \quad (3.176)$$

where  $\mathbf{0}_n$  denotes the  $n$ -dimensional zero vector. The normality condition thus states that, for  $\mathbf{k}$  to produce a stationary value of the positioning error—proportional to the

rms value of the structural error  $\mathbf{s}$ —the structural error  $\mathbf{s}$  must lie in the null space of the matrix product  $\mathbf{S}^T \mathbf{D}^{-1}$ . That is, the structural error of minimum norm need not vanish and, in general, it won't, but must verify eq.(3.176).

Now, contrary to the minimization of the design error, the minimization of the positioning error leads to a *nonlinear least-square problem*, which must be solved *iteratively*, as described in Subsection 3.7.1.

### 3.7.1 Minimizing the Structural Error

The approach followed here is similar to the Newton-Gauss method used to solve nonlinear least-square problems, as outlined in Subsection 1.6.1: for starters, a sequence  $\mathbf{s}^0, \mathbf{s}^1, \dots, \mathbf{s}^i, \mathbf{s}^{i+1}$  of structural-error vector values is generated, which, upon convergence, should verify the normality condition. For a given  $\mathbf{s}^i$ , an improved vector value  $\mathbf{s}^{i+1}$  is obtained from the *first-order approximation* of  $\mathbf{s}$ :

$$\mathbf{s}^{i+1} \approx \mathbf{s}^i + \left. \frac{\partial \mathbf{s}}{\partial \mathbf{k}} \right|_{\mathbf{k}=\mathbf{k}^i} \Delta \mathbf{k}^i = \mathbf{s}^i + \mathbf{D}_i^{-1} \mathbf{S}_i \Delta \mathbf{k}^i \quad (3.177)$$

where  $\mathbf{D}_i \equiv \mathbf{D}|_{\mathbf{k}=\mathbf{k}^i}$  and  $\mathbf{S}_i \equiv \mathbf{S}|_{\mathbf{k}=\mathbf{k}^i}$ . Hence,

$$\mathbf{D}_i^{-1} \mathbf{S}_i \Delta \mathbf{k}^i = \mathbf{s}^{i+1} - \mathbf{s}^i \quad (3.178)$$

Upon solving for  $\Delta \mathbf{k}^i$ , the above equation allows the updating of  $\mathbf{k}$  as  $\mathbf{k}^{i+1} = \mathbf{k}^i + \Delta \mathbf{k}^i$ . However, in eq.(3.178) we don't know  $\mathbf{s}^{i+1}$ . Moreover, upon convergence,  $\mathbf{s}$  needn't vanish, and most likely it won't. We can thus assume that  $\mathbf{s}^{i+1} \neq \mathbf{0}_m$ , but, if  $\mathbf{k}^{i+1}$  is an improvement over  $\mathbf{k}^i$ , then the corresponding structural error  $\mathbf{s}^{i+1}$  will be “close” to verifying the normality condition (3.176). In fact, let us assume that  $\mathbf{s}^{i+1}$  does verify the normality condition, with  $\mathbf{S}$  and  $\mathbf{D}$  evaluated at  $\mathbf{k} = \mathbf{k}^i$ , as we cannot evaluate them at  $\mathbf{k}^{i+1}$ . Further, let us multiply both sides of eq.(3.178) from the left by  $\mathbf{S}_i^T \mathbf{D}_i^{-1}$ , which yields

$$\mathbf{S}_i^T \mathbf{D}_i^{-1} \mathbf{D}_i^{-1} \mathbf{S}_i \Delta \mathbf{k}^i = -\mathbf{S}_i^T \mathbf{D}_i^{-1} \mathbf{s}^i \quad (3.179)$$

where the term linear in  $\mathbf{s}^{i+1}$  has dropped because it has been assumed to verify the normality conditions. In eq.(3.179) the coefficient of  $\Delta \mathbf{k}^i$  is a square  $n \times n$  matrix—with  $n$  being the dimension of vector  $\mathbf{k}$ —which allows for the computation of  $\Delta \mathbf{k}^i$  in the form

$$\Delta \mathbf{k}^i = -(\mathbf{S}_i^T \mathbf{D}_i^{-2} \mathbf{S}_i)^{-1} \mathbf{S}_i^T \mathbf{D}_i^{-1} \mathbf{s}^i \quad (3.180)$$

thereby showing that the correction  $\Delta \mathbf{k}^i$  can be computed with the numerical values available at the  $i$ th iteration. In fact, the expression for  $\Delta \mathbf{k}^i$  given in eq.(3.180) should be regarded as a *formula*, not as an algorithm. Indeed, the verbatim inversion of the matrix in parentheses in the foregoing equation is *to be avoided* due to its high *condition*

*number*<sup>10</sup>. As a matter of fact, the condition number, in either the Euclidean or the Frobenius norm, of the same  $n \times n$  matrix is exactly the square of the same norm of the  $m \times n$  matrix  $\mathbf{D}_i^{-1}\mathbf{S}_i$ . Hence, a formulation is sought that will allow the computation of  $\Delta\mathbf{k}^i$  from a system of equations involving the foregoing rectangular matrix. If we recall Subsection 1.4.5, the right-hand side of eq.(3.180) is the *least-square approximation* of the *overdetermined system*

$$(\mathbf{D}_i^{-1}\mathbf{S}_i)\Delta\mathbf{k}^i = -\mathbf{s}^i \quad (3.181)$$

which is identical to eq.(3.178) when the term  $\mathbf{s}^{i+1}$  is dropped. Notice, however, that this term couldn't simply be dropped from the above-mentioned equation on the basis that the said term vanishes, because the structural error is not expected to vanish at the optimum solution. The computation of  $\Delta\mathbf{k}^i$  from eq.(3.181) now should be pursued via an orthogonalization procedure, as studied in Subsection 1.4.5. With  $\Delta\mathbf{k}^i$  calculated, the  $i$ th iteration is complete, as a new, improved value  $\mathbf{k}^{i+1}$  of the design parameter vector  $\mathbf{k}$  is available. Now the new structural-error vector value  $\mathbf{s}^{i+1}$  can be computed, and then the normality condition verified. If the condition is not verified, a new iteration is in order; if the same condition is verified, then the procedure stops. An alternative convergence criterion, equivalent to the latter, is to verify whether  $\|\Delta\mathbf{k}^i\| < \epsilon$ , for a prescribed tolerance  $\epsilon$ . The equivalence of the two criteria should be apparent from the relation between  $\Delta\mathbf{k}^i$  and the product of the last three factors of the right-hand side of eq.(3.180).

**Caveat:** To the uninitiated, it may appear tempting to transfer  $\mathbf{D}_i^{-1}$  to the right-hand side of eq. (3.181), and obtain  $\Delta\mathbf{k}^i$  as the least-square approximation of  $\mathbf{S}_i\Delta\mathbf{k}^i = -\mathbf{D}_i\mathbf{S}_i$ . This is a bad idea, as the least-square solution obtained from the foregoing equation will be different from that obtained from eq. (3.181). Reason: eq. (3.181) is not necessarily verified, but only approximated.  $\mathbf{D}_i$ , or its inverse, carries weights that dictate the value of the least-square approximation.

### Branch-switching Detection

This Subsubsection is limited to planar linkages, its generalization to spherical and spatial linkages should be doable, as the problem under study is based on the concept of the sign of the transmission index. The latter was studied in Section 3.6.

In the foregoing analysis an implicit assumption was adopted: all generated values  $\{\phi_i\}_1^m$  lie on the same linkage branch. However, all four-bar linkages studied in this chapter, planar, spherical and spatial, were shown in Section 3.4 to be *bimodal*, i.e., they all entail two solution branches of their input-output equation. This means that, within an iteration loop, the occurrence of branch-switching should be monitored. Below we explain a simple means of doing this, as applicable to planar linkages. The two branches of a

---

<sup>10</sup>See the definition of this concept in Section 1.4.4.

typical planar four-bar linkage are apparent in Fig. 3.8(a). In this figure, the transmission angle is  $\mu = \angle BCD$  in one branch, in the second being  $\mu' = \angle BC'D$ . The qualitative difference between the two branches lies in *the sign of the sine of the transmission angle*, for, in the first branch, we have  $\sin \mu > 0$ ; in the second,  $\sin \mu' < 0$ . Moreover,  $\sin \mu$  vanishes at *deadpoints*, when the input angle reaches either a maximum or a minimum—linkages of this kind have an input rocker. Hence, a simple way of deciding whether all values  $\{\phi_i\}_1^m$  lie in the same branch relies on the computation of the sign of  $\sin \mu$ . This is most simply done by means of the 2D version of the cross product<sup>11</sup> of vectors  $\overrightarrow{CB} = \mathbf{b} - \mathbf{c}$  and  $\overrightarrow{CD} = \mathbf{d} - \mathbf{c}$ , in this order, where  $\mathbf{b}$ ,  $\mathbf{c}$  and  $\mathbf{d}$  are the position vectors of points  $B$ ,  $C$  and  $D$ , respectively, in the given coordinate frame. The product at stake is given by

$$p \equiv (\mathbf{b} - \mathbf{c})^T \mathbf{E}(\mathbf{d} - \mathbf{c}) = \|\mathbf{b} - \mathbf{c}\| \|\mathbf{d} - \mathbf{c}\| \sin \mu = a_3 a_4 \sin \mu \quad (3.182)$$

with  $\mathbf{E}$  introduced in eq.(1.1a). Given that the link lengths are positive, we have the relation

$$\operatorname{sgn}(\sin \mu) = \operatorname{sgn}(p) \quad (3.183)$$

which now can be used to monitor branch-switching.

### Introducing a Massive Number of Data Points

As shown by Hayes et al. (1999), one simple way of minimizing the structural error is via design-error minimization *in the presence of a large number of prescribed data-pairs*. We show with one example below that, as the cardinality  $m$  of the data set increases, the design and structural errors converge. The results are taken from the foregoing reference.

In the example below, the *weighted Euclidean norm* of the design and the structural error,  $\|\mathbf{e}\|_{2W}$  and  $\|\mathbf{s}\|_{2W}$ , respectively, are minimized. For any  $m$ -dimensional vector  $\mathbf{v}$ , this norm is defined as the rms value of its components, namely,

$$\|\mathbf{v}\|_{2W} \equiv \sqrt{\frac{1}{m} \mathbf{v}^T \mathbf{v}} \quad (3.184)$$

**Example 3.7.1** We synthesize here a planar and a spherical RRRR four-bar linkage to generate a quadratic I/O function for the values given below:

$$\psi_i = \alpha + \Delta\psi_i, \quad \phi_i = \beta + \Delta\phi_i, \quad \Delta\phi_i = \frac{9\Delta\psi_i^2}{8\pi}, \quad i = 1, \dots, m$$

For each linkage the I/O dial zeros ( $\alpha$  and  $\beta$ ) are selected to minimize the condition number  $\kappa$  of  $\mathbf{S}$  for each data-set, in following the procedure proposed by Liu and Angeles (1993). Then both the design and structural errors are determined for the linkages that minimize the respective Euclidean norms for data-sets with cardinalities of

---

<sup>11</sup>See Subsection 1.4.1.

$m = \{10, 40, 70, \text{ and } 100\}$ . These results are listed in Tables 3.5–3.8. Finally the structural errors, corresponding to  $m = 40$ , of the linkages that minimize the Euclidean norms of the design and structural errors are graphically displayed in Fig. 3.20.

Table 3.5: Results for  $m = 10$ .

	Planar RRRR	Spherical RRRR
$\alpha_{\text{opt}} (\circ)$	123.8668	43.3182
$\beta_{\text{opt}} (\circ)$	91.7157	89.5221
$\kappa_{\text{opt}}$	33.2974	200.5262
$\ \mathbf{e}\ _{2W}$	$2.2999 \times 10^{-3}$	$2.4033 \times 10^{-4}$
$\ \mathbf{s}\ _{2W}$	$1.8863 \times 10^{-3}$	$1.3187 \times 10^{-4}$

Table 3.6: Results for  $m = 40$ .

	Planar RRRR	Spherical RRRR
$\alpha_{\text{opt}} (\circ)$	117.4593	42.7696
$\beta_{\text{opt}} (\circ)$	89.4020	88.8964
$\kappa_{\text{opt}}$	32.5549	203.0317
$\ \mathbf{e}\ _{2W}$	$2.484 \times 10^{-3}$	$2.984 \times 10^{-4}$
$\ \mathbf{s}\ _{2W}$	$2.375 \times 10^{-3}$	$1.671 \times 10^{-4}$

Table 3.7: Results for  $m = 70$ .

	Planar RRRR	Spherical RRRR
$\alpha_{\text{opt}} (\circ)$	116.4699	42.7014
$\beta_{\text{opt}} (\circ)$	89.0488	88.8045
$\kappa_{\text{opt}}$	32.5242	204.7696
$\ \mathbf{e}\ _{2W}$	$2.496 \times 10^{-3}$	$3.031 \times 10^{-4}$
$\ \mathbf{s}\ _{2W}$	$2.438 \times 10^{-3}$	$1.701 \times 10^{-4}$

## 3.8 Synthesis Under Mobility Constraints

Read (Liu and Angeles, 1992).

Table 3.8: Results for  $m = 100$ .

	Planar RRRR	Spherical RRRR
$\alpha_{\text{opt}} (\circ)$	116.0679	42.6740
$\beta_{\text{opt}} (\circ)$	88.9057	88.7674
$\kappa_{\text{opt}}$	32.5170	205.5603
$\ \mathbf{e}\ _{2W}$	$2.499 \times 10^{-3}$	$3.047 \times 10^{-4}$
$\ \mathbf{s}\ _{2W}$	$2.464 \times 10^{-3}$	$1.712 \times 10^{-4}$

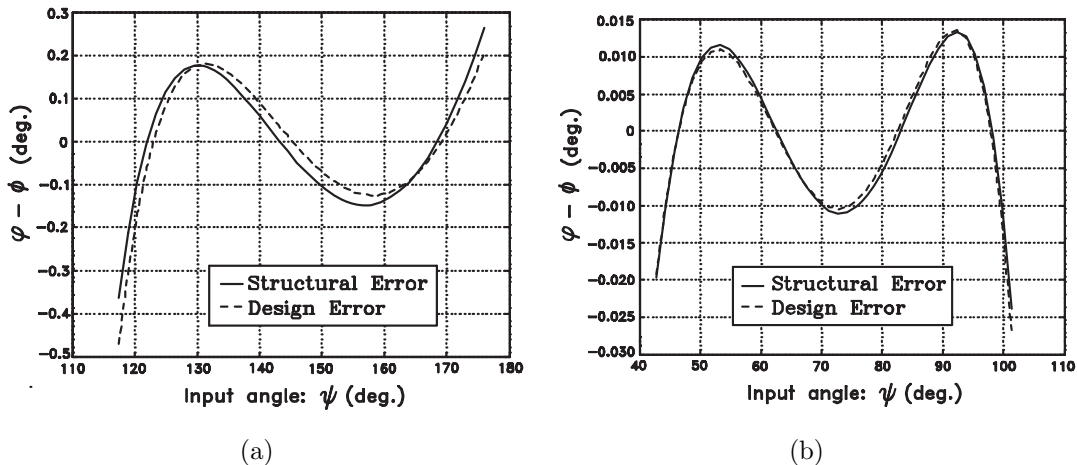


Figure 3.20: Structural error comparison for: (a) planar and (b) spherical RRRR linkages upon minimizing  $\|\mathbf{s}\|_{2W}$  &  $\|\mathbf{e}\|_{2W}$ .

## 3.9 Synthesis of Complex Linkages

To come.

### 3.9.1 Synthesis of Stephenson Linkages

To come.

# Chapter 4

## Motion Generation

### 4.1 Introduction

In the classical problem of *motion generation*, a.k.a. *rigid-body guidance*, a set of poses of a rigid-body is given. These poses are to be visited, in the prescribed order, by the coupler link of a four-bar linkage of *a given type*, whose geometric parameters are to be determined. In this chapter we study the four-bar linkages of the three types studied in Ch. 3, namely, planar, spherical and spatial.

The problem was originally formulated by Ludwig Burmester (1840-1927), for the synthesis of a planar four-bar linkage (Koetsier, 2010). Moreover, the problem discussed here is limited to *finitely separated poses*, which means that velocity and acceleration conditions of the body in question are not considered. Furthermore, the problem reduces to one of *dyad synthesis*, a dyad being a link that carries two kinematic pairs fixed at distinct points of the link. In the case of planar linkages, only R and P pairs are considered; in the spherical case, only R joints; in the case of spatial linkages, only R and C joints.

### 4.2 Planar Four-bar Linkages

A dyad is defined as a link coupled to two other links, one fixed, one mobile. In fact, this definition is not limited to planar linkages; it applies to spherical and spatial linkages as well. Regarding planar linkages, the coupling can take place via a R or a P joint, a dyad can be of any of four types: RR; RP; PR or PP. All four cases are considered in this problem. Furthermore, a planar R pair is defined by one point, its center, a P joint by a unit vector indicating its direction. The R joint is thus known when the position vector of its center is found, the P-joint when a unit vector parallel to its direction is found.

Shown in Fig. 4.1 is a four bar linkage resulting from the arrangement of two dyads,  $A_0B$  and  $A_0^*B^*$ , sharing two common links, the *fixed*  $BB^*$  and the *floating* or *coupler* link  $A_0A_0^*$ . In the problem of linkage synthesis, a set of poses attained by the coupler link is

given via the successive locations of a landmark point  $R$  of the body,  $\{R_j\}_0^m$ , and the corresponding set of position vectors  $\{\mathbf{r}_j\}_0^m$ , together with the attitude attained by the body at the given poses, denoted by the set  $\{\theta_j\}_0^m$ .

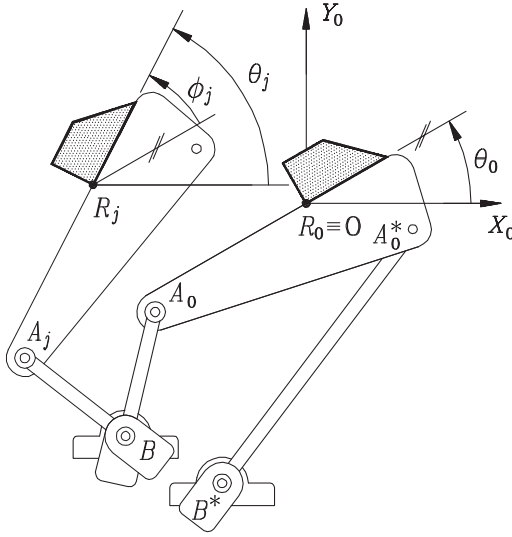


Figure 4.1: Two finitely separated poses of a rigid body carried by the coupler link of a four-bar linkage

Henceforth we use  $X_0$ - $Y_0$  of Fig. 4.1 as the reference coordinate frame. Under the usual rigid-body assumption, the *dyad-synthesis equation* is readily derived: the distance between points  $A_0$  and  $B$  equals that between  $A_j$  and  $B$ , for  $j = 1, \dots, m$ , and hence,

$$\underbrace{\|\mathbf{r}_j - \mathbf{b}\|}_{\mathbf{a}_j - \mathbf{b}} + \mathbf{Q}_j \mathbf{a}_0 = \|\mathbf{a}_0 - \mathbf{b}\|, \quad j = 1, \dots, m \quad (4.1)$$

where  $\mathbf{a}_0$  and  $\mathbf{b}$  are the position vectors of points  $A_0$  and  $B$ , respectively, which are the *design parameters* of the RR dyad, while  $\mathbf{Q}_j$  denotes the rotation matrix carrying the guided body,  $A_0A_0^*$ , from pose 0 to pose  $j$ , i.e.,

$$\mathbf{Q}_j = \begin{bmatrix} \cos \phi_j & -\sin \phi_j \\ \sin \phi_j & \cos \phi_j \end{bmatrix}, \quad \text{with } \phi_j \equiv \theta_j - \theta_0 \quad (4.2)$$

Upon expansion of eq.(4.1) and simplifying the expression thus resulting, we obtain

$$\mathbf{b}^T (\mathbf{1} - \mathbf{Q}_j) \mathbf{a}_0 + \mathbf{r}_j^T \mathbf{Q}_j \mathbf{a}_0 - \mathbf{r}_j^T \mathbf{b} + \frac{\mathbf{r}_j^T \mathbf{r}_j}{2} = 0, \quad j = 1, \dots, m \quad (4.3)$$

where  $\mathbf{1}$  is the  $2 \times 2$  identity matrix, thereby obtaining the dyad-synthesis equations allowing the computation of the design parameters.

It will be shown that a planar dyad can be synthesized exactly for up to five poses, i.e., for  $m = 2, 3, 4$ . These cases are studied below, following which *approximate synthesis* is discussed.

### 4.2.1 Dyad Synthesis for Three Poses

For the case at hand,  $m = 2$ , and hence, two equations of the form of eq.(4.3) are available. However, these equations involve four real unknowns, the two components of  $\mathbf{a}_0$  and the two of  $\mathbf{b}$ . The designer thus has the freedom to specify two of these unknowns. Although any of the four unknowns can be prescribed, it makes sense to specify the two coordinates of the same point,  $A_0$  or  $B$ . Moreover, since the space available to locate the anchor joint centers,  $B$  and  $B^*$ , is known, it is common practice to specify these. In this light, the two equations at hand are now arranged in a convenient form, with  $\mathbf{a}_0$  as unknown:

$$\underbrace{\begin{bmatrix} \mathbf{b}^T(\mathbf{1} - \mathbf{Q}_1) + \mathbf{r}_1^T \mathbf{Q}_1 \\ \mathbf{b}^T(\mathbf{1} - \mathbf{Q}_2) + \mathbf{r}_2^T \mathbf{Q}_2 \end{bmatrix}}_{\mathbf{B}} \mathbf{a}_0 = \underbrace{\begin{bmatrix} \mathbf{r}_1^T(\mathbf{b} - (1/2)\mathbf{r}_1) \\ \mathbf{r}_2^T(\mathbf{b} - (1/2)\mathbf{r}_2) \end{bmatrix}}_{\mathbf{r}} \quad (4.4)$$

whose solution can be obtained in closed form:

$$\mathbf{a}_0 = \mathbf{B}^{-1} \mathbf{r} \quad (4.5)$$

with  $\mathbf{B}^{-1}$  obtained from Fact 1.4.2, namely,

$$\mathbf{B}^{-1} = \frac{1}{\det(\mathbf{B})} \mathbf{E} [ -(\mathbf{1} - \mathbf{Q}_2^T) \mathbf{b} - \mathbf{Q}_2^T \mathbf{r}_2 \quad (\mathbf{1} - \mathbf{Q}_1^T) \mathbf{b} + \mathbf{Q}_1^T \mathbf{r}_1 ] \quad (4.6)$$

and  $\mathbf{E}$  representing the  $2 \times 2$  rotation matrix through  $90^\circ$ , as introduced in eq.(1.1a), while  $\det(\mathbf{B})$  is obtained by resorting to Fact 1.4.1:

$$\det(\mathbf{B}) = [\mathbf{b}^T(\mathbf{1} - \mathbf{Q}_2) + \mathbf{r}_2^T \mathbf{Q}_2] \mathbf{E}[(\mathbf{1} - \mathbf{Q}_1^T) \mathbf{b} + \mathbf{Q}_1^T \mathbf{r}_1] \quad (4.7)$$

thereby completing this case.

### 4.2.2 Dyad Synthesis for Four Poses

We start with some definitions and concepts of *algebraic geometry*, that will become useful in the balance of the chapter. For starters, according to Todd<sup>1</sup>: “Algebraic geometry is the study of geometries that come from algebra, in particular, from rings.” A ring, in turn, is a set  $\mathcal{S}$  together with two binary operators, denoted by “+” and “\*,” (commonly interpreted as addition and multiplication, respectively) that satisfy certain conditions that allow for operations similar to those of real numbers, except for division. The instance of rings that are of interest in our study is polynomials, and multivariate polynomials for that matter.

Of particular interest to our study is multivariate polynomials involving the two coordinates of a point in a plane,  $(x, y)$ , or the three coordinates of a point in three-dimensional space,  $(x, y, z)$ . More facts on algebraic geometry, as pertaining specifically to cubic curves in the plane and in the unit sphere, are provided at the end of this subsection.

---

<sup>1</sup>Todd, R., “Algebraic Geometry.” From MathWorld—A Wolfram Web Resource, created by Eric W.

In the four-pose problem at hand,  $m = 3$ , and hence, this case leads to an underdetermined system of three equations in four unknowns. The approach to the solution of this case is different from the previous case. Rather than finding one specific solution, we will find a *locus* of solutions, or rather *two loci*, one for point  $A_0$ , henceforth termed the *circlepoint*, one for  $B$ , henceforth termed the *centerpoint*. The names arise from the geometry of the linkage, as  $A_0$  lies in a circle with center at  $B$ .

In order to obtain the locus of points  $A_0$ , we eliminate  $\mathbf{b}$  from the three synthesis equations at hand. To this end, let  $\mathbf{z}$  denote the vector of homogeneous coordinates, introduced in eq.(2.18), of  $B$ , and rewrite eq.(4.3) in a more appropriate form, namely,

$$[\mathbf{a}_0^T(\mathbf{1} - \mathbf{Q}_j) - \mathbf{r}_j^T]\mathbf{b} + \frac{\mathbf{r}_j^T \mathbf{r}_j}{2} + \mathbf{r}_j^T \mathbf{Q}_j \mathbf{a}_0 = 0 , \quad j = 1, 2, 3 \quad (4.8)$$

Now, in terms of the homogeneous-coordinate vector  $\mathbf{z}$ , the synthesis equations (4.8) lead to

$$\mathbf{G}\mathbf{z} = \mathbf{0}_3 \quad (4.9)$$

where  $\mathbf{0}_3$  is the three-dimensional zero vector, while  $\mathbf{G}$  is a  $3 \times 3$  matrix linear function of  $\mathbf{a}_0$ , whose  $j$ th row is the three-dimensional vector  $\mathbf{g}_j^T$ , all defined below:

$$\mathbf{z} \equiv \begin{bmatrix} \mathbf{b} \\ 1 \end{bmatrix} = \begin{bmatrix} x \\ y \\ 1 \end{bmatrix}, \quad \mathbf{G} \equiv \begin{bmatrix} \mathbf{g}_1^T \\ \mathbf{g}_2^T \\ \mathbf{g}_3^T \end{bmatrix}, \quad \mathbf{g}_j = \begin{bmatrix} (\mathbf{1} - \mathbf{Q}_j)\mathbf{a}_0 - \mathbf{r}_j \\ \mathbf{r}_j^T(\mathbf{Q}_j\mathbf{a}_0 + \mathbf{r}_j/2) \end{bmatrix}, \quad j = 1, 2, 3 \quad (4.10)$$

Now, for eq.(4.9) to admit a non-trivial solution, as required by the third component of  $\mathbf{z}$ ,  $\mathbf{G}$  must be singular, and hence,

$$G(x, y) \equiv \det(\mathbf{G}) \equiv \mathbf{g}_1 \cdot \mathbf{g}_2 \times \mathbf{g}_3 = 0 \quad (4.11)$$

Since each row of  $\mathbf{G}$  is a linear function of  $\mathbf{a}_0$  and the matrix is of  $3 \times 3$ , it follows that eq.(4.11) defines an (implicit) *cubic* function<sup>2</sup>  $G(x, y)$  in the components of  $\mathbf{a}_0$ , and hence, a cubic curve  $\mathcal{K}$  in the  $X_0$ - $Y_0$  plane, termed the *circlepoint curve*, as it is the locus of the circlepoint  $A_0$ . Therefore, any point on  $\mathcal{K}$  can be used to locate the centerpoint  $A_0$ .

Once a given point  $A_0$  of  $\mathcal{K}$  has been chosen, eq.(4.8) represents an *overdetermined* linear system of three equations in only two unknowns, the components of  $\mathbf{b}$ . However, because  $\mathbf{a}_0$  is the position vector of a point in  $\mathcal{K}$ , the three equations in question are bound to be linearly dependent—remember that  $\mathbf{G}$  has been forced to be singular! Hence, any two of these equations yields the corresponding  $\mathbf{b}$ . The only difference in the three possible solutions obtained upon choosing two out of the three equations (4.8) is due to roundoff error. The difference can be large in the presence of an ill-conditioned  $2 \times 2$  submatrix of

---

Weisstein: <http://mathworld.wolfram.com/AlgebraicGeometry.html>

<sup>2</sup>The cubic nature of  $\det(\mathbf{G})$  is made apparent in eq.(4.11), which shows three factors linear in  $\mathbf{a}_0$ .

**G.** To alleviate the roundoff-error effect, it is advisable to regard the three equations as if they were independent, and compute  $\mathbf{b}$  as the *linear* least-square approximation of the three equations using one of the methods of Subsection 1.4.5.

By the same token,  $\mathbf{a}_0$  can be eliminated from eqs.(4.3). To this end, these are rewritten in the form

$$\mathbf{H}\mathbf{w} = \mathbf{0}_3 \quad (4.12)$$

with  $\mathbf{H}$  defined as a  $3 \times 3$  matrix linear function of  $\mathbf{b}$ , while  $\mathbf{w}$  is the *three-dimensional array of homogeneous coordinates* of  $A_0$ , i.e.,

$$\mathbf{w} \equiv \begin{bmatrix} \mathbf{a}_0 \\ 1 \end{bmatrix} = \begin{bmatrix} u \\ v \\ 1 \end{bmatrix}, \quad \mathbf{H} \equiv \begin{bmatrix} \mathbf{h}_1^T \\ \mathbf{h}_2^T \\ \mathbf{h}_3^T \end{bmatrix}, \quad \mathbf{h}_j = \begin{bmatrix} (\mathbf{1} - \mathbf{Q}_j^T)\mathbf{b} + \mathbf{Q}_j^T\mathbf{r}_j \\ -\mathbf{r}_j^T\mathbf{b} + \mathbf{r}_j^T\mathbf{r}_j/2 \end{bmatrix}, \quad j = 1, 2, 3 \quad (4.13)$$

Following the same reasoning as that leading to eq.(4.11), matrix  $\mathbf{H}$  is bound to be singular, and hence,

$$\det(\mathbf{H}) = 0 \quad (4.14)$$

which defines a cubic equation in  $\mathbf{b}$ , and hence, a cubic curve  $\mathcal{M}$  in the  $X_0$ - $Y_0$  plane, termed the *centerpoint curve*. This curve is the locus of all centerpoints  $B$  that satisfy the three given synthesis equations. Again, once a point  $B$  in  $\mathcal{M}$  has been chosen, and its position vector substituted into the synthesis equations (4.8), an overdetermined system of three equations in the two components of  $\mathbf{a}_0$  is obtained. Its least-square approximation determines point  $A_0$  in a form robust to roundoff-error effects.

## A Note on Cubic Equations

Curves  $\mathcal{K}$  and  $\mathcal{M}$  are cubic, meaning that they are endowed with special features worth highlighting. For starters, these curves are what is known as *algebraic*. A generic *planar* curve of this kind is represented by an *implicit function*  $f(x, y) = 0$ , whose left-hand side is a bivariate polynomial, namely, a linear combination of expressions  $x^i y^j$ , for integers  $i$  and  $j$ . The degree  $N$  of an algebraic curve is defined as  $N = \max(i + j)$ . As a result, an algebraic curve of degree  $N$  intersects a line at  $N$  points *at most*. In specific cases, the number of visible intersections of the plots of the curve and the line may be smaller than  $N$ , the reason being that some of the intersections are either points with complex coordinates, which are, hence, invisible in a plot, or points at infinity.

Furthermore, cubic curves bear the property of having one *asymptote*. This is a line that is tangent to the curve, with the points of tangency lying at infinity.

### 4.2.3 Dyad Synthesis for Five Poses

When  $m = 4$ , eq.(4.8) can be cast in a homogeneous form, similar to eq.(4.9), but now  $\mathbf{G}$  becomes a  $4 \times 3$  matrix, and hence,

$$\mathbf{G}\mathbf{z} = \mathbf{0}_4 \quad (4.15)$$

where  $\mathbf{0}_4$  is the four-dimensional zero vector, while  $\mathbf{G}$ , still a matrix linear function of  $\mathbf{a}_0$ , has won a fourth row,  $\mathbf{g}_4^T$ , vector  $\mathbf{z}$  remaining as in eq.(4.10), and all four vectors  $\mathbf{g}_j$  keeping the same pattern as in this equation.

The condition under which eq.(4.15) admits a non-trivial solution  $\mathbf{z}$  leads to the rank-deficiency of  $\mathbf{G}$ , which means that  $\text{rank}(\mathbf{G}) < 3$ . This condition can be imposed by noticing that it implies that every triplet of rows of  $\mathbf{G}$  is bound to be linearly dependent, thereby rendering every  $3 \times 3$  submatrix of  $\mathbf{G}$  singular.

If  $\mathbf{G}_j$  is the  $3 \times 3$  matrix formed by deleting the  $j$ th row from  $\mathbf{G}$ , then the singularity of every such square matrix defines one circlepoint curve  $\mathcal{K}_j$ , i.e.,

$$\mathcal{K}_j : \Delta_j(\mathbf{a}_0) \equiv \Delta_j(x, y) \equiv \det(\mathbf{G}_j) = 0, \quad j = 1, \dots, 4 \quad (4.16)$$

Each of the four equations (4.16) defines one circlepoint curve in the  $X_0$ - $Y_0$  plane. Therefore, one common intersection of the four curves  $\mathcal{K}_j$  yields one real circlepoint of the dyad sought. If no such intersection occurs, the problem admits no real solution. Of course, any pair of equations (4.16) suffices to determine a set of circlepoints  $\mathbf{a}_0$ . Moreover, a pair of cubic equations bearing a Bezout number<sup>3</sup> of 9, one can expect up to nine real intersections of two cubics. However, upon expressing the rotation matrix as  $\mathbf{Q}_j = \cos \phi_j \mathbf{1} + \sin \phi_j \mathbf{E}$ , with  $\mathbf{E}$  introduced in eq.(1.1a), and introduction of a change of variable, as suggested by Bottema and Roth (1978), the four cubic equations can be reduced to two quadratics, with a Bezout number of 4. Hence, the number of real solutions to be expected in this case is 0, 2, or 4, as demonstrated by Chang et al. (1991). Moreover, given that two dyads are needed to produce a planar four-bar linkage, the total number  $N$  of possible linkages is

$$N = \binom{4}{2} = 6$$

An alternative approach to solving the problem at hand is purely numeric: Regard the four cubic equations in  $\mathbf{a}_0$  as an overdetermined system of four equations in two unknowns, and solve it by means of the Newton-Gauss method, introduced in Subsection 1.6.1. Notice that, in this case, various initial guesses must be tried, to obtain all possible solutions.

Likewise, the centerpoints of a RR dyad can be found from relations similar to those of eq.(4.13), but now with a  $4 \times 3$  matrix  $\mathbf{H}$ , namely.

---

<sup>3</sup>See Section 1.3.

$$\mathbf{H}\mathbf{w} = \mathbf{0}_4 \quad (4.17)$$

with  $\mathbf{H}$  now gaining one fourth row,  $\mathbf{h}_4^T$ ,  $\mathbf{w}$  staying as in eq.(4.13), while the four vectors  $\mathbf{h}_j$  bear the same pattern as in the same equation.

Therefore, for eq.(4.17) to admit a non-trivial solution,  $\mathbf{H}$  must be rank-deficient, and hence, each of its four  $3 \times 3$  submatrices must be singular, which then defines four corresponding centerpoint curves  $\mathcal{M}_j$ :

$$\mathcal{M}_j : \tilde{\Delta}_j(\mathbf{b}) \equiv \tilde{\Delta}_j(u, v) \equiv \det(\mathbf{H}_j) = 0, \quad j = 1, \dots, 4 \quad (4.18)$$

where  $\mathbf{H}_j$  is formed by deleting the  $j$ th row from  $\mathbf{H}$ . The four equations thus obtained are functions of  $\mathbf{b} = [u, v]^T$ , and provide four centerpoint curves  $\mathcal{M}_j$  in the  $X_0$ - $Y_0$  plane, for  $j = 1, \dots, 4$ . The centerpoints are determined as the intersections of all four curves  $\mathcal{M}_j$ . Again, if no common intersection occurs, then the problem admits no real solution.

While *algebraically* any pair of eqs.(4.16) and (4.18) suffices to determine  $\mathbf{a}_0$  or, correspondingly,  $\mathbf{b}$ , for *numerical robustness* we recommend the use of all four equations involved. Upon regarding this system of equations in the two unknown components of  $\mathbf{a}_0$  ( $\mathbf{b}$ )—the Cartesian coordinates of  $A_0$  ( $B$ )—as an overdetermined system of *four* equations in *two* unknowns, we compute the two unknowns as the *least-square approximation* of eqs.(4.16) or (4.18), as the case may be. This approach is at the core of the *robustness* of the methodology proposed here.

#### 4.2.4 Case Study: Synthesis of a Landing Gear Mechanism

Throughout this section we will illustrate the synthesis procedure with the case study described below, for various numbers of given poses.

In developing a compact landing gear for small aircraft, a planar four-bar linkage is being considered. The linkage is to be anchored to the fuselage, indicated as the shaded region in Fig. 4.2. Produce a design that will do the job, with the fixed R joints as close as possible to the fuselage boundary, and outside of the *working region*, i.e., the region swept by the wheel when it is being either retracted or deployed, as shown in the same figure. It hasn't as yet been decided what tire model will be used. For this reason, the design should be proposed in terms of the tire radius  $r$ . To this end, the relations below are specified:

$$a = r, \quad b = 2r$$

Moreover, the tire can be assumed to fit in a rectangle of width  $r/3$  and height  $2r$ .

In order to make the operations of deployment and retraction as smooth as possible, a *smooth* trajectory  $\Gamma$  is to be followed by the *midpoint* of the tire, defined as the intersection

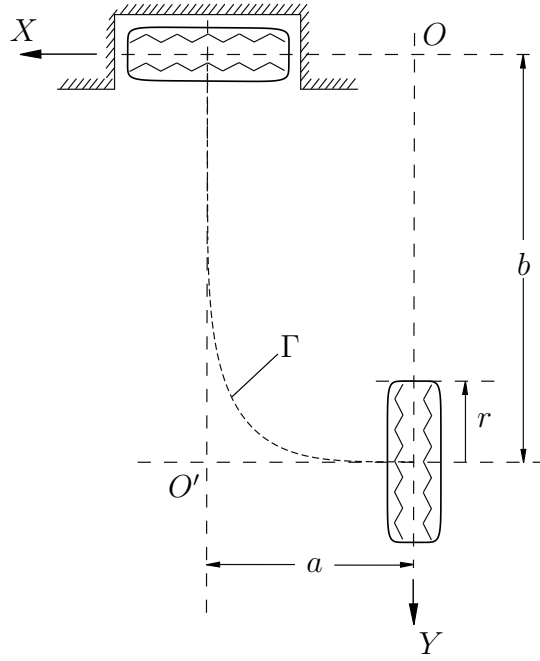


Figure 4.2: A landing gear for small aircraft

of the tire axis with the tire midplane, while the axis of the tire is to remain tangent to  $\Gamma$ . More precisely,  $\Gamma$  is defined as a *fourth-degree Lamé curve* (Gardner, 1965), namely,

$$\left(\frac{x}{a}\right)^4 + \left(\frac{y}{b}\right)^4 = 1 \quad (4.19)$$

A set of 11 poses is given in Table 4.1, from which subsets of poses are to be taken to illustrate the synthesis procedure for  $m = 2, 3, 4$ , and 11, in the coordinate frame  $X$ - $Y$  of the figure. A note on *data-conditioning* is in order here: The Lamé curve is as smooth as an ellipse—it bears the nickname of “superellipse”—but this smoothness carries certain features that need careful attention, as discussed below.

For starters, if the Cartesian coordinates of the sample points is given in a frame with origin at  $O'$  of Fig. 4.2, with axis  $X$  coinciding with the axis of the wheel at its deployed pose and axis  $Y$  coinciding with the same axis at its retracted pose, then the resolution of the  $y$ -coordinates at points close to the value  $x = a$  becomes rather poor. The same holds for the  $x$ -coordinates at points close to the value  $y = b$ . For this reason, the coordinate axes have been defined as shown in the same figure, with origin at  $O$ .

Moreover, calculating the coordinates from the *implicit equation* (4.19) upon assigning a value to, say  $x$ , and then solving for  $y$  is a bad idea, as this requires solving a quartic equation, which incurs roundoff error. A better approach is to resort to the *parametric equations* of the curve, which require no equation solving, namely,

$$x(\theta) = \frac{a}{(1 + \tan^m \theta)^{1/m}}, \quad y(\theta) = \frac{b \tan \theta}{(1 + \tan^m \theta)^{1/m}}, \quad 0 \leq \theta < \frac{\pi}{2} \quad (4.20)$$

Table 4.1: A set of prescribed poses for rigid-body guidance

$j$	$\mathbf{r}_j$ [mm]	$\phi_j$ [deg]
0	$r[1.0, 0.0]^T$	0.0
1	$r[0.99999, 0.1584]^T$	0.0142
2	$r[0.9998, 0.3249]^T$	0.1228
3	$r[0.9989, 0.5090]^T$	0.4737
4	$r[0.9957, 0.7234]^T$	1.3731
5	$r[0.9850, 0.9850]^T$	3.5763
6	$r[0.9507, 1.3085]^T$	9.2559
7	$r[0.8487, 1.6657]^T$	25.2897
8	$r[0.6237, 1.9196]^T$	61.2401
9	$r[0.3160, 1.9950]^T$	86.3626
10	$r[0.0, 2.0]^T$	90.0

where (a)  $\theta$  is the angle made by the position vector of a point  $P$  of  $\Gamma$  in the given frame and (b) the strict inequality is intended to avoid the *singularity*<sup>4</sup> of the  $\tan(\cdot)$  function. Moreover, the unit vector  $\mathbf{e}_t$  tangent to the curve at any value of  $\theta$  within the above range is given by

$$\mathbf{e}_t \equiv \frac{1}{\sqrt{x'(\theta)^2 + y'(\theta)^2}} \begin{bmatrix} -x'(\theta) \\ y'(\theta) \end{bmatrix} = \frac{1}{\sqrt{a^2 \tan^6 \theta + b^2}} \begin{bmatrix} -a \tan^3 \theta \\ b \end{bmatrix}$$

The coordinates of the sample of points and the slope of the tangent to the curve at its corresponding point are given in Table 4.1.

### Dyad Synthesis for Three Poses

Entries  $j = 0, 5$  and  $10$  of Table 4.1 are chosen here, the two ensuing rotation matrices, along with the two vectors  $\mathbf{r}_j$ , are now evaluated:

$$\mathbf{Q}_1 = \begin{bmatrix} 0.9981 & -0.0624 \\ 0.0624 & 0.9981 \end{bmatrix}, \quad \mathbf{Q}_2 = \begin{bmatrix} 0.0 & -1.0 \\ 1.0 & 0.0 \end{bmatrix}, \quad \mathbf{r}_1 = r \begin{bmatrix} 0.9850 \\ 0.9850 \end{bmatrix}, \quad \mathbf{r}_2 = r \begin{bmatrix} 0 \\ 2.0000 \end{bmatrix}$$

Now let us choose  $B$  and  $B^*$  symmetrically located on the  $X$ -axis with coordinates  $x = 0$  and  $x^* = 3r$ , respectively. Upon plugging these values into matrix  $\mathbf{B}$  and vector  $\mathbf{r}$

---

<sup>4</sup>Points at which the value of a function becomes unbounded are termed *singular*.

of eq.(4.4), the numerical values of  $\mathbf{B}$ ,  $\mathbf{B}^*$ ,  $\mathbf{r}$  and  $\mathbf{r}^*$  are obtained below, with an obvious notation:

$$\mathbf{B} = r \begin{bmatrix} 1.0445 & 0.9216 \\ 2.0 & 0.0 \end{bmatrix}, \mathbf{r} = -r^2 \begin{bmatrix} 0.9701 \\ 2.0 \end{bmatrix}, \mathbf{B}^* = r \begin{bmatrix} 1.0503 & 1.1087 \\ 5.0 & 3.0 \end{bmatrix}, \mathbf{r}^* = r^2 \begin{bmatrix} 1.9847 \\ -2 \end{bmatrix}$$

from which  $\mathbf{B}^{-1}$  and  $(\mathbf{B}^*)^{-1}$  are readily computed:

$$\mathbf{B}^{-1} = \frac{1}{r} \begin{bmatrix} 0.0 & 0.5 \\ 1.0851 & -0.5667 \end{bmatrix}, (\mathbf{B}^*)^{-1} = \frac{1}{r} \begin{bmatrix} -1.2538 & 0.4634 \\ 2.0897 & -0.4390 \end{bmatrix}$$

which readily lead to

$$\mathbf{a}_0 = r \begin{bmatrix} -1 \\ 0.0807 \end{bmatrix}, \mathbf{a}_0^* = r \begin{bmatrix} -3.4152 \\ 5.0254 \end{bmatrix}$$

thereby completing the solution.

### Dyad Synthesis for Four Poses

For this case we choose entries  $j = 0, 3, 6$  and  $10$  of Table 4.1, which lead to the three rotation matrices and the three vectors  $\mathbf{r}_j$  below:

$$\mathbf{Q}_1 = \begin{bmatrix} 0.99997 & -0.00827 \\ 0.00827 & 0.99997 \end{bmatrix}, \mathbf{Q}_2 = \begin{bmatrix} 0.9870 & -0.1608 \\ 0.1608 & 0.9870 \end{bmatrix}, \mathbf{Q}_3 = \begin{bmatrix} 0.0 & -1.0 \\ 1.0 & 0.0 \end{bmatrix}$$

$$\mathbf{r}_1 = r \begin{bmatrix} 0.9989 \\ 0.5090 \end{bmatrix}, \mathbf{r}_2 = r \begin{bmatrix} 0.9507 \\ 1.3085 \end{bmatrix}, \mathbf{r}_3 = r \begin{bmatrix} 0.0 \\ 2.0 \end{bmatrix}$$

while vectors  $\mathbf{g}_j$ , for  $j = 1, 2, 3$ , are readily obtained:

$$\mathbf{g}_1 = r \begin{bmatrix} 0.0083 \eta - 0.9989 \\ -0.0083 \xi - 0.5090 \\ r(1.0031 \xi + 0.5007 \eta + 0.6285) \end{bmatrix}, \mathbf{g}_2 = r \begin{bmatrix} 0.0130 \xi + 0.1608 \eta - 0.9507 \\ -0.1608 \xi + 0.0130 \eta - 1.3085 \\ r(1.1487 \xi + 1.1385 \eta + 1.3079) \end{bmatrix},$$

$$\mathbf{g}_3 = r \begin{bmatrix} \xi + \eta \\ -\xi + \eta - 2 \\ 2r(\xi + 1) \end{bmatrix}, \quad \text{with } \xi \equiv \frac{x}{r} \text{ \& } \eta \equiv \frac{y}{r}$$

Hence,  $\det(\mathbf{G})$  follows:

$$\begin{aligned} \det(\mathbf{G}) = r^4 &(0.0646 \eta^3 + 0.0646 \xi^2 \eta + 0.2283 + 0.1390 \xi^3 \\ &+ 0.9091 \xi^2 + 1.0087 \xi + 0.6771 \eta^2 - 0.5213 \eta + 0.1390 \xi \eta^2 + 0.1356 \xi \eta) \end{aligned}$$

whose plot, representing the circlepoint curve  $\mathcal{K}$ , is displayed in Fig. 4.3, with a value of  $r = 1$  unit—whatever the unit may be.

Next, the centerpoint curve  $\mathcal{M}$  is obtained for the same set of poses. To this end, the  $3 \times 3$  matrix  $\mathbf{H}$  is produced from the three three-dimensional vectors  $\mathbf{h}_j$ , namely,

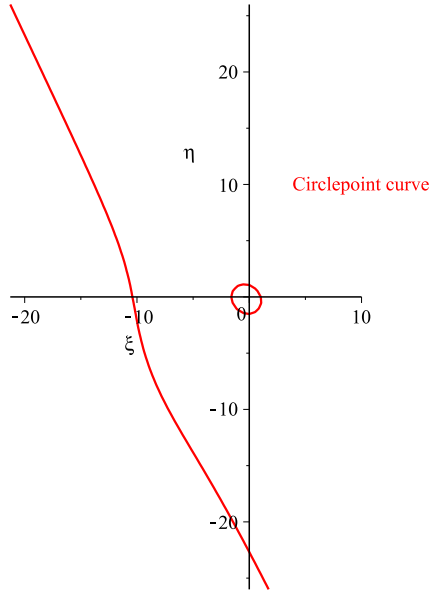


Figure 4.3: Circlepoint curve  $\mathcal{K}$  for  $m = 3$

$$\mathbf{h}_1 = r \begin{bmatrix} -0.0083 \eta^* + 1.0031 \\ 0.0083 \xi^* + 0.5007 \\ -r(0.9989 \xi^* + 0.5090 \eta^* - 0.6285) \end{bmatrix}, \quad \mathbf{h}_2 = r \begin{bmatrix} 0.0130 \xi^* - 0.1608 \eta^* + 1.1487 \\ 0.1608 \xi^* + 0.0130 \eta^* + 1.1385 \\ -r(0.9507 \xi^* + 1.3085 \eta^* - 1.3079) \end{bmatrix},$$

$$\mathbf{h}_3 = r \begin{bmatrix} \xi^* - \eta^* + 2 \\ \xi^* + \eta^* \\ 2r(1 - \eta^*) \end{bmatrix}, \quad \text{with } \xi^* \equiv \frac{u}{r} \text{ & } \eta^* \equiv \frac{v}{r}$$

With the above vectors,  $\mathbf{H}$  is obtained, its determinant being

$$\det(\mathbf{H}) = r^4(1.0125 - 0.3257 \xi^* \eta^* + 0.1398 \xi^* \eta^{*2} + 0.0647 \eta^{*3} + 0.0647 \xi^{*2} \eta^* + 0.6907 \xi^{*2} + 0.7821 \xi^* + 0.5661 \eta^{*2} - 1.6625 \eta^* + 0.1398 \xi^{*3})$$

whose plot is also obtained for a value of  $r = 1$  unit, as displayed in Fig. 4.4.

The reader is invited to choose points  $B$  and  $B^*$  on  $\mathcal{K}$  at convenient locations, and then find the corresponding points  $A_0$  and  $A_0^*$ , while ensuring that these points meet the design specs given at the outset.

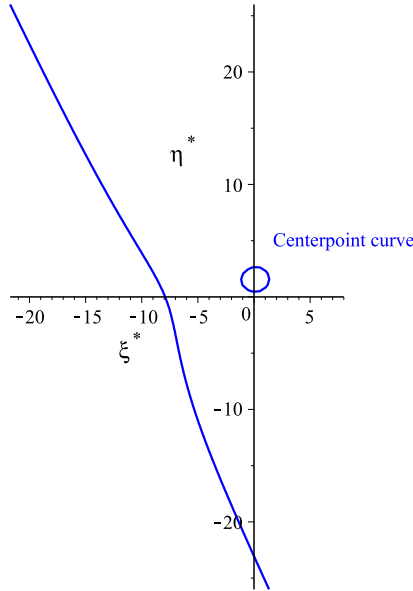


Figure 4.4: Centerpoint curve  $\mathcal{M}$  for  $m = 3$

### Dyad Synthesis for Five Poses

Now five poses are chosen from Table 4.1, namely, those of entries 0, 2, 5, 8 and 10. In this case, we have four  $\mathbf{g}_j$  and four  $\mathbf{h}_j$  vectors, namely,

$$\mathbf{g}_1 = r \begin{bmatrix} 0.0021\eta - 0.9998 \\ -0.0021\xi - 0.3249 \\ r(1.0005\xi + 0.3227\eta + 0.5526) \end{bmatrix}, \quad \mathbf{g}_2 = r \begin{bmatrix} 0.00195\xi + 0.0624\eta - 0.9850r \\ -0.0624\xi + 0.0019\eta - 0.9850r \\ r(1.0445\xi + 0.9216\eta + 0.9701) \end{bmatrix}$$

$$\mathbf{g}_3 = r \begin{bmatrix} 0.5189\xi + 0.8766\eta - 0.6237 \\ -0.8766\xi + 0.5189\eta - 1.9196 \\ r(1.9829\xi + 0.3768\eta + 2.0370) \end{bmatrix}, \quad \mathbf{g}_4 = r \begin{bmatrix} \xi + \eta \\ -\xi + \eta - 2 \\ 2r(\xi + 1) \end{bmatrix}$$

$$\mathbf{h}_1 = r \begin{bmatrix} -0.002144\eta^* + 1.0005 \\ 0.0021\xi^* + 0.3227 \\ r(-0.9998\xi^* - 0.3249\eta^* + 0.5526) \end{bmatrix}, \quad \mathbf{h}_2 = r \begin{bmatrix} 0.0019\xi^* - 0.0624\eta^* + 1.0445 \\ 0.0624\xi^* + 0.0019\eta^* + 0.9216 \\ r(-0.9850\xi^* - 0.9850\eta^* + 0.9701) \end{bmatrix}$$

$$\mathbf{h}_3 = r \begin{bmatrix} 0.5189\xi^* - 0.8766\eta^* + 1.9829 \\ 0.8766\xi^* + 0.5189\eta^* + 0.3768 \\ r(-0.6237\xi^* - 1.9196\eta^* + 2.0370) \end{bmatrix}, \quad \mathbf{h}_4 = r \begin{bmatrix} \xi^* - \eta^* + 2 \\ \xi^* + \eta^* \\ r(-2\eta^* + 2) \end{bmatrix}$$

The four determinants out of each of the  $4 \times 3$  matrices of  $\mathbf{G}$  are displayed below:

$$\det(\mathbf{G}_1) = r^4(0.0295\xi\eta^2 + 0.0089\xi^2\eta + 0.0057\xi\eta + 0.0089\eta^3 + 0.3169\eta^2)$$

$$-0.5264 \eta + 0.0295 \xi^3 + 0.3790 \xi^2 + 0.6498 \xi + 0.3941)$$

$$\det(\mathbf{G}_2) = r^4(0.5552 \xi^2 - 0.0125 \xi \eta + 1.1670 \xi + 0.4928 \eta^2 - 0.7816 \eta + 0.7822 + 0.0307 \xi^3 + 0.0307 \xi \eta^2)$$

$$\det(\mathbf{G}_3) = r^4(0.1714 \xi^2 - 0.0011 \xi \eta + 0.4820 \xi + 0.1680 \eta^2 - 0.3294 \eta + 0.4593 + 0.0011 \xi^3 + 0.0011 \xi \eta^2)$$

$$\det(\mathbf{G}_4) = r^4(0.0007 \xi^2 + 0.0167 \xi + 0.0006 \eta^2 - 0.0093 \eta + 0.1033)$$

those of  $\mathbf{H}$  being

$$\begin{aligned} \det(\mathbf{H}_1) = r^4 &(0.0296 \xi^{*3} + 0.3273 \xi^{*2} + 0.4205 \xi^* + 0.0089 \eta^{*3} + 0.3051 \eta^{*2} \\ &- 0.9217 \eta^* + 0.0089 \xi^{*2} \eta^* + 0.0296 \xi^* \eta^{*2} - 0.0673 \xi^* \eta^* + 0.6543) \end{aligned}$$

$$\begin{aligned} \det(\mathbf{H}_2) = r^4 &(0.4947 \xi^{*2} - 0.0689 \xi^* \eta^* + 0.6640 \xi^* + 0.4920 \eta^{*2} \\ &- 1.2361 \eta^* + 0.7945 + 0.0307 \xi^{*3} + 0.0307 \xi^* \eta^{*2}) \end{aligned}$$

$$\begin{aligned} \det(\mathbf{H}_3) = r^4 &(0.1692 \xi^{*2} - 0.0018 \xi^* \eta^* + 0.3110 \xi^* + 0.1680 \eta^{*2} \\ &- 0.3832 \eta^* + 0.3177 + 0.0011 \xi^{*3} + 0.0011 \xi^* \eta^{*2}) \end{aligned}$$

$$\det(\mathbf{H}_4) = r^4(0.0007 \xi^{*2} + 0.0160 \xi^* + 0.0006 \eta^{*2} - 0.0095 \eta^* + 0.0963)$$

#### 4.2.5 The Presence of a P Joint in Dyad Synthesis

The three cases studied above are considered here. We will do this under the assumption that a PR dyad is sought, i.e., one with a P joint coupling the dyad under synthesis with the fixed link  $BB^*$ . A similar procedure follows if a dyad of the RP type is sought. For starters, division of the two sides of eq.(4.3) by  $\|\mathbf{b}\|$  lead to:

$$[(\underbrace{(\mathbf{1} - \mathbf{Q}_j)\mathbf{a}_0 - \mathbf{r}_j}_{-\mathbf{u}_j}]^T \frac{\mathbf{b}}{\|\mathbf{b}\|} + \left( \mathbf{r}_j^T \mathbf{Q}_j \mathbf{a}_0 + \frac{\mathbf{r}_j^T \mathbf{r}_j}{2} \right) \frac{1}{\|\mathbf{b}\|} = 0, \quad j = 1, \dots, m \quad (4.21)$$

Furthermore, we define a unit vector  $\beta$  as

$$\beta = \frac{\mathbf{b}}{\|\mathbf{b}\|} \quad (4.22)$$

When  $\|\mathbf{b}\| \rightarrow \infty$ , the second term of the right-hand side of eq.(4.21) goes to zero, while the centrepoint  $B$  goes to infinity, which leads to a PR dyad. The unit vector  $\beta$ , in turn, gives the *line of sight* of  $B$  at infinity, the normal direction to  $\beta$  indicating the direction of the translations allowed by the P joint sought.

Moreover, upon substitution of eq.(4.22) into eq.(4.21), we obtain

$$\mathbf{u}_j^T \beta = 0, \quad j = 1, \dots, m \quad (4.23)$$

where  $\mathbf{u}_j \equiv \mathbf{a}_j - \mathbf{a}_0$  is the displacement of the circlepoint  $A_0$  at the  $j$ th pose, i.e.,

$$\mathbf{u}_j = \mathbf{r}_j - (\mathbf{1} - \mathbf{Q}_j)\mathbf{a}_0, \quad j = 1, \dots, m \quad (4.24)$$

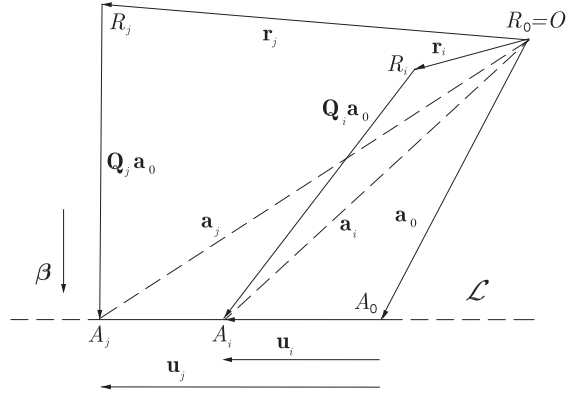


Figure 4.5: Relation between the  $i$ th and  $j$ th poses and the circlepoints

With reference to Fig. 4.5,  $\mathbf{u}_i$  ( $i = 1, \dots, m$ ) is the  $i$ th displacement vector of the circlepoint. For a PR dyad, all  $m$  vectors  $\mathbf{u}_i$  must be parallel. In other words, the cross product of any two displacement vectors must vanish. However, rather than working with cross products, we simplify the analysis by resorting to the two-dimensional representation of the cross product introduced in Subsection 1.4.1. This is based on matrix  $\mathbf{E}$  rotating vectors in the plane through  $90^\circ$  ccw. Hence, the parallelism condition between  $\mathbf{u}_i$  and  $\mathbf{u}_j$  can be expressed as

$$\Delta_{ij} = \mathbf{u}_j^T \mathbf{E} \mathbf{u}_i = 0, \quad i, j = 1, \dots, m, \quad i \neq j \quad (4.25)$$

which expands to

$$\begin{aligned} \Delta_{ij} &= \mathbf{a}_0^T (-\mathbf{E} \mathbf{Q}_i - \mathbf{Q}_j^T \mathbf{E} + \mathbf{Q}_j^T \mathbf{E} \mathbf{Q}_i) \mathbf{a}_0 \\ &\quad - (\mathbf{E} \mathbf{r}_i - \mathbf{Q}_j^T \mathbf{E} \mathbf{r}_i - \mathbf{E} \mathbf{r}_j + \mathbf{Q}_i^T \mathbf{E} \mathbf{r}_j)^T \mathbf{a}_0 + \mathbf{r}_j^T \mathbf{E} \mathbf{r}_i = 0 \end{aligned} \quad (4.26)$$

We develop below all quadratic terms of eq.(4.26), those in the first line of this equation, by writing  $\mathbf{Q}_i$  in the form  $\mathbf{Q}_i = c_i \mathbf{1} + s_i \mathbf{E}$ , in which  $c_i \equiv \cos\phi_i$  and  $s_i \equiv \sin\phi_i$ . Hence,

$$-\mathbf{a}_0^T \mathbf{E} \mathbf{Q}_i \mathbf{a}_0 = -\mathbf{a}_0^T \mathbf{E} (c_i \mathbf{1} + s_i \mathbf{E}) \mathbf{a}_0 = -c_i \mathbf{a}_0^T \mathbf{E} \mathbf{a}_0 - s_i \mathbf{a}_0^T \mathbf{E}^2 \mathbf{a}_0 = s_i \|\mathbf{a}_0\|^2 \quad (4.27a)$$

$$-\mathbf{a}_0^T \mathbf{Q}_j^T \mathbf{E} \mathbf{a}_0 = -\mathbf{a}_0^T \mathbf{E}^T \mathbf{Q}_j \mathbf{a}_0 = \mathbf{a}_0^T \mathbf{E} \mathbf{Q}_j \mathbf{a}_0 = -s_j \|\mathbf{a}_0\|^2 \quad (4.27b)$$

$$\begin{aligned} \mathbf{a}_0^T \mathbf{Q}_j^T \mathbf{E} \mathbf{Q}_i \mathbf{a}_0 &= \mathbf{a}_0^T (c_j \mathbf{1} - s_j \mathbf{E}) (c_i \mathbf{E} + s_i \mathbf{1}) \mathbf{a}_0 = \mathbf{a}_0^T [-(c_j s_i - s_j c_i) \mathbf{1} + (s_j s_i + c_j c_i) \mathbf{E}] \mathbf{a}_0 \\ &= (-c_j s_i + s_j c_i) \|\mathbf{a}_0\|^2 = -\sin(\phi_i - \phi_j) \|\mathbf{a}_0\|^2 \end{aligned} \quad (4.27c)$$

Notice that the foregoing relations could have been obtained by pure geometric reasoning, as  $\mathbf{E} \mathbf{Q}_i$  is a rotation through an angle  $\phi_i + \pi/2$ , given that angles of rotation are additive in planar motion. By the same token,  $\mathbf{Q}_j^T \mathbf{E}$  is a rotation through an angle  $\pi/2 - \phi_j$ , while  $\mathbf{Q}_j^T \mathbf{E} \mathbf{Q}_i$  is one through an angle  $\phi_i + \pi/2 - \phi_j$ . Moreover, terms of the form  $\mathbf{a}_0^T \mathbf{E} \mathbf{a}_0$  vanish because  $\mathbf{E}$  is skew-symmetric.

Further, let

$$\mathbf{v}_{ij} \equiv -\mathbf{E} \mathbf{r}_i + \mathbf{Q}_j^T \mathbf{E} \mathbf{r}_i + \mathbf{E} \mathbf{r}_j - \mathbf{Q}_i^T \mathbf{E} \mathbf{r}_j \quad (4.28)$$

as appearing in the second line of eqs.(4.26), which are now rewritten as

$$\Delta_{ij} = (s_i - s_j - s_{i\bar{j}}) \|\mathbf{a}_0\|^2 + \mathbf{v}_{ij}^T \mathbf{a}_0 + \mathbf{r}_j^T \mathbf{E} \mathbf{r}_i = 0, \quad i, j = 1, \dots, m, \quad i \neq j \quad (4.29)$$

and represent the loci of  $A_0$ , of position vector  $\mathbf{a}_0$ , namely, a family of circles  $\{\mathcal{C}_{ij}\}_{i,j=1;i \neq j}^m$ , where  $s_{i\bar{j}} \equiv \sin(\phi_i - \phi_j)$ . A line  $\mathcal{L}$  passing through  $A_0$  and parallel to the direction of sliding of the P joint is shown normal to vector  $\beta$  in Fig. 4.5. Given that P joints have a direction, *but no position*, the slider implementing this joint can be placed anywhere on the fixed frame, as long as its sliding direction is parallel to  $\mathcal{L}$ . It is common practice to represent the P joint of a PR dyad as a line passing through the centre of the R joint, but this by no means limits the actual implementation of the joint in question.

### Remarks:

1. The foregoing relations have been derived from the condition of the vanishing of the product  $\mathbf{u}_j^T \mathbf{E} \mathbf{u}_i$  in eq.(4.25). This product can be shown to be identical to the determinant of a  $2 \times 2$  matrix  $\mathbf{D}$ , namely,

$$\mathbf{D} = [\mathbf{u}_j \quad \mathbf{u}_i] \quad (4.30)$$

Obviously, the vanishing of  $\det(\mathbf{D})$  is equivalent to the linear dependence, and hence, the parallelism of vectors  $\mathbf{u}_i$  and  $\mathbf{u}_j$ . Fact 1.4.1 should shed light on this relation.

2. The locus of the centrepoints of a PR dyad, for every pair of parallel unit vectors  $(\mathbf{u}_i, \mathbf{u}_j)$ , is a circle  $\mathcal{C}_{ij}$ , which is sometimes referred to as the “circle of sliders.”

Indeed, this circle was derived from geometric arguments by Hall (1961), although without giving a specific name to the circle. In the same reference, Hall points out that, in the limit, as the three poses defining that circle become infinitesimally separated, the circle becomes the *inflection circle* of curvature theory.

### Three-pose Synthesis

In this case  $m = 2$ , and hence, eqs.(4.29) reduce to a single one:

$$(s_1 - s_2 - s_{1\bar{2}})\|\mathbf{a}_0\|^2 + \mathbf{v}_{12}^T \mathbf{a}_0 + \mathbf{r}_2^T \mathbf{E} \mathbf{r}_1 = 0$$

which can be cast in the form

$$\|\mathbf{a}_0\|^2 + \frac{\mathbf{v}_{12}^T}{s_1 - s_2 - s_{1\bar{2}}} \mathbf{a}_0 + \frac{\mathbf{r}_2^T \mathbf{E} \mathbf{r}_1}{s_1 - s_2 - s_{1\bar{2}}} = 0 \quad (4.31)$$

The radius and the position vector  $\mathbf{c}$  of the center of the circle are readily found when comparing this equation with that of the circle with the foregoing characteristics, and applied to one point  $A_0$  of the circle, of position vector  $\mathbf{a}_0$ :

$$\|\mathbf{a}_0\|^2 - 2\mathbf{c}^T \mathbf{a}_0 + \|\mathbf{c}\|^2 - r^2 = 0 \quad (4.32)$$

In summary, for three positions, the problem admits infinitely many solutions, all with a circlepoint  $A_0$  lying in a circle of center  $C$ , of position vector  $\mathbf{c}$ , and radius  $r$ , as given above.

### Four-pose Synthesis

It is noteworthy that a PR dyad always exists in this case, as we have one single centerpoint curve, the corresponding P joint being equivalent to a R joint with its center at infinity. The direction of the unit vector  $\beta$  identical to the direction of the line of sight of point  $B$  lying at infinity and normal to the sliding of the P joint is given by the asymptote of the centerpoint curve. Hence, one single P joint is to be expected here.

Moreover, we have three displacements  $\{\mathbf{u}_i\}_1^3$ , and hence, three *independent* parallelism conditions, namely,  $\mathbf{u}_1 \parallel \mathbf{u}_2$ ,  $\mathbf{u}_2 \parallel \mathbf{u}_3$  and  $\mathbf{u}_3 \parallel \mathbf{u}_1$ , as given by eq.(4.29). In principle, two of these conditions imply the third. However, if  $\mathbf{u}_2$  happens to vanish, then, while the first two conditions still hold, the third does not necessarily do so. To guarantee the parallelism condition in any event, we use the three equations available in this case.

Now, the three equations at hand represent, each, a circle in the  $X_0$ - $Y_0$  plane. It is apparent that we can always find a suitable linear combination of two distinct pairs of the three equations (4.29), with  $m = 3$ , that will yield, correspondingly, two lines, upon subtraction of one from the other two, which will lead to the elimination of the quadratic terms  $\|\mathbf{a}_0\|^2$  in the latter. Hence, the parallelism condition leads to one circle  $\mathcal{C}$  and two

lines  $\mathcal{L}_1$  and  $\mathcal{L}_2$ . The geometric interpretation of the problem of finding the point  $A_0$  is then straightforward: the circlepoint sought (a) is the intersection of the two lines and (b) lies on the circle.

### Remarks:

1. If the coefficient of  $\|\mathbf{a}_0\|^2$  in one of eqs.(4.29) vanishes, then the resulting equation is already a line. A second line is then obtained by a suitable linear combination of the remaining two circle equations, which will then lead to the general case.
2. If the same coefficient vanishes in two of eqs.(4.29), then we need not look for any linear combination to obtain the two lines of the general case.
3. If the same coefficient vanishes in the three eqs.(4.29), then we have three lines that must be concurrent at one common point, the circlepoint  $A_0$  sought.
4. The above statement on the existence of one single circlepoint  $A_0$  is best explained by noticing that, from the plot of the centerpoint curve, its asymptote can be estimated by inspection—a precise value can be obtained from the equation of the asymptote, of course. If this estimate is plugged into eq.(4.8), and the second term of the equation is deleted because, as  $\|\mathbf{b}\| \rightarrow \infty$ , this term tends to zero, we obtain three linear equations in  $\mathbf{a}_0$ . In the absence of roundoff error, only two are independent<sup>5</sup>, and hence, determine uniquely  $\mathbf{a}_0$ .

Once  $\mathbf{a}_0$  is obtained, solving for  $\beta$  is straightforward<sup>6</sup>:

$$\beta = \frac{\mathbf{E}\hat{\mathbf{u}}}{\|\mathbf{E}\hat{\mathbf{u}}\|}, \quad \hat{\mathbf{u}} = \frac{1}{m} \sum_{j=1}^m \mathbf{u}_j \quad (4.33)$$

### Five-pose Synthesis

In this case we have four displacements  $\{\mathbf{u}_i\}_1^4$ , and hence, six possible pairs<sup>7</sup>  $(\mathbf{u}_i, \mathbf{u}_j)$ , for  $j \neq i$ . It is noteworthy that the parallelism relation is *transitive*, i.e., if  $\mathbf{u}_1 \parallel \mathbf{u}_2$  and  $\mathbf{u}_2 \parallel \mathbf{u}_3$ , then  $\mathbf{u}_1 \parallel \mathbf{u}_3$ . Hence, the number of independent relations reduces to three. However, and within the spirit of robustness, we recommend the use of the full six parallelism conditions available.

We can always find a suitable linear combination of the first equation with each of the remaining five equations (4.29) that will yield, correspondingly, five lines, upon elimination of the quadratic terms  $\|\mathbf{a}_0\|^2$ , in the four-pose case. Hence, the parallelism conditions lead

<sup>5</sup>To account for roundoff error, we recommend to regard the three equations as independent, and compute the unique value of  $\mathbf{a}_0$  as their least-square approximation.

<sup>6</sup>One single vector  $\mathbf{u}_j$  would suffice. We take the mean value here in order to filter out roundoff error.

<sup>7</sup>The combinatoric number of four objects taking two at a time.

to one circle  $\mathcal{C}$  and five lines  $\mathcal{L}_1, \dots, \mathcal{L}_5$ . A geometric interpretation of the solution then follows: the circlepoint  $A_0$  sought (a) is the common intersection of the five lines and (b) lies on the circle.

A similar discussion for the cases in which the coefficient of  $\|\mathbf{a}_0\|^2$  in eq.(4.29) vanishes in all four equations is straightforward, and follows the same line of reasoning as Remark 3 of the four-pose case.

If there is one common point to the five lines and the circle, this point is then the solution  $A_0$  sought. Otherwise, there is no solution. After  $\mathbf{a}_0$  is obtained,  $\beta$  can be found from Eq. (4.33).

The whole section was devoted to the synthesis of a PR joint. To handle the case of a RP joint the procedure is the same: divide both sides of eq.(4.3) by  $\|\mathbf{a}_0\|$  and then let  $\|\mathbf{a}_0\| \rightarrow \infty$ . The procedure that ensues parallels that described above. The reader is invited to develop it on her/his own, but details are given by Chen et al. (2008).

Finally, notice that, in this case, a P joint is not to be taken for granted. Indeed, for a centerpoint to lie at infinity, and hence, for a PR dyad to be possible, the asymptotes of all centerpoint curves  $\mathcal{K}_j$  must be parallel. Likewise, for a RP dyad to be possible, the asymptotes of all circlepoint curves  $\mathcal{M}_j$  must be parallel. The condition for a PP dyad to occur in this case follows immediately.

#### 4.2.6 Approximate Synthesis

When the number of prescribed poses is greater than five, i.e., when  $m > 4$  in eq.(4.3), the problem admits no solution. However, it is always possible to find a linkage that *best* meets the given poses with *a minimum error in the least-square sense*. To this end, we regard the left-hand side of eqs.(4.3) as functions  $e_j$  of  $\mathbf{a}_0$  and  $\mathbf{b}$  that represent the error incurred in the approximation of the  $j$ th pose. We thus define this error as

$$e_j \equiv \mathbf{b}^T(\mathbf{1} - \mathbf{Q}_j)\mathbf{a}_0 + \mathbf{r}_j^T\mathbf{Q}_j\mathbf{a}_0 - \mathbf{r}_j^T\mathbf{b} + \frac{\mathbf{r}_j^T\mathbf{r}_j}{2} \quad j = 1, \dots, m \geq 5 \quad (4.34)$$

**Caveat:** A *pose error*, in fact, is impossible to define (Angeles, 2006), the reason being that the concept includes items with different dimensions, length for the position and dimensionless for the orientation. Nevertheless, the pose error defined in eq.(4.34) is dimensionally homogeneous, as it is measured in units of surface, i.e., in  $\text{m}^2$ .

The problem is now handled as one of *optimum design*. In this vein, an *objective function*  $z(\mathbf{x})$  is defined, that is positive-definite—i.e., positive, unless the error vanishes, in which case the function vanishes as well—with  $\mathbf{x}$  denoting the vector of *design variables*, namely, the position vectors of the circlepoint and the centerpoint,  $\mathbf{a}_0$  and  $\mathbf{b}$ , respectively. To guarantee positive-definiteness, moreover,  $z(\mathbf{x})$  is defined as a norm of the error vector  $\mathbf{e}$ , introduced below. Moreover, to ease the ensuing calculations, the Euclidian norm is

adopted, as the gradient of its square with respect to the design-variable vector is a vector linear function of the error, as we know from the experience gained in Ch. 1.

The optimum-design problem at hand is thus formulated as

$$z \equiv \frac{1}{2} \|\mathbf{e}\|^2 = \frac{1}{2} \sum_1^m e_j^2(\mathbf{x}) \rightarrow \min_{\mathbf{x}} \quad \text{with} \quad \mathbf{e} \equiv \begin{bmatrix} e_1 \\ \vdots \\ e_m \end{bmatrix} \quad \& \quad \mathbf{x} \equiv \begin{bmatrix} \mathbf{a}_0 \\ \mathbf{b} \end{bmatrix} \quad (4.35)$$

Since the optimization problem requires no constraints, its *first-order normality conditions* (FONC) (Hillier and Liebermann, 1995) reduce to the vanishing of the gradient of  $z$  with respect to  $\mathbf{x}$ :

$$\nabla z \equiv \begin{bmatrix} \sum_1^m e_j \frac{\partial e_j}{\partial \mathbf{a}_0} \\ \sum_1^m e_j \frac{\partial e_j}{\partial \mathbf{b}} \end{bmatrix} = \mathbf{0}_4 \quad (4.36)$$

with

$$\frac{\partial e_j}{\partial \mathbf{a}_0} = (\mathbf{1} - \mathbf{Q}_j^T) \mathbf{b} + \mathbf{Q}_j^T \mathbf{r}_j \quad \& \quad \frac{\partial e_j}{\partial \mathbf{b}} = (\mathbf{1} - \mathbf{Q}_j) \mathbf{a}_0 - \mathbf{r}_j \quad (4.37)$$

Upon substitution of the two foregoing expressions into the FONC of eq.(4.36), while recalling the expression for  $e_j$  displayed in eq.(4.34), the FONC decompose into two two-dimensional subsystems, namely,

$$\frac{\partial z}{\partial \mathbf{a}_0} \equiv \sum_1^m [\mathbf{b}^T (\mathbf{1} - \mathbf{Q}_j) \mathbf{a}_0 + \mathbf{r}_j^T \mathbf{Q}_j \mathbf{a}_0 - \mathbf{r}_j^T \mathbf{b} + \frac{\mathbf{r}_j^T \mathbf{r}_j}{2}] [(\mathbf{1} - \mathbf{Q}_j^T) \mathbf{b} + \mathbf{Q}_j^T \mathbf{r}_j] = \mathbf{0}_2 \quad (4.38)$$

and

$$\frac{\partial z}{\partial \mathbf{b}} \equiv \sum_1^m [\mathbf{b}^T (\mathbf{1} - \mathbf{Q}_j) \mathbf{a}_0 + \mathbf{r}_j^T \mathbf{Q}_j \mathbf{a}_0 - \mathbf{r}_j^T \mathbf{b} + \frac{\mathbf{r}_j^T \mathbf{r}_j}{2}] [(\mathbf{1} - \mathbf{Q}_j) \mathbf{a}_0 - \mathbf{r}_j] = \mathbf{0}_2 \quad (4.39)$$

In light of the two foregoing expressions, we now have two useful results:

**Lemma 4.2.1** *The partial derivative of  $z$  with respect to  $\mathbf{a}_0$  is linear in  $\mathbf{a}_0$  and quadratic in  $\mathbf{b}$ , this derivative thus being cubic in  $\mathbf{x}$ .*

**Lemma 4.2.2** *The partial derivative of  $z$  with respect to  $\mathbf{b}$  is quadratic in  $\mathbf{a}_0$  and linear in  $\mathbf{b}$ , this derivative thus being cubic in  $\mathbf{x}$  as well.*

As a result of the two above lemmas, the normality conditions (4.36) are both cubic in  $\mathbf{x}$ , and hence, lead to a total of four cubic scalar equations in  $\mathbf{x}$ , the Bezout number of the foregoing algebraic system then being  $N_B = 3^4 = 81$ . This means that up to 81 solutions are to be expected, some real, some complex. Of course, we are interested only in the real solutions.

Furthermore, note that the first two-dimensional subsystem of eq.(4.36) is linear in  $\mathbf{a}_0$ , the second linear in  $\mathbf{b}$ , although both are quadratic in the other vector block of  $\mathbf{x}$ . This feature eases the reduction of the polynomial system to two scalar equations in only two unknowns, either the coordinates of  $A_0$  or those of  $B$ . For concreteness, the second two-dimensional subsystem of the system in question is used to solve for  $\mathbf{b}$  in terms of  $\mathbf{a}_0$ , the resulting expression then substituted into the first two-dimensional subsystem of the same system, thereby obtaining a new two-dimensional vector equation in  $\mathbf{a}_0$ . First, each term of the second summation of eq.(4.36), i.e., the intermediate side of eq.(4.39), is expanded:

$$e_j \frac{\partial e_j}{\partial \mathbf{b}} = [\underbrace{\mathbf{b}^T(\mathbf{1} - \mathbf{Q}_j)\mathbf{a}_0 + \mathbf{r}_j^T \mathbf{Q}_j^T \mathbf{a}_0 - \mathbf{r}_j^T \mathbf{b} + \frac{\mathbf{r}_j^T \mathbf{r}_j}{2}}_{\mathbf{a}_0^T(\mathbf{1} - \mathbf{Q}_j^T)\mathbf{b}}][(1 - \mathbf{Q}_j)\mathbf{a}_0 - \mathbf{r}_j]$$

Then, after rearranging, to assemble all terms including  $\mathbf{b}$  in one single term,

$$e_j \frac{\partial e_j}{\partial \mathbf{b}} = [(1 - \mathbf{Q}_j)\mathbf{a}_0 - \mathbf{r}_j] \underbrace{[\mathbf{a}_0^T(\mathbf{1} - \mathbf{Q}_j^T) - \mathbf{r}_j^T]}_{[(1 - \mathbf{Q}_j)\mathbf{a}_0 - \mathbf{r}_j]^T} \mathbf{b} + \mathbf{r}_j^T (\mathbf{Q}_j^T \mathbf{a}_0 + \frac{\mathbf{r}_j}{2}) [(1 - \mathbf{Q}_j)\mathbf{a}_0 - \mathbf{r}_j]$$

That is,

$$e_j \frac{\partial e_j}{\partial \mathbf{b}} = [(1 - \mathbf{Q}_j)\mathbf{a}_0 - \mathbf{r}_j] [(1 - \mathbf{Q}_j)\mathbf{a}_0 - \mathbf{r}_j]^T \mathbf{b} + \underbrace{\mathbf{r}_j^T (\mathbf{Q}_j^T \mathbf{a}_0 + \frac{\mathbf{r}_j}{2})}_{(\mathbf{Q}_j^T \mathbf{a}_0 + \mathbf{r}_j/2)^T \mathbf{r}_j} [(1 - \mathbf{Q}_j)\mathbf{a}_0 - \mathbf{r}_j]$$

which, when substituted into eq.(4.39), leads to a linear equation in  $\mathbf{b}$ , in terms of  $\mathbf{a}_0$  and the data:

$$\mathbf{B}\mathbf{b} + \mathbf{r} = \mathbf{0}_2 \quad (4.40)$$

with  $\mathbf{B}$  and  $\mathbf{r}$  defined as<sup>8</sup>

$$\mathbf{B} \equiv \sum_1^m [(1 - \mathbf{Q}_j)\mathbf{a}_0 - \mathbf{r}_j] [(1 - \mathbf{Q}_j)\mathbf{a}_0 - \mathbf{r}_j]^T, \quad \mathbf{r} \equiv \sum_1^m [(\mathbf{Q}_j^T \mathbf{a}_0 + \frac{\mathbf{r}_j}{2})^T \mathbf{r}_j] [(1 - \mathbf{Q}_j)\mathbf{a}_0 - \mathbf{r}_j]$$

and hence,

$$\mathbf{b} = -\mathbf{B}^{-1}\mathbf{r} \quad \text{with} \quad \mathbf{B}^{-1} \equiv \frac{\text{Adj}(\mathbf{B})}{\det(\mathbf{B})} \quad (4.41)$$

Apparently,  $\mathbf{B}$  is a sum of  $m > 4$  rank-one<sup>9</sup>  $2 \times 2$  matrices, all, in general, linearly independent. As it takes only two such matrices to make up a  $2 \times 2$  nonsingular matrix, and the sum has at least five terms, matrix  $\mathbf{B}$  is, except for pathological cases, invertible. Furthermore, upon invoking Facts 1.4.1 and 1.4.2, it becomes apparent that  $\mathbf{B}^{-1}$  is a rational expression, whose matrix numerator,  $\text{Adj}(\mathbf{B})$ , is *quadratic* in  $\mathbf{a}_0$ , its denominator,  $\det(\mathbf{B})$  *quartic* in the same. Therefore, the product  $\det(\mathbf{B})e_j \partial e_j / \partial \mathbf{b}$  is *nonic* in  $\mathbf{a}_0$ , and hence, we have

---

<sup>8</sup> $\mathbf{B}$  in eq.(4.40) not to be confused with  $\mathbf{B}$  in eq.(4.4).

<sup>9</sup>See footnote 1 in Ch. 2 for a definition of *rank-one matrix*.

**Lemma 4.2.3** *The vanishing of the partial derivative of  $z$  with respect to  $\mathbf{a}_0$  leads to two nonic equations in  $\mathbf{a}_0$ , free of  $\mathbf{b}$ .*

Since we have two scalar nonic equations to solve for the circlepoint  $A_0$ , the Bezout number of the system in question is  $N_B = 9^2 = 81$ , i.e., the problem admits up to 81 solutions, some real, some complex.

By symmetry, we can conclude further one complementary result:

**Lemma 4.2.4** *The vanishing of the partial derivative of  $z$  with respect to  $\mathbf{b}$  leads to two nonic equations in  $\mathbf{b}$ , free of  $\mathbf{a}_0$ .*

Therefore, the system of two nonic equations arising from the vanishing of the partial derivative of  $z$  with respect to  $\mathbf{b}$  also has a Bezout number of 81. However, once one particular circlepoint  $A_0$  has been found, of position vector  $\mathbf{a}_0$ , the corresponding centerpoint  $B$ , of position vector  $\mathbf{b}$  can be computed in closed form, namely, via eq.(4.41).

Each of the two scalar equations in  $\mathbf{a}_0 = [x, y]^T$  defines a contour  $\mathcal{K}_j$ , for  $j = 1, 2$ , in the  $X_0$ - $Y_0$  plane. This means that the real values of  $\mathbf{a}_0$  can be found by *inspection*, at the intersection of the two contours. Notice that these two contours can be fairly regarded as circlepoint curves, as each represents a *locus* of circlepoint candidates. The intersections of the two loci then determine which of the infinitely many candidates is a valid circlepoint. The same holds for the centerpoints. All valid circlepoints and centerpoints, however, are *stationary points* (SPs) of the optimization problem at hand. Each can be a *local maximum*, a *local minimum* or a *saddle point*. The nature of each SP is elucidated by means of the Hessian matrix  $\mathbf{H}$  of  $z$  with respect to  $\mathbf{x}$ , namely,

$$\mathbf{H} = \begin{bmatrix} \frac{\partial^2 z}{\partial \mathbf{a}_0^2} & \frac{\partial^2 z}{\partial \mathbf{a}_0 \partial \mathbf{b}} \\ \frac{\partial^2 z}{\partial \mathbf{b} \partial \mathbf{a}_0} & \frac{\partial^2 z}{\partial \mathbf{b}^2} \end{bmatrix} \quad (4.42)$$

Now, since  $z(\mathbf{a}_0, \mathbf{b})$  is a biquadratic equation in  $\mathbf{a}_0$  and  $\mathbf{b}$ , i.e., *quartic*—and hence, *algebraic*—in  $\mathbf{x}$ , it satisfies the conditions of Schwarz's Theorem (Brand, 1955); therefore,  $\mathbf{H}$  is symmetric, i.e.,

$$\frac{\partial^2 z}{\partial \mathbf{a}_0^2} = \left( \frac{\partial^2 z}{\partial \mathbf{a}_0^2} \right)^T, \quad \frac{\partial^2 z}{\partial \mathbf{b}^2} = \left( \frac{\partial^2 z}{\partial \mathbf{b}^2} \right)^T, \quad \frac{\partial^2 z}{\partial \mathbf{b} \partial \mathbf{a}_0} = \left( \frac{\partial^2 z}{\partial \mathbf{a}_0 \partial \mathbf{b}} \right)^T \quad (4.43)$$

Hence, the four eigenvalues of  $\mathbf{H}$  are all real, the corresponding eigenvectors mutually orthogonal. Now the identification of the nature of each SP is summarized below:

1. A SP is a local maximum if  $\mathbf{H}$  is negative-definite, i.e., if all its eigenvalues are negative at this point;
2. A SP is a local minimum if  $\mathbf{H}$  is positive-definite, i.e., if all its eigenvalues are positive at this point; and

3. A SP is a saddle point if  $\mathbf{H}$  is sign-indefinite at this point.

Our interest being the minimization of the Euclidian norm of the error, we look only at the local minima. Of these, the smallest one is the *global minimum*.

### Example of Synthesis with 11 Poses

In this case we aim at a planar four-bar linkage that can best meet all the 11 poses displayed in Table 4.1. To this end,  $\mathbf{b}$  is expressed as a rational vector function of  $\mathbf{a}_0$ , as per eqs.(4.41). The expression thus resulting is then substituted into eq.(4.38), which leads to two nonic equations in  $\mathbf{a}_0$ ,  $F_i(x, y) = 0$ ,  $i = 1, 2$ , free of  $u$  and  $v$ , the components of  $\mathbf{b}$ . Notice that  $F_1(x, y) = 0$  represents the normality condition  $\partial z/\partial x = 0$  as one equation in  $x$  and  $y$ ,  $F_2(x, y) = 0$  representing  $\partial z/\partial y = 0$ —or their corresponding nondimensional versions with  $\xi$  replacing  $x$  and  $\eta$  replacing  $y$ —likewise.

The two foregoing *implicit functions* of  $x$  and  $y$ — $\xi$  and  $\eta$ , correspondingly, when normalized—which can be regarded as circlepoint curves  $\mathcal{K}$  for the case at hand, are plotted in Fig. 4.6. In this figure,  $\partial z/\partial \xi$  appears as a continuous curve,  $\partial z/\partial \eta$  as a dashed curve.

While the system of two nonic equations is expected to admit up to  $9^2$  solutions, only two real solutions were found within a *reasonable* distance of the origin, i.e., within a region commensurate with the dimensions of the landing gear operation of deployment and retraction. Alas, these two solutions are a) too close to each other, which would make a rather too short coupler link, and b) close to the fuselage boundary.

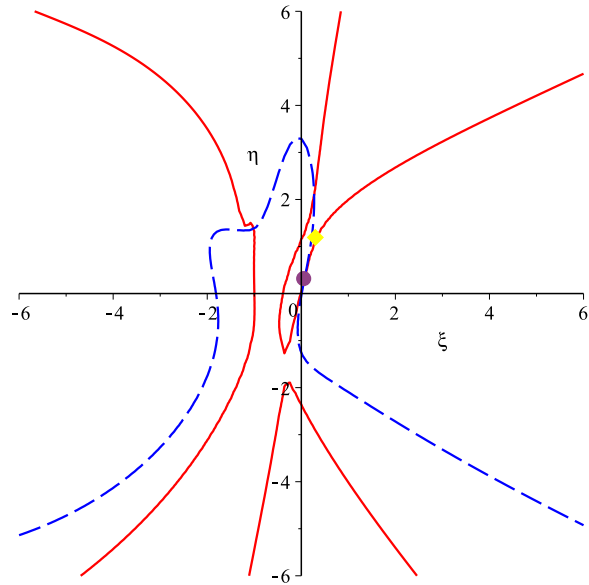


Figure 4.6: Circlepoint curves  $\mathcal{K}$  for  $m = 10$

### 4.3 Spherical Four-bar Linkages

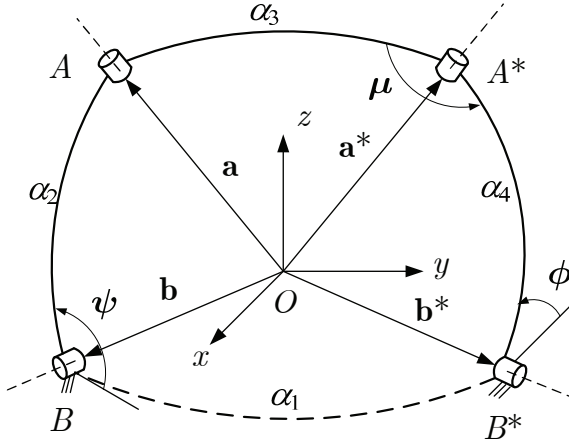


Figure 4.7: The spherical 4R linkage

The spherical four-bar linkage under synthesis is depicted in Fig. 4.7, with its four linkage dimensions  $\{\alpha_j\}_1^4$ . Just as in the planar case of Section 4.2, the linkage is composed of four links coupled by four R joints, this time around with their axes intersecting at one common point,  $O$ , as depicted in Fig. 4.7. The two fixed axes,  $OB$  and  $OB^*$ , intersect the unit sphere at points  $B$  and  $B^*$ , the two moving axes,  $OA$  and  $OA^*$ , at points  $A$  and  $A^*$ . For brevity, the axes will be referred to only by their intersection points with the sphere. More accurately, one should refer here not to centerpoints and circlepoints, but, rather, to *cone axis* and *cone element*, as axis  $A_0$  sweeps a circular conical surface of apex  $O$ , one of its elements being  $A_0$ .

The reference locations of the moving axes are denoted by  $A_0$  and  $A_0^*$ , the linkage then being fully defined by the two dyads  $BA_0$  and  $B^*A_0^*$ . By analogy with the planar case, points  $B$  and  $B^*$  are called the *centerpoints*, while  $A_0$  and  $A_0^*$  the *circlepoints*.

As the coupler link moves, while visiting the  $m$  prescribed *attitudes*, the circlepoint attains positions  $A_1, \dots, A_m$ , the moving revolute axis thus attaining locations  $\overline{OA}_j$ , for  $j = 1, \dots, m$ , as shown in Fig. 4.8.

The two dyads of this linkage are thus arc  $A_0B$ , defined by axes  $\overline{OA}_0$  and  $\overline{OB}$ , arc  $A_0^*B$ , defined by axes  $\overline{OA}_0^*$  and  $\overline{OB}^*$ , respectively; the position vectors of  $A_0$  and  $B$  are  $\mathbf{a}_0$  and  $\mathbf{b}$ , respectively, both of unit magnitude, i.e.,

$$\|\mathbf{a}_0\| = 1, \quad \|\mathbf{b}\| = 1 \quad (4.44)$$

which will be termed henceforth the *normality conditions*.

Likewise, the position vectors of points  $A_0^*$  and  $B^*$  are denoted by the unit vectors  $\mathbf{a}_0^*$  and  $\mathbf{b}^*$ , respectively.

With the foregoing definitions, the *spherical Burmester problem*, the counterpart of the problem studied in Section 4.2, is stated as:

Find a spherical four-bar linkage that will conduct its coupler link through a set of  $m$  attitudes given by a corresponding set of orthogonal matrices,  $\mathcal{Q} = \{\mathbf{Q}_j\}_1^m$ , defined with respect to a reference attitude given by  $\mathbf{Q}_0 = \mathbf{1}$ ,  $\mathbf{1}$  now denoting the  $3 \times 3$  identity matrix.

By virtue of the link rigidity, the angle between  $\overline{OA}_j$  and  $\overline{OB}$  remains equal to  $\alpha_2$ , and hence, constant. The *synthesis equation* is thus obtained upon imposing this geometric constraint:

$$\mathbf{a}_j^T \mathbf{b} = \mathbf{a}_0^T \mathbf{b} \quad \text{or} \quad (\mathbf{a}_j - \mathbf{a}_0)^T \mathbf{b} = 0, \quad j = 1, \dots, m \quad (4.45)$$

where, apparently,

$$\mathbf{a}_j = \mathbf{Q}_j \mathbf{a}_0 \quad (4.46)$$

Therefore, conditions (4.45) become

$$\mathbf{a}_0^T (\mathbf{Q}_j^T - \mathbf{1}) \mathbf{b} = 0, \quad j = 1, \dots, m \quad (4.47)$$

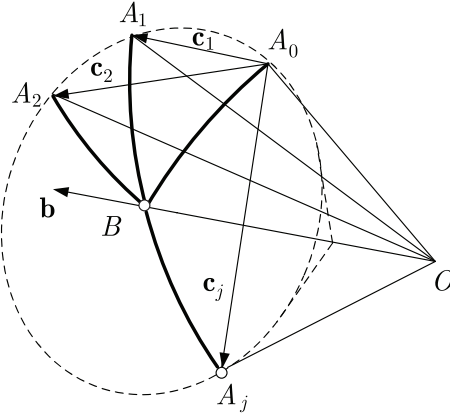


Figure 4.8: A spherical dyad and the cone formed by the moving axis  $OA$

In order to ease the ensuing discussion, let

$$\mathbf{c}_j \equiv (\mathbf{Q}_j - \mathbf{1}) \mathbf{a}_0 \quad (4.48)$$

eq.(4.47) then taking the form

$$\mathbf{c}_j^T \mathbf{b} = 0, \quad j = 1, \dots, m \quad (4.49)$$

Geometrically, Eq. (4.49) states that vector  $\mathbf{b}$  is perpendicular to any vector  $\mathbf{c}_j$ . Referring to Fig. 4.8, this means that segment  $\overline{OB}$  is perpendicular to segments  $\overline{A_0 A_j}$ , for  $j = 1, \dots, m$ . That is, as link  $AB$  attains the set of attitudes  $\mathcal{A} = \{A_j B\}_0^m$ , all points  $\{A_j\}_0^m$  lie in a circle whose plane is normal to vector  $\mathbf{b}$ .

Note that the rotation matrices  $\mathbf{Q}_j$  admit various parameterizations, the one adopted here is in terms of the *natural invariants* of the rotation, namely the unit vector  $\mathbf{e}_j$  parallel

to the axis of the rotation represented by  $\mathbf{Q}_j$ , and the corresponding angle of rotation,  $\phi_j$ , as described in Section 2.2. The rotation matrix  $\mathbf{Q}_j$  thus takes the form of eq.(2.1b), reproduced below for quick reference.

$$\mathbf{Q}_j = \mathbf{1} + s_j \mathbf{E}_j + (1 - c_j) \mathbf{E}_j^2, \quad c_j \equiv \cos \phi_j, \quad s_j \equiv \sin \phi_j \quad (4.50)$$

with  $\mathbf{E}_j \equiv \text{CPM}(\mathbf{e}_j)$  and the operator  $\text{CPM}(\cdot)$  defined in turn as the cross-product matrix of the three-dimensional vector  $(\cdot)$  in eq.(2.1d). Hence,

$$\mathbf{Q}_j - \mathbf{1} = [s_j \mathbf{1} + (1 - c_j) \mathbf{E}_j] \mathbf{E}_j \quad (4.51)$$

Therefore, eq.(4.47) becomes

$$\mathbf{a}_0^T \mathbf{E}_j [s_j \mathbf{1} - (1 - c_j) \mathbf{E}_j] \mathbf{b} = 0, \quad j = 1, \dots, m \quad (4.52)$$

which is the *synthesis equation* of the problem at hand. Its solution for various values of  $m$  is discussed below.

### 4.3.1 Dyad Synthesis for Three Attitudes

In this case,  $m = 2$ , two constraint equations thus occurring in eq.(4.49), namely,

$$\mathbf{c}_1^T \mathbf{b} = 0, \quad \text{and} \quad \mathbf{c}_2^T \mathbf{b} = 0 \quad (4.53)$$

Hence, one of the two vectors  $\mathbf{a}_0$  and  $\mathbf{b}$  can be prescribed arbitrarily. If, for example, the former is prescribed, then  $\mathbf{c}_1$  and  $\mathbf{c}_2$  are known. The conditions of Eq. (4.53) are thus verified for  $\mathbf{b}$  defined as the unit vector derived from the cross product of the two other vectors in the above equations, i.e.,

$$\mathbf{b} = \frac{\mathbf{c}_1 \times \mathbf{c}_2}{\|\mathbf{c}_1 \times \mathbf{c}_2\|} \quad (4.54)$$

However, as in the planar case, most commonly the centerpoints  $B$  and  $B^*$  are given, as the space available to anchor the mechanism is known in a practical design project. In this case, two equations are given explicitly with  $\mathbf{a}_0$  as unknown:

$$\mathbf{d}_j^T \mathbf{a}_0 = 0, \quad j = 1, 2 \quad (4.55)$$

with  $\mathbf{d}_j$  defined as

$$\mathbf{d}_j \equiv (\mathbf{Q}_j^T - \mathbf{1}) \mathbf{b}, \quad j = 1, 2 \quad (4.56)$$

and hence, the solution sought takes the form

$$\mathbf{a}_0 = \frac{\mathbf{d}_1 \times \mathbf{d}_2}{\|\mathbf{d}_1 \times \mathbf{d}_2\|} \quad (4.57)$$

thereby showing that, in this case, the problem has a unique solution—obtained in closed form—modulo the *antipodal* of  $B$  or of  $A_0$ , as the case may be. Indeed, in formulas (4.54)

and (4.57), nothing prevents the designer from using the alternative cross product  $\mathbf{c}_2 \times \mathbf{c}_1$  or, correspondingly,  $\mathbf{d}_2 \times \mathbf{d}_1$ . The result would be the same, the only difference being that the new vector  $\mathbf{b}$ , or  $\mathbf{a}_0$ , would be pointing in the direction opposite to that of its previous counterpart. That is, the designer would be looking at a different branch of the same circular-conical surface, both sharing one common point, the cone apex.

### 4.3.2 Dyad Synthesis for Four Attitudes

Now we have  $m = 3$ , the constraints being

$$\mathbf{c}_1^T \mathbf{b} = 0, \quad \mathbf{c}_2^T \mathbf{b} = 0 \quad \text{and} \quad \mathbf{c}_3^T \mathbf{b} = 0 \quad (4.58)$$

or correspondingly,

$$\mathbf{d}_1^T \mathbf{a}_0 = 0, \quad \mathbf{d}_2^T \mathbf{a}_0 = 0 \quad \text{and} \quad \mathbf{d}_3^T \mathbf{a}_0 = 0 \quad (4.59)$$

In order to be able to find a vector  $\mathbf{b}$  simultaneously perpendicular to all three vectors  $\mathbf{c}_j$  in eq.(4.58), these vectors must be coplanar, and hence, this triplet must obey the condition

$$\mathcal{K} : F(x, y, z) \equiv \mathbf{c}_1 \times \mathbf{c}_2 \cdot \mathbf{c}_3 = 0 \quad (4.60)$$

which is a product of three factors, each linearly homogeneous in  $\mathbf{a}_0$ , as per eq.(4.48), and hence, it is cubic and homogeneous in  $\mathbf{a}_0$ . As well, any vector  $\mathbf{a}_0$  verifying eq.(4.60) is an element of a conic surface with apex at the origin  $O$ . Its intersection with the unit sphere described by the first of eqs.(4.44) is thus a spherical surface, labeled  $\mathcal{K}$  to mimic the planar case of Subsection 4.2.2. Notice that every conical surface has two sheets sharing one common point, the surface apex. Therefore,  $\mathcal{K}$  consists of two parts, one the *antipodal* of the other. Any point on the curve represents a solution  $\mathbf{a}_0$ . In this light, we call  $\mathcal{K}$  the *circlepoint curve*.

As in the case of a planar cubic curve, its spherical counterpart intersects the spherical-surface equivalent of the planar line, namely, a major circle, at a maximum of three points. Likewise, a spherical cubic curve has one asymptote, which in this case is, again, a major circle.

Furthermore, once a point on  $\mathcal{K}$  has been chosen as  $A_0$ , its corresponding centerpoint  $B$ , of position vector  $\mathbf{b}$ , is chosen as any of the three possible cross products  $\mathbf{c}_j \times \mathbf{c}_{j+1}$ , for  $j = 1, 2, 3$  and  $j + 1 \equiv j + 1 \bmod 3$ , upon normalizing the product to yield a unit vector. Algebraically, these three products, although not necessarily identical—the angle between any pair of their factors are, in general, different—yield identical unit vectors upon normalization. However, due to roundoff errors, the three unit vectors will be numerically different. In order to filter the roundoff error, the obvious strategy is to compute all three products, then take their mean value. Normalizing this value to render it of unit norm yields vector  $\mathbf{b}$ .

By a similar reasoning, the *centerpoint conical surface*  $\mathcal{M}$  and its corresponding *centerpoint curve*<sup>10</sup> are obtained as

$$\mathcal{M} : G(u, v, w) \equiv \mathbf{d}_1 \times \mathbf{d}_2 \cdot \mathbf{d}_3 = 0 \quad (4.61)$$

with  $\mathbf{d}_j$  defined in eq.(4.56). Any point on  $\mathcal{M}$  gives one corresponding circlepoint  $A_0$  on the unit sphere and any point of  $\mathcal{K}$  gives one centerpoint  $B$  on the unit sphere.

### 4.3.3 Dyad Synthesis Five Attitudes

For  $m = 4$ , the synthesis equations lead to a system of four homogeneous bilinear equations in the unknown vectors  $\mathbf{a}_0$  and  $\mathbf{b}$ . As these are three-dimensional vectors, the total number of unknowns at hand is six, but then again, two additional equations are available, namely, eqs.(4.44), and the problem is fully determined. The four homogeneous equations can then be cast in the form

$$\underbrace{\begin{bmatrix} \mathbf{a}_0^T \mathbf{E}_1[s_1 \mathbf{1} - (1 - c_1)\mathbf{E}_1] \\ \mathbf{a}_0^T \mathbf{E}_2[s_2 \mathbf{1} - (1 - c_2)\mathbf{E}_2] \\ \mathbf{a}_0^T \mathbf{E}_3[s_3 \mathbf{1} - (1 - c_3)\mathbf{E}_3] \\ \mathbf{a}_0^T \mathbf{E}_4[s_4 \mathbf{1} - (1 - c_4)\mathbf{E}_4] \end{bmatrix}}_{\mathbf{C}} \mathbf{b} = \mathbf{0}_4 \quad (4.62)$$

whose matrix coefficient  $\mathbf{C}$  is a  $4 \times 3$  array. In light of the second of equations (4.44), moreover, the trivial solution of eqs.(4.62) is not acceptable, and hence,  $\mathbf{C}$  must be *rank-deficient*, i.e., its three columns must be linearly dependent. This happens if and only if the four distinct  $3 \times 3$  determinants obtained by taking three rows of  $\mathbf{C}$  at a time vanish. Let

$$\Delta_j(\mathbf{a}_0) \equiv \det(\mathbf{C}_j) = 0, \quad j = 1, \dots, 4 \quad (4.63)$$

with  $\mathbf{C}_j$  denoting the  $3 \times 3$  matrix obtained from  $\mathbf{C}$  upon deleting its  $j$ th row. From Subsection 4.3.2 it is known that each of the four determinants defines a conical cubic surface whose apex is the origin. The common intersections of all four surfaces are common elements of these surfaces; they are candidate axes capable of guiding the coupler link through the five prescribed poses.

Likewise, surface equations for  $\mathbf{b}$  can be formulated with

$$\mathbf{D}\mathbf{a}_0 = \mathbf{0}_4 \quad (4.64)$$

in which the  $4 \times 3$  matrix  $\mathbf{D} = [\mathbf{d}_1^T, \dots, \mathbf{d}_4^T]^T$  with  $\mathbf{d}_j$  defined in eq.(4.56) for  $m = 2$ ; the same pattern holds for the case at hand,  $m = 4$ . The rank-deficiency of matrix  $\mathbf{D}$  yields

$$\Delta_j(\mathbf{b}) \equiv \det(\mathbf{D}_j) = 0, \quad j = 1, \dots, 4 \quad (4.65)$$

---

<sup>10</sup>McCarthy and Soh (2011) call the conical surfaces generating these curves the *center-axis cone* and

with  $\mathbf{D}_j$  denoting the  $3 \times 3$  matrix obtained from  $\mathbf{D}$  upon deleting its  $j$ th row.

The Bezout number of the four cubic equations (4.63) is thus  $3^4 = 81$ . Ditto that of the four cubic equations (4.65). This number is an overestimate of the actual number of possible solutions. Indeed, McCarthy and Soh (2011), by invoking the *Burmester-Roth Theorem* (Roth, 1967), showed that the four cubic equations in  $\mathbf{a}_0$  can be reduced, by elimination of two of the three coordinates of  $A_0$ , to a sextic polynomial. As a consequence, the problem admits six, four, two or zero circlepoint solutions. The same reasoning leads to the conclusion that the problem also admits six, four, two or zero centerpoint solutions. Therefore, the number of possible dyads that solve the problem is six, four, two or zero. Correspondingly, the number of spherical four-bar linkages that can guide their coupler link through the five given attitudes is the number of combinations of six, four, two or zero objects taking two at a time, i.e., 15, six, one or zero.

#### 4.3.4 Spherical Dyads with a P Joint

While it may appear counterintuitive to associate a P joint with a spherical linkage, such a joint is possible in this linkage type. In fact, the putative P joint is still of the R type, but with a special feature: it allows the motion of its coupling link via a circular guideway, defined by a major circle on the unit sphere.

In a spherical dyad, a P joint is a special case of the R dyad, whose arc subtends an angle of  $90^\circ$ . The foregoing method of synthesis still applies, if with some modifications. Indeed, for the prescribed attitudes to lead to a linkage that admits a P joint, at a circlepoint for example, the circle traced by  $A$ , or  $A^*$  for that matter, becomes a major circle. In this case  $A_j$  moves on a major circle lying in a plane normal to  $\mathbf{b}$ , eq.(4.45) then becoming

$$\mathbf{b}^T \mathbf{a}_0 = \mathbf{b}^T \Rightarrow \mathbf{Q}_j \mathbf{a}_0 = 0, \quad j = 0, \dots, m \quad (4.66)$$

with  $\mathbf{Q}_0 = \mathbf{1}$ , the  $3 \times 3$  identity matrix. The foregoing equation means that all vectors  $\{\mathbf{a}_j\}_0^m$  are coplanar,  $\mathbf{b}$  then being the unit normal to the plane of the set. Furthermore, relations (4.66) can be rewritten as an array of  $m + 1$  scalar equations:

$$\mathbf{H}\mathbf{a}_0 = \mathbf{0}_{m+1} \quad (4.67)$$

where  $\mathbf{H}$  is a  $(m + 1) \times 3$  matrix. Again, matrix  $\mathbf{H}$  has to be *rank-deficient*, as only  $m \geq 2$  conditions are considered<sup>11</sup>. This implies, for the four-attitude synthesis problem, that

$$\det(\mathbf{H}_i) = 0, \quad i = 1, \dots, 4 \quad (4.68)$$

the  $3 \times 3$  matrix  $\mathbf{H}_i$  obtained by deleting the  $i$ th row from matrix  $\mathbf{H}$ . In the case of five poses,  $\mathbf{H}_i$  is obtained by deleting the  $i$ th and  $(i + 1)$ st rows from matrix  $\mathbf{H}$ .

---

the *circling-axis cone*, respectively.

<sup>11</sup>For  $m = 1$  it is always possible to find two linearly independent vectors normal to a given one!

### 4.3.5 Approximate Dyad Synthesis

Exactly as in the case of planar linkages, whenever  $m \geq 5$  the synthesis equations, in general, cannot be satisfied exactly. In this case, as in its planar counterpart, the approach is to formulate the synthesis problem as one of optimum design. To this end, an objective function  $z$  is defined as in the planar case, namely, as one-half the Euclidian norm of an error vector  $\mathbf{e}$  defined exactly as in the planar case as well. Contrary to the latter, however, the optimization task at hand is no longer unconstrained, because vectors  $\mathbf{a}_0$  and  $\mathbf{b}$  are now subjected to the normality conditions (4.44), which play the role of equality constraints in the optimization task. Unfortunately, the literature on the solution of the approximate synthesis problem for spherical four-bar linkages is rather scarce.

The challenge posed by the approximate synthesis of spherical linkages lies in that solving a *constrained optimization problem* is more complex than solving an unconstrained one, as the former must incorporate the constraints, first in the formulation, then in the solution algorithm (Hillier and Liebermann, 1995).

The basic optimization problem is stated below. First, the error incurred at the  $j$ th pose is defined:

$$e_j \equiv \mathbf{a}_0^T (\mathbf{Q}_j^T - \mathbf{1}) \mathbf{b}, \quad j = 1, \dots, m \geq 5 \quad (4.69)$$

the optimization problem now being formulated as

$$z \equiv \frac{1}{2} \|\mathbf{e}\|^2 = \frac{1}{2} \sum_1^m e_j^2(\mathbf{x}) \rightarrow \min_{\mathbf{x}}, \quad \text{with } \mathbf{x} \equiv \begin{bmatrix} \mathbf{a}_0 \\ \mathbf{b} \end{bmatrix} \in \mathbb{R}^6 \& \mathbf{e} \equiv \begin{bmatrix} e_1 \\ \vdots \\ e_m \end{bmatrix} \quad (4.70)$$

subject to<sup>12</sup>

$$\mathbf{h}(\mathbf{x}) \equiv \frac{1}{2} \begin{bmatrix} (\|\mathbf{a}_0\|^2 - 1) \\ (\|\mathbf{b}\|^2 - 1) \end{bmatrix} = \mathbf{0}_2 \quad (4.71)$$

In order to handle the constraints, we can cite two approaches: *i*) adjoin the constraints to the objective function  $z(\mathbf{x})$ , defined above, by means of *Lagrange multipliers*, which become additional unknowns to the optimization problem, as done by Liu and Angeles (1992); and *ii*) introduce an alternative parametrization of the problem, that allows formulating the synthesis task as an *unconstrained optimization problem* (Léger and Angeles, 2014). There are pros and cons to the two approaches, as described below.

#### Constrained-minimization Approach

In this case, a new objective function is defined, that allows the handling of the problem as in the unconstrained case, by means of a vector  $\boldsymbol{\lambda}$  of Lagrange multipliers, of dimension identical to the number of scalar constraints, which, in our case, is two. The new objective

---

<sup>12</sup>The purpose of the 1/2 factor in the definition of  $\mathbf{h}(\mathbf{x})$  is to avoid carrying a factor of 2 when calculating  $\nabla \mathbf{h}$ .

function then becomes

$$F(\mathbf{x}, \boldsymbol{\lambda}) \equiv z(\mathbf{x}) + \boldsymbol{\lambda}^T \mathbf{h}(\mathbf{x}) \rightarrow \min_{\mathbf{x}, \boldsymbol{\lambda}}, \quad \boldsymbol{\lambda} \in \mathbb{R}^2 \quad (4.72)$$

subject to no constraints.

The FONC of the unconstrained problem are now:

$$\frac{\partial F}{\partial \mathbf{x}} = \frac{\partial z}{\partial \mathbf{x}} + \mathbf{J}(\mathbf{x})^T \boldsymbol{\lambda} = \mathbf{0}_6, \quad \mathbf{J}(\mathbf{x}) \equiv \frac{\partial \mathbf{h}}{\partial \mathbf{x}} = \begin{bmatrix} \mathbf{a}_0^T & \mathbf{0}^T \\ \mathbf{0}^T & \mathbf{b}^T \end{bmatrix} \in \mathbb{R}^{2 \times 6} \quad (4.73)$$

$$\frac{\partial F}{\partial \boldsymbol{\lambda}} = \mathbf{h}(\mathbf{x}) = \mathbf{0}_2 \quad (4.74)$$

with  $\mathbf{J}(\mathbf{x})$  termed the *constraint Jacobian*, and eq.(4.74) being a restatement of the constraint, eq.(4.71).

Given the simplicity of  $z(\mathbf{x})$ , which is a *quartic* scalar function of  $\mathbf{x}$ , and of  $\mathbf{h}(\mathbf{x})$ , which is, in turn, a *quadratic* vector function of the same, their gradients  $\partial z / \partial \mathbf{x}$  and  $\mathbf{J}(\mathbf{x})$ , are also algebraic functions, but now *cubic* and, correspondingly, *linear* in  $\mathbf{x}$ , their FONC are algebraically simple equations that should lead to simplifications. For one thing, in light of the linearity of eq.(4.73) in  $\boldsymbol{\lambda}$ , it is possible to eliminate this vector from the same equation system. Rather than eliminating  $\boldsymbol{\lambda}$  by means of equation-solving, an alternative approach is introduced below.

The concept of orthogonal complement, introduced in Subsection 3.5.3, is key to the elimination of the vector of Lagrange multipliers: let  $\mathbf{L}$  be an orthogonal complement of the constraint Jacobian  $\mathbf{J}$ , in the sense that the columns of  $\mathbf{L}$  span the null space of  $\mathbf{J}$ . Since the later is a  $2 \times 6$  matrix,  $\mathbf{L}$  is bound to be a  $6 \times 4$  matrix because  $\mathbf{J}$  is of full rank, since its two rows are apparently linearly independent. The range of  $\mathbf{J}$  is thus 2, and hence, four linearly independent six-dimensional vectors can be found that are all orthogonal to the two columns of  $\mathbf{J}$ . These four vectors thus span the null space of  $\mathbf{J}$ , and hence, can be chosen at the four columns of  $\mathbf{L}$ . It should be apparent that the choice of these four vectors is not unique, as long as they are linearly independent.

An obvious choice of the four columns of  $\mathbf{L}$  is given below:

$$\mathbf{L} = \begin{bmatrix} \mathbf{A}_0 \mathbf{u} & \mathbf{0} & \mathbf{A}_0 \mathbf{v} & \mathbf{0} \\ \mathbf{0} & \mathbf{B} \mathbf{u} & \mathbf{0} & \mathbf{B} \mathbf{v} \end{bmatrix} \quad (4.75)$$

where  $\mathbf{A}_0 = \text{CPM}(\mathbf{a}_0)$ ,  $\mathbf{B} = \text{CPM}(\mathbf{b})$ , while  $\mathbf{u}$  and  $\mathbf{v}$  are arbitrary linearly independent three-dimensional vectors that, for purposes of numerical stability, might as well be chosen of unit magnitude. Under these conditions, the reader can readily prove that

$$\mathbf{J} \mathbf{L} = \mathbf{O} \in \mathbb{R}^{2 \times 4} \quad (4.76)$$

Upon multiplying both sides of the first of eqs.(4.73) by  $\mathbf{L}^T$  from the left, a new system of first-order normality conditions for the problem at hand is obtained, free of  $\boldsymbol{\lambda}$ , namely,

$$\mathbf{L}^T \nabla z = \mathbf{0} \in \mathbb{R}^4 \quad (4.77)$$

with  $\nabla z$  representing the gradient of  $z(\mathbf{x})$ , i.e.,

$$\nabla z = \begin{bmatrix} \partial z / \partial \mathbf{a}_0 \\ \partial z / \partial \mathbf{b} \end{bmatrix} \quad (4.78)$$

whose two three-dimensional blocks are readily computed below:

From the definition of  $z(\mathbf{x})$  in eq.(4.70),  $\partial z / \partial \mathbf{a}_0$  readily follows:

$$\frac{\partial z}{\partial \mathbf{a}_0} = \sum_1^m e_j \frac{\partial e_j}{\partial \mathbf{a}_0} = \sum_1^m [\mathbf{a}_0^T (\mathbf{Q}_j^T - \mathbf{1}) \mathbf{b}] \frac{\partial e_j}{\partial \mathbf{a}_0} \quad (4.79)$$

the last partial derivative being displayed below:

$$\frac{\partial e_j}{\partial \mathbf{a}_0} = (\mathbf{Q}_j^T - \mathbf{1}) \mathbf{b} \quad (4.80)$$

with a similar expression for  $\partial e_j / \partial \mathbf{b}$ :

$$\frac{\partial e_j}{\partial \mathbf{b}} = (\mathbf{Q}_j - \mathbf{1}) \mathbf{a}_0 \quad (4.81)$$

Hence,

$$\frac{\partial z}{\partial \mathbf{a}_0} = \sum_1^m e_j \frac{\partial e_j}{\partial \mathbf{a}_0} = \sum_1^m [\mathbf{a}_0^T (\mathbf{Q}_j^T - \mathbf{1}) \mathbf{b}] (\mathbf{Q}_j^T - \mathbf{1}) \mathbf{b} \quad (4.82a)$$

which can be cast in the form

$$\frac{\partial z}{\partial \mathbf{a}_0} = \mathbf{Z}_a \mathbf{b} \quad (4.82b)$$

with  $\mathbf{Z}_a$  defined as

$$\mathbf{Z}_a \equiv \sum_1^m e_j [\mathbf{a}_0^T (\mathbf{Q}_j^T - \mathbf{1}) \mathbf{b}] (\mathbf{Q}_j^T - \mathbf{1}) \quad (4.82c)$$

Likewise,  $\partial z / \partial \mathbf{b}$  is computed as

$$\frac{\partial z}{\partial \mathbf{b}} = \mathbf{Z}_b \mathbf{a} \quad (4.83a)$$

with  $\mathbf{Z}_b$  defined as

$$\mathbf{Z}_b \equiv \sum_1^m e_j [\mathbf{a}_0^T (\mathbf{Q}_j^T - \mathbf{1}) \mathbf{b}] (\mathbf{Q}_j - \mathbf{1}) \quad (4.83b)$$

It is noteworthy that the last factor in  $\mathbf{Z}_b$  differs from its counterpart in  $\mathbf{Z}_a$ , in that matrix  $\mathbf{Q}_j$  is not transposed, a consequence of the definition of the derivative of a scalar,  $e_j$  in this case, with respect to a vector,  $\mathbf{a}_0$  or  $\mathbf{b}$ , as per the definitions introduced in Subsection 1.4.4.

In summary, then, system (4.77) yields four equations in the six unknowns  $\mathbf{x} =$

$[\mathbf{a}_0^T, \mathbf{b}^T]^T$ , to be complemented with the two scalar constraints, eqs.(4.71), thereby ending up with a system of six nonlinear equations in six unknowns. The number of possible solutions to the foregoing system can be predicted via its Bezout number. First, notice that  $\mathbf{Z}_a$  and  $\mathbf{Z}_b$  are quadratic in  $\mathbf{a}_0$  and  $\mathbf{b}$ , i.e., in  $\mathbf{x}$ . Since the first block of  $\nabla z$  is linear in  $\mathbf{Z}_a$  and in  $\mathbf{b}$ , while its second block is linear in  $\mathbf{Z}_b$  and  $\mathbf{a}_0$ , it follows that  $\nabla z$  is cubic in  $\mathbf{x}$ . Moreover, the two scalar constraints (4.71) are quadratic in  $\mathbf{x}$ , the overall system of six algebraic equations in six unknowns has a Bezout number  $N_B = 4^4 \times 2 \times 2 = 1024$ . Upon removing the antipodal solutions, the total number of distinct solutions can be as high as 512.

This system can be solved numerically via the Newton-Raphson method, whose convergence, as pointed out in Section 1.5.1, cannot be predicted. For this reason, a robust alternative is investigated.

The alternative solution aims at an overdetermined, although *consistent*, system of nonlinear equations, to be solved numerically via the Newton-Gauss method, whose convergence is guaranteed, as per the results of Subsection 1.6.1. To this end, an alternative, although *expanded* orthogonal complement of  $\mathbf{J}(\mathbf{x})$  is explored. What the qualifier in italics means is an orthogonal complement with a surplus of columns. This is a  $6 \times 6$  matrix, namely,

$$\mathbf{L} = \begin{bmatrix} \mathbf{A}_0 & \mathbf{O} \\ \mathbf{O} & \mathbf{B} \end{bmatrix} \in \mathbb{R}^{6 \times 6} \quad (4.84)$$

where  $\mathbf{A}_0 = \text{CPM}(\mathbf{a}_0)$  and  $\mathbf{B} = \text{CPM}(\mathbf{b})$ , while  $\mathbf{O} \in \mathbb{R}^{3 \times 3}$  is the  $3 \times 3$  zero matrix. The reader is invited to prove that  $\mathbf{J}\mathbf{L} = \mathbf{O} \in \mathbb{R}^{2 \times 6}$ .

Further, upon premultiplying the first of eqs.(4.72) by  $\mathbf{L}^T$ , with  $\mathbf{L}$  given as in eq.(4.84), a new system of first-order normality conditions is obtained, free of Lagrange multipliers:

$$\mathbf{L}^T \nabla F = \begin{bmatrix} -\mathbf{A}_0 \mathbf{Z}_a \mathbf{b} \\ -\mathbf{B} \mathbf{Z}_b \mathbf{a}_0 \end{bmatrix} = \mathbf{0} \in \mathbb{R}^6 \quad (4.85)$$

which, together with the constraints (4.71), lead to an overdetermined system of eight nonlinear equations in six unknowns, to be solved with the Newton-Gauss method, which is guaranteed to converge to one of the multiple solutions admitted by the problem.

An alternative to the Newton-Gauss method is, of course, a semigraphical method, aimed at eliminating all but two of the six unknowns of the first six-dimensional system or of the eight-dimensional system in the second approach. All real solutions can then be obtained by contour intersection.

## Unconstrained-minimization Approach

If, rather than using Cartesian coordinates, one uses spherical coordinates tailored to points lying on the unit sphere, then not only are the constraints eliminated, but the

number of design variables is reduced, from three per point to only two, as the third spherical coordinate, the distance of a point in 3D space to the origin, is constant. Indeed, all points of interest lie in the unit sphere.

However, introduction of spherical coordinates brings about its own complexity, as the point-coordinates entail the harmonic functions, sine and cosine, of the spherical coordinates, thereby destroying the algebraic nature of the problem. While the tan-half identities, introduced in eq.(3.73), can be invoked, that would bring the system of equations back to algebraic, the degree of the error, eq.(4.69), would be now higher than quadratic. One alternative to cope with the new algebraic system is to resort to *dialytic elimination* (Salmon, 1964), which allows a systematic means of eliminating unknowns from a system of algebraic equations. This is an interesting research topic, but it will not be pursued here.

One practical means of coping with the nonlinearity of the problem is by resorting to a purely numerical approach, if with some massaging of the relations involved, as outlined presently. Given that the optimization problem is now unconstrained, it can be regarded as one of *nonlinear least squares*, as studied in Section 1.6, and solved by means of the Newton-Gauss method.

The spherical coordinates to be used here are *longitude* and *latitude*. Let, then<sup>13</sup>,  $\vartheta_A$  and  $\varphi_A$  be the longitude and the latitude of  $A_0$ ,  $\vartheta_B$  and  $\varphi_B$  those of  $B$ . Hence, the position vectors of interest,  $\mathbf{a}_0$  and  $\mathbf{b}$ , are now given, each, in terms of only two design variables:

$$\mathbf{a}_0 = \begin{bmatrix} \cos \varphi_A \cos \vartheta_A \\ \cos \varphi_A \sin \vartheta_A \\ \sin \varphi_A \end{bmatrix}, \quad \mathbf{b} = \begin{bmatrix} \cos \varphi_B \cos \vartheta_B \\ \cos \varphi_B \sin \vartheta_B \\ \sin \varphi_B \end{bmatrix} \quad (4.86)$$

As the synthesis problem admits two valid solutions, one the antipodal of the other, we will now limit the search of the optimum solution to only one of the two alternatives. This is readily done by specifying the ranges of all spherical coordinates as

$$\{\varphi_A, \vartheta_A, \varphi_B, \vartheta_B\} \in [-\pi/2, \pi/2] \quad (4.87)$$

In order to formulate the unconstrained optimization problem we recall the error  $e_j$  of eq.(4.69) for the  $j$ th prescribed attitude. The approximate-synthesis problem is now formulated as

$$z \equiv \frac{1}{2} \|\mathbf{e}\|^2 = \frac{1}{2} \sum_1^m e_j^2(\mathbf{x}) \rightarrow \min_{\mathbf{x}}, \quad \text{with } \mathbf{e} \equiv \begin{bmatrix} e_1 \\ \vdots \\ e_m \end{bmatrix} \& \mathbf{x} \equiv \begin{bmatrix} \boldsymbol{\alpha} \\ \boldsymbol{\beta} \end{bmatrix} \in \mathbb{R}^4 \quad (4.88)$$

with vectors  $\boldsymbol{\alpha}$  and  $\boldsymbol{\beta}$  defined, in turn, as

$$\boldsymbol{\alpha} \equiv \begin{bmatrix} \varphi_A \\ \vartheta_A \end{bmatrix} \quad \text{and} \quad \boldsymbol{\beta} \equiv \begin{bmatrix} \varphi_B \\ \vartheta_B \end{bmatrix} \quad (4.89)$$

---

<sup>13</sup> $\vartheta$  and  $\varphi$  are read “vartheta” and “varphi,” respectively.

The simplest way of solving the foregoing problem is by means of the approach used for overdetermined systems of nonlinear equations, as introduced in Section 1.6. That is, we look at an overdetermined system of  $m \geq 5$  equations in four unknowns, of the form

$$\mathbf{e}(\mathbf{x}) = \mathbf{0}_m, \quad \text{with } m \geq 5 \text{ & } \mathbf{x} \in \mathbb{R}^4 \quad (4.90)$$

Further, the Newton-Gauss method requires the Jacobian of  $\mathbf{e}$  with respect to  $\mathbf{x}$ , namely,

$$\Phi(\mathbf{x}) \equiv \frac{\partial \mathbf{e}(\mathbf{x})}{\partial \mathbf{x}} \quad (4.91)$$

However, the components  $e_j$  of  $\mathbf{e}$  are given in eq.(4.69) in terms of  $\mathbf{a}_0$  and  $\mathbf{b}$ . The gradients of these components w.r.t.  $\boldsymbol{\alpha}$  and  $\boldsymbol{\beta}$  thus call for application od the chain rule for vector arguments, as introduced in eq.(1.35). To do this, notice that an increment  $\Delta \mathbf{e}$  of  $\mathbf{e}$ , as a result of an increment  $\Delta \mathbf{x}$  in  $\mathbf{x}$ , is given, to a *first-order approximation*, which is good enough for a *reasonably small* increment  $\Delta \mathbf{x}$ , by

$$\Delta \mathbf{e} = \Phi \Delta \mathbf{x}, \quad \Phi \equiv \frac{\partial \mathbf{e}}{\partial \mathbf{x}} \in \mathbb{R}^{m \times 4} \quad (4.92)$$

where, in light of the partitioning of  $\mathbf{x}$ , as per eq.(4.88),  $\Phi$  admits the partitioning

$$\Phi = [\Phi_\alpha \quad \Phi_\beta], \quad \text{with } \Phi_\alpha \equiv \frac{\partial \mathbf{e}}{\partial \boldsymbol{\alpha}} \quad \& \quad \Phi_\beta \equiv \frac{\partial \mathbf{e}}{\partial \boldsymbol{\beta}} \in \mathbb{R}^{m \times 2} \quad (4.93)$$

Further, in order to obtain matrices  $\Phi_\alpha$  and  $\Phi_\beta$ , the Jacobians of  $\mathbf{e}$  w.r.t.  $\boldsymbol{\alpha}$  and  $\boldsymbol{\beta}$ , in terms of the corresponding Jacobians of  $\mathbf{a}_0$  and  $\mathbf{b}$  with respect to  $\boldsymbol{\alpha}$  and  $\boldsymbol{\beta}$ , respectively—notice that  $\mathbf{a}_0$  is a function of  $\boldsymbol{\alpha}$  alone, while  $\mathbf{b}$  is, in turn, a function of  $\boldsymbol{\beta}$  alone—, *the chain rule of differentiation for vector arrays*, introduced in eq.(1.35), is now recalled:

$$\frac{\partial e_j}{\partial \boldsymbol{\alpha}} = \left( \frac{\partial \mathbf{a}_0}{\partial \boldsymbol{\alpha}} \right)^T \frac{\partial e_j}{\partial \mathbf{a}_0}, \quad \frac{\partial e_j}{\partial \boldsymbol{\beta}} = \left( \frac{\partial \mathbf{b}}{\partial \boldsymbol{\beta}} \right)^T \frac{\partial e_j}{\partial \mathbf{b}}, \quad j = 1, \dots, m \quad (4.94)$$

The Jacobians of interest are now computed from eqs.(4.86):

$$\mathbf{A} \equiv \frac{\partial \mathbf{a}_0}{\partial \boldsymbol{\alpha}} = \begin{bmatrix} -\sin \varphi_A \cos \vartheta_A & -\cos \varphi_A \sin \vartheta_A \\ -\sin \varphi_A \sin \vartheta_A & \cos \varphi_A \cos \vartheta_A \\ \cos \varphi_A & 0 \end{bmatrix} \in \mathbb{R}^{3 \times 2} \quad (4.95)$$

and

$$\mathbf{B} \equiv \frac{\partial \mathbf{b}}{\partial \boldsymbol{\beta}} = \begin{bmatrix} -\sin \varphi_B \cos \vartheta_B & -\cos \varphi_B \sin \vartheta_B \\ -\sin \varphi_B \sin \vartheta_B & \cos \varphi_B \cos \vartheta_B \\ \cos \varphi_B & 0 \end{bmatrix} \in \mathbb{R}^{3 \times 2} \quad (4.96)$$

while the gradients of  $e_j$  w.r.t.  $\mathbf{a}_0$  and  $\mathbf{b}$  were already obtained, as displayed in eqs.(4.80) and (4.81), respectively.

Upon substitution of eqs.(4.95) and (4.96), along with eqs.(4.80) and (4.81), into eqs.(4.94), the gradients of  $e_j$  with respect to  $\boldsymbol{\alpha}$  and  $\boldsymbol{\beta}$  are obtained:

$$\frac{\partial e_j}{\partial \boldsymbol{\alpha}} = \mathbf{A}^T (\mathbf{Q}_j^T - \mathbf{1}) \mathbf{b}, \quad \frac{\partial e_j}{\partial \boldsymbol{\beta}} = \mathbf{B}^T (\mathbf{Q}_j - \mathbf{1}) \mathbf{a}_0 \in \mathbb{R}^2, \quad j = 1, \dots, m \quad (4.97)$$

Table 4.2: Five Given Attitudes of a Rigid Link

No.	$\phi_j$ [rad]	$\mathbf{e}^T$
0	0	undefined
1	0.2034	$[-0.0449, -0.5133, -0.8569]^T$
2	1.1957	$[0.1827, 0.7709, -0.6101]^T$
3	1.1932	$[0.5212, 0.8414, -0.1422]^T$
4	1.0512	$[0.5384, 0.8114, 0.2271]^T$

which are all two-dimensional vector arrays. Now, upon assembling these arrays into the two arrays  $\Phi_\alpha$  and  $\Phi_\beta$  of eqs.(4.93), the  $m \times 2$  gradients appearing therein, we obtain

$$\Phi_\alpha = \begin{bmatrix} \mathbf{b}^T(\mathbf{Q}_1 - \mathbf{1})\mathbf{A} \\ \mathbf{b}^T(\mathbf{Q}_2 - \mathbf{1})\mathbf{A} \\ \vdots \\ \mathbf{b}^T(\mathbf{Q}_m - \mathbf{1})\mathbf{A} \end{bmatrix}, \quad \Phi_\beta = \begin{bmatrix} \mathbf{a}_0^T(\mathbf{Q}_1^T - \mathbf{1})\mathbf{B} \\ \mathbf{a}_0^T(\mathbf{Q}_2^T - \mathbf{1})\mathbf{B} \\ \vdots \\ \mathbf{a}_0^T(\mathbf{Q}_m^T - \mathbf{1})\mathbf{B} \end{bmatrix} \in \mathbb{R}^{m \times 2} \quad (4.98)$$

the Jacobian  $\Phi$  of  $\mathbf{e}$  w.r.t.  $\mathbf{x}$ , introduced in eq.(4.91), thus being completed:

$$\Phi = \begin{bmatrix} \mathbf{b}^T(\mathbf{Q}_1 - \mathbf{1})\mathbf{A} & \mathbf{a}_0^T(\mathbf{Q}_1^T - \mathbf{1})\mathbf{B} \\ \mathbf{b}^T(\mathbf{Q}_2 - \mathbf{1})\mathbf{A} & \mathbf{a}_0^T(\mathbf{Q}_2^T - \mathbf{1})\mathbf{B} \\ \vdots & \vdots \\ \mathbf{b}^T(\mathbf{Q}_m - \mathbf{1})\mathbf{A} & \mathbf{a}_0^T(\mathbf{Q}_m^T - \mathbf{1})\mathbf{B} \end{bmatrix} \in \mathbb{R}^{m \times 4} \quad (4.99)$$

Once the Jacobian  $\Phi$  is available, the Newton-Gauss method can be implemented for a given initial guess  $\mathbf{x}^0$ , which is all that this algorithm needs.

### 4.3.6 Examples

A set of attitudes of a rigid link is given in Table 4.2, from which data will be taken for the synthesis examples below.

#### Synthesis of a Spherical Dyad for Three Attitudes

Attitudes No. 1 and 2 are taken from Table 4.2 to design a RR dyad. First, the rotation matrices  $\mathbf{Q}_1$  and  $\mathbf{Q}_2$ , taking the dyad end-link from the reference attitude, 0 in the table and represented by  $\mathbf{1}$ , are calculated, based on the angle of rotation  $\phi$  and the unit vector  $\mathbf{e}$  given in rows 1 and 2 of the table. These are

$$\mathbf{Q}_1 = \begin{bmatrix} 0.9794 & 0.1736 & -0.1029 \\ -0.1726 & 0.9848 & 0.0181 \\ 0.1045 & 0 & 0.9945 \end{bmatrix}, \quad \mathbf{Q}_2 = \begin{bmatrix} 0.3876 & 0.6569 & 0.6467 \\ -0.4784 & 0.7430 & -0.4680 \\ -0.7879 & -0.1280 & 0.6023 \end{bmatrix}$$

Furthermore, a first centerpoint  $\mathbf{b}$  is chosen a

$$\mathbf{b} = [0.5774 \quad 0.5774 \quad 0.5774]^T$$

which leads to vectors

$$\mathbf{d}_1 = \begin{bmatrix} -0.1955 \\ 0.0236 \\ -0.0039 \end{bmatrix}, \quad \mathbf{d}_2 = \begin{bmatrix} -0.0072 \\ -0.1492 \\ -0.1907 \end{bmatrix}$$

With the two foregoing vectors, the corresponding circlepoint is found as

$$\mathbf{a}_0 = [0.9199 \quad 0.36117 \quad 0.1532]^T$$

A second centerpoint  $\mathbf{b}$  is specified as

$$\mathbf{b} = [0.0 \quad -0.7071 \quad 0.7071]^T$$

which leads, in turn, to vectors

$$\mathbf{d}_1 = \begin{bmatrix} -0.1955 \\ 0.0236 \\ -0.0039 \end{bmatrix}, \quad \mathbf{d}_2 = \begin{bmatrix} -0.0072 \\ -0.1492 \\ -0.1907 \end{bmatrix}$$

the corresponding circlepoint being given by the position vector

$$\mathbf{a}_0 = [-0.1063 \quad -0.7812 \quad 0.6152]^T$$

thereby completing the synthesis of the two dyads making up the desired spherical four-bar linkage.

### Synthesis of a Spherical Dyad for Four Attitudes

Attitudes 1, 2 and 3 of Table 4.2 are taken now, which produce one third rotation matrix, besides  $\mathbf{Q}_1$  and  $\mathbf{Q}_2$  used above for the three-attitude synthesis, namely,

$$\mathbf{Q}_3 = \begin{bmatrix} 0.5403 & 0.4090 & 0.7353 \\ 0.1447 & 0.8157 & -0.5600 \\ -0.8289 & 0.4089 & 0.3816 \end{bmatrix}$$

With  $\mathbf{a}_0 = [x, y, z]^T$  and the three foregoing matrices, vectors  $\mathbf{c}_j$ , for  $j = 1, 2, 3$ , are obtained, as per eq.(4.48); when the latter is substituted into eq.(4.60), the cubic equation in  $\mathbf{a}_0 = [x, y, z]^T$  defining the circlepoint spherical curve  $\mathcal{K}$  is obtained, namely,

$$\mathcal{K} : F(x, y, z) = -0.01766 x^3 + 0.03116 x^2 y + 0.04156 x^2 z + 0.02939 x y^2 + 0.08747 x y z$$

$$-0.06021 xz^2 - 0.01747 y^3 - 0.02155 y^2 z + 0.02673 yz^2 - 0.00482 z^3 = 0$$

Likewise, the centerpoint spherical curve  $\mathcal{M}$  is obtained for unit vector  $\mathbf{b} = [u, v, w]^T$  as

$$\begin{aligned} \mathcal{M} : G(u, v, w) = & 0.01678 u^3 + 0.05157 u^2 v + 0.01743 u^2 w - 0.04005 u v^2 + 0.02803 u v w \\ & - 0.05074 u w^2 - 0.00259 v^3 - 0.05317 v^2 w - 0.00933 v w^2 + 0.02762 w^3 = 0 \end{aligned}$$

The spherical circlepoint and centerpoint curves are shown in Fig. 4.9. Dyad synthesis now proceeds as discussed in Subsection 4.3.2. In the same figure, the reader can appreciate the asymptotes of the two cubic curves, as two major circles.

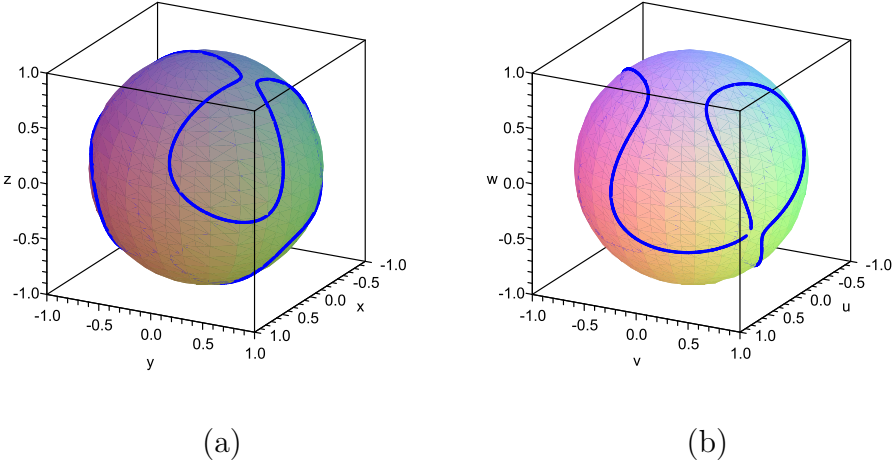


Figure 4.9: Four-pose synthesis curves on the unit sphere, (a) the circlepoint curve and (b) the centerpoint curve

### Synthesis of Spherical Dyads for Five Attitudes

In this example, attitudes 1, 2, 3, and 4 of Table 4.2 are to be met by a spherical dyad. In order to enable the visual determination of the solutions from the intersections of the four circlepoint equations arising from the data, we adopt here spherical coordinates, as introduced in Subsection 4.3.5 for the unconstrained approach to the approximate synthesis of spherical dyads.

The four circlepoint contours in the  $\varphi_a$ -vs.- $\vartheta_a$  plane are illustrated in Fig. 4.10a, those of the centerpoint in the  $\varphi_b$ -vs.- $\vartheta_b$  plane in Fig. 4.10b. Four common intersections can be identified by inspection on each of the two figures, which provide plausible values for the initial guess of numerical solutions via the Newton-Gauss method. To match each solution for  $\mathbf{a}_0$  and its corresponding solution for  $\mathbf{b}$ , the linear equations derived from a value of  $\mathbf{a}_0$  are used: for example, each solution of  $\mathbf{a}_0$  is substituted into the synthesis equation (4.47), which yields a system of  $m$  linear equations in  $\mathbf{b}$ . The values of  $\mathbf{b}$  that verify the linear equations correspond to the given value of  $\mathbf{a}_0$ . The matched solutions are

Table 4.3: Solutions for the Spherical-dyad 5-attitude Synthesis

	$\mathbf{a}_0(\text{or } \mathbf{a}_0^*)$	$\mathbf{b}(\text{or } \mathbf{b}^*)$
# 1	[0.7085, -0.6418, -0.2932]	[0.2640, -0.6636, -0.6998]
# 2	[0.0385, 0.3163, 0.9478]	[0.1143, 0.7263, -0.6777]
# 3	[0.1642, 0.6977, 0.6972]	[0.5218, 0.8413, -0.1403]
# 4	[0.8077, 0.1493, 0.5702]	[0.9524, -0.2535, 0.1686]

recorded in Table 4.3. Note that the results are also the solutions of vectors  $\mathbf{a}_0^*$  and  $\mathbf{b}^*$ . Six linkages<sup>14</sup>, shown in Fig. 4.11, are generated from the four dyads. In the foregoing subfigures, notation  $L\# : i + j$  stands for a linkage generated using solutions  $i$  and  $j$  of Table 4.3.

Branching-detection on the six mechanism was conducted by means of the sign of  $\sin \mu$ , with  $\mu$  denoting the transmission angle for spherical linkages defined in Subsection 3.6.2. Sign changes of the sine of the transmission angle were found in linkages L3 and L4, which indicates the presence of branching defect in these two solutions. The remaining linkages were found to be defect-free. Linkage animations confirmed this point. It was also found from animations that linkages L1, L2 and L5 are of the crank-rocker type, while linkage L6 is a double-rocker.

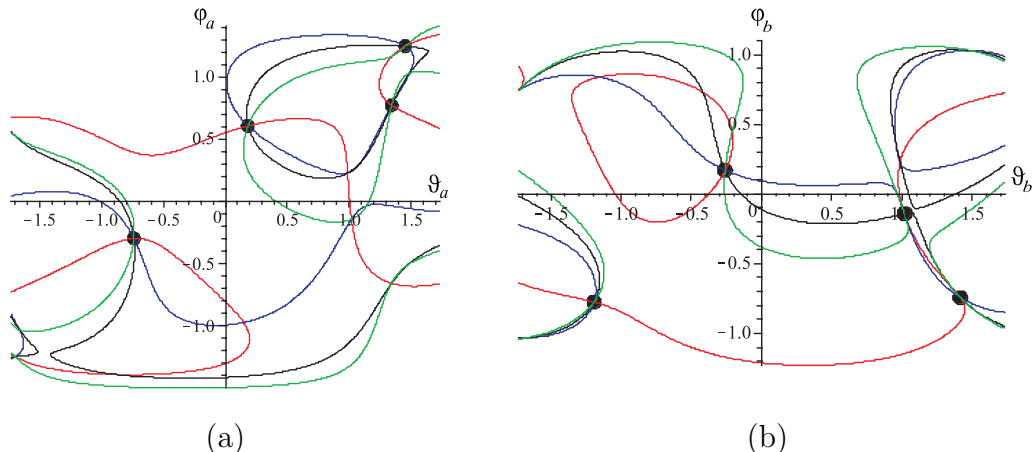


Figure 4.10: The four contours for five-attitude dyad synthesis leading to four possible solutions: (a) for the circlepoint; (b) for the centerpoint

Accurate values of the four circlepoint and centerpoint coordinates, displayed in Table 4.3, were obtained numerically, using nonlinear least-squares.

---

<sup>14</sup>The number of possible combinations of four objects taken two at a time.

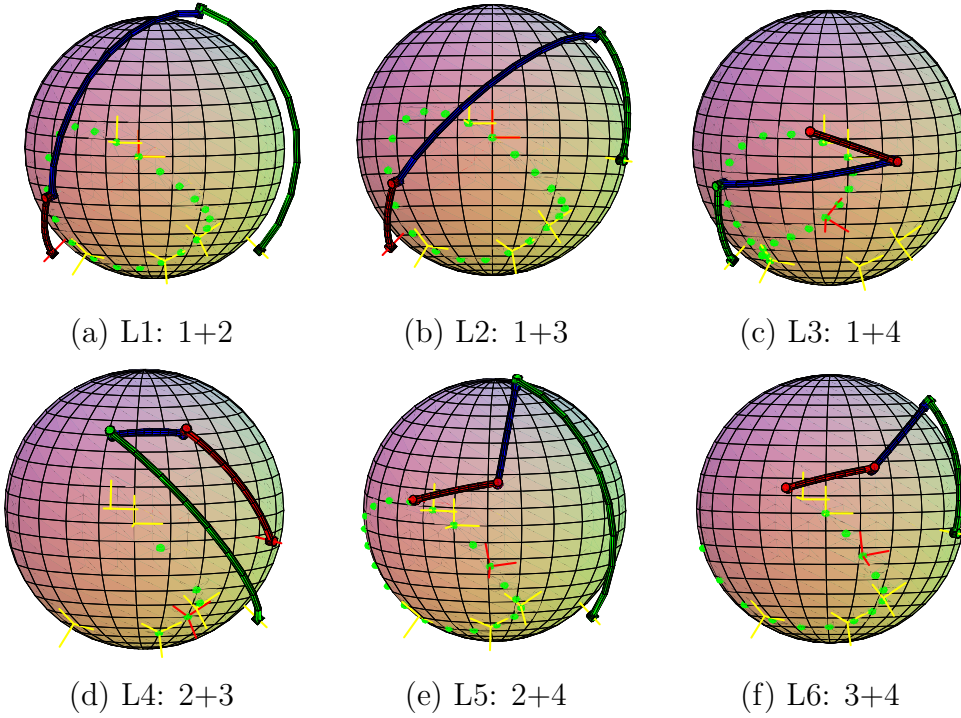


Figure 4.11: Six synthesized mechanisms, shown together with all task orientations in yellow. Solid dots show traces of a point of the coupler link

Table 4.4: Five attitudes for the synthesis of a PR spherical dyad

$\phi_j$ [rad]	$\mathbf{e}^T$
0	[0,0,1]
0.2563	[-0.2280, -0.4553, -0.8606]
1.1307	[-0.0578, 0.2370, -0.9697]
1.1938	[0.5049, 0.8505, -0.1468]
1.3665	[0.7119, 0.6601, 0.2393]

### Synthesis of a Spherical Dyad with a P Joint

For concreteness, let us assume that the P joint is located at the centerpoint  $B$ , coupling the dyad under synthesis with the fixed link. Then the axis of the R joint at  $A_0$  intersects the foregoing major circle at right angles. In the example at hand, five attitudes are given, as displayed in Table 4.4.

By means of eq.(4.68), and a representation of vector  $\mathbf{a}_0$  with spherical coordinates  $\vartheta_a$  and  $\varphi_a$ , contours of four determinant equations are plotted in Fig. 4.12. It is seen that there is only one real solution  $\{\vartheta_a, \varphi_a\}$ . The corresponding unit vector  $\mathbf{b}^*$  is thus obtained, followed by the unit vector  $\mathbf{a}_0^*$ . For the remaining dyad consisting of two R joints, four solutions are found with the general procedure. Of the four solutions of  $\mathbf{a}_0$  and  $\mathbf{b}$ , one is identical to the solution already found for  $\mathbf{a}_0^*$  and  $\mathbf{b}^*$ , which restates that a P joint is a special case of the general spherical RR dyad. All results are listed in Table 4.5.

Table 4.5: Solutions of Example 3

	$\mathbf{a}_0$	$\mathbf{b}$
# 1	[0.2845, 0.3863, 0.8773]	[0.1219, -0.7089, -0.6946]
# 2	[0.7226, 0.5295, 0.4442]	[0.2309, 0.4566, 0.8591]
# 3	[0.9573, -0.2433, 0.1555]	[0.8134, 0.1643, 0.5579]
	$\mathbf{a}_0^*$	$\mathbf{b}^*$
# 4	[0.5221, 0.8442, -0.1208]	[0.0655, 0.1015, 0.9926]

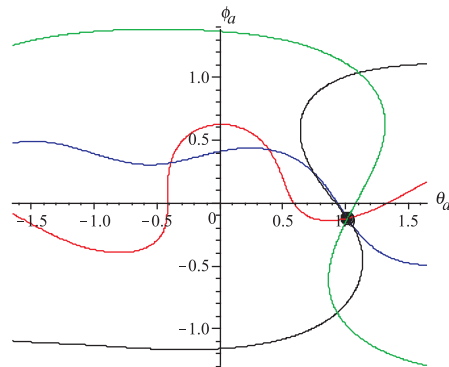


Figure 4.12: Contour plot to find position vectors for the unit vector of the P joint.

Altogether, there are three possible four-bar linkages containing one P joint for the given solutions. One is shown in Fig. 4.13, which is a branching-free linkage, as made apparent by animation.

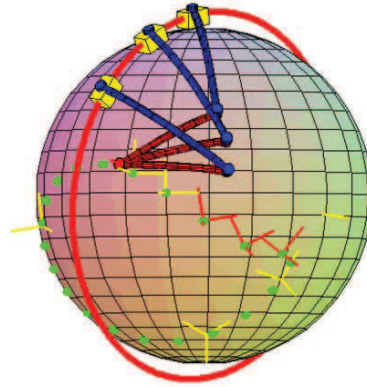


Figure 4.13: Spherical four-bar linkage with a P joint

As a matter of fact, circular guideways are common joints in machinery, available from manufacturers. One circular guideway from Germany-based Schaeffler AG<sup>15</sup> is included in Fig. 4.14.

<sup>15</sup><http://www.schaeffler.com/content.schaeffler.com/en/divisions/industrial/industrial.jsp>



Figure 4.14: An instance of an industrial circular guideway

### Approximate Synthesis of Spherical Dyads

Read (Léger and Angeles, 2014) plus the pertinent references therein.

## 4.4 Spatial Four-bar Linkages

This section is still under construction. It is based on (Bai and Angeles, 2012; 2014).



# Chapter 5

## Path Generation

**Disclaimer:** This chapter is still work in progress. It should be taken with a grain of salt!

### 5.1 Introduction

A recurrent problem in mechanical engineering design is the tracing of a continuous path by means of a mechanism. Examples abound in practice: cranes to upload and download containers from ships, a task that requires horizontal segments to ease the load on the motor; guiding of laser beams to cut a profile from a metal plate; guiding the centre of the wheel in the landing gear of small aircraft through a planar curve; and so on. The foregoing examples pertain to planar linkages. Other tasks call for *spherical curves*, i.e., curves lying on the surface of a sphere, which are to be implemented by means of *spherical linkages*. An example of this task is the linkage needed to guide the focal axis of a solar collector in the form of a paraboloid of revolution. The axis must aim at the centre of the Sun as this moves on the sky throughout the day, with daily adjustments, of course. One more class of tasks involve the tracing of the path generated by a line, namely, a ruled surface, which is to be implemented with a spatial linkage. An application example here is the design of the landing gear (LG) of large aircraft, in which case the generating line is the axis of one of the wheels of the LG, as large aircraft carry several wheels on each of the two halves of their LG.

While the foregoing operations can be realized by means of robots, these become impractical when the operation involves endless repetitions through the same path. A single-dof linkage is the solution here not only because of its low cost in terms of production, maintenance and servicing, but also because of reliability and repeatability. A robot cannot compete with a linkage in terms of repeatability. Other applications include the synthesis of *dwell* in production lines. For example, the gluing of labels or the filling of a bottle, presented to the pertinent mechanism of a packaging system, calls for contact

of a mechanism link with the bottle during a finite amount of time. From the results of Subsection 3.3.1, it is apparent that a four-bar linkage cannot produce dwell, which requires that output velocity and acceleration *vanish simultaneously* during a finite time interval. This then calls for a multiloop linkage, e.g., a six-bar linkage with two kinematic loops. The synthesis of a dwell mechanism then requires the addition of an extra triad<sup>1</sup> to a four-bar linkage. The triad can be of two types, RRR or RPR, with the extreme R joints coupled to the machine frame and to the coupler link of the four-bar linkage, at a designated point  $P$ . For triads of the first type, dwell is obtained by choosing the point  $P$  so that it traces, during a certain finite interval, a coupler curve (CC) that *locally* approximates a circle of radius  $r$  to a third order, meaning that the curvature of the CC is  $1/r$  at the linkage posture at which the curvature becomes *stationary* with respect to the input angle of the four-bar linkage. Points of the coupler curve with the *stationarity property* are known (Hartenberg and Denavit, 1964) to lie on a *cubic curve* fixed to the coupler link, this curve being quite appropriately known as the *cubic of stationary curvature*. For triads of the second type,  $P$  is chosen so that its coupler curve *locally* approximates a line segment to a second order, meaning that the curvature of the CC traced by  $P$  vanishes at a given posture of the linkage. It is known (Hartenberg and Denavit, 1964) that the locus of points of the coupler link with a vanishing curvature is a circle, which is rightfully known as the *inflection circle*. Both loci are unique at a given linkage posture, meaning that these loci, fixed on the coupler link, change as the linkage moves from posture to posture.

The balance of the chapter discusses the methodology behind the synthesis of planar, spherical and spatial four-bar linkages with the property that one point, the planar case, or one line, the case of the spherical and the spatial cases, of their coupler link, will visit a discrete set of points or, correspondingly, lines.

## 5.2 Planar Path Generation

The problem to be solved here is formulated as:

**Problem 5.2.1** *Synthesize a planar four-bar linkage, as shown in Fig. 5.1, whose coupler point  $P$  will attain a set of positions  $\{P_j\}_0^m$ , as the linkage is driven by its input link.*

In the problem statement above, the input link is to be decided by the designer. It could be any one of the two links pinned to the machine frame,  $BA$  or  $B^*A^*$ . Before the assignment of the driving function to one of the two foregoing links, it is futile to speak of the transmission angle<sup>2</sup> in this case, although it is common in the literature to find

---

<sup>1</sup>Similar to a dyad, a tryad is a two-link chain, with two LKPs at its free ends and one third pair coupling both.

<sup>2</sup>This concept is defined in Section 3.2.1.

synthesis problems in which the transmission angle is to be optimized at this stage.

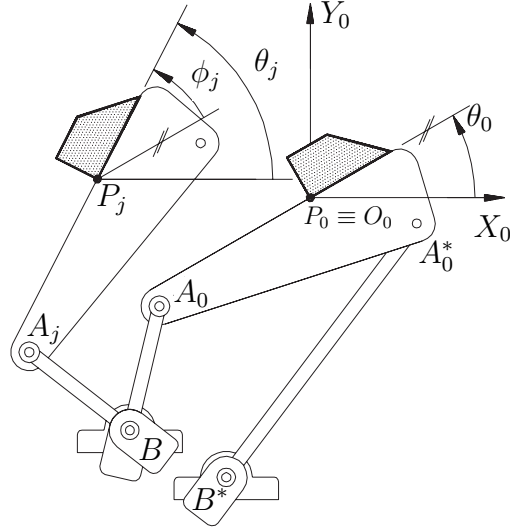


Figure 5.1: A planar four-bar linkage whose point  $R$  is to visit a set of positions  $\{R_j\}_0^m$

The general method of linkage synthesis for path generation is based on the synthesis equations derived for motion generation (Chen et al., 2008), which stem from Fig. 5.2, and recalled below for quick reference: for dyad  $BA_0$ ,

$$\mathbf{b}^T(\mathbf{1} - \mathbf{Q}_j)\mathbf{a}_0 + \mathbf{p}_j^T \mathbf{Q}_j \mathbf{a}_0 - \mathbf{p}_j^T \mathbf{b} + \frac{1}{2} \mathbf{p}_j^T \mathbf{p}_j = 0, \text{ for } j = 1, \dots, m \quad (5.1a)$$

while, for dyad  $B^*A_0^*$ ,

$$(\mathbf{b}^*)^T(\mathbf{1} - \mathbf{Q}_j)\mathbf{a}_0^* + \mathbf{p}_j^T \mathbf{Q}_j \mathbf{a}_0^* - \mathbf{p}_j^T \mathbf{b}^* + \frac{1}{2} \mathbf{p}_j^T \mathbf{p}_j = 0, \text{ for } j = 1, \dots, m \quad (5.1b)$$

If matrix  $\mathbf{Q}_j$  in the above equations is substituted by the expression given in eq.(1.6), with  $\phi_j$  in lieu of  $\theta$ , eq.(5.1a) becomes

$$(\mathbf{b} + \mathbf{p}_j)^T(c_j \mathbf{1} + s_j \mathbf{E})\mathbf{a}_0 + \mathbf{p}_j^T \left( \mathbf{b} + \frac{1}{2} \mathbf{p}_j \right) = 0, \text{ for } j = 1, \dots, m$$

with a similar expression for eq.(5.1b) and the definitions:  $c_j \equiv \cos \phi_j$  and  $s_j \equiv \sin \phi_j$ . If now the tan-half identities of eq.(3.73) are introduced in the above equation, a set of polynomial equations is obtained upon clearing denominators: for dyad  $BA_0$ ,

$$(\mathbf{b} + \mathbf{p}_j)^T[(1 - T_j^2)\mathbf{1} + 2T_j \mathbf{E}]\mathbf{a}_0 + \mathbf{p}_j^T \left( \mathbf{b} + \frac{1}{2} \mathbf{p}_j \right) (1 + T_j^2) = 0, \text{ for } j = 1, \dots, m \quad (5.2a)$$

while, for dyad  $B^*A_0^*$ ,

$$(\mathbf{b}^* + \mathbf{p}_j)^T[(1 - T_j^2)\mathbf{1} + 2T_j \mathbf{E}]\mathbf{a}_0^* + \mathbf{p}_j^T \left( \mathbf{b}^* + \frac{1}{2} \mathbf{p}_j \right) (1 + T_j^2) = 0, \text{ for } j = 1, \dots, m \quad (5.2b)$$

In summary, then, the problem involves  $8 + m$  unknowns, the two components of the four position vectors  $\mathbf{a}_0$ ,  $\mathbf{b}$ ,  $\mathbf{a}_0^*$  and  $\mathbf{b}^*$ , plus the  $m$  angles of orientation of the coupler link,  $\{\theta_j\}_1^m$ . The number of equations is  $2m$ , i.e.,  $m$  equations for each set of eqs. (5.2a & b). The maximum number of points that can be visited with a planar four-bar linkage is obtained by equating the number of equations with that of unknowns, namely,

$$8 + m = 2m, \quad \Rightarrow \quad m_{\max} = 8 \quad (5.3)$$

and, if the reference location  $P_0$  is considered, the total number of points in the plane that can be visited with a planar four-bar linkage is nine.

It should be apparent now that each of equations (5.2a & b) is *quartic* in the  $8 + m$  unknowns,  $\mathbf{a}_0$ ,  $\mathbf{b}$ ,  $\mathbf{a}_0^*$  and  $\mathbf{b}^*$ ,  $\{T_j\}_1^m$ . The *Bezout number*  $N_B$  of the system of equations (Salmon, 1964), for the maximum number of prescribed points, is, then,

$$N_B = 4^{2m_{\max}} = 4^{16} = 2^{32} = 4294967296 \quad (5.4)$$

which is about 4.3 billion! As a matter of fact, because of a concept from *algebraic geometry* known as *circularity*, the actual number of expected roots drops dramatically. An interesting case is  $m = 4$ , which leads to eight equations in 12 unknowns, thereby allowing for the free choice of four of these unknowns. Morgan and Wampler (1990) solved an instance of this problem in which they specified the two fixed joint centres  $B$  and  $B^*$ . In this case the problem is reduced to four quartic equations in four unknowns, with a Bezout number of  $4^4 = 256$ . They showed that this problem admits, in fact, up to 36 nonzero real solutions only.

The algebraic complexity of this problem reduces when the prescribed points are to be visited at prescribed values of the input angle, a problem known as *path generation with prescribed timing*. This problem is the subject of Section 5.3.

### 5.3 Planar Path Generation With Prescribed Timing

If the problem of path generation calls for a *synchronization* of the points  $\{P_j\}_0^m$  with the values of the input angle, that will be assumed to be that made by  $\overline{BA}$  with  $X_0$ , as per Fig. 5.1 and denoted  $\{\psi_j\}_0^m$  at the prescribed poses, then we have a problem of *path generation with prescribed timing*. This is the case in which one may need, for example, to have points  $\{P_j\}_0^m$  laid down on a line with equal spacing between consecutive points, for equal increments of the input angle.

The data are thus given as  $\{P_j, \psi_j\}_0^m$ . As  $\mathbf{Q}_j$  is unknown, the synthesis equations are derived now upon elimination of this matrix from eqs.(5.1a & b), as described below. Notice, however, that the set of values of the input angle,  $\{\psi_j\}_0^m$ , are now given.

## Elimination of $\mathbf{Q}_j$

Since the input link  $BA$  undergoes rotations about  $B$ , we can write

$$\mathbf{a}_j - \mathbf{b} = \mathbf{R}_j(\mathbf{a}_0 - \mathbf{b}), \quad \text{for } j = 1, \dots, m \quad (5.5)$$

where  $\mathbf{R}_j$  is the rotation matrix carrying  $\overrightarrow{BA_0}$  into  $\overrightarrow{BA_j}$  through angle  $\beta_j = \psi_j - \psi_0$ . Since timing is prescribed, introduction of matrices  $\mathbf{R}_j$  does not introduce additional unknowns. Moreover, matrix  $\mathbf{R}_j$  can be represented using eq.(1.6), with  $\theta$  replaced by  $\beta_j$ , namely,

$$\mathbf{R}_j = \cos \beta_j \mathbf{1} + \sin \beta_j \mathbf{E}, \quad \text{for } j = 1, \dots, m$$

where  $\mathbf{1}$  is the  $2 \times 2$  identity matrix and  $\mathbf{E}$  is the  $90^\circ$ -ccw rotation matrix introduced in eq.(1.1a). With reference to Fig. 5.2,

$$\mathbf{a}_j - \mathbf{p}_j = \overrightarrow{P_j A_j} = \mathbf{Q}_j \overrightarrow{P_0 A_0} = \mathbf{Q}_j \mathbf{a}_0, \quad \text{for } j = 1, \dots, m$$

Upon substituting eq.(5.5) into the above equation, we obtain

$$\mathbf{Q}_j \mathbf{a}_0 = \mathbf{R}_j \mathbf{a}_0 + (\mathbf{1} - \mathbf{R}_j) \mathbf{b} - \mathbf{p}_j, \quad j = 1, \dots, m \quad (5.6)$$

Now, if we substitute eq.(1.6) into the above equation, with  $\phi_j$  in lieu of  $\theta$ , we end up with

$$c\phi_j \mathbf{a}_0 + s\phi_j \mathbf{E} \mathbf{a}_0 = \mathbf{R}_j \mathbf{a}_0 + (\mathbf{1} - \mathbf{R}_j) \mathbf{b} - \mathbf{p}_j, \quad j = 1, \dots, m$$

which can be cast in the form

$$[\mathbf{a}_0 \ \mathbf{E} \mathbf{a}_0] \begin{bmatrix} c\phi_j \\ s\phi_j \end{bmatrix} = \underbrace{\mathbf{R}_j \mathbf{a}_0 + (\mathbf{1} - \mathbf{R}_j) \mathbf{b} - \mathbf{p}_j}_{\mathbf{c}_j}, \quad j = 1, \dots, m$$

Consequently, we can readily solve the above equation for  $c\phi_j$  and  $s\phi_j$  as

$$\begin{bmatrix} c\phi_j \\ s\phi_j \end{bmatrix} = [\mathbf{a}_0 \ \mathbf{E} \mathbf{a}_0]^{-1} \mathbf{c}_j = \frac{1}{\|\mathbf{a}_0\|^2} \begin{bmatrix} \mathbf{a}_0^T \mathbf{E}^T \\ -\mathbf{a}_0^T \end{bmatrix} \mathbf{E} \mathbf{c}_j = \frac{1}{\|\mathbf{a}_0\|^2} \begin{bmatrix} \mathbf{a}_0^T \mathbf{c}_j \\ -\mathbf{a}_0^T \mathbf{E} \mathbf{c}_j \end{bmatrix}, \quad j = 1, \dots, m$$

where we have recalled the formula for the inverse of a  $2 \times 2$  matrix given in Fact 1.4.2.

## The Equation for the $BAP$ Dyad

When the expression for  $\mathbf{Q}_j \mathbf{a}_0$  of eq.(5.6) is substituted into the synthesis equations (5.1a), we obtain

$$\mathbf{b}^T \mathbf{a}_0 - \mathbf{b}^T \mathbf{R}_j \mathbf{a}_0 - \mathbf{b}^T (\mathbf{1} - \mathbf{R}_j) \mathbf{b} + \mathbf{p}_j^T \mathbf{R}_j \mathbf{a}_0 + \mathbf{p}_j^T \mathbf{R}_j \mathbf{b} - \mathbf{p}_j^T \mathbf{b} - \frac{1}{2} \mathbf{p}_j^T \mathbf{p}_j = 0, \quad j = 1, \dots, m$$

which simplifies to

$$\mathbf{b}^T (\mathbf{1} - \mathbf{R}_j) \mathbf{b} + \mathbf{b}^T (\mathbf{R}_j - \mathbf{1}) \mathbf{a}_0 + \mathbf{p}_j^T (\mathbf{R}_j - \mathbf{1}) \mathbf{b} - \mathbf{p}_j^T \mathbf{R}_j \mathbf{a}_0 + \frac{1}{2} \mathbf{p}_j^T \mathbf{p}_j = 0, \quad (5.7)$$

thereby deriving the  $m$  synthesis equations for the left-hand dyad of Fig. 5.2 for the problem at hand. Apparently, these equations are quadratic in  $\mathbf{b}$  and linear in  $\mathbf{a}_0$ , their degree being two.

## The Equation for the $B^*A^*P$ Dyad

Vector  $\mathbf{Q}_j \mathbf{a}_0^*$  appearing in eq.(5.1b) can be derived by mimicking eq.(5.6), which yields

$$\mathbf{Q}_j \mathbf{a}_0^* = [\mathbf{a}_0^* \mathbf{E} \mathbf{a}_0^*] \begin{bmatrix} c\phi_j \\ s\phi_j \end{bmatrix} = \frac{1}{\|\mathbf{a}_0\|^2} [(\mathbf{a}_0^T \mathbf{c}_j) \mathbf{a}_0^* - (\mathbf{a}_0^T \mathbf{E} \mathbf{c}_j) \mathbf{E} \mathbf{a}_0^*], \quad \text{for } j = 1, \dots, m$$

or

$$\mathbf{Q}_j \mathbf{a}_0^* = \frac{1}{\|\mathbf{a}_0\|^2} [(\mathbf{a}_0^T \mathbf{c}_j) \mathbf{1} - (\mathbf{a}_0^T \mathbf{E} \mathbf{c}_j) \mathbf{E}] \mathbf{a}_0^*, \quad j = 1, \dots, m$$

Substituting the above expression into eq.(5.1b), we obtain, after clearing the denominator,

$$\begin{aligned} (\mathbf{b}^*)^T [(\|\mathbf{a}_0\|^2 - \mathbf{a}_0^T \mathbf{c}_j) \mathbf{1} + (\mathbf{a}_0^T \mathbf{E} \mathbf{c}_j) \mathbf{E}] \mathbf{a}_0^* + \mathbf{p}_j^T [(\mathbf{a}_0^T \mathbf{c}_j) \mathbf{1} - (\mathbf{a}_0^T \mathbf{E} \mathbf{c}_j) \mathbf{E}] \mathbf{a}_0^* \\ - \|\mathbf{a}_0\|^2 \mathbf{p}_j^T \mathbf{b}^* + \frac{1}{2} \|\mathbf{a}_0\|^2 \|\mathbf{p}_j\|^2 = 0, \quad j = 1, \dots, m \end{aligned} \quad (5.8)$$

which are the synthesis equations for the right-hand dyad of Fig. 5.2 for the problem at hand. Apparently, these  $m$  equations are all *cubic*.

## Remarks

- We have  $2m$  equations, (5.7 & 5.8), to solve for eight unknowns—the components of  $\mathbf{a}_0$ ,  $\mathbf{b}$ ,  $\mathbf{a}_0^*$ ,  $\mathbf{b}^*$ . Therefore, to have a determined system of equations, we must have  $m = 4$ , which implies that up to *five points* can be visited in a plane using a four-bar linkage, with prescribed timing.
- Since the system of eqs.(5.7 & 5.8) involves four *quadratic* and four *cubic* equations in the unknowns  $\{\mathbf{a}_0, \mathbf{b}\}$ , the *Bezout number*  $N_B$  of the system, which gives an upper bound for the number of roots to expect, thus being  $N_B = 2^4 \times 3^4 = 1296$
- Equations (5.7) are linear in  $\mathbf{a}_0$  and quadratic in  $\mathbf{b}$ . Consequently, we can eliminate  $\mathbf{a}_0$  by casting the said system in the form

$$\mathbf{Bx} = \mathbf{0} \quad (5.9)$$

in which  $\mathbf{x} = [\mathbf{a}_0^T \mathbf{1}]^T$  and  $\mathbf{B}$  is a  $4 \times 3$  matrix function of  $\mathbf{b}$  of the form

$$\mathbf{B} = \begin{bmatrix} \mathbf{b}^T (\mathbf{R}_1 - \mathbf{1}) - \mathbf{p}_1^T \mathbf{R}_1 \mathbf{b}^T (\mathbf{1} - \mathbf{R}_1) \mathbf{b} + \mathbf{p}_1^T (\mathbf{R}_1 - \mathbf{1}) \mathbf{b} + (1/2) \mathbf{p}_1^T \mathbf{p}_1 \\ \mathbf{b}^T (\mathbf{R}_2 - \mathbf{1}) - \mathbf{p}_2^T \mathbf{R}_2 \mathbf{b}^T (\mathbf{1} - \mathbf{R}_2) \mathbf{b} + \mathbf{p}_2^T (\mathbf{R}_2 - \mathbf{1}) \mathbf{b} + (1/2) \mathbf{p}_2^T \mathbf{p}_2 \\ \mathbf{b}^T (\mathbf{R}_3 - \mathbf{1}) - \mathbf{p}_3^T \mathbf{R}_3 \mathbf{b}^T (\mathbf{1} - \mathbf{R}_3) \mathbf{b} + \mathbf{p}_3^T (\mathbf{R}_3 - \mathbf{1}) \mathbf{b} + (1/2) \mathbf{p}_3^T \mathbf{p}_3 \\ \mathbf{b}^T (\mathbf{R}_4 - \mathbf{1}) - \mathbf{p}_4^T \mathbf{R}_4 \mathbf{b}^T (\mathbf{1} - \mathbf{R}_4) \mathbf{b} + \mathbf{p}_4^T (\mathbf{R}_4 - \mathbf{1}) \mathbf{b} + (1/2) \mathbf{p}_4^T \mathbf{p}_4 \end{bmatrix}$$

For the  $4 \times 3$  matrix  $\mathbf{B}$  to have a nontrivial null space, which is needed in light of the form of  $\mathbf{x}$ ,  $\mathbf{B}$  must be rank-deficient. This means that every  $3 \times 3$  submatrix of

$\mathbf{B}$  must be singular. We can thus derive four bivariate polynomial equations in the Cartesian coordinates  $u$  and  $v$  of  $B$ , the components of  $\mathbf{b}$ , namely,

$$\Delta_j(u, v) = \det(\mathbf{B}_j), \quad \text{for } j = 1, \dots, 4 \quad (5.10)$$

where  $\Delta_j$  is the determinant of the  $j$ th  $3 \times 3$  submatrix  $\mathbf{B}_j$ , obtained by deleting the  $j$ th row of  $\mathbf{B}$ . Notice that  $\Delta_j$  can be computed by the cofactors of the third column of its corresponding matrix. Moreover, this column is quadratic in  $\mathbf{b}$ , the corresponding cofactors being determinants of  $2 \times 2$  matrices whose entries are linear in  $\mathbf{b}$ . Such a determinant is expanded in Fact 1.4.1, Subsection 1.4.2, in which it is apparent that this determinant is a bilinear expression of its rows or, correspondingly, of its columns. Hence, each  $2 \times 2$  cofactor is quadratic in  $\mathbf{b}$ , the result being that  $\Delta_j$  is quartic in  $\mathbf{b}$ . Therefore, the Bezout number of any pair of those equations is  $N_B = 4^2 = 16$ .

Moreover, each eq.(5.10) defines a *contour* in the  $u$ - $v$  plane. The real solutions of system (5.9) can be visually estimated by plotting the  $m$  contours in the same figure. Notice that, at the outset, we do not have bounds for the location of  $B$  in the  $u$ - $v$  plane. However, we always have a region available of this plane in which we can anchor the revolute centre  $B$ . Our first attempt of finding real solutions for  $B$  is thus this region.

Once  $\mathbf{b}$  is known, we can solve for  $\mathbf{a}_0$  from eq.(5.9) using a least-square approximation. To this end, we rewrite eq.(5.9) in the form

$$\mathbf{M}\mathbf{a}_0 = \mathbf{n}$$

where

$$\mathbf{M} = \begin{bmatrix} \mathbf{b}^T(\mathbf{R}_1 - \mathbf{1}) - \mathbf{p}_1^T \mathbf{R}_1 \\ \mathbf{b}^T(\mathbf{R}_2 - \mathbf{1}) - \mathbf{p}_2^T \mathbf{R}_2 \\ \mathbf{b}^T(\mathbf{R}_3 - \mathbf{1}) - \mathbf{p}_3^T \mathbf{R}_3 \\ \mathbf{b}^T(\mathbf{R}_4 - \mathbf{1}) - \mathbf{p}_4^T \mathbf{R}_4 \end{bmatrix}, \quad \mathbf{n} = \begin{bmatrix} \mathbf{b}^T(\mathbf{R}_1 - \mathbf{1})\mathbf{b} - \mathbf{p}_1^T(\mathbf{R}_1 - \mathbf{1})\mathbf{b} - (1/2)\mathbf{p}_1^T \mathbf{p}_1 \\ \mathbf{b}^T(\mathbf{R}_2 - \mathbf{1})\mathbf{b} - \mathbf{p}_2^T(\mathbf{R}_2 - \mathbf{1})\mathbf{b} - (1/2)\mathbf{p}_2^T \mathbf{p}_2 \\ \mathbf{b}^T(\mathbf{R}_3 - \mathbf{1})\mathbf{b} - \mathbf{p}_3^T(\mathbf{R}_3 - \mathbf{1})\mathbf{b} - (1/2)\mathbf{p}_3^T \mathbf{p}_3 \\ \mathbf{b}^T(\mathbf{R}_4 - \mathbf{1})\mathbf{b} - \mathbf{p}_4^T(\mathbf{R}_4 - \mathbf{1})\mathbf{b} - (1/2)\mathbf{p}_4^T \mathbf{p}_4 \end{bmatrix}$$

- Equation (5.8) is bilinear in  $\mathbf{b}^*$  and  $\mathbf{a}_0^*$ . Once we have  $\mathbf{a}_0$  and  $\mathbf{b}$  from eq.(5.9), we can solve eq.(5.8) for  $\mathbf{a}_0^*$  and  $\mathbf{b}^*$  using dialytic elimination, as we did in the motion-generation case. That is, computing  $\mathbf{b}^*$  and  $\mathbf{a}_0^*$  leads to the solution of one quartic polynomial. We need not find the roots of this polynomial numerically, if we apply the contour technique introduced in Chapter 4.

## Reducing the Degree of the Synthesis Equations of the BAP Dyad

Using the definition of  $\mathbf{Q}_j$  of eq.(1.6), the first term of eq.(5.7) can be further simplified to

$$\mathbf{b}^T(\mathbf{1} - \mathbf{R}_j)\mathbf{b} = \mathbf{b}^T[(1 - c\beta_j)\mathbf{1} + s\beta_j \mathbf{E}]\mathbf{b} = (1 - c\beta_j)\|\mathbf{b}\|^2, \quad j = 1, \dots, m$$

where we used the identity  $\mathbf{b}^T \mathbf{E} \mathbf{b} \equiv 0$ , because matrix  $\mathbf{E}$  is *skew-symmetric*. Thus, eq.(5.7) reduces to

$$(1 - c\beta_j) \|\mathbf{b}\|^2 + \mathbf{b}^T (\mathbf{R}_j - \mathbf{1}) \mathbf{a}_0 + \mathbf{p}_j^T (\mathbf{R}_j - \mathbf{1}) \mathbf{b} - \mathbf{p}_j^T \mathbf{R}_j \mathbf{a}_0 + \frac{1}{2} \mathbf{p}_j^T \mathbf{p}_j = 0 \quad (5.11)$$

for  $j = 1, \dots, m$ .

Let  $M$  be  $j \in \{1, \dots, m\}$  that maximizes  $|1 - c\beta_j|$  and use the  $M$ th equation of eqs.(5.11) as a pivot, to reduce the order of the remaining equations. After a reshuffling of the equations, we let  $M = 1$ , so that now the pivot equation is the first one of the set. Just as in Gaussian elimination, subtract a “suitable” multiple of the first equation from the remaining ones, so as to eliminate the quadratic term of those equations, which leads, for  $j = 2, \dots, m$ , to

$$(1 - c\beta_1) \|\mathbf{b}\|^2 + \mathbf{b}^T (\mathbf{R}_1 - \mathbf{1}) \mathbf{a}_0 + \mathbf{p}_1^T (\mathbf{R}_1 - \mathbf{1}) \mathbf{b} - \mathbf{p}_1^T \mathbf{R}_1 \mathbf{a}_0 + \frac{1}{2} \mathbf{p}_1^T \mathbf{p}_1 = 0 \quad (5.12a)$$

$$\begin{aligned} & \mathbf{b}^T [\mathbf{R}_j - \mathbf{1} - q_j(\mathbf{R}_j - \mathbf{1})] \mathbf{a}_0 + [\mathbf{p}_j^T (\mathbf{R}_j - \mathbf{1}) - q_j \mathbf{p}_j^T (\mathbf{R}_1 - \mathbf{1})] \mathbf{b} \\ & - (\mathbf{p}_j^T \mathbf{R}_j - q_j \mathbf{p}_1^T \mathbf{R}_1) \mathbf{a}_0 + \frac{1}{2} (\mathbf{p}_j^T \mathbf{p}_j - \mathbf{p}_1^T \mathbf{p}_1) = 0 \quad (5.12b) \\ & j = 2, \dots, m \end{aligned}$$

where

$$q_j = \frac{1 - c\beta_j}{1 - c\beta_1}$$

System (5.12) can be cast in linear-homogeneous form in  $\mathbf{x}$ , if this vector is defined as  $\mathbf{x} = [\mathbf{a}_0^T \ 1]^T$ , thereby obtaining

$$\mathbf{Bx} = \mathbf{0}_4 \quad (5.13a)$$

with

$$\mathbf{B} = \begin{bmatrix} \mathbf{b}^T (\mathbf{R}_1 - \mathbf{1}) - \mathbf{p}_1^T \mathbf{R}_1 & s_1 \\ (1 - q_2) \mathbf{b}^T (\mathbf{R}_2 - \mathbf{1}) - (\mathbf{p}_2^T \mathbf{R}_2 - q_2 \mathbf{p}_1^T \mathbf{R}_1) & s_2 \\ (1 - q_3) \mathbf{b}^T (\mathbf{R}_3 - \mathbf{1}) - (\mathbf{p}_3^T \mathbf{R}_3 - q_3 \mathbf{p}_1^T \mathbf{R}_1) & s_3 \\ (1 - q_4) \mathbf{b}^T (\mathbf{R}_4 - \mathbf{1}) - (\mathbf{p}_4^T \mathbf{R}_4 - q_4 \mathbf{p}_1^T \mathbf{R}_1) & s_4 \end{bmatrix} \quad (5.13b)$$

and

$$s_1 = (1 - c\beta_1) \|\mathbf{b}\|^2 + \mathbf{p}_1^T (\mathbf{R}_1 - \mathbf{1}) \mathbf{b} + \frac{1}{2} \mathbf{p}_1^T \mathbf{p}_1 \quad (5.13c)$$

$$s_j = [\mathbf{p}_j^T (\mathbf{R}_j - \mathbf{1}) - q_j \mathbf{p}_j^T (\mathbf{R}_1 - \mathbf{1})] \mathbf{b} + \frac{1}{2} (\mathbf{p}_j^T \mathbf{p}_j - \mathbf{p}_1^T \mathbf{p}_1) \quad j = 2, \dots, m \quad (5.13d)$$

Notice that  $s_1$  is quadratic and  $\{s_j\}_2^m$  are all linear in  $\mathbf{b}$ . Thus, the corresponding  $\Delta_1$  of eq.(5.10) for system (5.13) is quadratic, but  $\{\Delta_j\}_2^m$  are all cubic in  $\mathbf{b}$ . Consequently, the Bezout number of any pair of equations  $(1, j)$ , for  $j = 2, \dots, m$ , is  $N_B = 3 \times 4 = 12$ .

## 5.4 Coupler Curves of Planar Four-Bar Linkages

The four-bar linkage of Fig. 5.2 is given in a Cartesian frame  $\mathcal{F}$  with origin at the midpoint of segment  $\overline{BB^*}$  and axis  $X$  containing the foregoing segment. The trajectory traced by point  $P$  of its coupler link is called the *coupler curve* traced by that point.

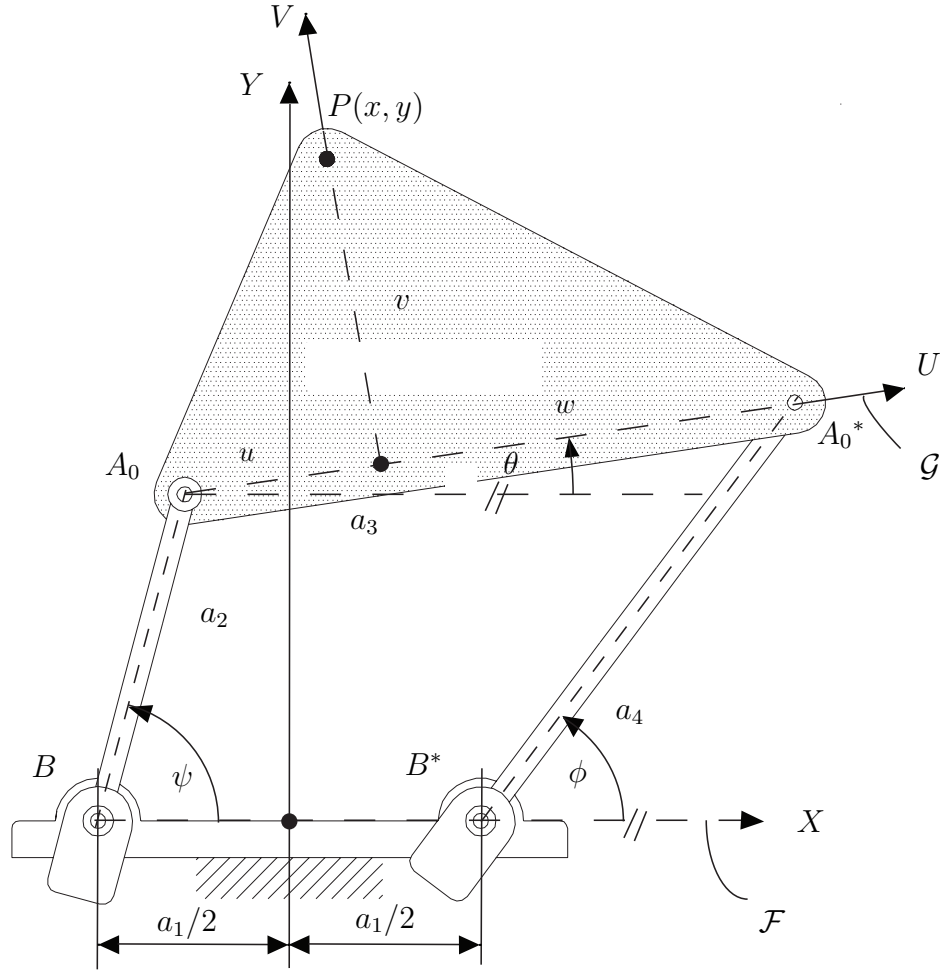


Figure 5.2: Determination of the coupler curve traced by point  $P$  of a planar four-bar linkage

### Construction of the Coupler Curve

We start by proving a basic result in planar kinematics regarding the nature of the coupler curve of a planar four-bar linkage, namely,

**Theorem 5.4.1 (Coupler Curve of a Planar Four-Bar Linkage)** *The curve traced by any point of the coupler link of a planar four-bar linkage is algebraic, of sixth degree.*

In general, a curve can be either *algebraic* or *non-algebraic*. A planar curve is algebraic if it is given by an implicit function  $F(x, y) = 0$ , with  $F(x, y)$  being the sum of products of integer powers of  $x$  and  $y$ . The *degree* of the curve is the highest degree of the various terms making up  $F(x, y)$ . Moreover, a curve of degree  $n$  intersects a straight line at a maximum of  $n$  points, which the reader is invited to prove. Thus, the coupler curve of a four-bar linkage intersects a straight line at a maximum of six points. As a consequence, the coupler curve under discussion *cannot have straight segments of finite length*. There are, however, well-known examples of planar four-bar linkages that trace coupler curves that, to the naked eye, appear as having line segments. The best known of these linkages are those bearing the eponyms of Roberts and Chebyshev. Linkages capable of tracing *exactly* line segments are also known, but these comprise more than four links and more than one kinematic loop, e.g., those of Peaucellier and Hart (Bricard, 1927; Dudită et al., 1989; McCarthy and Soh, 2011).

The coupler link carries a point  $P(x, y)$  lying on the  $V$ -axis of a second Cartesian frame,  $\mathcal{G}$ , its  $U$ -axis passing through  $A_0$  and  $A_0^*$ . What we need now is an implicit function  $F(x, y) = 0$ , free of any linkage variable, and having as parameters the link lengths.

The desired function is obtained by first noticing that, irrespective of the linkage posture,

$$\|\overrightarrow{BA_0}\|^2 = a_2^2, \quad \|\overrightarrow{B^*A_0^*}\|^2 = a_4^2 \quad (5.14)$$

Vectors  $\overrightarrow{BA_0}$  and  $\overrightarrow{B^*A_0^*}$  can be expressed as

$$\overrightarrow{BA_0} = \mathbf{a}_0 - \mathbf{b} = \mathbf{p} - \overrightarrow{A_0P} - \mathbf{b} \quad (5.15a)$$

$$\overrightarrow{B^*A_0^*} = \mathbf{a}_0^* - \mathbf{b}^* = \mathbf{p} - \overrightarrow{A_0^*P} - \mathbf{b}^* \quad (5.15b)$$

where, in our standard notation,  $\mathbf{a}_0$  ( $\mathbf{a}_0^*$ ),  $\mathbf{b}$  ( $\mathbf{b}^*$ ) and  $\mathbf{p}$  denote the position vectors of  $A_0$  ( $A_0^*$ ),  $B$  ( $B^*$ ) and  $P$  in  $\mathcal{F}$ .

In light of the two foregoing expressions, the left-hand sides of eqs.(5.14) take the forms

$$\|\overrightarrow{BA_0}\|^2 = \|\mathbf{p}\|^2 + \|\overrightarrow{A_0P}\|^2 + \|\mathbf{b}\|^2 - 2\mathbf{p}^T \overrightarrow{A_0P} - 2\mathbf{p}^T \mathbf{b} + 2\mathbf{b}^T \overrightarrow{A_0P} \quad (5.16a)$$

$$\|\overrightarrow{B^*A_0^*}\|^2 = \|\mathbf{p}\|^2 + \|\overrightarrow{A_0^*P}\|^2 + \|\mathbf{b}^*\|^2 - 2\mathbf{p}^T \overrightarrow{A_0^*P} - 2\mathbf{p}^T \mathbf{b}^* + 2\mathbf{b}^{*T} \overrightarrow{A_0^*P} \quad (5.16b)$$

Vectors  $\mathbf{a}_0$ ,  $\mathbf{a}_0^*$ ,  $\mathbf{b}$  and  $\mathbf{b}^*$  are given directly in frame  $\mathcal{F}$ ,  $\overrightarrow{PA_0}$  and  $\overrightarrow{PA_0^*}$  in  $\mathcal{G}$ . In order to express the latter in  $\mathcal{F}$  a *rotation*  $\mathbf{Q}$  that takes  $\mathcal{F}$  into  $\mathcal{G}$  is introduced:

$$\mathbf{Q} = \begin{bmatrix} \cos \theta & -\sin \theta \\ -\sin \theta & \cos \theta \end{bmatrix} \quad (5.17a)$$

which can be expressed as

$$\mathbf{Q} = \mathbf{1} \cos \theta + \mathbf{E} \sin \theta \quad (5.17b)$$

with  $\mathbf{1}$  denoting the  $2 \times 2$  identity matrix, while  $\mathbf{E}$  is the  $2 \times 2$  matrix defined in eq.(1.1a).

Now vectors  $\overrightarrow{PA_0}$  and  $\overrightarrow{PA_0^*}$  can be represented in  $\mathcal{F}$  as

$$[\overrightarrow{PA_0}]_{\mathcal{F}} = \mathbf{Q}^T [\overrightarrow{PA_0}]_{\mathcal{G}} = \mathbf{Q}^T \mathbf{g}, \quad [\overrightarrow{PA_0^*}]_{\mathcal{F}} = \mathbf{Q}^T [\overrightarrow{PA_0^*}]_{\mathcal{G}} = \mathbf{Q}^T \mathbf{g}^* \quad (5.18)$$

where

$$\mathbf{g} = [-u \quad -v]^T, \quad \mathbf{g}^* = [w \quad -v]^T \quad (5.19)$$

Substitution of eqs.(5.16a), (5.16b) and (5.18) into eqs.(5.14), while taking into account that

$$\|\overrightarrow{PA_0}\|^2 = u^2 + v^2, \quad \|\overrightarrow{PA_0^*}\|^2 = w^2 + v^2, \quad \|\mathbf{b}\|^2 = \|\mathbf{b}^*\|^2 = \frac{a_1^2}{4} \quad (5.20)$$

leads, correspondingly, to

$$\|\mathbf{p}\|^2 + 2\mathbf{g}^T(\mathbf{b} - \mathbf{p}) \cos \theta + 2\mathbf{g}^T \mathbf{E}(\mathbf{b} - \mathbf{p}) \sin \theta - 2\mathbf{b}^T \mathbf{p} + u^2 + v^2 + \frac{a_1^2}{4} - a_2^2 = 0 \quad (5.21a)$$

$$\|\mathbf{p}\|^2 + 2\mathbf{g}^{*T}(\mathbf{b}^* - \mathbf{p}) \cos \theta + 2\mathbf{g}^{*T} \mathbf{E}(\mathbf{b}^* - \mathbf{p}) \sin \theta - 2\mathbf{b}^{*T} \mathbf{p} + w^2 + v^2 + \frac{a_1^2}{4} - a_4^2 = 0 \quad (5.21b)$$

In order to transform the above trigonometric equations into algebraic form, the tangent-half identities are introduced:

$$\cos \theta = \frac{1 - T^2}{1 + T^2}, \quad \sin \theta = \frac{2T}{1 + T^2}, \quad T \equiv \tan\left(\frac{\theta}{2}\right)$$

Hence, eqs.(5.21a & b) become quadratic in  $T$ , namely,

$$A_1 T^2 - 2B_1 T + C_1 = 0 \quad (5.22a)$$

$$A_2 T^2 - 2B_2 T + C_2 = 0 \quad (5.22b)$$

where

$$A_1 = \|\mathbf{p}\|^2 - 2\mathbf{g}^T(\mathbf{b} - \mathbf{p}) - 2\mathbf{b}^T \mathbf{p} + u^2 + v^2 + a_1^2/4 - a_2^2 \quad (5.23a)$$

$$B_1 = -2\mathbf{g}^T \mathbf{E}(\mathbf{b} - \mathbf{p}) \quad (5.23b)$$

$$C_1 = \|\mathbf{p}\|^2 + 2\mathbf{g}^{*T}(\mathbf{b}^* - \mathbf{p}) - 2\mathbf{b}^{*T} \mathbf{p} + u^2 + v^2 + \frac{a_1^2}{4} - a_4^2 \quad (5.23c)$$

$$A_2 = \|\mathbf{p}\|^2 - 2\mathbf{g}^{*T}(\mathbf{b}^* - \mathbf{p}) - 2\mathbf{b}^{*T} \mathbf{p} + w^2 + v^2 + a_1^2/4 - a_4^2 \quad (5.23d)$$

$$B_2 = -2\mathbf{g}^{*T} \mathbf{E}(\mathbf{b}^* - \mathbf{p}) \quad (5.23e)$$

$$C_2 = \|\mathbf{p}\|^2 + 2\mathbf{g}^{*T}(\mathbf{b}^* - \mathbf{p}) - 2\mathbf{b}^{*T} \mathbf{p} + w^2 + v^2 + \frac{a_1^2}{4} - a_4^2 \quad (5.23f)$$

Apparently, coefficients  $A_1$ ,  $A_2$ ,  $C_1$  and  $C_2$  are *quadratic*,  $B_1$  and  $B_2$  *linear in  $\mathbf{p}$* . Moreover, all four coefficients quadratic in  $\mathbf{p}$  involve only one such term, namely,  $\|\mathbf{p}\|^2$ . Hence, upon subtracting both sides of eq.(5.22b) from the corresponding sides of eq.(5.22a), one third equation in  $T$  is obtained, namely,

$$A_3 T^2 - 2B_3 T + C_3 = 0 \quad (5.24)$$

with coefficients

$$A_3 = 2(\mathbf{g} - \mathbf{g}^* - \mathbf{b} + \mathbf{b}^*)^T \mathbf{p} - 2(\mathbf{g}^T \mathbf{b} - \mathbf{g}^{*T} \mathbf{b}^*) + u^2 - w^2 - a_2^2 + a_4^2 \quad (5.25a)$$

$$B_3 = 2(\mathbf{g} - \mathbf{g}^*)^T \mathbf{E} \mathbf{p} - 2(\mathbf{g}^T \mathbf{E} \mathbf{b} - \mathbf{g}^{*T} \mathbf{E} \mathbf{b}^*) \quad (5.25b)$$

$$C_3 = -2(\mathbf{g} - \mathbf{g}^* + \mathbf{b} - \mathbf{b}^*)^T \mathbf{p} + 2(\mathbf{g}^T \mathbf{b} - \mathbf{g}^{*T} \mathbf{b}^*) + u^2 - w^2 - a_2^2 + a_4^2 \quad (5.25c)$$

Further, multiplying both sides of eqs.(5.22a) and (5.24) by  $T$ , two additional polynomial equations in  $T$  are derived:

$$A_1 T^3 - 2B_1 T^2 + C_1 T = 0 \quad (5.26a)$$

$$A_3 T^3 - 2B_3 T^2 + C_3 T = 0 \quad (5.26b)$$

eqs.(5.22a), (5.24), (5.26a) and (5.26b) thus forming a system of four linear homogeneous equations in the four powers of  $T$ :  $T^0, \dots$  and  $T^3$ , namely,

$$\mathbf{M} \mathbf{t} = \mathbf{0}_4 \quad (5.27)$$

with  $\mathbf{M}$  and  $\mathbf{t}$  defined as

$$\mathbf{M} = \begin{bmatrix} A_1 & -2B_1 & C_1 & 0 \\ A_3 & -2B_3 & C_3 & 0 \\ 0 & A_1 & -2B_1 & C_1 \\ 0 & A_3 & -2B_3 & C_3 \end{bmatrix}, \quad \mathbf{t} = \begin{bmatrix} T^3 \\ T^2 \\ T \\ 1 \end{bmatrix} \quad (5.28)$$

Since eq.(5.27) must admit nontrivial solutions—the fourth component of  $\mathbf{t}$  is identically unity—matrix  $\mathbf{M}$  must be singular, and hence,

$$\Delta \equiv \det(\mathbf{M}) = 0 \quad (5.29)$$

The entries of  $\mathbf{M}$  are apparently all scalar functions of vector  $\mathbf{p}$ . In particular,  $A_1$  and  $C_1$  are quadratic, while  $A_3, B_1, B_3$  and  $C_3$  are linear in  $\mathbf{p}$ . Therefore, two rows of  $\mathbf{M}$  are quadratic two are linear in  $\mathbf{p}$ , which leads to a determinant of degree sixth in  $\mathbf{p}$ , as the reader is invited to prove. Upon expansion,

$$\Delta = 4 A_1 B_1 B_3 C_3 - 4 A_1 B_3^2 C_1 - A_1^2 C_3^2 + 2 A_1 A_3 C_1 C_3 - 4 A_3 B_1^2 C_3 + 4 A_3 B_1 B_3 C_1 - A_3^2 C_1^2 \quad (5.30)$$

Apparently, each of the seven terms of  $\Delta$  is at most, sextic in  $\mathbf{p}$ , which means that  $\Delta(\mathbf{p})$  is indeed a sextic polynomial in  $\mathbf{p}$ .

In summary,  $\Delta(\mathbf{p}) = \Delta(x, y) = 0$  defines a sextic curve in the  $X$ - $Y$  plane, thereby proving Theorem 5.4.1.

### Example 5.4.1 (Coupler curve of a planar four-bar linkage<sup>3</sup>)

A planar four-bar linkage and a point  $P$  of its coupler link are defined by the linkage parameters given below:

$$a_1 = 200, a_2 = 100, a_3 = 230, a_4 = 230, u = 80, v = 170, w = 150$$

all in the same units. Draw the coupler curve traced by point  $P$  in the two conjugate configurations of the linkage.

Figures 5.3 and 5.4 show the coupler curve traced by point  $P$  of the above linkage when postured in its two conjugate configurations. For simplicity, the coordinate axes are not included, but they are obvious.

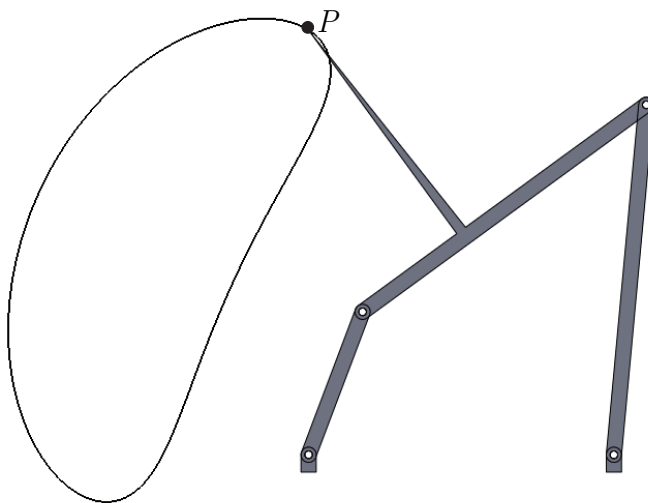


Figure 5.3: Curve of a planar four-bar linkage traced by a point  $P$  of its coupler link

## 5.5 The Theorem of Roberts-Chebyshev

In the realm of planar-linkage synthesis for path generation it is noteworthy that the solution to any problem is not unique. In fact, for every coupler curve generated by a planar four-bar linkage, there exist two more four-bar linkages, called the *cognates* of the first one, that trace exactly the same coupler curve.

A proof of this result is available in (Bricard, 1927) and (Malik et al., 1994).

---

<sup>3</sup>The algorithm and the code to plot the coupler curves of this example were produced by Salvatore Grande, University of Cassino, Italy.

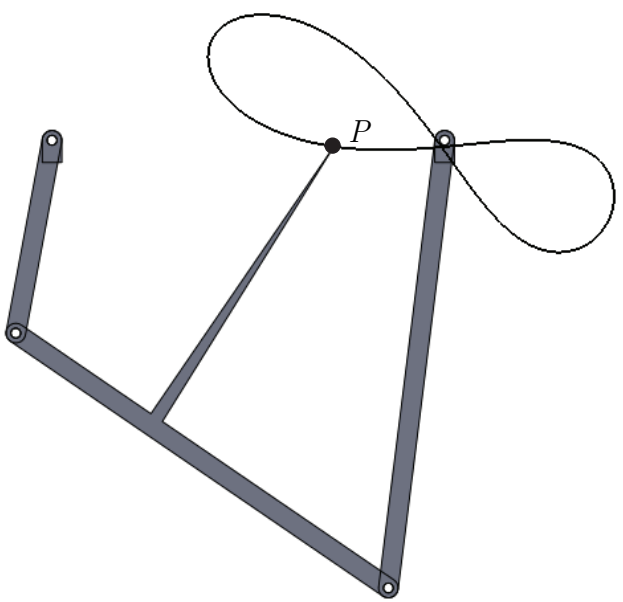


Figure 5.4: Coupler curve of the same point  $P$  of the same linkage as that of Fig. 5.3, as traced by its conjugate configuration

# Appendix A

## A Summary of Dual Algebra

The algebra of dual numbers is recalled here, with extensions to vector and matrix operations. This material is reproduced from a chapter in a NATO Advanced Study Institute book<sup>1</sup>

### A.1 Introduction

The aim of this Appendix is to outline the applications of dual algebra to kinematic analysis. To this end, the algebra of dual scalars, vectors, and matrices is first recalled. The applications included here refer to the computation of the parameters of the screw of a rigid body between two finitely-separated positions and of the instant screw. However, the applications of dual numbers go beyond that in kinematics. Indeed, the well-known *Principle of Transference* (Dimentberg, 1965; Bottema and Roth, 1978; Rico Martínez and Duffy, 1993) has been found extremely useful in spatial kinematics, since it allows the derivation of spatial kinematic relations by simply *dualizing* the corresponding relations of spherical kinematics.

*Dual numbers* were first proposed by Clifford (1873), their first applications to kinematics being attributed to both Kotel'nikov (1895) and Study (1903). A comprehensive analysis of dual numbers and their applications to the kinematic analysis of spatial linkages was conducted by Yang (1963) and Yang and Freudenstein (1964). Bottema and Roth(1978) include a treatment of theoretical kinematics using dual numbers. More

---

<sup>1</sup>Angeles, J., 1998, “The Application of Dual Algebra to Kinematic Analysis”, in Angeles, J. and Zakhariiev, E. (editors), Computational Methods in Mechanical Systems, Springer-Verlag, Heidelberg, Vol. 161, pp. 3-31.

recently, Agrawal (1987) reported on the application of dual quaternions to spatial kinematics, while Pradeep, Yoder, and Mukundan (1989) used the dual-matrix exponential in the analysis of robotic manipulators. Shoham and Brodsky (1993, 1994) have proposed a dual inertia operator for the dynamical analysis of mechanical systems. A comprehensive introduction to dual quaternions is to be found in (McCarthy, 1990), while an abstract treatment is found in (Chevallier, 1991).

## A.2 Definitions

A *dual number*  $\hat{a}$  is defined as the sum of a *primal part*  $a$ , and a *dual part*  $a_0$ , namely,

$$\hat{a} = a + \epsilon a_0 , \quad (\text{A.1})$$

where  $\epsilon$  is the dual unity, which verifies  $\epsilon \neq 0$ ,  $\epsilon^2 = 0$ , and  $a$  and  $a_0$  are real numbers, the former being the *primal part* of  $\hat{a}$ , the latter its *dual part*. Actually, dual numbers with complex parts can be equally defined (Cheng and Thompson, 1996). For the purposes of this chapter, real numbers will suffice.

If  $a_0 = 0$ ,  $\hat{a}$  is called a *real number*, or, correspondingly, a *complex number*; if  $a = 0$ ,  $\hat{a}$  is called a *pure dual number*; and if neither is zero  $\hat{a}$  is called a *proper dual number*.

Let  $\hat{b} = b + \epsilon b_0$  be another dual number. Equality, addition, multiplication, and division are defined, respectively, as

$$\hat{a} = \hat{b} \Leftrightarrow a = b, \quad a_0 = b_0 \quad (\text{A.2a})$$

$$\hat{a} + \hat{b} = (a + b) + \epsilon(a_0 + b_0) \quad (\text{A.2b})$$

$$\hat{a}\hat{b} = ab + \epsilon(ab_0 + a_0b) \quad (\text{A.2c})$$

$$\frac{\hat{a}}{\hat{b}} = \frac{a}{b} - \epsilon \left( \frac{ab_0 - a_0b}{b^2} \right), \quad b \neq 0 . \quad (\text{A.2d})$$

From eq.(A.2d) it is apparent that the division by a pure dual number is not defined. Hence, dual numbers do not form a *field* in the algebraic sense; they do form a *ring* (Simmons, 1963).

All formal operations involving dual numbers are identical to those of ordinary algebra, while taking into account that  $\epsilon^2 = \epsilon^3 = \dots = 0$ . Therefore, the series expansion of the *analytic function*  $f(\hat{x})$  of a dual argument  $\hat{x}$  is given by

$$f(\hat{x}) = f(x + \epsilon x_0) = f(x) + \epsilon x_0 \frac{df(x)}{dx} . \quad (\text{A.3})$$

As a direct consequence of eq.(A.3), we have the expression below for the exponential of a dual number  $\hat{x}$ :

$$e^{\hat{x}} = e^x + \epsilon x_0 e^x = e^x(1 + \epsilon x_0) , \quad (\text{A.4})$$

and hence, *the dual exponential cannot be a pure dual number.*

The *dual angle*  $\hat{\theta}$  between two skew lines  $\mathcal{L}_1$  and  $\mathcal{L}_2$ , introduced by Study (1903), is defined as

$$\hat{\theta} = \theta + \epsilon s , \quad (\text{A.5})$$

where  $\theta$  and  $s$  are, respectively, the twist angle and the distance between the two lines. The *dual trigonometric functions* of the dual angle  $\hat{\theta}$  are derived directly from eq.(A.3), namely,

$$\cos \hat{\theta} = \cos \theta - \epsilon s \sin \theta , \quad \sin \hat{\theta} = \sin \theta + \epsilon s \cos \theta , \quad \tan \hat{\theta} = \tan \theta + \epsilon s \sec^2 \theta . \quad (\text{A.6})$$

Moreover, all identities for ordinary trigonometry hold for dual angles. Likewise, the square root of a dual number can be readily found by a straightforward application of eq.(A.3), namely,

$$\sqrt{\hat{x}} = \sqrt{x} + \epsilon \frac{x_0}{2\sqrt{x}} , \quad (\text{A.7})$$

A *dual vector*  $\hat{\mathbf{a}}$  is defined as the sum of a primal vector part  $\mathbf{a}$ , and a dual vector part  $\mathbf{a}_0$ , namely,

$$\hat{\mathbf{a}} = \mathbf{a} + \epsilon \mathbf{a}_0 , \quad (\text{A.8})$$

where both  $\mathbf{a}$  and  $\mathbf{a}_0$  are Cartesian, 3-dimensional vectors. Henceforth, all vectors are assumed to be of this kind. Further, let  $\hat{\mathbf{a}}$  and  $\hat{\mathbf{b}}$  be two dual vectors and  $\hat{c}$  be a dual scalar. The concepts of dual-vector equality, multiplication of a dual vector by a dual scalar, inner product and vector product of two dual vectors are defined below:

$$\hat{\mathbf{a}} = \hat{\mathbf{b}} \Leftrightarrow \mathbf{a} = \mathbf{b} \quad \text{and} \quad \mathbf{a}_0 = \mathbf{b}_0 ; \quad (\text{A.9a})$$

$$\hat{c} \hat{\mathbf{a}} = c \mathbf{a} + \epsilon (c_0 \mathbf{a} + c \mathbf{a}_0) ; \quad (\text{A.9b})$$

$$\hat{\mathbf{a}} \cdot \hat{\mathbf{b}} = \mathbf{a} \cdot \mathbf{b} + \epsilon (\mathbf{a} \cdot \mathbf{b}_0 + \mathbf{a}_0 \cdot \mathbf{b}) ; \quad (\text{A.9c})$$

$$\hat{\mathbf{a}} \times \hat{\mathbf{b}} = \mathbf{a} \times \mathbf{b} + \epsilon (\mathbf{a} \times \mathbf{b}_0 + \mathbf{a}_0 \times \mathbf{b}) . \quad (\text{A.9d})$$

In particular, when  $\hat{\mathbf{b}} = \hat{\mathbf{a}}$ , eq.(A.9c) leads to the *Euclidean norm* of the dual vector  $\hat{\mathbf{a}}$ , i.e.,

$$\|\hat{\mathbf{a}}\|^2 = \|\mathbf{a}\|^2 + \epsilon 2 \mathbf{a} \cdot \mathbf{a}_0 . \quad (\text{A.9e})$$

Furthermore, the six *normalized Plücker coordinates* of a line  $\mathcal{L}$  passing through a point  $P$  of position vector  $\mathbf{p}$  and parallel to the unit vector  $\mathbf{e}$  are given by the pair  $(\mathbf{e}, \mathbf{p} \times \mathbf{e})$ , where the product  $\mathbf{e}_0 \equiv \mathbf{p} \times \mathbf{e}$  denotes the *moment* of the line. The foregoing coordinates can be represented by a *dual unit vector*  $\hat{\mathbf{e}}^*$ , whose six real components in  $\mathbf{e}$  and  $\mathbf{e}_0$  are the Plücker coordinates of  $\mathcal{L}$ , namely,

$$\hat{\mathbf{e}}^* = \mathbf{e} + \epsilon \mathbf{e}_0, \quad \text{with} \quad \|\mathbf{e}\| = 1 \quad \text{and} \quad \mathbf{e} \cdot \mathbf{e}_0 = 0. \quad (\text{A.10})$$

The reader is invited to verify the results summarized below:

**Lemma A.2.1** *For  $\hat{\mathbf{e}}^* \equiv \mathbf{e} + \epsilon \mathbf{e}_0$  and  $\hat{\mathbf{f}}^* \equiv \mathbf{f} + \epsilon \mathbf{f}_0$  defined as two dual unit vectors representing lines  $\mathcal{L}$  and  $\mathcal{M}$ , respectively, we have:*

- (i) *If  $\hat{\mathbf{e}}^* \times \hat{\mathbf{f}}^*$  is a pure dual vector, then  $\mathcal{L}$  and  $\mathcal{M}$  are parallel;*
- (ii) *if  $\hat{\mathbf{e}}^* \cdot \hat{\mathbf{f}}^*$  is a pure dual number, then  $\mathcal{L}$  and  $\mathcal{M}$  are perpendicular;*
- (iii)  *$\mathcal{L}$  and  $\mathcal{M}$  are coincident if and only if  $\hat{\mathbf{e}}^* \times \hat{\mathbf{f}}^* = \mathbf{0}$ ; and*
- (iv)  *$\mathcal{L}$  and  $\mathcal{M}$  intersect at right angles if and only if  $\hat{\mathbf{e}}^* \cdot \hat{\mathbf{f}}^* = 0$ .*

Dual matrices can be defined likewise, i.e., if  $\mathbf{A}$  and  $\mathbf{A}_0$  are two real  $n \times n$  matrices, then the dual  $n \times n$  matrix  $\hat{\mathbf{A}}$  is defined as

$$\hat{\mathbf{A}} \equiv \mathbf{A} + \epsilon \mathbf{A}_0. \quad (\text{A.11})$$

We will work with  $3 \times 3$  matrices in connection with dual vectors, but the above definition can be applied to any square matrices, which is the reason why  $n$  has been left arbitrary. Equality, multiplication by a dual scalar, and multiplication by a dual vector are defined as in the foregoing cases. Moreover, matrix multiplication is defined correspondingly, but then the order of multiplication must be respected. We thus have that, if  $\hat{\mathbf{A}}$  and  $\hat{\mathbf{B}}$  are two  $n \times n$  dual matrices, with their primal and dual parts self-understood, then

$$\hat{\mathbf{A}} \hat{\mathbf{B}} = \mathbf{AB} + \epsilon (\mathbf{AB}_0 + \mathbf{A}_0 \mathbf{B}). \quad (\text{A.12})$$

Therefore, matrix  $\hat{\mathbf{A}}$  is real if  $\mathbf{A}_0 = \mathbf{O}$ , where  $\mathbf{O}$  denotes the  $n \times n$  zero matrix; if  $\mathbf{A} = \mathbf{O}$ , then  $\hat{\mathbf{A}}$  is called a *pure dual matrix*. Moreover, as we shall see below, a square dual matrix admits an inverse if and only if its primal part is nonsingular.

Now we can define the inverse of a dual matrix, if this is nonsingular. Indeed, it suffices to make  $\hat{\mathbf{B}} = \hat{\mathbf{A}}^{-1}$  in eq.(A.12) and the right-hand side of this equation equal to the  $n \times n$  identity matrix,  $\mathbf{1}$ , thereby obtaining two matrix equations that allow us to find the primal and the dual parts of  $\hat{\mathbf{A}}^{-1}$ , namely,

$$\mathbf{AB} = \mathbf{1}, \quad \mathbf{AB}_0 + \mathbf{A}_0\mathbf{B} = \mathbf{O},$$

whence

$$\mathbf{B} = \mathbf{A}^{-1}, \quad \mathbf{B}_0 = -\mathbf{A}^{-1}\mathbf{A}_0\mathbf{A}^{-1},$$

which are defined because  $\mathbf{A}$  is invertible by hypothesis, and hence, for any nonsingular dual matrix  $\hat{\mathbf{A}}$ ,

$$\hat{\mathbf{A}}^{-1} = \mathbf{A}^{-1} - \epsilon \mathbf{A}^{-1}\mathbf{A}_0\mathbf{A}^{-1}. \quad (\text{A.13})$$

Note the striking similarity of the dual part of the foregoing expression with the time-derivative of the inverse of  $\mathbf{A}(t)$ , namely,

$$\frac{d}{dt}[\mathbf{A}^{-1}(t)] = -\mathbf{A}^{-1}(t)\dot{\mathbf{A}}(t)\mathbf{A}^{-1}(t).$$

In order to find an expression for the determinant of an  $n \times n$  dual matrix, we need to recall the general expression for the dual function defined in eq.(A.3). However, that expression has to be adapted to a dual-matrix argument, which leads to

$$f(\hat{\mathbf{A}}) = f(\mathbf{A}) + \epsilon \operatorname{tr} \left[ \mathbf{A}_0 \left( \frac{df}{d\hat{\mathbf{A}}} \right)^T \right] \Big|_{\hat{\mathbf{A}}=\mathbf{A}}. \quad (\text{A.14})$$

In particular, when  $f(\hat{\mathbf{A}}) = \det(\hat{\mathbf{A}})$ , we have, recalling the formula for the derivative of the determinant with respect to its matrix argument (Angeles, 1982), for any  $n \times n$  matrix  $\mathbf{X}$ ,

$$\frac{d}{d\mathbf{X}}[\det(\mathbf{X})] = \det(\mathbf{X})\mathbf{X}^{-T},$$

where  $\mathbf{X}^{-T}$  denotes the transpose of the inverse of  $\mathbf{X}$  or, equivalently, the transpose of  $\mathbf{X}^{-1}$ . Therefore,

$$\operatorname{tr} \left[ \mathbf{A}_0 \left( \frac{df}{d\hat{\mathbf{A}}} \right)^T \right] \Big|_{\hat{\mathbf{A}}=\mathbf{A}} = \det(\mathbf{A})\operatorname{tr}(\mathbf{A}_0\mathbf{A}^{-1}),$$

and hence,

$$\det(\hat{\mathbf{A}}) = \det(\mathbf{A})[1 + \epsilon \operatorname{tr}(\mathbf{A}_0\mathbf{A}^{-1})]. \quad (\text{A.15})$$

Now we can define the eigenvalue problem for the dual matrix  $\hat{\mathbf{A}}$  defined above. Let  $\hat{\lambda}$  and  $\hat{\mathbf{e}}$  be a dual eigenvalue and a dual (unit) eigenvector of  $\hat{\mathbf{A}}$ , respectively. Then,

$$\hat{\mathbf{A}}\hat{\mathbf{e}} = \hat{\lambda}\hat{\mathbf{e}}, \quad \|\hat{\mathbf{e}}\| = 1. \quad (\text{A.16a})$$

For the foregoing linear homogeneous equation to admit a nontrivial solution, we must have

$$\det(\hat{\lambda}\mathbf{1} - \hat{\mathbf{A}}) = 0, \quad (\text{A.16b})$$

which yields an  $n$ th-order dual polynomial in the dual number  $\hat{\lambda}$ . Its  $n$  dual roots, real and complex, constitute the  $n$  *dual eigenvalues* of  $\hat{\mathbf{A}}$ . Note that, associated with each dual eigenvalue  $\hat{\lambda}_i$ , a corresponding *dual (unit) eigenvector*  $\hat{\mathbf{e}}_i^*$  is defined, for  $i = 1, 2, \dots, n$ . Moreover, if we recall eq.(A.4), we can write

$$e^{\hat{\mathbf{A}}} = e^{\mathbf{A}} + \epsilon \mathbf{A}_0 e^{\mathbf{A}}. \quad (\text{A.17})$$

Upon expansion, the foregoing expression can be cast in the form

$$e^{\hat{\mathbf{A}}} = (\mathbf{1} + \epsilon \mathbf{A}_0)e^{\mathbf{A}} \neq e^{\mathbf{A}}(\mathbf{1} + \epsilon \mathbf{A}_0), \quad (\text{A.18})$$

the inequality arising because, in general,  $\mathbf{A}$  and  $\mathbf{A}_0$  do not commute. They do so only in the case in which they share the same set of eigenvectors. A special case in which the two matrices share the same set of eigenvectors is when one matrix is an *analytic function* of the other. More formally, we have

**Lemma A.2.2** *If  $\mathbf{F}$  is an analytic matrix function of matrix  $\mathbf{A}$ , then the two matrices*

- (i) *share the same set of eigenvectors, and*
- (ii) *commute under multiplication.*

Typical examples of analytic matrix functions are  $\mathbf{F} = \mathbf{A}^N$  and  $\mathbf{F} = e^{\mathbf{A}}$ , for an integer  $N$ .

### A.3 Fundamentals of Rigid-Body Kinematics

We review in this section some basic facts from rigid-body kinematics. For the sake of conciseness, some proofs are not given, but the pertinent references are cited whenever necessary.

### A.3.1 Finite Displacements

A rigid body is understood as a particular case of the continuum with the special feature that, under any given motion, *any* two points of the rigid body remain equidistant. A rigid body is available through a *configuration* or *pose* that will be denoted by  $\mathcal{B}$ . Whenever a *reference configuration* is needed, this will be labelled  $\mathcal{B}^0$ . Moreover, the position vector of a point  $P$  of the body in configuration  $\mathcal{B}$  will be denoted by  $\mathbf{p}$ , that in  $\mathcal{B}^0$  being denoted correspondingly by  $\mathbf{p}^0$ .

A rigid-body motion leaving a point  $O$  of the body fixed is called a *pure rotation*, and is represented by a *proper orthogonal matrix*  $\mathbf{Q}$ , i.e.,  $\mathbf{Q}$  verifies the two properties below:

$$\mathbf{Q}\mathbf{Q}^T = \mathbf{1}, \quad \det(\mathbf{Q}) = +1. \quad (\text{A.19})$$

According to Euler's Theorem (Euler, 1776), a pure rotation leaves a set of points of the body immutable, this set lying on a line  $\mathcal{L}$ , which is termed the *axis of rotation*. If we draw the perpendicular from an arbitrary point  $P$  of the body to  $\mathcal{L}$  and denote its intersection with  $\mathcal{L}$  by  $P'$ , the angle  $\phi$  between  $P'P^0$  and  $P'P$ , where, according to our convention,  $P^0$  denotes the point  $P$  in the reference configuration  $\mathcal{B}^0$  of the body, is called the *angle of rotation*. Note that a direction must be specified along this line to define the sign of the angle. Furthermore, the direction of the line is specified by the unit vector  $\mathbf{e}$ . We term  $\mathbf{e}$  and  $\phi$  the *natural invariants* of  $\mathbf{Q}$ .

As a result of Euler's Theorem, the rotation  $\mathbf{Q}$  can be represented in terms of its natural invariants. This representation takes the form

$$\mathbf{Q} = \mathbf{e}\mathbf{e}^T + \cos\phi(\mathbf{1} - \mathbf{e}\mathbf{e}^T) + \sin\phi\mathbf{E}, \quad (\text{A.20})$$

where  $\mathbf{E}$  denotes the *cross-product matrix* of  $\mathbf{e}$ , i.e., for any 3-dimensional vector  $\mathbf{v}$ ,

$$\mathbf{e} \times \mathbf{v} = \mathbf{E}\mathbf{v}.$$

As a result of the foregoing definition,  $\mathbf{E}$  is skew-symmetric, i.e.,  $\mathbf{E} = -\mathbf{E}^T$  and, moreover, it has the properties below:

$$\mathbf{E}^{2k+1} = (-1)^k\mathbf{E}, \quad \mathbf{E}^{2k} = (-1)^k(\mathbf{1} - \mathbf{e}\mathbf{e}^T), \quad \text{for } k = 1, 2, \dots$$

By virtue of the foregoing properties of the cross-product matrix  $\mathbf{E}$  of  $\mathbf{e}$ , the rotation matrix  $\mathbf{Q}$  can be written in the alternative form

$$\mathbf{Q} = \mathbf{1} + \sin\phi\mathbf{E} + (1 - \cos\phi)\mathbf{E}^2. \quad (\text{A.21})$$

Now, if we recall the *Cayley-Hamilton Theorem* (Halmos, 1974), we can realize that the right-hand side of the foregoing equation is nothing but the exponential of  $\phi\mathbf{E}$ , i.e.,

$$\mathbf{Q} = e^{\phi\mathbf{E}} , \quad (\text{A.22})$$

which is the *exponential form of the rotation matrix*. Now it is a simple matter to obtain the eigenvalues of the rotation matrix if we first notice that one eigenvalue of  $\mathbf{E}$  is 0, the other eigenvalues being readily derived as  $\pm\sqrt{-1}$ , where  $\sqrt{-1}$  is the imaginary unit, i.e.,  $\sqrt{-1} \equiv \sqrt{-1}$ . Therefore, if  $\mathbf{Q}$  is the exponential of  $\phi\mathbf{E}$ , then the eigenvalues of  $\mathbf{Q}$  are the exponentials of the eigenvalues of  $\phi\mathbf{E}$ :

$$\lambda_1 = e^0 = 1, \quad \lambda_{2,3} = e^{\pm\sqrt{-1}\phi} = \cos\phi \pm \sqrt{-1}\sin\phi . \quad (\text{A.23})$$

Moreover, we recall below the *Cartesian decomposition* of an  $n \times n$  matrix  $\mathbf{A}$ , namely,

$$\mathbf{A} = \mathbf{A}_s + \mathbf{A}_{ss} , \quad (\text{A.24a})$$

where  $\mathbf{A}_s$  is symmetric and  $\mathbf{A}_{ss}$  is skew-symmetric. These matrices are given by

$$\mathbf{A}_s \equiv \frac{1}{2}(\mathbf{A} + \mathbf{A}^T), \quad \mathbf{A}_{ss} \equiv \frac{1}{2}(\mathbf{A} - \mathbf{A}^T) . \quad (\text{A.24b})$$

Any  $3 \times 3$  skew-symmmetric matrix is fully defined by three scalars, which means that such a matrix can then be made isomorphic to a 3-dimensional vector. Indeed, let  $\mathbf{S}$  be a  $3 \times 3$  skew-symmetric matrix and  $\mathbf{v}$  be an arbitrary 3-dimensional vector. Then, we have

$$\mathbf{S}\mathbf{v} \equiv \mathbf{s} \times \mathbf{v} . \quad (\text{A.25})$$

When the above items are expressed in a given coordinate frame  $\mathcal{F}$ , the components of  $\mathbf{S}$ , indicated as  $\{s_{i,j}\}_{i,j=1}^3$ , and of  $\mathbf{s}$ , indicated as  $\{s_i\}_1^3$ , bear the relations below:

$$\mathbf{S} = \begin{bmatrix} 0 & -s_3 & s_2 \\ s_3 & 0 & -s_1 \\ -s_2 & s_1 & 0 \end{bmatrix}, \quad \mathbf{s} = \frac{1}{2} \begin{bmatrix} s_{32} - s_{23} \\ s_{13} - s_{31} \\ s_{21} - s_{12} \end{bmatrix} . \quad (\text{A.26})$$

In general, we define the *axial vector* of an arbitrary  $3 \times 3$  matrix  $\mathbf{A}$  in terms of the difference of its off-diagonal entries, as appearing in eq.(A.26) for the entries of matrix  $\mathbf{S}$ . Apparently, the axial vector of any  $3 \times 3$  matrix is identical to that of its skew-symmetric component; this vector, represented as  $\mathbf{a} \equiv \text{vect}(\mathbf{A})$ , is the *vector linear invariant* of  $\mathbf{A}$ .

The *scalar linear invariant* of the same matrix is its trace,  $\text{tr}(\mathbf{A})$ . With this notation, note that

$$\frac{1}{2}(\mathbf{A} - \mathbf{A}^T)\mathbf{v} = \mathbf{a} \times \mathbf{v}.$$

Further, with reference to Fig. A.3.1, let  $A$  and  $P$  be two points of a rigid body, which is shown in its reference and its current configurations.

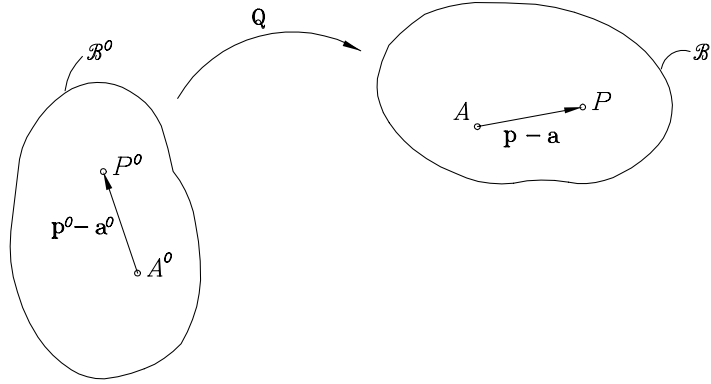


Figure A.1: Displacements of two points of a rigid body in two finitely-separated configurations

We can regard vector  $\mathbf{p} - \mathbf{a}$  as the image of  $\mathbf{p}^0 - \mathbf{a}^0$  under the rotation  $\mathbf{Q}$ , namely,

$$\mathbf{p} - \mathbf{a} = \mathbf{Q}(\mathbf{p}^0 - \mathbf{a}^0), \quad (\text{A.27})$$

whence an expression for  $\mathbf{p}$  can be derived as

$$\mathbf{p} = \mathbf{a} + \mathbf{Q}(\mathbf{p}^0 - \mathbf{a}^0). \quad (\text{A.28})$$

Furthermore, the *displacement*  $\mathbf{d}_A$  of  $A$  is defined as the difference  $\mathbf{a} - \mathbf{a}^0$ , with a similar definition for the displacement  $\mathbf{d}_P$  of  $P$ . From the above equation, it is now apparent that a linear relation between the two displacements follows:

$$\mathbf{d}_P = \mathbf{d}_A + (\mathbf{Q} - \mathbf{1})(\mathbf{p}^0 - \mathbf{a}^0). \quad (\text{A.29})$$

Therefore,

**Theorem A.3.1** *The displacements of all the points of a rigid body have identical projections onto the axis of the concomitant rotation.*

The proof of the foregoing result follows upon dot-multiplying both sides of eq.(A.29) by  $\mathbf{e}$ :

$$\mathbf{e} \cdot \mathbf{d}_P = \mathbf{e} \cdot \mathbf{d}_A .$$

From the previous result it is apparent that  $\|\mathbf{d}_P\|$  can attain infinitely large values, depending on  $\|\mathbf{p}^0 - \mathbf{a}^0\|$ , but, in general,  $\mathbf{d}_P$  does not vanish. Hence, a minimum of  $\|\mathbf{d}_P\|$  can be found, a result summarized in the Mozzi-Chasles Theorem (Mozzi, 1763;Chasles, 1830). This theorem states that the points of  $\mathcal{B}$  of minimum-norm displacement lie in a line  $\mathcal{M}$  that is parallel to the axis of the rotation represented by matrix  $\mathbf{Q}$ , the minimum-norm displacement being a vector parallel to the same axis. If we recall that  $\mathbf{e}$  and  $\phi$  denote the natural invariants of  $\mathbf{Q}$ , then the position vector  $\mathbf{p}^*$  of the point  $P^*$  of  $\mathcal{M}$  lying closest to the origin  $O$  is given by (Angeles, 1997)

$$\mathbf{p}^* = \frac{(\mathbf{Q} - \mathbf{1})^T (\mathbf{Q}\mathbf{a}^0 - \mathbf{a})}{2(1 - \cos \phi)}, \quad \text{for } \phi \neq 0 , \quad (\text{A.30})$$

the special case in which  $\phi = 0$  corresponding to a *pure translation*, whereby all points of  $\mathcal{B}$  undergo identical displacements. In this case, then, the axis  $\mathcal{M}$  is indeterminate, because all points of the body can be thought of as undergoing minimum-norm displacements. Henceforth, line  $\mathcal{M}$  will be termed the *Mozzi-Chasles axis*. Note that the Plücker coordinates of the Mozzi-Chasles axis are given by  $\mathbf{e}$  and  $\mathbf{e}_0 \equiv \mathbf{p}^* \times \mathbf{e}$ . We shall denote with  $\mathbf{d}^*$  the minimum-norm displacement, which can be represented in the form

$$\mathbf{d}^* = d^* \mathbf{e}, \quad d^* = \mathbf{d}_P \cdot \mathbf{e} . \quad (\text{A.31})$$

Therefore, the body under study can be regarded as undergoing, from  $\mathcal{B}^0$  to  $\mathcal{B}$ , a screw motion, as if the body were rigidly attached to the bolt of a screw of axis  $\mathcal{M}$  and *pitch p* given by

$$p = \frac{d^*}{\phi} = \frac{\mathbf{e} \cdot \mathbf{d}_P}{\phi} . \quad (\text{A.32})$$

We list below further results:

**Lemma A.3.1** *Let  $A$  and  $P$  be two points of a rigid body undergoing a general motion from a reference pose  $\mathcal{B}^0$  to a current pose  $\mathcal{B}$ . Then, under the notation adopted above, the difference  $\mathbf{p} - \mathbf{Q}\mathbf{p}^0$  remains constant and is denoted by  $\mathbf{d}$ , i.e.,*

$$\mathbf{p} - \mathbf{Q}\mathbf{p}^0 = \mathbf{a} - \mathbf{Q}\mathbf{a}^0 = \mathbf{d} . \quad (\text{A.33})$$

*Proof:* If we recall eq.(A.28) and substitute the expression therein for  $\mathbf{p}$  in the difference  $\mathbf{p} - \mathbf{Q}\mathbf{p}^0$ , we obtain

$$\mathbf{p} - \mathbf{Q}\mathbf{p}^0 = \mathbf{a} + \mathbf{Q}(\mathbf{p}^0 - \mathbf{a}^0) - \mathbf{Q}\mathbf{p}^0 = \mathbf{a} - \mathbf{Q}\mathbf{a}^0 = \mathbf{d} ,$$

thereby completing the intended proof.

Note that the kinematic interpretation of  $\mathbf{d}$  follows directly from eq.(A.33):  $\mathbf{d}$  represents the displacement of the point of  $\mathcal{B}$  that coincides with the origin in the reference pose  $\mathcal{B}^0$ .

The geometric interpretation of the foregoing lemma is given in Fig. A.2. What this figure indicates is that the pose  $\mathcal{B}$  can be attained from  $\mathcal{B}^0$  in two stages: (a) first, the body is given a rotation  $\mathbf{Q}$  about the origin  $O$ , that takes the body to the intermediate pose  $\mathcal{B}'$ ; (b) then, from  $\mathcal{B}'$ , the body is given a pure translation of displacement  $\mathbf{d}$  that takes the body into  $\mathcal{B}$ .

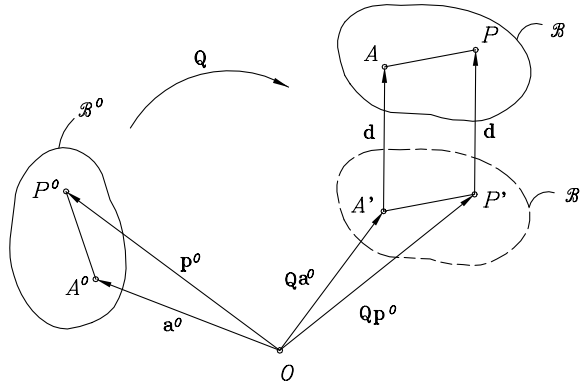


Figure A.2: Geometric interpretation of Lemma 3.1

Therefore, eq.(A.30) for the position vector of the point of the Mozzi-Chasles axis lying closest to the origin can be expressed in terms of vector  $\mathbf{d}$  as

$$\mathbf{p}^* = \frac{(\mathbf{1} - \mathbf{Q})^T \mathbf{d}}{2(1 - \cos \phi)}, \quad \text{for } \phi \neq 0 . \quad (\text{A.34})$$

Note that, in general,  $\mathbf{d}$  is not of minimum norm. Additionally,  $\mathbf{d}$  is origin-dependent, and hence, is not an invariant of the motion under study. Now, if we choose the origin on the Mozzi-Chasles axis  $\mathcal{M}$ , then we have the layout of Fig. A.3, and vector  $\mathbf{d}$  becomes a multiple of  $\mathbf{e}$ , namely,  $\mathbf{d} = d^* \mathbf{e}$ .

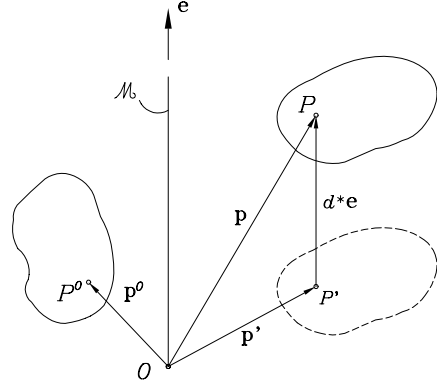


Figure A.3: Rigid-body displacement with origin on the Mozzi-Chasles axis

We can now express the Plücker coordinates of a line  $\mathcal{L}$  of a rigid body  $\mathcal{B}$  in terms of those of the line in its reference configuration  $\mathcal{L}^0$  (Bottema and Roth, 1978; Pradeep, Yoder, and Mukundan, 1989), as shown in Fig. A.3.1. To this end, we let  $\mathbf{f}$  be the unit vector parallel to  $\mathcal{L}$  and  $P$  be a point of  $\mathcal{L}$ , and arrange the Plücker coordinates of  $\mathcal{L}^0$  and  $\mathcal{L}$  in the 6-dimensional arrays  $\boldsymbol{\lambda}^0$  and  $\boldsymbol{\lambda}$ , respectively, defined as

$$\boldsymbol{\lambda}^0 \equiv \begin{bmatrix} \mathbf{f}^0 \\ \mathbf{p}^0 \times \mathbf{f}^0 \end{bmatrix}, \quad \boldsymbol{\lambda} \equiv \begin{bmatrix} \mathbf{f} \\ \mathbf{p} \times \mathbf{f} \end{bmatrix}. \quad (\text{A.35})$$

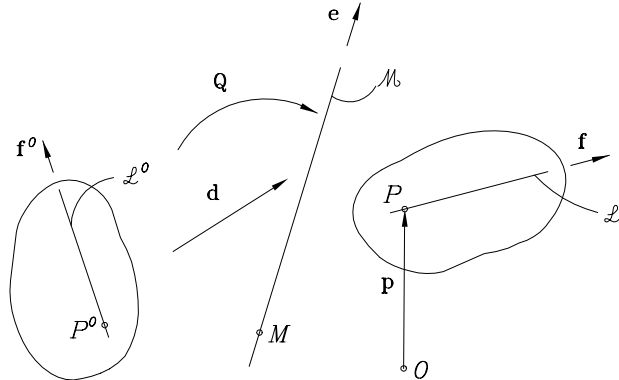


Figure A.4: The reference and the current configurations of a body and one of its lines

We thus have

$$\mathbf{f} = \mathbf{Q}\mathbf{f}^0, \quad \mathbf{p} = \mathbf{Q}\mathbf{p}^0 + \mathbf{d},$$

and hence,

$$\mathbf{p} \times \mathbf{f} = (\mathbf{Q}\mathbf{p}^0 + \mathbf{d}) \times \mathbf{Q}\mathbf{f}^0 = (\mathbf{Q}\mathbf{p}^0) \times \mathbf{Q}\mathbf{f} + \mathbf{d} \times \mathbf{Q}\mathbf{f}^0.$$

Now, the first term of the rightmost-hand side of the above equation can be simplified upon noticing that the cross product of two rotated vectors is identical to the rotated

cross product. Furthermore, the second term of the same side can be expressed in terms of  $\mathbf{D}$ , the cross-product matrix of  $\mathbf{d}$ , thereby obtaining

$$\mathbf{p} \times \mathbf{f} = \mathbf{Q}(\mathbf{p}^0 \times \mathbf{f}^0) + \mathbf{D}\mathbf{Q}\mathbf{f}^0.$$

Upon substituting the foregoing expressions for  $\mathbf{f}$  and  $\mathbf{p} \times \mathbf{f}$  into eq.(A.35), we obtain

$$\boldsymbol{\lambda} = \begin{bmatrix} \mathbf{Q}\mathbf{f}^0 \\ \mathbf{D}\mathbf{Q}\mathbf{f}^0 + \mathbf{Q}(\mathbf{p}^0 \times \mathbf{f}^0) \end{bmatrix},$$

which can be readily cast in the form of a linear transformation of  $\boldsymbol{\lambda}^0$ , i.e.,

$$\begin{bmatrix} \mathbf{f} \\ \mathbf{p} \times \mathbf{f} \end{bmatrix} = \begin{bmatrix} \mathbf{Q} & \mathbf{O} \\ \mathbf{D}\mathbf{Q} & \mathbf{Q} \end{bmatrix} \begin{bmatrix} \mathbf{f}^0 \\ \mathbf{p}^0 \times \mathbf{f}^0 \end{bmatrix}, \quad (\text{A.36a})$$

where  $\mathbf{O}$  denotes the  $3 \times 3$  zero matrix.

As the reader can readily verify, the inverse relation of eq.(A.36a) takes the form

$$\begin{bmatrix} \mathbf{f}^0 \\ \mathbf{p}^0 \times \mathbf{f}^0 \end{bmatrix} = \begin{bmatrix} \mathbf{Q}^T & \mathbf{O} \\ -\mathbf{Q}^T\mathbf{D} & \mathbf{Q}^T \end{bmatrix} \begin{bmatrix} \mathbf{f} \\ \mathbf{p} \times \mathbf{f} \end{bmatrix}. \quad (\text{A.36b})$$

By inspection of eq.(A.36a), and recalling the dual-unit-vector representation of a line, as given in eq.(A.10), we can realize that the dual unit vector of  $\mathcal{L}$  can be expressed as the image of the dual unit vector of  $\mathcal{L}^0$  upon a linear transformation given by a dual matrix  $\hat{\mathbf{Q}}$ . Moreover, the dual matrix of interest can be readily derived from the real matrix of eq.(A.36a). Indeed, it can be realized from Section 2 that the difference between the primal and the dual parts of a dual quantity is that the units of the dual part are those of the primal part times units of length. Hence, the primal part of the dual matrix sought is bound to be  $\mathbf{Q}$ , which is dimensionless, the corresponding dual part being  $\mathbf{D}\mathbf{Q}$ , which has units of length. A plausible form of the matrix sought is, then,

$$\hat{\mathbf{Q}} = \mathbf{Q} + \epsilon \mathbf{D}\mathbf{Q}. \quad (\text{A.37})$$

The correctness of the above expression can be readily realized. Indeed, let  $\hat{\mathbf{f}}^* = \mathbf{f} + \epsilon \mathbf{p} \times \mathbf{f}$  and  $\hat{\mathbf{f}}^{0*} = \mathbf{f}^0 + \epsilon \mathbf{p}^0 \times \mathbf{f}^0$  be the dual unit vectors of  $\mathcal{L}$  and  $\mathcal{L}^0$ , respectively. Then upon performing the product  $\hat{\mathbf{Q}}\hat{\mathbf{f}}^{0*}$ , we note that the product is rightfully  $\hat{\mathbf{f}}^*$ , i.e.,  $\hat{\mathbf{f}}^* = \hat{\mathbf{Q}}\hat{\mathbf{f}}^{0*}$ . In the derivations below, we will need expressions for the vector and scalar linear invariants of the product of two matrices, one of which is skew-symmetric. These expressions are derived in detail in (Angeles, 1997). For quick reference, we recall these relations below:

**Theorem A.3.2** Let both  $\mathbf{A}$  and  $\mathbf{S}$  be  $3 \times 3$  matrices, the former arbitrary, the latter skew-symmetric. Then,

$$\text{vect}(\mathbf{SA}) = \frac{1}{2}[\text{tr}(\mathbf{A})\mathbf{1} - \mathbf{A}]\mathbf{s}, \quad (\text{A.38})$$

where  $\mathbf{s} \equiv \text{vect}(\mathbf{S})$ .

Now, as a direct consequence of the above result, we have

**Corollary A.3.1** If  $\mathbf{A}$  in Theorem A.3.2 is skew-symmetric, then the axial vector of the product  $\mathbf{SA}$  reduces to

$$\text{vect}(\mathbf{SA}) = -\frac{1}{2}\mathbf{As} = -\frac{1}{2}\mathbf{a} \times \mathbf{s}, \quad (\text{A.39})$$

where  $\mathbf{a} \equiv \text{vect}(\mathbf{A})$ .

Moreover,

**Theorem A.3.3** Let  $\mathbf{A}$ ,  $\mathbf{S}$ , and  $\mathbf{s}$  be defined as in Theorem A.3.2. Then,

$$\text{tr}(\mathbf{SA}) = -2\mathbf{s} \cdot [\text{vect}(\mathbf{A})]. \quad (\text{A.40})$$

Furthermore, we prove now that  $\hat{\mathbf{Q}}$  is proper orthogonal. Indeed, orthogonality can be proven by performing the product  $\hat{\mathbf{Q}}\hat{\mathbf{Q}}^T$  and noticing that this product yields the  $3 \times 3$  identity matrix, i.e.,  $\hat{\mathbf{Q}}\hat{\mathbf{Q}}^T = \mathbf{1}$ . Proper orthogonality is proven, in turn, upon application of formula (A.15) to matrix  $\hat{\mathbf{Q}}$ , as given by eq.(A.37), namely,

$$\det(\hat{\mathbf{Q}}) = \det(\mathbf{Q})[1 + \epsilon \text{tr}(\mathbf{D}\mathbf{Q}\mathbf{Q}^{-1})] = \det(\mathbf{Q})[1 + \epsilon \text{tr}(\mathbf{D})] = 1,$$

thus completing the proof.

The exponential form of the dual rotation matrix can be obtained if we note that the exponential of a pure dual number  $\hat{x} = \epsilon x_0$  reduces to

$$e^{\epsilon x_0} = 1 + \epsilon x_0. \quad (\text{A.41})$$

On the other hand, we can write

$$\hat{\mathbf{Q}} = (\mathbf{1} + \epsilon \mathbf{D})\mathbf{Q}. \quad (\text{A.42})$$

In analogy with eq.(A.41), the foregoing expression takes the form

$$\hat{\mathbf{Q}} = e^{\epsilon \mathbf{D}} \mathbf{Q} .$$

Furthermore, if we recall the exponential form of  $\mathbf{Q}$ , as given in eq.(A.22), the foregoing expression simplifies to

$$\hat{\mathbf{Q}} = e^{\epsilon \mathbf{D}} e^{\phi \mathbf{E}} . \quad (\text{A.43})$$

However, since  $\mathbf{D}$  and  $\mathbf{E}$  are unrelated, they do not share the same set of eigenvectors, and hence, they do not commute under multiplication, the foregoing expression thus not being further reducible to one single exponential. Nevertheless, if the origin is placed on the Mozzi-Chasles axis, as depicted in Fig. A.3, then the dual rotation matrix becomes

$$\hat{\mathbf{Q}} = \mathbf{Q} + \epsilon d^* \mathbf{E} \mathbf{Q} , \quad (\text{A.44})$$

where  $d^* \mathbf{E}$  is, apparently, the cross-product matrix of vector  $d^* \mathbf{e}$ . Furthermore, the exponential form of the dual rotation matrix, eq.(A.43), then simplifies to  $\hat{\mathbf{Q}} = e^{(\phi + \epsilon d^*) \mathbf{E}}$  or, if we let  $\hat{\phi} = \phi + \epsilon d^*$ , then we can write  $\hat{\mathbf{Q}} = e^{\hat{\phi} \mathbf{E}}$ .

### A.3.2 Velocity Analysis

Upon differentiation with respect to time of both sides of eq.(A.27), we obtain

$$\dot{\mathbf{p}} - \dot{\mathbf{a}} = \dot{\mathbf{Q}}(\mathbf{p}^0 - \mathbf{a}^0) ,$$

and, if we solve for  $(\mathbf{p}^0 - \mathbf{a}^0)$  from the equation mentioned above, we obtain

$$\dot{\mathbf{p}} - \dot{\mathbf{a}} = \dot{\mathbf{Q}} \mathbf{Q}^T (\mathbf{p} - \mathbf{a}) , \quad (\text{A.45})$$

where  $\dot{\mathbf{Q}} \mathbf{Q}^T$  is defined as the angular-velocity matrix of the motion under study, and is represented as  $\boldsymbol{\Omega}$ , namely,

$$\boldsymbol{\Omega} \equiv \dot{\mathbf{Q}} \mathbf{Q}^T . \quad (\text{A.46a})$$

It can be readily proven that the foregoing matrix is skew-symmetric, i.e.,

$$\boldsymbol{\Omega}^T = -\boldsymbol{\Omega} . \quad (\text{A.46b})$$

Moreover, the axial vector of  $\boldsymbol{\Omega}$  is the angular-velocity vector  $\boldsymbol{\omega}$ :

$$\boldsymbol{\omega} = \text{vect}(\boldsymbol{\Omega}) . \quad (\text{A.46c})$$

We can now write eq.(A.45) in the form

$$\dot{\mathbf{p}} = \dot{\mathbf{a}} + \boldsymbol{\Omega}(\mathbf{p} - \mathbf{a}) = \dot{\mathbf{a}} + \boldsymbol{\omega} \times (\mathbf{p} - \mathbf{a}) , \quad (\text{A.47})$$

whence,

$$\dot{\mathbf{p}} - \boldsymbol{\omega} \times \mathbf{p} = \dot{\mathbf{a}} - \boldsymbol{\omega} \times \mathbf{a} \equiv \mathbf{v}^0 = \text{const} . \quad (\text{A.48})$$

Therefore, the difference  $\dot{\mathbf{p}} - \boldsymbol{\omega} \times \mathbf{p}$  is the same for all points of a rigid body. The kinematic interpretation of this quantity is straightforward: If we rewrite  $\mathbf{v}^0$  in the form  $\mathbf{v}^0 = \dot{\mathbf{p}} + \boldsymbol{\omega} \times (-\mathbf{p})$ , then we can readily realize that,  $-\mathbf{p}$  being the vector directed from point  $P$  of the rigid body to the origin  $O$ ,  $\mathbf{v}^0$  represents the velocity of the point of the body that coincides instantaneously with the origin. Furthermore, we express  $\mathbf{d}$ , as given by eq.(A.33), in terms of the position vector of an arbitrary point  $P$ ,  $\mathbf{p}$ , thus obtaining

$$\mathbf{d} = \mathbf{p} - \mathbf{Q}\mathbf{p}^0 . \quad (\text{A.49})$$

Upon differentiation of the two sides of the above expression with respect to time, we obtain

$$\dot{\mathbf{d}} = \dot{\mathbf{p}} - \dot{\mathbf{Q}}\mathbf{p}^0 ,$$

which can be readily expressed in terms of the current value of the position vector of  $P$ , by solving for  $\mathbf{p}^0$  from eq.(A.49), namely,

$$\dot{\mathbf{d}} = \dot{\mathbf{p}} - \boldsymbol{\Omega}(\mathbf{p} - \mathbf{d}) \quad \text{or} \quad \dot{\mathbf{d}} - \boldsymbol{\omega} \times \mathbf{d} = \dot{\mathbf{p}} - \boldsymbol{\omega} \times \mathbf{p} , \quad (\text{A.50})$$

and hence, the difference  $\dot{\mathbf{d}} - \boldsymbol{\omega} \times \mathbf{d}$  is identical to the difference  $\dot{\mathbf{p}} - \boldsymbol{\omega} \times \mathbf{p}$ , i.e.,

$$\dot{\mathbf{d}} - \boldsymbol{\omega} \times \mathbf{d} = \mathbf{v}^0 . \quad (\text{A.51})$$

Furthermore, upon dot-multiplying the two sides of eq.(A.48) by  $\boldsymbol{\omega}$ , we obtain an interesting result, namely,

$$\boldsymbol{\omega} \cdot \dot{\mathbf{p}} = \boldsymbol{\omega} \cdot \dot{\mathbf{a}} , \quad (\text{A.52})$$

and hence,

**Theorem A.3.4** *The velocities of all points of a rigid body have the same projection onto the angular-velocity vector of the motion under study.*

Similar to the Mozzi-Chasles Theorem, we have now

**Theorem A.3.5** Given a rigid body  $\mathcal{B}$  under general motion, a set of its points, on a line  $\mathcal{L}$ , undergoes the identical minimum-magnitude velocity  $\mathbf{v}^*$  parallel to the angular velocity  $\boldsymbol{\omega}$ .

The Plücker coordinates of line  $\mathcal{L}$ , grouped in the 6-dimensional array  $\boldsymbol{\lambda}$ , are given as

$$\boldsymbol{\lambda} \equiv \begin{bmatrix} \mathbf{f} \\ \boldsymbol{\pi} \times \mathbf{f} \end{bmatrix}, \quad \mathbf{f} \equiv \frac{\boldsymbol{\omega}}{\|\boldsymbol{\omega}\|}, \quad \boldsymbol{\pi} \equiv \frac{\boldsymbol{\omega} \times \mathbf{v}^0}{\|\boldsymbol{\omega}\|^2}, \quad (\text{A.53})$$

where  $\mathbf{v}^0$  was previously introduced as the velocity of the point of  $\mathcal{B}$  that coincides instantaneously with the origin. Line  $\mathcal{L}$  is termed the *instant screw axis*–ISA, for brevity.

Thus, the instantaneous motion of  $\mathcal{B}$  is defined by a screw of axis  $\mathcal{L}$  and pitch  $p'$ , given by

$$p' = \frac{\dot{\mathbf{p}} \cdot \boldsymbol{\omega}}{\|\boldsymbol{\omega}\|^2}, \quad (\text{A.54})$$

where  $\dot{\mathbf{p}}$  is the velocity of an arbitrary point  $P$  of  $\mathcal{B}$ , the product  $\dot{\mathbf{p}} \cdot \boldsymbol{\omega}$  being constant by virtue of Theorem A.3.4. A proof of the foregoing results is available in (Angeles, 1997).

### A.3.3 The Linear Invariants of the Dual Rotation Matrix

We start by recalling the *linear invariants* of the real rotation matrix (Angeles, 1997).

These are defined as

$$\mathbf{q} \equiv \text{vect}(\mathbf{Q}) = (\sin \phi) \mathbf{e}, \quad q_0 \equiv \frac{\text{tr}(\mathbf{Q}) - 1}{2} = \cos \phi. \quad (\text{A.55a})$$

Note that the linear invariants of any  $3 \times 3$  matrix can be obtained from simple differences of its off-diagonal entries and sums of its diagonal entries. Once the foregoing linear invariants are calculated, the natural invariants can be obtained uniquely as indicated below: First, note that the sign of  $\mathbf{e}$  can be changed without affecting  $\mathbf{q}$  if the sign of  $\phi$  is changed accordingly, which means that the sign of  $\phi$ —or that of  $\mathbf{e}$ , for that matter—is undefined. In order to define this sign uniquely, we will adopt a positive sign for  $\sin \phi$ , which means that  $\phi$  is assumed, henceforth, to lie in the interval  $0 \leq \phi \leq \pi$ .

We can thus obtain the inverse relations of eq.(A.55a) in the form

$$\mathbf{e} = \frac{\mathbf{q}}{\|\mathbf{q}\|}, \quad \phi = \arctan \left( \frac{\|\mathbf{q}\|}{q_0} \right), \quad \mathbf{q} \neq \mathbf{0}, \quad (\text{A.55b})$$

the case  $\mathbf{q} = \mathbf{0}$  being handled separately. Indeed,  $\mathbf{q}$  vanishes under two cases: (a)  $\phi = 0$ , in which case the body undergoes a pure translation and the axis of rotation is obviously

undefined; and (b)  $\phi = \pi$ , in which case  $\mathbf{Q}$  is symmetric and takes the form

$$\text{For } \phi = \pi : \quad \mathbf{Q} = -\mathbf{1} + 2\mathbf{e}\mathbf{e}^T , \quad (\text{A.55c})$$

whence the natural invariants become apparent and can be readily extracted from  $\mathbf{Q}$ .

Similar to the linear invariants of the real rotation matrix, in the dual case we have

$$\hat{\mathbf{q}} \equiv \text{vect}(\hat{\mathbf{Q}}), \quad \hat{q}_0 \equiv \frac{\text{tr}(\hat{\mathbf{Q}}) - 1}{2} . \quad (\text{A.56})$$

Expressions for the foregoing quantities in terms of the motion parameters are derived below; in the sequel, we also derive expressions for the *dual natural invariants* in terms of the same parameters. We start by expanding the vector linear invariant:

$$\text{vect}(\hat{\mathbf{Q}}) = \text{vect}(\mathbf{Q} + \epsilon \mathbf{D}\mathbf{Q}) = \text{vect}(\mathbf{Q}) + \epsilon \text{vect}(\mathbf{D}\mathbf{Q}) . \quad (\text{A.57a})$$

But, by virtue of eq.(A.20),

$$\text{vect}(\mathbf{Q}) = (\sin \phi)\mathbf{e} . \quad (\text{A.57b})$$

Furthermore, the second term of the rightmost-hand side of eq.(A.57a) can be readily calculated if we recall Theorem A.3.2, with  $\mathbf{d} \equiv \text{vect}(\mathbf{D})$ :

$$\text{vect}(\mathbf{D}\mathbf{Q}) = \frac{1}{2}[\text{tr}(\mathbf{Q})\mathbf{1} - \mathbf{Q}]\mathbf{d} . \quad (\text{A.57c})$$

Now, if we recall expression (A.20), we obtain

$$\text{tr}(\mathbf{Q})\mathbf{1} - \mathbf{Q} = (1 + \cos \phi)\mathbf{1} - \sin \phi \mathbf{E} - (1 - \cos \phi)\mathbf{e}\mathbf{e}^T .$$

Upon substitution of the foregoing expression into eq.(A.57c), the desired expression for  $\text{vect}(\mathbf{D}\mathbf{Q})$  is readily derived, namely,

$$\text{vect}(\mathbf{D}\mathbf{Q}) = \frac{1}{2}[(1 + \cos \phi)\mathbf{d} - \sin \phi \mathbf{e} \times \mathbf{d} - (1 - \cos \phi)(\mathbf{e} \cdot \mathbf{d})\mathbf{e}] , \quad (\text{A.57d})$$

and hence,

$$\hat{\mathbf{q}} = (\sin \phi)\mathbf{e} + \epsilon \frac{1}{2}[(\cos \phi)(\mathbf{e} \cdot \mathbf{d})\mathbf{e} + (1 + \cos \phi)\mathbf{d} + (\sin \phi)\mathbf{d} \times \mathbf{e} - (\mathbf{e} \cdot \mathbf{d})\mathbf{e}] . \quad (\text{A.57e})$$

On the other hand, the position vector  $\mathbf{p}^*$  of the Mozzi-Chasles axis, given by eq.(A.34), can be expressed as

$$\mathbf{p}^* = \frac{1}{2} \frac{\sin \phi}{1 - \cos \phi} \mathbf{e} \times \mathbf{d} + \frac{1}{2}\mathbf{d} - \frac{1}{2}(\mathbf{e} \cdot \mathbf{d})\mathbf{e} , \quad (\text{A.58a})$$

and hence,

$$\mathbf{p}^* \times \mathbf{e} = \frac{1}{2} \frac{\sin \phi}{1 - \cos \phi} \mathbf{d} - \frac{1}{2} \frac{\sin \phi}{1 - \cos \phi} (\mathbf{e} \cdot \mathbf{d}) \mathbf{e} + \frac{1}{2} \mathbf{d} \times \mathbf{e} . \quad (\text{A.58b})$$

Moreover, let us recall the identity

$$\frac{1 + \cos \phi}{\sin \phi} = \frac{\sin \phi}{1 - \cos \phi} , \quad (\text{A.58c})$$

which allows us to rewrite eq.(A.58b) in the form

$$\mathbf{p}^* \times \mathbf{e} = \frac{1}{2} \frac{1 + \cos \phi}{\sin \phi} \mathbf{d} - \frac{1}{2} \frac{1 + \cos \phi}{\sin \phi} (\mathbf{e} \cdot \mathbf{d}) \mathbf{e} + \frac{1}{2} \mathbf{d} \times \mathbf{e} , \quad (\text{A.58d})$$

whence,

$$(\sin \phi) \mathbf{p}^* \times \mathbf{e} = \frac{1}{2} [(1 + \cos \phi) \mathbf{d} - (1 + \cos \phi) (\mathbf{e} \cdot \mathbf{d}) \mathbf{e} + (\sin \phi) \mathbf{d} \times \mathbf{e}] ,$$

and  $\hat{\mathbf{q}}$  takes the form

$$\hat{\mathbf{q}} = (\sin \phi) \mathbf{e} + \epsilon [(\cos \phi) (\mathbf{e} \cdot \mathbf{d}) \mathbf{e} + (\sin \phi) \mathbf{p}^* \times \mathbf{e}] . \quad (\text{A.59})$$

If we now recall eqs.(A.31) and (A.32),  $\mathbf{d} \cdot \mathbf{e} \equiv d^* = p\phi$ , while  $\mathbf{p}^* \times \mathbf{e}$  is the moment of the associated Mozzi-Chasles axis,  $\mathbf{e}_0$ , and hence, eq.(A.59) becomes

$$\hat{\mathbf{q}} = (\sin \phi) \mathbf{e} + \epsilon [(\cos \phi) p\phi \mathbf{e} + (\sin \phi) \mathbf{e}_0] , \quad (\text{A.60})$$

and hence,  $\hat{\mathbf{q}}$  can be further simplified to

$$\hat{\mathbf{q}} = \hat{\mathbf{e}}^* \sin \hat{\phi}, \quad \hat{\phi} \equiv \phi 1 + \epsilon p) , \quad (\text{A.61})$$

where  $\hat{\mathbf{e}}^*$  is the dual unit vector representing the Mozzi-Chasles axis, i.e.,  $\hat{\mathbf{e}}^* = \mathbf{e} + \epsilon \mathbf{e}_0$ .

Now, such as in the real case, we can calculate the dual natural invariants of the motion under study in terms of the foregoing dual linear invariants. We do this by mimicking eqs.(A.55b), namely,

$$\hat{\mathbf{e}}^* = \frac{\hat{\mathbf{q}}}{\|\hat{\mathbf{q}}\|}, \quad \hat{\phi} = \arctan \left( \frac{\|\hat{\mathbf{q}}\|}{\hat{q}_0} \right), \quad \|\hat{\mathbf{q}}\| \neq 0 , \quad (\text{A.62})$$

where  $\|\hat{\mathbf{q}}\|$  is calculated from eq.(A.9e), which gives  $\|\hat{\mathbf{q}}\|^2$ , the square root of the latter then following from eq.(A.7), thus obtaining

$$\|\hat{\mathbf{q}}\| = \sin \hat{\phi} = \sin \phi + \epsilon (\mathbf{e} \cdot \mathbf{d}) \cos \phi , \quad (\text{A.63})$$

and hence, upon simplification,

$$\hat{\mathbf{e}}^* = \mathbf{e} + \epsilon \mathbf{p}^* \times \mathbf{e} = \mathbf{e} + \epsilon \mathbf{e}_0 , \quad (\text{A.64})$$

which is rightfully the dual unit vector of the Mozzi-Chasles axis. Furthermore,

$$\text{tr}(\hat{\mathbf{Q}}) = \text{tr}(\mathbf{Q}) + \epsilon \text{tr}(\mathbf{D}\mathbf{Q}) , \quad (\text{A.65a})$$

where, from Theorem A.3.3,  $\text{tr}(\mathbf{D}\mathbf{Q})$  turns out to be

$$\text{tr}(\mathbf{D}\mathbf{Q}) = -2[\text{vect}(\mathbf{Q})] \cdot \mathbf{d} = -2 \sin \phi (\mathbf{e} \cdot \mathbf{d}) , \quad (\text{A.65b})$$

whence,

$$\text{tr}(\hat{\mathbf{Q}}) = 1 + 2 \cos \phi - \epsilon 2(\sin \phi) \mathbf{e} \cdot \mathbf{d} , \quad (\text{A.65c})$$

and so, from the second of eqs.(A.56),

$$\hat{q}_0 \equiv \cos \hat{\phi} = \cos \phi - \epsilon (\sin \phi) (\mathbf{e} \cdot \mathbf{d}) ,$$

which, by virtue of eqs.(A.31), leads to

$$\hat{q}_0 = \cos \phi - \epsilon (\sin \phi) d^*, \quad \hat{\phi} = \phi + \epsilon d^* = \phi(1 + \epsilon p) . \quad (\text{A.65d})$$

In summary, the dual angle of the dual rotation under study comprises the angle of rotation of  $\mathbf{Q}$  in its primal part and the axial component of the displacement of all points of the moving body onto the Mozzi-Chasles axis. Upon comparison of the dual angle between two lines, as given in eq.(A.5), with the dual angle of rotation  $\hat{\phi}$ , it is then apparent that the primal part of the latter plays the role of the angle between two lines, while the corresponding dual part plays the role of the distance  $s$  between those lines. It is noteworthy that a pure rotation has a dual angle of rotation that is real, while a pure translation has an angle of rotation that is a pure dual number.

### **Example 1: Determination of the screw parameters of a rigid-body motion.**

We take here an example of (Angeles, 1997): The cube of Fig. A.5 is displaced from configuration  $A^0B^0\dots H^0$  into configuration  $AB\dots H$ . Find the Plücker coordinates of the Mozzi-Chasles axis of the motion undergone by the cube.

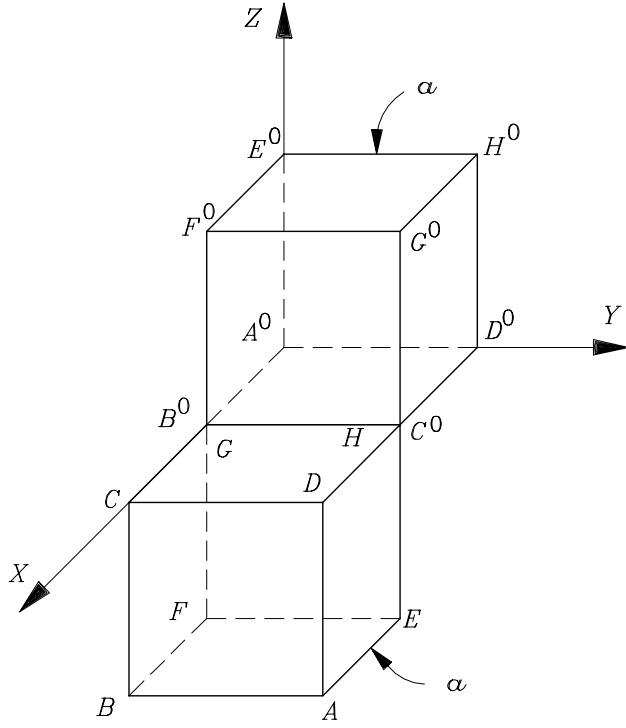


Figure A.5: Motion of a cube

*Solution:* We start by constructing  $\hat{\mathbf{Q}}$ :  $\hat{\mathbf{Q}} \equiv [\hat{\mathbf{i}}^* \ \hat{\mathbf{j}}^* \ \hat{\mathbf{k}}^*]$ , where  $\hat{\mathbf{i}}^*$ ,  $\hat{\mathbf{j}}^*$ , and  $\hat{\mathbf{k}}^*$  are the dual unit vectors of lines  $AB$ ,  $AD$ , and  $AE$ , respectively. These lines are, in turn, the images of lines  $A^0B^0$ ,  $A^0D^0$ , and  $A^0E^0$  under the rigid-body motion at hand. The dual unit vectors of the latter are denoted by  $\hat{\mathbf{i}}^{0*}$ ,  $\hat{\mathbf{j}}^{0*}$ , and  $\hat{\mathbf{k}}^{0*}$ , respectively, and are parallel to the  $X$ ,  $Y$ , and  $Z$  axes of the figure. We thus have

$$\hat{\mathbf{i}}^* = -\mathbf{j}^0 + \epsilon \mathbf{a} \times (-\mathbf{j}^0), \quad \hat{\mathbf{j}}^* = \mathbf{k}^0 + \epsilon \mathbf{a} \times \mathbf{k}^0, \quad \hat{\mathbf{k}}^* = -\mathbf{i}^0 + \epsilon \mathbf{a} \times (-\mathbf{i}^0),$$

where  $\mathbf{a}$  is the position vector of  $A$ , and is given by

$$\mathbf{a} = [2 \quad 1 \quad -1]^T a .$$

Hence,

$$\hat{\mathbf{i}}^* = -\mathbf{j}^0 + \epsilon a(-\mathbf{i}^0 - 2\mathbf{k}^0)$$

$$\hat{\mathbf{j}}^* = \mathbf{k}^0 + \epsilon a(\mathbf{i}^0 - 2\mathbf{j}^0)$$

$$\hat{\mathbf{k}}^* = -\mathbf{i}^0 + \epsilon a(\mathbf{j}^0 + \mathbf{k}^0)$$

Therefore,

$$\hat{\mathbf{Q}} = \begin{bmatrix} -\epsilon a & +\epsilon a & -1 \\ -1 & -\epsilon 2a & +\epsilon a \\ -\epsilon 2a & 1 & +\epsilon a \end{bmatrix},$$

whence,

$$\text{vect}(\hat{\mathbf{Q}}) = \frac{1}{2} \begin{bmatrix} 1 - \epsilon a \\ -1 + \epsilon 2a \\ -1 - \epsilon a \end{bmatrix}, \quad \text{tr}(\hat{\mathbf{Q}}) = -\epsilon(2a),$$

and

$$\|\text{vect}(\hat{\mathbf{Q}})\|^2 = \left\| \frac{1}{2} \begin{bmatrix} 1 \\ -1 \\ -1 \end{bmatrix} \right\|^2 + \epsilon 2 \frac{1}{2} [1 \ -1 \ -1] \begin{bmatrix} -1 \\ 2 \\ -1 \end{bmatrix} \frac{a}{2} = \frac{3}{4} - \epsilon a.$$

Thus,

$$\|\text{vect}(\hat{\mathbf{Q}})\| = \frac{\sqrt{3}}{2} + \epsilon \frac{-a}{\sqrt{3}} = \frac{\sqrt{3}}{2} - \epsilon \frac{\sqrt{3}}{3}a.$$

Therefore, the unit dual vector representing the Mozzi-Chasles axis of the motion at hand,  $\hat{\mathbf{e}}^*$ , is given by  $\hat{\mathbf{e}}^* = \text{vect}(\hat{\mathbf{Q}})/\|\text{vect}(\hat{\mathbf{Q}})\|$ , i.e.,

$$\hat{\mathbf{e}}^* = \frac{1}{\sqrt{3}/2} \frac{1}{2} \begin{bmatrix} 1 \\ -1 \\ -1 \end{bmatrix} - \epsilon \frac{a}{3/4} \left( \frac{1}{2} \begin{bmatrix} 1 \\ -1 \\ -1 \end{bmatrix} \frac{-\sqrt{3}}{3} - \frac{1}{2} \begin{bmatrix} -1 \\ 2 \\ -1 \end{bmatrix} \frac{\sqrt{3}}{2} \right).$$

After various stages of simplification, the foregoing expression reduces to

$$\hat{\mathbf{e}}^* = \frac{\sqrt{3}}{3} \begin{bmatrix} 1 \\ -1 \\ -1 \end{bmatrix} + \epsilon \frac{\sqrt{3}}{9} \begin{bmatrix} -1 \\ 4 \\ -5 \end{bmatrix} a.$$

Thus, the Mozzi-Chasles axis is parallel to the unit vector  $\mathbf{e}$ , which is given by the primal part of  $\hat{\mathbf{e}}$ , while the dual part of the same dual unit vector represents the moment of the Mozzi-Chasles axis, from which the position vector  $\mathbf{p}^*$  of  $P^*$ , the point of the Mozzi-Chasles axis closest to the origin, is readily found as

$$\mathbf{p}^* = \mathbf{e} \times \mathbf{e}_0 = \frac{a}{3} [3 \ 2 \ 1]^T.$$

#### A.3.4 The Dual Euler-Rodrigues Parameters of a Rigid-Body Motion

We first recall the definition of the Euler-Rodrigues parameters of a pure rotation, which are isomorphic to the *quaternion* of the rotation (Hamilton, 1844). These are most naturally introduced as the linear invariants of the square root of the rotation at hand, and

represented, paralleling the definition of the linear invariants, as

$$\mathbf{r} \equiv \text{vect}(\sqrt{\mathbf{Q}}), \quad r_0 \equiv \frac{\text{tr}(\sqrt{\mathbf{Q}}) - 1}{2}, \quad (\text{A.66})$$

the *proper orthogonal* square root of  $\mathbf{Q}$  being given as (Angeles, 1997):

$$\sqrt{\mathbf{Q}} = \mathbf{1} + \sin\left(\frac{\phi}{2}\right) \mathbf{E} + \left[1 - \cos\left(\frac{\phi}{2}\right)\right] \mathbf{E}^2. \quad (\text{A.67})$$

The *dual Euler-Rodrigues parameters* of a rigid-body motion are thus defined as

$$\hat{\mathbf{r}} \equiv \text{vect}(\sqrt{\hat{\mathbf{Q}}}), \quad \hat{r}_0 \equiv \frac{\text{tr}(\sqrt{\hat{\mathbf{Q}}}) - 1}{2}. \quad (\text{A.68})$$

Below we derive an expression for  $\sqrt{\hat{\mathbf{Q}}}$ . Prior to this, we introduce a relation that will prove useful:

**Lemma A.3.2** *Let  $\mathbf{a}$  and  $\mathbf{b}$  be arbitrary 3-dimensional vectors, and  $\mathbf{c} \equiv \mathbf{a} \times \mathbf{b}$ . The cross-product matrix  $\mathbf{C}$  of  $\mathbf{c}$  is given by*

$$\mathbf{C} = \mathbf{b}\mathbf{a}^T - \mathbf{a}\mathbf{b}^T. \quad (\text{A.69})$$

*Proof:* This follows by noticing that, for any 3-dimensional vector  $\mathbf{u}$ ,

$$\mathbf{c} \times \mathbf{u} = (\mathbf{a} \times \mathbf{b}) \times \mathbf{u} = \mathbf{b}(\mathbf{a}^T \mathbf{u}) - \mathbf{a}(\mathbf{b}^T \mathbf{u}),$$

which readily leads to

$$\mathbf{Cu} = (\mathbf{ba}^T - \mathbf{ab}^T)\mathbf{u},$$

thereby completing the proof.

Now we proceed to determine  $\sqrt{\hat{\mathbf{Q}}}$ . To this end, we regard the motion at hand, from a reference configuration  $\mathcal{B}^0$  to a current configuration  $\mathcal{B}$ , as consisting of a rotation  $\mathbf{Q}$  about the origin  $O$  followed by a translation  $\mathbf{d}$ . Then, this motion is decomposed into two parts, as shown in Fig. A.3.4: First, the body is rotated about the origin  $O$  by a rotation  $\sqrt{\mathbf{Q}}$  and a translation  $\mathbf{d}_s$ ; then, from the configuration  $\mathcal{B}'$  thus attained, the body is given a new rotation  $\sqrt{\mathbf{Q}}$  about  $O$  as well, followed by the same translation  $\mathbf{d}_s$ .

It is apparent that, from the general expression for the dual rotation matrix, eq.(A.42),

$\sqrt{\hat{\mathbf{Q}}}$  can be represented as

$$\sqrt{\hat{\mathbf{Q}}} = (\mathbf{1} + \epsilon \mathbf{D}_s) \sqrt{\mathbf{Q}}, \quad (\text{A.70})$$

the calculation of  $\sqrt{\hat{\mathbf{Q}}}$  thus reducing to that of the skew-symmetric matrix  $\mathbf{D}_s$ , which is the cross-product matrix of  $\mathbf{d}_s$ . This matrix is calculated below in terms of  $\sqrt{\mathbf{Q}}$  and  $\mathbf{D}$ . We thus have

$$\mathbf{p}^2 = \sqrt{\mathbf{Q}} \mathbf{p}^0 + \mathbf{d}_s, \quad (\text{A.71})$$

$$\mathbf{p}^4 = \sqrt{\mathbf{Q}} \mathbf{p}^2 + \mathbf{d}_s = \mathbf{Q} \mathbf{p}^0 + (\mathbf{1} + \sqrt{\mathbf{Q}}) \mathbf{d}_s. \quad (\text{A.72})$$

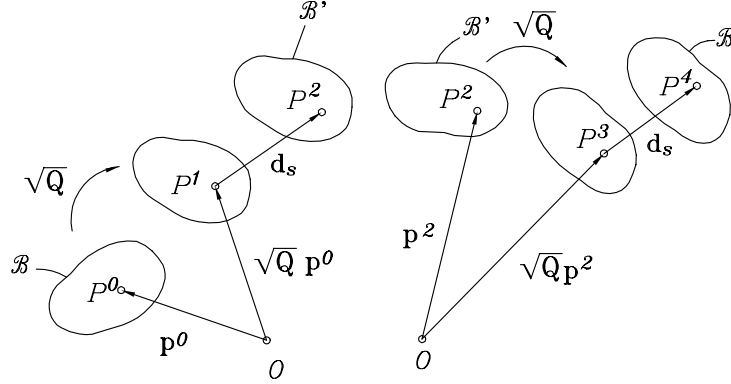


Figure A.6: Decomposition of the motion of a rigid body

But  $\mathbf{p}^4$  is the position vector of point  $P$  in  $\mathcal{B}$ , which can be attained by a rotation  $\mathbf{Q}$  about  $O$  followed by a translation  $\mathbf{d}$ , i.e.,

$$\mathbf{p}^4 = \mathbf{Q} \mathbf{p}^0 + \mathbf{d}. \quad (\text{A.73})$$

Upon comparing the right-hand sides of eqs.(A.72) and (A.73), we obtain

$$(\mathbf{1} + \sqrt{\mathbf{Q}}) \mathbf{d}_s = \mathbf{d},$$

whence,

$$\mathbf{d}_s = (\mathbf{1} + \sqrt{\mathbf{Q}})^{-1} \mathbf{d}. \quad (\text{A.74})$$

An expression for the above inverse can be derived if we realize that this inverse is an analytic function of  $\sqrt{\mathbf{Q}}$ , which is, in turn, an analytic function of  $\mathbf{Q}$ . We can thus conclude that by virtue of the Cayley-Hamilton Theorem, invoked when deriving the exponential

form of the rotation matrix in eq.(A.22), the inverse sought must be a linear combination of the first three powers of  $\mathbf{E}$ :  $\mathbf{e}^0 \equiv \mathbf{1}$ ,  $\mathbf{E}$ , and  $\mathbf{E}^2$ , namely,

$$(\mathbf{1} + \sqrt{\mathbf{Q}})^{-1} = \alpha \mathbf{1} + \beta \mathbf{E} + \gamma \mathbf{E}^2 , \quad (\text{A.75})$$

where  $\alpha$ ,  $\beta$ , and  $\gamma$  are to be determined. To this end, we write

$$(\mathbf{1} + \sqrt{\mathbf{Q}})^{-1}(\alpha \mathbf{1} + \beta \mathbf{E} + \gamma \mathbf{E}^2) = \mathbf{1} .$$

If we now substitute in the above equation the expression for  $\sqrt{\mathbf{Q}}$  displayed in eq.(A.67), we obtain three equations for the three unknowns  $\alpha$ ,  $\beta$ , and  $\gamma$ , from which it is a simple matter to solve for these unknowns, namely,

$$\alpha = \frac{1}{2}, \quad \beta = -\frac{\sin(\phi/2)}{2[1 + \cos(\phi/2)]}, \quad \gamma = 0 , \quad (\text{A.76})$$

the inverse sought thus taking the form

$$(\mathbf{1} + \sqrt{\mathbf{Q}})^{-1} = \frac{1}{2} \left[ \mathbf{1} - \frac{\sin(\phi/2)}{1 + \cos(\phi/2)} \mathbf{E} \right] . \quad (\text{A.77})$$

Therefore, eq.(A.74) yields

$$\mathbf{d}_s = (\mathbf{1} + \sqrt{\mathbf{Q}})^{-1} \mathbf{d} = \frac{1}{2} \left[ \mathbf{1} - \frac{\sin(\phi/2)}{1 + \cos(\phi/2)} \mathbf{E} \right] \mathbf{d} ,$$

i.e.,

$$\mathbf{d}_s = \frac{1}{2} \left[ \mathbf{d} - \frac{\sin(\phi/2)}{1 + \cos(\phi/2)} \mathbf{e} \times \mathbf{d} \right] . \quad (\text{A.78})$$

Thus,  $\mathbf{D}_s$  is the cross-product matrix of the sum of two vectors, and hence,  $\mathbf{D}_s$  reduces to the sum of the corresponding cross-product matrices. The cross-product matrix of the first term of the right-hand side of the foregoing equation is apparently proportional to  $\mathbf{D}$ , that of the second term being proportional to the cross-product matrix of  $\mathbf{e} \times \mathbf{d}$ . The latter can be readily obtained by application of Lemma A.3.2, which leads to

$$\mathbf{D}_s = \frac{1}{2} \left[ \mathbf{D} - \frac{\sin(\phi/2)}{1 + \cos(\phi/2)} (\mathbf{d}\mathbf{e}^T - \mathbf{e}\mathbf{d}^T) \right] . \quad (\text{A.79})$$

Hence,

$$\sqrt{\hat{\mathbf{Q}}} = \mathbf{1} + \epsilon \frac{1}{2} \left[ \mathbf{D} - \frac{\sin(\phi/2)}{1 + \cos(\phi/2)} (\mathbf{d}\mathbf{e}^T - \mathbf{e}\mathbf{d}^T) \right] \sqrt{\mathbf{Q}} . \quad (\text{A.80})$$

Now, the linear invariants of  $\sqrt{\hat{\mathbf{Q}}}$  are

$$\text{vect}(\sqrt{\hat{\mathbf{Q}}}) = \text{vect}(\sqrt{\mathbf{Q}}) + \epsilon \text{vect}(\mathbf{D}_s \sqrt{\mathbf{Q}}) \quad (\text{A.81a})$$

and

$$\text{tr}(\sqrt{\hat{\mathbf{Q}}}) = \text{tr}(\sqrt{\mathbf{Q}}) + \epsilon \text{tr}(\mathbf{D}_s \sqrt{\mathbf{Q}}) . \quad (\text{A.81b})$$

An expression for  $\text{vect}(\sqrt{\mathbf{Q}})$ , appearing in the first term of  $\text{vect}(\sqrt{\hat{\mathbf{Q}}})$ , can be obtained from eq.(A.67), namely,

$$\text{vect}(\sqrt{\mathbf{Q}}) = \sin\left(\frac{\phi}{2}\right) \text{vect}(\mathbf{E}) = \sin\left(\frac{\phi}{2}\right) \mathbf{e} , \quad (\text{A.82})$$

while an expression for the second term of the right-hand side of eq.(A.81b) is obtained by application of Theorem A.3.2:

$$\text{vect}(\mathbf{D}_s \sqrt{\mathbf{Q}}) = \frac{1}{2} [\text{tr}(\sqrt{\mathbf{Q}}) \mathbf{1} - \sqrt{\mathbf{Q}}] \mathbf{d}_s ,$$

which can be further expanded without intermediate lengthy derivations if we realize that the above expression is the counterpart of that appearing in eq.(A.57c); the latter is expanded in eq.(A.57d). Thus, all we need now is mimic eq.(A.57d), if with  $\phi$  and  $\mathbf{d}$  substituted by their counterparts  $\phi/2$  and  $\mathbf{d}_s$ , respectively, i.e.,

$$\begin{aligned} \text{vect}(\mathbf{D}_s \sqrt{\mathbf{Q}}) &= \frac{1}{2} \left\{ \left[ 1 + \cos\left(\frac{\phi}{2}\right) \right] \mathbf{d}_s - \sin\left(\frac{\phi}{2}\right) \mathbf{e} \times \mathbf{d}_s \right. \\ &\quad \left. - \left[ 1 - \cos\left(\frac{\phi}{2}\right) \right] (\mathbf{e} \cdot \mathbf{d}) \mathbf{e} \right\} . \end{aligned} \quad (\text{A.83})$$

If we now simplify the above expression for  $\text{vect}(\mathbf{D}_s \sqrt{\mathbf{Q}})$ , and substitute the simplified expression into eq.(A.81a), along with eq.(A.82), we obtain the desired expression for  $\hat{\mathbf{r}}$ . Note that the latter is defined in eq.(A.68), and hence,

$$\hat{\mathbf{r}} = \sin\left(\frac{\phi}{2}\right) \mathbf{e} + \epsilon \left[ \cos\left(\frac{\phi}{2}\right) p_s \frac{\phi}{2} \mathbf{e} + \sin\left(\frac{\phi}{2}\right) \mathbf{e}_0 \right] , \quad (\text{A.84})$$

where  $p_s$  is the pitch associated with the motion represented by  $\sqrt{\hat{\mathbf{Q}}}$ , namely,

$$p_s \equiv \mathbf{d}_s \cdot \mathbf{e} = \frac{1}{2} \mathbf{d} , \quad (\text{A.85})$$

where we have recalled the expression for  $\mathbf{d}_s$  displayed in eq.(A.78). Similar to eq.(A.61), then, the dual vector of the Euler-Rodrigues parameters is given by

$$\hat{\mathbf{r}} = \hat{\mathbf{e}}^* \sin\left(\frac{\hat{\phi}}{2}\right) , \quad \hat{\phi} \equiv \phi + \epsilon d_s^*, \quad d_s^* \equiv \mathbf{d}_s \cdot \mathbf{e} . \quad (\text{A.86})$$

The scalar of the Euler-Rodrigues parameters under study,  $\hat{r}_0$ , is now found in terms of the trace of  $\sqrt{\hat{\mathbf{Q}}}$ , which is displayed in eq.(A.81b). In that equation,

$$\text{tr}(\sqrt{\mathbf{Q}}) = 1 + 2 \cos\left(\frac{\phi}{2}\right) ,$$

the dual part of the right-hand side of eq.(A.81b) being calculated by application of Theorem A.3.3:

$$\text{tr}(\mathbf{D}_s \sqrt{\mathbf{Q}}) = -2\mathbf{d}_s \cdot \text{vect}(\sqrt{\mathbf{Q}}) = -2\mathbf{d}_s \cdot \mathbf{e} \sin\left(\frac{\phi}{2}\right)$$

or, in terms of the corresponding pitch  $p_s$ ,

$$\text{tr}(\mathbf{D}_s \sqrt{\mathbf{Q}}) = -2p_s \sin\left(\frac{\phi}{2}\right) .$$

Therefore,

$$\text{tr}(\sqrt{\hat{\mathbf{Q}}}) = 1 + 2 \cos\left(\frac{\phi}{2}\right) - \epsilon 2p_s \sin\left(\frac{\phi}{2}\right) ,$$

and hence,

$$\hat{r}_0 = \cos\left(\frac{\phi}{2}\right) - \epsilon p_s \sin\left(\frac{\phi}{2}\right) , \quad (\text{A.87})$$

which is the counterpart of the second of eqs.(A.55a). The set  $(\hat{\mathbf{r}}, \hat{r}_0)$  constitutes the *dual quaternion* of the motion under study (McCarthy, 1990).

## A.4 The Dual Angular Velocity

Similar to the angular-velocity matrix  $\boldsymbol{\Omega}$  introduced in eq.(A.46a), the *dual angular velocity matrix*  $\hat{\boldsymbol{\Omega}}$  is defined as

$$\hat{\boldsymbol{\Omega}} \equiv \dot{\hat{\mathbf{Q}}} \hat{\mathbf{Q}}^T . \quad (\text{A.88})$$

Now we differentiate with respect to time the expression for  $\hat{\mathbf{Q}}$  introduced in eq.(A.42), which yields

$$\dot{\hat{\mathbf{Q}}} = (\mathbf{1} + \epsilon \mathbf{D}) \dot{\mathbf{Q}} + \epsilon \dot{\mathbf{D}} \mathbf{Q} .$$

Upon substitution of the above expression for  $\dot{\hat{\mathbf{Q}}}$  and of the expression for  $\dot{\mathbf{Q}}$  of eq.(A.42) into eq.(A.88), we obtain

$$\hat{\boldsymbol{\Omega}} = \boldsymbol{\Omega} + \epsilon (\mathbf{D}\boldsymbol{\Omega} - \boldsymbol{\Omega}\mathbf{D} + \dot{\mathbf{D}}) . \quad (\text{A.89})$$

The *dual angular-velocity vector*  $\hat{\omega}$  of the motion under study is then obtained as the axial vector of the foregoing expression, namely,

$$\hat{\omega} = \text{vect}(\hat{\Omega}) = \omega + \epsilon [\text{vect}(\mathbf{D}\Omega - \Omega\mathbf{D}) + \dot{\mathbf{d}}] , \quad (\text{A.90})$$

with  $\dot{\mathbf{d}}$  being the time-derivative of vector  $\mathbf{d}$ , introduced in eq.(A.33). Thus, in order to determine  $\hat{\omega}$ , all we need is the axial vector of the difference  $\mathbf{D}\Omega - \Omega\mathbf{D}$ . An expression for this difference can be obtained in various manners, one of which is outlined below: First, note that this difference is skew-symmetric, and hence,

$$\text{vect}(\mathbf{D}\Omega - \Omega\mathbf{D}) = 2 \text{vect}(\mathbf{D}\Omega) .$$

Further, the vector of  $\mathbf{D}\Omega$  is computed by means of Corollary A.3.1, eq.(A.39), upon substituting  $\mathbf{A}$  by  $\Omega$  in that expression. Thus,

$$\text{vect}(\mathbf{D}\Omega) = -\frac{1}{2}\omega \times \mathbf{d} . \quad (\text{A.91})$$

Therefore,

$$\hat{\omega} = \omega + \epsilon (\dot{\mathbf{d}} - \omega \times \mathbf{d}) , \quad (\text{A.92})$$

and, if we recall eq.(A.51), the foregoing expression takes the alternative form

$$\hat{\omega} = \omega + \epsilon \mathbf{v}^0 . \quad (\text{A.93})$$

In consequence, the dual angular velocity is the dual representation of the *twist*  $\mathbf{t}$  of  $\mathcal{B}$ , defined as the 6-dimensional array

$$\mathbf{t} \equiv \begin{bmatrix} \omega \\ \mathbf{v}^0 \end{bmatrix} . \quad (\text{A.94})$$

We can therefore find the angular velocity vector and the moment of the ISA about the given origin—i.e., the *instant screw parameters* of the motion at hand—if we are given enough information as to allow us to compute  $\hat{\omega}$ . The information required to determine the screw parameters of the motion under study can be given as the position and velocity vectors of three noncollinear points of a rigid body (Angeles, 1997). However, note that the dual rotation matrix was obtained in Example 1 in terms of the dual unit vectors representing three mutually orthogonal lines. Notice that, by virtue of Lemma A.2.1, the three lines of Example 1 were chosen concurrent and mutually orthogonal.

Now, in order to find the instant-screw parameters of interest, we need the time-derivatives of the dual unit vectors representing three concurrent, mutually orthogonal lines, but all we have at our disposal is the position and velocity vectors of three non-collinear points. Nevertheless, once we know three noncollinear points of a rigid body, say  $A$ ,  $B$ , and  $C$ , along with their velocities, it is possible to find the position and velocity vectors of three pairs of points defining a triad of concurrent, mutually orthogonal lines, an issue that falls beyond the scope of this chapter. Rather than discussing the problem at hand in its fullest generality, we limit ourselves to the special case in which the position vector  $\mathbf{p}$  of a point  $P$  of the rigid body under study can be determined so that the three lines  $PA$ ,  $PB$ , and  $PC$  are mutually orthogonal. Further, we let the position vectors of the three given points be  $\mathbf{a}$ ,  $\mathbf{b}$ , and  $\mathbf{c}$ . Thus, point  $P$  of the body in this case forms a rectangular trihedron with vertex at  $P$  and edges  $PA$ ,  $PB$ , and  $PC$ . We can thus express  $\mathbf{p}$  as a nonlinear function of the three position vectors  $\mathbf{a}$ ,  $\mathbf{b}$ , and  $\mathbf{c}$ :

$$\mathbf{p} = \mathbf{p}(\mathbf{a}, \mathbf{b}, \mathbf{c}) . \quad (\text{A.95})$$

Moreover, the velocity of point  $P$ ,  $\dot{\mathbf{p}}$ , can be calculated now as a linear combination of the velocities of the three given points, by straightforward differentiation of the foregoing expression, namely,

$$\dot{\mathbf{p}} = \mathbf{P}_a \dot{\mathbf{a}} + \mathbf{P}_b \dot{\mathbf{b}} + \mathbf{P}_c \dot{\mathbf{c}} , \quad (\text{A.96})$$

where  $\mathbf{P}_a$ ,  $\mathbf{P}_b$ , and  $\mathbf{P}_c$  denote the partial derivatives of  $\mathbf{p}$  with respect to  $\mathbf{a}$ ,  $\mathbf{b}$ , and  $\mathbf{c}$ , respectively. Once the position and the velocity vectors of point  $P$  are known, it is possible to determine the time-rates of change of the dual unit vectors representing the three lines  $PA$ ,  $PB$  and  $PC$ , as described below.

Let  $\hat{\mathbf{e}}^*$  denote the dual unit vector representing the line determined by points  $A$  and  $P$ , its primary and dual parts,  $\mathbf{e}$  and  $\mathbf{e}_0$ , being given by

$$\mathbf{e} = \frac{\mathbf{a} - \mathbf{p}}{\|\mathbf{a} - \mathbf{p}\|}, \quad \mathbf{e}_0 = \mathbf{p} \times \frac{\mathbf{a} - \mathbf{p}}{\|\mathbf{a} - \mathbf{p}\|} . \quad (\text{A.97})$$

Straightforward differentiation of the foregoing expressions with respect to time leads to

$$\begin{aligned} \dot{\mathbf{e}} &= \frac{1}{\|\mathbf{a} - \mathbf{p}\|} \left( \dot{\mathbf{a}} - \dot{\mathbf{p}} - \mathbf{e} \frac{d}{dt} \|\mathbf{a} - \mathbf{p}\| \right) , \\ \dot{\mathbf{e}}_0 &= \dot{\mathbf{p}} \times \frac{\mathbf{a} - \mathbf{p}}{\|\mathbf{a} - \mathbf{p}\|} + \mathbf{p} \times \frac{1}{\|\mathbf{a} - \mathbf{p}\|} \left( \dot{\mathbf{a}} - \dot{\mathbf{p}} - \mathbf{e} \frac{d}{dt} \|\mathbf{a} - \mathbf{p}\| \right) . \end{aligned}$$

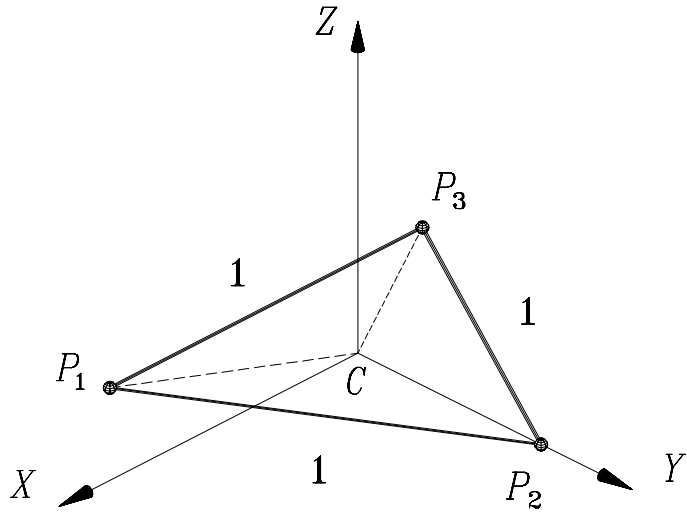


Figure A.7: A rigid triangular plate undergoing a motion given by the velocity of its vertices

Upon simplification, we obtain the desired expression for  $\dot{\mathbf{e}}^*$ , namely,

$$\dot{\mathbf{e}}^* = \frac{1}{\|\mathbf{a} - \mathbf{p}\|} [\dot{\mathbf{a}} - \dot{\mathbf{p}} + \epsilon(\mathbf{p}\dot{\mathbf{a}} + \dot{\mathbf{p}} \times \mathbf{a})] . \quad (\text{A.98})$$

Therefore, knowing the velocity of two points of a line, we can determine the time-rate of change of the dual unit vector representing the line. The foregoing idea is best illustrated with the aid of the example included below.

### **Example 2: Determination of the ISA of a rigid-body motion.**

For comparison purposes, we take an example from (Angeles, 1997): The three vertices of the equilateral triangular plate of Fig. A.4, which lie in the  $X$ - $Y$  plane,  $\{P_i\}_1^3$ , have the position vectors  $\{\mathbf{p}_i\}_1^3$ . Moreover, the origin of the coordinate frame  $X$ ,  $Y$ ,  $Z$  lies at the centroid  $C$  of the triangle, and the velocities of the foregoing points,  $\{\dot{\mathbf{p}}_i\}_1^3$ , are given in this coordinate frame as

$$\dot{\mathbf{p}}_1 = \frac{4 - \sqrt{2}}{4} \begin{bmatrix} 0 \\ 0 \\ 1 \end{bmatrix}, \quad \dot{\mathbf{p}}_2 = \frac{4 - \sqrt{3}}{4} \begin{bmatrix} 0 \\ 0 \\ 1 \end{bmatrix}, \quad \dot{\mathbf{p}}_3 = \frac{4 + \sqrt{2}}{4} \begin{bmatrix} 0 \\ 0 \\ 1 \end{bmatrix} .$$

With the above information, compute the instant-screw parameters of the motion under study.

*Solution:* Since the centroid  $C$  of the triangle coincides with that of the three given points, we have  $\mathbf{c} = \mathbf{0}$ , where  $\mathbf{c}$  is the position vector of  $C$ . Moreover,

$$\mathbf{p}_1 = \begin{bmatrix} 1/2 \\ -\sqrt{3}/6 \\ 0 \end{bmatrix}, \quad \mathbf{p}_2 = \begin{bmatrix} 0 \\ \sqrt{3}/3 \\ 0 \end{bmatrix}, \quad \mathbf{p}_3 = \begin{bmatrix} -1/2 \\ -\sqrt{3}/6 \\ 0 \end{bmatrix}.$$

First and foremost, we have to verify the compatibility of the data. To do this, we calculate the component of the relative velocities of two given points onto the line that they define. It can be readily shown that the data are compatible, and hence, the motion is possible. Next, we obtain the position vector of the point  $P$  that, along with  $\{\mathbf{p}_i\}_1^3$ , forms an orthogonal trihedron. It is not difficult to realize that the position vector of point  $P$  can be expressed as<sup>2</sup>

$$\mathbf{p} = \mathbf{c} + \frac{\sqrt{2}}{3}(\mathbf{p}_2 - \mathbf{p}_1) \times (\mathbf{p}_3 - \mathbf{p}_1),$$

and hence,

$$\dot{\mathbf{p}} = \dot{\mathbf{c}} + \frac{\sqrt{2}}{3}[(\mathbf{p}_3 - \mathbf{p}_2) \times \dot{\mathbf{p}}_1 + (\mathbf{p}_1 - \mathbf{p}_3) \times \dot{\mathbf{p}}_2 + (\mathbf{p}_2 - \mathbf{p}_1) \times \dot{\mathbf{p}}_3],$$

with the numerical values of  $\mathbf{p}$  and  $\dot{\mathbf{p}}$  given below:

$$\mathbf{p} = \frac{\sqrt{6}}{6} \begin{bmatrix} 0 \\ 0 \\ 1 \end{bmatrix}, \quad \dot{\mathbf{p}} = \frac{1}{12} \begin{bmatrix} 2\sqrt{3} \\ \sqrt{6} \\ 12 - \sqrt{3} \end{bmatrix}.$$

Now, let  $\hat{\mathbf{e}}_i^*$  denote the dual unit vector representing the line that passes through  $P$  and  $P_i$ , i.e.,

$$\hat{\mathbf{e}}_i^* = \frac{1}{\|\mathbf{p}_i - \mathbf{p}\|} [\mathbf{p}_i - \mathbf{p} + \epsilon \mathbf{p} \times \mathbf{p}_i],$$

where

$$\|\mathbf{p}_i - \mathbf{p}\| = \frac{\sqrt{2}}{2}, \quad i = 1, 2, 3.$$

Next, the three foregoing dual unit vectors are stored columnwise in the dual rotation matrix  $\hat{\mathbf{Q}}$ , i.e.,

$$\hat{\mathbf{Q}} = [\hat{\mathbf{e}}_1^* \quad \hat{\mathbf{e}}_2^* \quad \hat{\mathbf{e}}_3^*].$$

Upon substitution of the numerical values of these vectors into the above expression, we obtain

$$\hat{\mathbf{Q}} = \frac{\sqrt{12}}{12} \begin{bmatrix} 6 + \epsilon 2 & -\epsilon 2\sqrt{2} & -6 + \epsilon \sqrt{2} \\ -2\sqrt{3} + \epsilon \sqrt{6} & 4\sqrt{3} & -2\sqrt{3} - \epsilon \sqrt{6} \\ -2\sqrt{6} & -2\sqrt{6} & -2\sqrt{6} \end{bmatrix}.$$

---

<sup>2</sup>Although  $\mathbf{c} = \mathbf{0}$  in this case,  $\dot{\mathbf{c}} \neq \mathbf{0}$ , and hence,  $\mathbf{c}$  must be written explicitly in the expression for  $\mathbf{p}$ .

Likewise, the time derivative of  $\hat{\mathbf{Q}}$  is computed as

$$\dot{\hat{\mathbf{Q}}} = \frac{\sqrt{2}}{24} \left( \begin{bmatrix} -4\sqrt{3} & -4\sqrt{3} & -4\sqrt{3} \\ -2\sqrt{6} & -2\sqrt{6} & -2\sqrt{6} \\ -6\sqrt{2} + 2\sqrt{3} & -4\sqrt{3} & 6\sqrt{2} + 2\sqrt{3} \end{bmatrix} \right. \\ \left. + \epsilon \begin{bmatrix} -1 + 4\sqrt{3} & 2 - 8\sqrt{3} & -1 + 4\sqrt{3} \\ 12 - \sqrt{3} & 0 & -12 + \sqrt{3} \\ -(2 + \sqrt{6}) & 4 & -2 + \sqrt{6} \end{bmatrix} \right).$$

Therefore,

$$\hat{\boldsymbol{\Omega}} = \dot{\hat{\mathbf{Q}}} \hat{\mathbf{Q}}^T = \frac{1}{12} \begin{bmatrix} 0 & -\epsilon(12 - \sqrt{3}) & 6\sqrt{2} \\ +\epsilon(12 - \sqrt{3}) & 0 & 6 \\ -6\sqrt{2} & -6 & 0 \end{bmatrix},$$

which, as expected, is a dual skew-symmetric matrix. Hence,

$$\hat{\boldsymbol{\omega}} = \text{vect}(\hat{\boldsymbol{\Omega}}) = \frac{1}{2} \begin{bmatrix} -1 \\ \sqrt{2} \\ 0 \end{bmatrix} + \epsilon \frac{12 - \sqrt{3}}{12} \begin{bmatrix} 0 \\ 0 \\ 1 \end{bmatrix},$$

from which we can readily identify

$$\boldsymbol{\omega} = \frac{1}{2} \begin{bmatrix} -1 \\ \sqrt{2} \\ 0 \end{bmatrix}, \quad \mathbf{v}^0 = \frac{12 - \sqrt{3}}{12} \begin{bmatrix} 0 \\ 0 \\ 1 \end{bmatrix}.$$

Furthermore, the position vector  $\boldsymbol{\pi}^*$  of the point  $P^*$  of the ISA lying closest to the origin can be obtained from  $\mathbf{v}^0$ . Indeed, let  $\mathbf{v}^*$  be the velocity of  $P^*$ , which thus allows us to write

$$\mathbf{v}^0 = \mathbf{v}^* + \boldsymbol{\omega} \times (-\mathbf{p}^*) = \mathbf{v}^* + \mathbf{p}^* \times \boldsymbol{\omega}.$$

Upon cross-multiplying the two sides of the foregoing expression by  $\boldsymbol{\omega}$ , we obtain

$$\mathbf{v}^0 \times \boldsymbol{\omega} = \mathbf{v}^* \times \boldsymbol{\omega} + (\mathbf{p}^* \times \boldsymbol{\omega}) \times \boldsymbol{\omega},$$

whose first term of the right-hand side vanishes because  $\mathbf{v}^*$  and  $\boldsymbol{\omega}$  are parallel. Therefore,

$$\mathbf{v}^0 \times \boldsymbol{\omega} = (\mathbf{p}^* \times \boldsymbol{\omega}) \times \boldsymbol{\omega} = (\mathbf{p}^* \cdot \boldsymbol{\omega})\boldsymbol{\omega} - \|\boldsymbol{\omega}\|^2 \mathbf{p}^*.$$

The first term of the rightmost-hand side of the foregoing equation vanishes because  $\mathbf{p}^*$  being the position vector of the point of the ISA that lies closest to the origin, and the ISA being parallel to  $\boldsymbol{\omega}$ , these two vectors are orthogonal. We can thus solve for  $\mathbf{p}^*$  from the above expression, which yields

$$\mathbf{p}^* = -\frac{\mathbf{v}^0 \times \boldsymbol{\omega}}{\|\boldsymbol{\omega}\|^2}.$$

The quantities involved in the foregoing expression are now evaluated:

$$-\mathbf{v}^0 \times \boldsymbol{\omega} = \boldsymbol{\omega} \times \mathbf{v}^0 = \frac{12 - \sqrt{3}}{24} \begin{bmatrix} \sqrt{2} \\ 1 \\ 0 \end{bmatrix}, \quad \|\boldsymbol{\omega}\|^2 = \frac{3}{4}.$$

Finally,  $\mathbf{p}^* = \{(12 - \sqrt{3})]/18\}[\sqrt{2} \ 1 \ 0]^T$ , which coincides with the results reported in (Angeles, 1997), obtained by another method.

## A.5 Conclusions

We revisited dual algebra in the context of kinematic analysis, which led us to a straightforward introduction of dual quaternions. In the process, we showed that the parameters of both the finite screw and the instant screw of a rigid-body motion can be computed from the sum of the diagonal and the difference of the off-diagonal entries of the dual rotation and, correspondingly, the dual angular-velocity matrices.



# Bibliography

Agrawal, O.P., 1987, “Hamilton operators and dual-number-quaternions in spatial kinematics,” *Mechanism and Machine Theory*, Vol. 22, No. 6, pp. 569–575.

Alizadeh, D., Angeles, J. and Nokleby, S., 2013, “Optimum design of a spherical quasi-homokinetic linkage for motion transmission between orthogonal axes,” *Mechanism and Machine Theory*, Vol. 59, pp. 107–118.

Altuzarra, O., Salgado, O., Hernandez, A. and Angeles, J., 2009, “Multiobjective optimum design of a symmetric parallel Schönflies-motion generator,” *ASME Journal of Mechanical Design*, Vol. 131, No. 3, pp. 031002-1–031002-11.

Angeles, J., 1982, *Spatial Kinematic Chains. Analysis, Synthesis, Optimization*, Springer-Verlag, Berlin-Heidelberg-New York.

Angeles, J., 2012, “The dual generalized inverses and their applications in kinematic synthesis,” in Lenarčič, J. and Hustý, M. (editors), *Latest Advances in Robot Kinematics*, Springer, Dordrecht, pp. 1–10.

Angeles, J., 2014, *Fundamentals of Robotic Mechanical Systems. Theory, Methods, and Algorithms*, 4rd ed., Springer, New York.

Angeles, J. and Gosselin, C., 1988, “Détermination du degré de liberté des chaînes cinématiques,” *Transactions of the Canadian Society of Mechanical Engineering*, Vol. 12, No. 4, pp. 219–226.

Arai, T., Hervé, J.M. and Tanikawa, T., 1996, “Development of 3 dof micro finger,” *Proc. IROS'96*, Osaka, pp. 981–987.

Bai, S.P. and Angeles, J., 2008, “A unified input-output analysis of four-bar link-

ages". *Mechanism and Machine Theory*, Vol. 43, pp. 240–251.

Bai, S., Hansen, M.R. and Angeles, J., 2009, "A robust forward-displacement analysis of spherical parallel robots," to appear in *Mechanism and Machine Theory*.

Beck, T., 1859, *Beiträge zur Geschichte des Maschinenbaues*, J. Springer, Berlin.

Björck, Å. and Dahlquist, G., 1974, *Numerical Methods*, Prentice-Hall, Inc., Upper Saddle River, NJ.

Bogolyubov, A. N., 1976, *Teoriya mekhanismov v istoricheskem razvitiu (Theory of Mechanisms and its Historical Development)*, Nauka, Moscow (in Russian).

Borgnis, G.A., 1818, *Traité Complet de Mécanique Appliquée aux Arts. Traité des Compositions des Machines*, Paris.

Bottema, O. and Roth, B., 1978. *Theoretical Kinematics*, North-Holland Publishers Co., North-Holland Publishing Company, Amsterdam.

Bricard, R., 1927, *Leçons de Cinématique..* Vols. I & II, Gauthier-Villars et Cie. Publishers, Paris.

Chen, C. and Angeles, J., 2008, "A novel family of linkages for advanced motion synthesis," *Mechanism and Machine Theory*, Vol. 43, pp. 882-890.

Chen, C., Bai, S.P. and Angeles, J., 2008, "A comprehensive solution of the classic Burmester problem," *CSME Transactions*, Vol. 32, No. 2, pp. 137–154.

Chasles, M., 1830, "Notes sur les propriétés générales de deux corps semblables entr'eux et placés d'une manière quelconque dans l'espace, et sur le déplacement fini ou infiniment petit d'un corps solide libre," *Bull. Sci. Math. Ferrusaa*, Vol. 14, pp. 321–32.

Cheng, H.H. and Thompson, S., 1996, "Dual polynomials and complex dual numbers for analysis of spatial mechanisms," *Proc. ASME Design Engineering Technical Conference and Computers in Engineering Conference*, Irvine, California.

Chevallier, D.P., 1991, "Lie algebras, modules, dual quaternions and algebraic meth-

ods in kinematics," *Mechanism and Machine Theory*, Vol. 26, No. 6, pp. 613–627.

Chiang, C.H., 1988, *Kinematics of Spherical Mechanisms*. Cambridge University Press, Cambridge.

Clavel, R., 1988, "Delta, a fast robot with parallel geometry," *Proc. 18th Int. Symp. Industrial Robots*, Lausanne, pp. 91–100.

Clavel, R., 1990, *Device for the Movement and Positioning of an Element in Space*, U.S. Patent No. 4,976,582.

Clifford, W.K., 1873, "Preliminary sketch of bi-quaternions," *London Math. Soc.*, Vol. 4, pp. 381–395.

de Laclos, C., 1782, *Les liaisons dangereuses ou lettres recueillies dans une société, et publiées pour l'instruction de quelques autres*, Durand Publishers, Paris (the first edition seems to have been published in Amsterdam), 1907 edition by Maurice Bauche Publishers, Paris.

Dietmaier, P., 1992, "Inverse kinematics of manipulators with 3 revolute and 3 parallelogram joints," *Proc. ASME 22nd Biennial Mechanisms Conference*. Sept. 13–16, Scottsdale, Vol. 45, pp. 35–40.

Dimentberg, F.M., 1965, *The Screw Calculus and Its Applications in Mechanics*, Izdat. Nauka, Moscow.

Dudiță, F.D., and Diaconescu, D., 1987, *Optimizarea Structurală a Mecanismelor (Optimization of Mechanisms)*, Tehnică Publishers, Bucharest.

Dudiță, F.D., Diaconescu, D. and Gogu, Gr., *Mecanisme Articulate, Inventica și Cinematica în Abordare Filogenetica*, Tehnică Publishers, Bucharest.

Erdman, A.G. and Sandor, S.K., 2001, *Mechanism Design Analysis and Synthesis*, Vol. 2, Prentice Hall, Upper Saddle River, N.J.

Euler, L., 1753, "De machinis in genere," *Novii Comentarii Academiæ Scientiarum Petropolitanæ*, III.

Euler, L., 1775, “Nova methodus motum corporum rigidorum determinandi,” *Novii Comentarii Academiae Scientiarum Petropolitanæ*, pp. 208–238= *Opera Omnia* (2) 9, Vol. 2, No. 9, pp. 99–125.

Forsythe, G.E., 1970, “Pitfalls in computation, or why a math book isn’t enough” *American Mathematical Monthly*, Vol. 27, pp. 931–956.

French, M.E. ,1992, *Form, Structure and Mechanism*, Macmillan, London.

Freudenstein, F., 1955, “Approximate synthesis of four-bar linkages” *Trans. ASME*, Vol. 77, pp. 853–861.

Frolov, K.V., 1987, *Teoriya Mechanismov i Mashin*, Vyschaya Shkola, Moscow.

Gleick, J., 1988, *Chaos. Making a New Science*, Penguin Books, New York.

Golub, G.H. and Van Loan, C.F., 1983. *Matrix Computations*, The Johns Hopkins University Press, Baltimore.

Hachette, 1811, *Traité Elémentaire des Machines*, Paris.

Halmos, P., 1974, *Finite-Dimensional Vector Spaces*, Springer-Verlag, New York.

Hamilton, W.R., 1844, “On quaternions: or a new system of imaginaries in algebra,” *Phil. Mag.*.

Harary, F., 1972, *Graph Theory*, Addison-Wesley Publishing Company, Reading, MA.

Hartenberg, R. and Denavit, J., 1964. *Kinematic Synthesis of Linkages*, McGraw-Hill Book Company ,New York.

Hervé, J, 1978, “Analyse structurelle des mécanismes par groupes de déplacements,” *Mechanism and Machine Theory*, Vol. 13, pp. 437–450.

Hervé, J, 1999, “The Lie group of rigid body displacements, a fundamental tool for mechanism design,” *Mechanism and Machine Theory*, Vol. 34, pp. 719–730.

Hervé, J. and Sparacino, F., 1992, “Star, a new concept in robotics,” *Proc. 3rd Int.*

*Workshop on Advances in Robot Kinematics*, pp. 176–183, Ferrara.

IFToMM PC for Standardization of Terminology, 2003, *Mechanism and Machine Theory*, Vol. 38, Nos. 7–10.

Kimbrell, J.T., 1991, *Kinematic Analysis and Synthesis*, McGraw-Hill, Inc., New York.

Klein, B., 1981, “Zum Einsatz nichtlinearer Optimierungsverfahren zur rechnerunterstützten Konstruktion ebener Koppelgetriebe,” *Mechanism and Machine Theory*, Vol. 16, No. 5, pp. 567–576.

Koenigs, F., 1901, “Etude critique sur la théorie générale des mécanismes,” *Comptes Rendus de l’Académie des Sciences*, Vol. 133.

Kotel’nikov, A. P., 1895, *Screw calculus and some of its applications to geometry and mechanics*.

Leupold, J., 1724, *Theatrum Machinarium Generale*, Leipzig.

Ma, O. and Angeles, J., 1992, “Architecture Singularities of Parallel Manipulators,” *Journal of Robotics and Automation*, Vol. 7, No. 1, pp. 23–29.

Malik, A.K., Ghosh, A. and Dittrich, G., 1994, *Kinematic Analysis and Synthesis of Mechanisms*, CRC Press, Boca Raton.

Mandelbrot, B.B., 1983, *The Fractal Geometry of Nature*, W.H. Freeman and Company, 3rd ed., New York.

McAree, P.R. and Daniel, R.W., 1996, “A Fast, Robust Solution to the Stewart Platform Kinematics,” *Journal of Robotic Systems*, Vol. 13, No. 7, pp. 407–427.

McCarthy, J.M., 1990, *An Introduction to Theoretical Kinematics*, The MIT Press, Cambridge (MA).

McCarthy, J.M. and Soh, G.S., 2011, *Geometric Design of Linkages*, Springer, New York.

Modler, K., 1972, "Beitrag zur Theorie der Burmesterschen Mittelpunktkurve," *Maschinenbautechnik*, Vol. 21, No. 5, pp. 98–102.

Morgan, A. and Wampler, C.W., 1990, "Solving a planar four-bar design problem using continuation," *ASME Journal of Mechanical Design*, Vol. 112, pp. 544–550.

Mozzi, G., 1763, *Discorso Matematico Sopra il Rotamento Momentaneo dei Corpi*, Stamperia di Donato Campo, Naples.

Nash, S.G. and Sofer, A., 1996, *Linear and Nonlinear Programming*, The McGraw-Hill Companies, Inc., New York.

Parenti-Castelli, V. and Di Gregorio, R., 1995, "A Three-Equation Numerical Method for the Direct Kinematics of the Generalized Gough-Stewart Platform," *Proc. Ninth World Congress on the Theory of Machines and Mechanisms*, Aug. 29–Sept. 2, Milan, Vol. 2, pp. 837–841.

Pierrot, F., Shibukawa, T. and Morita, K., March 21, 2001, *Four-degree-of-freedom Parallel Robot*, European Patent No. EP1084802.

Plecnik, M.M. and McCarthy, J.M., 2013, "Synthesis of a Stephenson II function generator for eight precision positions," *Proc. ASME 2013 Int. Design Engineering Technical Conferences and Computers and Information in Engineering Conference IDETC/CIE 2013*, August 4–7, 2013, Portland, OR, Paper DETC2013-12763.

Plecnik, M.M. and McCarthy, J.M., 2012, "Design of a 5-SS spatial steering linkage," *Proc. ASME 2012 Int. Design Engineering Technical Conf. & Computers and Information in Engineering Conference (IDETC/CIE 2012)*, August 12–15, 2012, Chicago, IL. Paper DETC2012-71405.

Poncelet, J.V., 1824. *Traité de Mécanique Appliquée aux Machines*, Liège.

Pradeep, A.K., Yoder, P.J. and Mukundan, R., 1989, "On the use of dual matrix exponentials in robot kinematics," *The Int. J. Robotics Res.*, Vol. 8, No. 5, pp. 57–66.

Reuleaux, F., 1875, *Theoretische Kinematik*, Braunschweig.

- Reuleaux, F, 1900, *Lehrbuch der Kinematik*, Braunschweig.
- Rico Martínez, J.M. and Duffy, J., 1994, “The principle of transference: History, statement and proof,” *Mechanism and Machine Theory*, Vol. 28, No. 1, pp. 165–177.
- Robert, P., 1994, *Le Petit Robert 1. Dictionnaire alphabétique et analogique de la langue française*, Paris.
- Salmon, G., 1964, *Higher Algebra*, Chelsea Publishing Co., New York.
- Sandor, G.N. and Erdman, A.G., 1984, *Advanced Mechanism Design: Analysis and Synthesis*, Vol. 2, Prentice-Hall, Inc., Englewood Cliffs.
- Shoham, M. and Brodsky, V., 1993, “Analysis of mechanisms by the dual inertia operator,” in Angeles, J., Hommel, G. and Kovács, P. (eds.), *Computational Kinematics*, Kluwer Academic Publishers, Dordrecht, pp. 129–138.
- Shoham, M. and Brodsky, V., 1994, “The dual inertia operator and its application to robot dynamics,” *ASME J. Mechanical Design*, Vol. 116, pp. 1089–1095.
- Simmons, G.F., 1963, *Introduction to Topology and Modern Analysis*, McGraw-Hill Book Co., New York.
- Stein, J., 1979, *Random House College Dictionary*, Random House, New York.
- Sternberg, S., 1994, *Group Theory and Physics*, Cambridge University Press, Cambridge.
- Strang, G., 1988, *Linear Algebra*, 3rd ed., Harcourt Brace Jovanovich College Publishers, Fort Worth.
- Study, E., 1903, *Geometrie der Dynamen*, Leipzig.
- Teng, C.P. and Angeles, J., 2001, “A sequential-quadratic-programming algorithm using orthogonal decomposition with Gershgorin stabilization”, *ASME J. of Mechanical Design*, Vol. 123, pp. 501–509.
- The Concise Oxford Dictionary of Current English*, 1995, Clarendon Press, Oxford.

Tinubu, S.O. and Gupta, K.C., 1984, "Optimal synthesis of function generators without the branch defect," *ASME, J. Mech., Trs., and Auto. in Design*, Vol. 106, pp. 348–354.

Uspensky, J., 1948, *Theory of Equations*, McGraw-Hill Book Company, Inc., New York.

Vitruvius, P.M., 28 BCE, *De Architectura*, Vol. X.

Waldron, K.J. and Kinzel,G .L., 1999, *Kinematics, Dynamics, and Design of Machinery*, John Wiley & Sons, Inc., New York.

Webster's Collegiate Dictionary, 2003, (on-line).

Wohlhart, K., 1991, "Der homogene Paralleltrieb-Mechanismus," *Mathematica Panonica*, Vol. 2, No. 2, pp. 59–76.

Wohlhart, K., 1992, "Displacement analysis of the general spatial parallelogram manipulator," *Proc. 3rd International Workshop on Advances in Robot Kinematics*, Ferrara, Italy, pp. 104–111.

Wright, D., Desai S., and Henderson, W., 1964, "Action of the subtalar and ankle-joint complex during the stance phase of walking," *The J. Bone and Joint Surgery*, Vol. 46-A, No. 2, pp. 361–382.

Yang, A.T., 1963. *Application of Quaternion Algebra and Dual Numbers to the Analysis of Spatial Mechanisms*, Doctoral Dissertation, Columbia University, New York, No. 64-2803 (University Microfilm, Ann Arbor, Michigan).

Yang, A.T. and Freudenstein, F., 1964, "Application of dual-number quaternion algebra to the analysis of spatial mechanisms," *J. of Applied Mechanics*, Vol. 31, pp. 300–308.

Koetsier, T., 2010, *Ludwig Burmester (1840–1927)*, in Ceccarelli, M. (editor), *Distinguished Figures in Mechanism and Machine Science. Their Contributions and Legacies, Part 2*, Springer.

Bottema, O. and Roth, B., 1978. *Theoretical Kinematics*, North-Holland Publishers Co., North-Holland Publishing Company, Amsterdam.

Chang, C.Y., Angeles, J. and González-Palacios, M.A., 1991, “A semigraphical method for the solution of the Burmester problem,” *Proc. 1991 ASME Design Automation Conference. Advances in Design Automation*, Sept. 22–25, Miami, Vol. 2, pp. 321–326.

Hall, Jr., A.S., 1961, *Kinematics and Linkage Design*, Balt Publishers, West Lafayette, IN.

Chen, C., Bai, S.P. and Angeles, J., 2008, “A comprehensive solution of the classic Burmester problem,” *CSME Transactions*, Vol. 32, No. 2, pp. 137–154.

Angeles, J., 2006, “Is there a characteristic length of a rigid-body displacement?,” *Mechanism and Machine Theory*, Vol. 41, pp. 884–896.

Hillier, S. and Liebermann, G.J., 1995, *Introduction to Mathematical Programming*, McGraw-Hill, Inc., New York.

Brand, L., 1955, *Advanced Calculus*, John Wiley & Sons, Inc., New York.

Chiang, C.H., 1988, *Kinematics of Spherical Mechanisms*, Cambridge University Press, Cambridge.

McCarthy, J.M. and Soh, G.S., 2011, *Geometric Design of Linkages*, Springer, New York.

Roth, B., 1967, “On the screw axes and other special lines associated with spatial displacements of a rigid body,” *ASME J. Engineering for Industry*, February, pp. 102-110.

Angeles, J. and Bai, S.P., 2010, “A robust solution of the spherical Burmester problem,” *Proc. ASME Int. Design Engineering Technical Conf. & Computers and Information in Engineering Conf., DETC2010-28189*, Montreal, Quebec, Canada, Aug. 15–18.

Liu, Z. and Angeles, J., 1992, "The constrained least-square optimization of spherical four-bar linkages for rigid-body guidance," *Trans. Canadian Society of Mechanical Engineering*, Vol. 16, No. 1, pp. 47–60.

Léger, J. and Angeles, J., 2014, "A solution to the approximate spherical Burmester problem," in Ceccarelli, M. and Hernández-Martínez, E.E. (editors), *Multibody Mechatronic Systems. Proc. MUSME Conference held in Huatulco, Mexico, Oct. 21–24, 2014*, pp. 521–529.

Salmon, G., 1964, *Higher Algebra*, 5th Edition (reprinted from the 1885 edition), Chelsea Publishing Co., New York.

# Index

- Π-joint, 53
- algebraic equation
  - degree, 14
- approximate synthesis
  - for function generation, 121
- assemblability, 75
- augmented synthesis equations, 126
- bimodal linkage, 104
- bivariate equations, 14
- branch switching, 143
- chain
  - exceptional, 71
- chain rule, 24
- Chebyshev-Grübler-Kutzbach-Hervé Formu-  
la, 66
- chirality, 46
- circularity, 192
- contour-intersection, 88
- cubic of stationary curvature, 190
- damping, 36
- damping factor, 36
- Denavit-Hartenberg
  - frames, 83
  - notation, 83
- Denavit-Hartenberg parameters, 9
- design
  - functions, 6
  - specifications, 6
  - variants, 6
- design vs. structural error, 139
- determined system, 32
- dimensioning, 9
- displacement
  - groups, 45
- dwell, 189
- eliminant, 14
- engineering design, 5
  - process, 6
- error vector, 22
- exceptional chains, 67
- floating-point operation, 26
- flop, *see* floating-point operation
- four-bar linkage
  - planar, 80
  - spatial, 89
  - spherical, 84
- fractal, 35
- Freudenstein equation
  - for planar linkages, 82
- Freudenstein parameters

for the spherical linkage, 86  
 function generation  
     exact synthesis, 93  
     exact synthesis for planar four-bar linkages, 93  
     exact synthesis for spherical four-bar linkages, 98  
 generalized Chebyshev-Grübler-Kutzbach formula, 68  
 generalized CGK formula, 68  
 groups of displacements, 66  
 Index, 247  
 inflection circle, 190  
 input-output equation  
     for spherical linkages, 87  
 input-output functions, 80  
 IO equation, 80  
 Jacobian matrix, 34  
 kinematic bond, 64  
 kinematic chain  
     architecture, 83  
 kinematic chains  
     multiloop, 45  
 kinematic synthesis, 7  
 kinetostatics, 15  
 least-square error, 24, 35  
     normality condition, 23  
 least-square solution, 36  
 left Moore-Penrose generalized inverse, 25  
 LKP, 45  
 lower kinematic pairs, 45  
 machine, 5  
     function, 5  
 mechanical system, 5  
 model  
     parametric, 7  
 monovariate polynomial equation, 14  
 motion  
     representation, 45  
 multiobjective optimization, 7  
 multivariate polynomial equations, 14  
 nonlinear system, 32  
 normality condition, 37  
 overdetermined system, 35  
 paradoxical chains, 67, 74  
 path generation, 189  
     with timing, 192  
 performance evaluation, 131  
 planar four-bar linkage  
     coupler curve, 197  
     feasibility condition, 95  
 Planar Linkages  
     transmission angle, quality, 131  
 planar linkages  
     Bloch synthesis, 96  
     planar path-generation, 190  
     projection  
         theorem, 25

QR decomposition, 123  
qualitative synthesis, 74

resolvent, 14  
rigid body, 46

Roberts-Chebyshev Theorem, 201

Sarrus mechanism, 71

semigraphical method, 88

signum function, 31

spatial linkages

- mobility analysis, 120
- synthesis for function generation, 118

stationary point, 37

structure, 5

- function, 5

Sylvester's Theorem, 26

synthesis

- approximate, 13
- equations, 13
- exact, 13
- qualitative, 8, 45
- semigraphical methods, 13

synthesized linkage

- analysis, 101
- mobility analysis, 114

synthesized planar linkage

- analysis, 101
- mobility analysis, 108

synthesized spatial linkage

- analysis, 114
- analysis with  $d_1$  as input, 117

synthesized spherical linkage analysis, 112

trivial chains, 66

trivial-chains, 67

weighting matrix, 36